UNIVERSITAT DE BARCELONA

Effects of ageing and genetic risk variants at 4q25 on the calcium homeostasis in cardiac myocytes

Adela Herraiz Martínez

ADVERTIMENT. La consulta d'aquesta tesi queda condicionada a l'acceptació de les següents condicions d'ús: La difusió d'aquesta tesi per mitjà del servei TDX (**www.tdx.cat**) i a través del Dipòsit Digital de la UB (**diposit.ub.edu**) ha estat autoritzada pels titulars dels drets de propietat intel·lectual únicament per a usos privats emmarcats en activitats d'investigació i docència. No s'autoritza la seva reproducció amb finalitats de lucre ni la seva difusió i posada a disposició des d'un lloc aliè al servei TDX ni al Dipòsit Digital de la UB. No s'autoritza la presentació del seu contingut en una finestra o marc aliè a TDX o al Dipòsit Digital de la UB (framing). Aquesta reserva de drets afecta tant al resum de presentació de la tesi com als seus continguts. En la utilització o cita de parts de la tesi és obligat indicar el nom de la persona autora.

ADVERTENCIA. La consulta de esta tesis queda condicionada a la aceptación de las siguientes condiciones de uso: La difusión de esta tesis por medio del servicio TDR (**www.tdx.cat**) y a través del Repositorio Digital de la UB (**diposit.ub.edu**) ha sido autorizada por los titulares de los derechos de propiedad intelectual únicamente para usos privados enmarcados en actividades de investigación y docencia. No se autoriza su reproducción con finalidades de lucro ni su difusión y puesta a disposición desde un sitio ajeno al servicio TDR o al Repositorio Digital de la UB. No se autoriza la presentación de su contenido en una ventana o marco ajeno a TDR o al Repositorio Digital de la UB (framing). Esta reserva de derechos afecta tanto al resumen de presentación de la tesis como a sus contenidos. En la utilización o cita de partes de la tesis es obligado indicar el nombre de la persona autora.

WARNING. On having consulted this thesis you're accepting the following use conditions: Spreading this thesis by the TDX (**www.tdx.cat**) service and by the UB Digital Repository (**diposit.ub.edu**) has been authorized by the titular of the intellectual property rights only for private uses placed in investigation and teaching activities. Reproduction with lucrative aims is not authorized nor its spreading and availability from a site foreign to the TDX service or to the UB Digital Repository. Introducing its content in a window or frame foreign to the TDX service or to the UB Digital Repository is not authorized (framing). Those rights affect to the presentation summary of the thesis as well as to its contents. In the using or citation of parts of the thesis it's obliged to indicate the name of the author.

EFFECTS OF AGEING AND GENETIC RISK VARIANTS AT 4q25 ON THE CALCIUM HOMEOSTASIS IN CARDIAC MYOCYTES

Tesis presentada por

Adela Herraiz Martínez

para optar al grado de Doctor por la Universidad de Barcelona

UNIVERSITAT DE BARCELONA

Programa de doctorado de Medicina

Facultad de Medicina

Este trabajo ha sido realizado bajo la dirección del Dr. Leif Hove Madsen, Científico Titular del Centro de Investigación Cardiovascular CSIC-ICCC

El director — La doctoranda

Leif Hove Madsen — Adela Herraiz Martínez

Barcelona, 2016

A mis padres,

“Inside every old person is a young person

wondering what happened”

AGRADECIMIENTOS

AGRADECIMIENTOS

En primer lugar me gustaría agradecer a mi director Leif, por haberme dado la oportunidad de realizar la tesis en su laboratorio. Muchas gracias por la confianza que has depositado en mí y por todo lo que me has aportado y ayudado durante este tiempo.

También quisiera agradecer a mis compañeras de laboratorio, empezando por las que ya no están Montse, Nuria y en especial a Anna, por el traspaso de conocimiento intensivo en tan breve tiempo compartido. Como no, agradecer a Selma su compañerismo, su entusiasmo y su humor, por hacernos pasar tan buenos momentos en el laboratorio (todavía queda por esclarecer las imágenes de Cuarto Milenio de la aparición de "la monja"). A Carmen, por su toque andaluz, su comprensión y por todos los momentos que hemos compartido (ah! y por ayudarme con los ratones!!). Y a Verónica, el nuevo fichaje del laboratorio que estoy segura que aportará muchas cosas buenas a este equipo!

Agradecer también al equipo del Dr. Cinca por su ayuda científica en nuestros resultados y al equipo de Cirugía Cardíaca del Hospital de Sant Pau por recibirnos siempre con los brazos abiertos en el quirófano.

Gracias a todo el personal del ICCC que de alguna manera me ha ayudado durante esta etapa, en especial al laboratorio 110 por su paciencia con los genotipados y con las demás tareas ratoniles…

A mis compañeros de piso, los de la primera temporada, Mili por ser la "compi" que toda persona le gustaría tener, por tener un corazón tan grande y aunque con sufrimiento (ya sabes que llevamos el sello de sufridoras en los genes) estas consiguiendo tu meta. También gracias a Felipe, por ser tan buena gente. Me alegro de vuestros éxitos conseguidos!

A mis compañeras de piso de la segunda temporada, María y Blanca. Gracias por vuestra compañía. Blanqui, gracias por este reencuentro después de tantos años, por tu apoyo moral y por hacer que Barcelona sea más divertida (aunque no terminemos de encontrar esa zona de marcha…)

Por último quisiera agradecer el apoyo incondicional de mi familia, a mis padres por todo el esfuerzo hecho por mi educación, por haberme inculcado la importancia de ser responsable y trabajadora. A mi hermano, por ser "un cacho de pan", a mi cuñada y a mis sobrinas por alegrarme el corazón; a mis tías María, "las Pilares" y a Pili peque, por toda vuestra ayuda y por estar siempre al pie del cañón en los momentos buenos y

no tan buenos. A mis primos Eugenio y en especial a Jose Ángel, el primer científico de la familia, sé que habrías estado orgulloso de verme concluir esta etapa.

Y como no, gracias a Joaquín, por preocuparse tanto por mí, por ayudarme, por confiar en mí…. Podría escribirte páginas enteras de agradecimiento, pero en resumidas cuentas gracias por estar a mi lado y haberme hecho disfrutar de tantos buenos momentos.

CONTENTS

ABREVIATIONS

AF	atrial fibrillation
AP	action potential
APD	action potential duration
AR	adrenergic receptor
AVN	atrioventricular node
BSA	bovine serum albumin
Ca^{2+}	calcium ion
$[Ca^{2+}]i$	intracellular calcium concentration
CACNA1C	alpha 1C subunit of the voltage-gated L-type calcium channel
CAF	caffeine
CaM	calmodulin
CaMKII	Ca-calmodulin dependent protein kinase II
cAMP	cyclic AMP
CICR	calcium-induced calcium release
CSQ2	cardiac calsequestrin (type 2)
DAD	delayed afterdepolarization
DHPR	dihydropyridine receptor
ECG	electrocardiogram
FDHM	full duration at half maximum
FWHM	full width at half maximum
GWAS	genome wide association studies
HGPS	Hutchinson-Gilford progeria syndrome
I_{Ca}	calcium current
I_h	holding current
I_{ion}	ionic current
I_k	potassium current
I-V	Current-Voltage
i.p.	Intraperitoneal
LA	left atrium
LTCC	L-type calcium channels
LV	left ventricular
LVH	left ventricular hypertrophy

NCX	Na^+/Ca^{2+} Exchange
NCX-1	cardiac Na^+/Ca^{2+} Exchanger (type 1)
PBS	phosphate buffer solution
PKA	c-AMP dependent protein kinase
PLC	phospholipase C
RA	right atrium
RT-PCR	real time-polymerase chain reaction
RyR2	cardiac ryanodine receptor (type 2)
SAN	sinoatrial node
SERCA2	cardiac SR Ca-ATPase pump protein (type 2)
SL	sarcolemma
SNP	single nucleotide polymorphism
SR	sarcoplasmic reticulum
T-tubules	transverse tubules
TnC	troponin C
TnI	troponin I
TnT	troponin T
V_m	membrane potential
WB	western blot

ABREVIATURAS

AD	aurícula derecha
AI	aurícula izquierda
ARA-II	antagonistas del receptor de angiotensina II
FA	fibrilación auricular
FEVI	fracción de eyección del ventrículo izquierdo
IECAs	inhibidores de la enzima convertidora de angiotensina
RS	retículo sarcoplásmico

RESUMEN

RESUMEN

Introducción

En las últimas décadas, el envejecimiento progresivo de la población se ha convertido en un patrón epidemiológico característico en los países desarrollados.[1] La media de la esperanza de vida en humanos está aumentando, y con ello el porcentaje de personas mayores de 65 años está creciendo rápidamente y lo continuará haciendo en los próximos años. Esto refuerza el interés en la fisiología del envejecimiento y en enfermedades cardiovasculares asociadas como la aterosclerosis, la insuficiencia cardíaca, la fibrilación auricular o trastornos del ritmo cardíaco, enfermedades que conjuntamente suponen la primera causa de muerte en los países desarrollados.

Alteraciones en la función o estructura del corazón que se relacionan con el envejecimiento pueden ser el resultado de una variedad de mecanismos entre los cuales, las principales proteínas involucradas en la contracción y relajación cardíaca son de especial relevancia.[2] Así mismo, el calcio juega un papel muy importante en la regulación de la contracción y relajación del cardiomiocito. Resumiendo el mecanismo, la contracción cardiaca se activa cuando un potencial de acción despolariza la membrana celular y activa la apertura de los canales de calcio tipo-L en los cardiomiocitos, provocando así un incremento del calcio intracelular y la activación de una mayor liberación de calcio del retículo sarcoplasmático. Este fenómeno conocido como “calcium induced calcium release” (CICR), eleva el calcio citosólico que a su vez se une a la troponina C y activa la contracción celular. Del mismo modo, la relajación se produce con la eliminación del calcio del citosol, principalmente por su reacumulación en el retículo sarcoplásmico y también por su expulsión del cardiomiocito a través del intercambiador Na^{+}-Ca^{2+}.[3]

Dado que las enfermedades prevalentes asociadas al envejecimiento como la fibrilación auricular también se ha asociado con cambios patológicos en la

homeostasis del calcio, hay un creciente interés en el efecto del envejecimiento sobre el manejo del calcio intracelular. A pesar de ello, no existe información que relacione el envejecimiento con los mecanismos involucrados en la homeostasis del calcio en cardiomiocitos humanos y parece oportuno analizar el efecto del envejecimiento sobre la homeostasis del calcio en miocitos auriculares humanos.

Para reforzar el estudio y profundizar en los mecanismos subyacentes a los efectos del envejecimiento sobre la homeostasis del calcio, se llevarán a cabo experimentos electrofisiológicos y moleculares en muestras auriculares humanas y en un modelo murino de envejecimiento. Se utilizarán ratones progéricos *Zmpste24*$^{-/-}$, en los que la acumulación de prelamina A provoca características típicas de la enfermedad de progeria prematura[4,5] Hutchinson-Gilford, entre las que se encuentran importantes alteraciones cardiovasculares que contribuyen a la muerte prematura en este modelo.

Además, dado que la fibrilación auricular es la más común de las arritmias cardíacas[6] y provoca un remodelado eléctrico de los miocitos auriculares, sería de gran interés estudiar la relación que existe entre alteraciones en la homeostasis del calcio inducido por envejecimiento y las alteraciones observadas en pacientes con fibrilación auricular.

En relación con los mecanismos moleculares subyacentes a alteraciones en la homeostasis del calcio en la fibrilación auricular, se desconoce prácticamente el papel que desempeñan las variaciones genéticas. Se han descrito mutaciones puntuales en los genes que codifican los canales de calcio asociado con fibrilación auricular familiar[7] pero esta solo representa una pequeña fracción del total de los casos de fibrilación auricular (<10%). Sin embargo, recientes estudios de GWAS (genome-wide asociation studies) han identificado variantes genéticas frecuentes asociadas con la fibrilación auricular. Entre ellas, variantes localizadas en el cromosoma 4q25, próximas al factor de transcripción Pitx2, que juega un papel muy importante en el desarrollo cardíaco durante la embriogénesis.[8] Así, parece existir una relación entre los variantes de riesgo, la actividad/expresión de Pitx2 y las alteraciones en la homeostasis del calcio en la fibrilación auricular.

Por ello, se pretende conocer los mecanismos moleculares que asocian las variantes de riesgo en el cromosoma 4q25, los niveles de Pitx2 y la fibrilación auricular. Concretamente, se pretende investigar como dichas variantes de riesgo y los niveles de Pitx2 afectan a las características electrofisiológicas de miocitos auriculares de pacientes con y sin fibrilación auricular.

Para poder llevar a cabo esta investigación, se utilizará un modelo de ratón deficiente en Pitx2 de forma total, parcial o no deficiente, pudiendo comparar los efectos electrofisiológicos que produce la delección de este factor de transcripción.

Por último, dado que ambos factores objetivo de estudio (envejecimiento y variantes de riesgo en el cromosoma 4q25) se han relacionado con alteraciones en el manejo del calcio, se estudiará si existe relación sinérgica entre ellos, en pacientes tanto con fibrilación auricular como sin ella, clasificándolos en grupos de edades.

Así, se pretende tener una información de los mecanismos afectados por estos dos factores objetivo de estudio, envejecimiento y variantes de riesgo genéticas (en concreto tres de las presentes en el cromosoma 4q25) sobre la homeostasis del calcio en células auriculares.

Hipótesis y Objetivos

El envejecimiento y las alteraciones en la homeostasis del calcio intracelular han sido descritos como posibles causas de enfermedades cardíacas como la fibrilación auricular o la insuficiencia cardíaca. Sin embargo, se sabe muy poco sobre el efecto que ejerce el envejecimiento en la homeostasis del calcio en la aurícula humana. Además, existen variantes genéticas (single nucleotide polymorphims - SNP) en el cromosoma 4q25 identificadas recientemente y asociadas a un mayor riesgo de padecer fibrilación auricular, pero se desconoce el efecto de estas variantes sobre la homeostasis del calcio y si la edad incrementa su efecto.

Por lo tanto, esta tesis tiene como objetivo probar la hipótesis de que el envejecimiento y las variantes de riesgo en 4q25 producen alteraciones en la homeostasis del calcio intracelular en miocitos auriculares, que por sí solas o en combinación contribuyen a aumentar la propensión a la fibrilación auricular.

Para probar esta hipótesis, los cardiomiocitos se aislaron a partir de muestras de aurícula derecha humana y de diferentes modelos de ratones transgénicos, sometidos a protocolos electrofisiológicos específicos diseñados para abordar los siguientes objetivos:

- Analizar los efectos del envejecimiento en los mecanismos que regulan la homeostasis del calcio en miocitos auriculares humanos.
- Utilizar modelos murinos transgénicos de envejecimiento para identificar los mecanismos moleculares que subyacen a los cambios en la homeostasis del calcio debido al envejecimiento.
- Investigar cómo las variantes de riesgo en el cromosoma 4q25 asociadas con un mayor riesgo de FA, afectan a las características electrofisiológicas de los miocitos auriculares humanos e identificar los mecanismos moleculares subyacentes.
- Investigar como la edad modula los efectos de las variantes de riesgo en 4q25 en miocitos auriculares humanos.

Resultados

Los resultados de esta tesis se estructuran en capítulos independientes, tratando de identificar los mecanismos que pueden dar explicación al aumento de frecuencia de la fibrilación auricular debido al envejecimiento, y la asociación de esta arritmia con alteraciones en la regulación del calcio intracelular. La mayoría de los resultados presentados aquí están incluidos en los manuscritos en preparación, presentados para su publicación, o ya publicados.

El primer capítulo está dedicado al primer y principal objetivo de esta tesis, tratando de dilucidar los mecanismos implicados en las alteraciones del manejo del calcio intracelular con la edad en miocitos auriculares humanos, y su potencial contribución en el incremento del riesgo de padecer fibrilación auricular con la edad. Los resultados de este capítulo han sido ya publicados.[9]

El segúndo capítulo describe los resultados hayados en el modelo de ratón progérico *Zmpste24*$^{-/-}$, donde el procesamiento defectivo de la lamina, el cual se ha asociado a envejecimiento natural y prematuro, reproduce los efectos vistos en miocitos auriculares humanos. Este capítulo contiene resultados incluidos en el manuscrito "Cardiac electrical defects in progeroid mice and Hutchinson-Gilford progeria syndrome patients with nuclear lamina alterations" recientemente publicado,[10] así como otros experimentos adicionales no incluidos en este manuscrito.

En el tercer capítulo se investiga si las variantes de riesgo en el cromosoma 4q25, asociadas a un mayor riesgo de sufrir FA, afectan al manejo del calcio intracelular en miocitos auriculares humanos. Los resultados de este manuscrito han sido enviados recientemente para su publicación.

El cuarto capítulo investiga como el factor de transcripción Pitx2, propuesto como el mediador del efecto de las varientes de riesgo del cromosoma 4q25, modula la homeostasis del calcio y si su insuficiencia reproduce los efectos observados en los miocitos de pacientes con las variantes de riesgo 4q25. Para este propósito, se utilizó un modelo transgénico de ratón con delección total, parcial o

nula de Pitx2. Algunos de estos reusltados son parte de un manuscrito publicado, el cual investiga los mecanismos que provocan alteración en la expresión y función de proteínas implicadas en la regulación del calcio.[11]

Finalmente, en el capítulo quinto se integran los efectos de ambos factores estudiados, la edad y las variantes de riesgo, para determinar si el envejecimiento modula el efecto de las varientes de riesgo 4q25 sobre la homeostasis del calcio intracelular. Estos resultados forman parte de un manuscrito en preparación.

A continuación se muestras los resultados obtenidos en cada uno de los capítulos:

I. El envejecimiento está asociado con el deterioro de la homeostasis de calcio en miocitos auriculares aislados.

Para determinar como el envejecimiento *per se* afecta al manejo del calcio en los miocitos auriculares humanos sanos, fueron medidas las corrientes de calcio intracelular en miocitos auriculares humanos de un total de 80 pacientes sin historia de fibrilación auricular previa y de tamaño auricular normal (<2.3 cm/m^2). Los pacientes fueron clasificados en tres grupos: jóvenes (<55 años, n = 21), de edad media (55 a 74 años, n = 42) y viejos (≥ 75 años, n = 17). Los niveles de las principales proteínas involucradas en la contracción y relajación cardíaca se determinaron mediante western blot.

Los resultados encontrados fueron que el envejecimiento está asociado con los siguientes cambios electrofisiológicos:

(i) Disminución de 3.2 veces del calcio transitorio celular ($p<0.01$) y con una propagación más lenta desde la membrana hacia el centro celular, no atribuible a la presencia de túbulos-t al no ser detectados en ninguna de las muestras analizadas en los tres grupos. También es más lenta la desaparición del calcio transitorio reflejado como una mayor duración al 50% de la amplitud máxima (FDHM);

(ii) Reducción de la amplitud de la corriente de calcio tipo L (2.4+0.3 pA/pF vs.1.4+0.2 pA/pF, $p<0.01$), sin cambios en las propiedades intrínsecas del canal;

(iii) Menor expresión de la subunidad alfa del canal de calcio tipo L ($p<0.05$), medidos por WB;

(iv) Se ralentiza la inactivación de la corriente de calcio rápida (14.5+0.9 ms vs. 20.9+1.9, $p<0.01$) y lenta (73+3 vs. 120+12 ms, $p<0.001$);

(v) Disminución en el contenido de calcio del retículo sarcoplásmico (10.1+0.8 vs. 6.4+0.6 amol/pF, $p<0.005$), que se puede liberar por cafeína ;

(vi) Menor expresión en las proteínas SERCA2 ($p<0.05$) y calsequestrin-2 ($p<0.05$) involucradas en regulación del calcio del retículo sarcoplásmico;

Por el contrario, el envejecimiento no afecto a la liberación espontánea de calcio del retículo sarcoplásmico, parámetro importante por la provocación de eventos arrítmicos. Tampoco hay un efecto del envejecimiento sobre la capacitancia celular, parámetro que refleja que la superficie de los miocitos no cambia con la edad, es decir, no se produce hipertrofia de las células auriculares en pacientes sin fibrilación auricular con la edad.

Los efectos descritos se analizaron estadísticamente, demostrando que fueron independientes de los posibles factores de confusión que a continuación se indican: sexo, fracción de eyección del ventrículo izquierdo (FEVI), enfermedad valvular, enfermedad isquémica, tratamiento farmacológico con inhibidores de la enzima convertidora de angiotensina (IECAs), antagonistas del receptor de angiotensina II (ARA-II) betabloqueantes y antagonistas del canal de calcio.

II. El modelo de ratón progérico *Zmpste 24*$^{-/-}$ reproduce las alteraciones en la homeostasis del calcio

Se utilizó el modelo de ratón de envejecimiento *Zmpste24*$^{-/-}$ para profundizar en los mecanismos subyacentes a la alteración del calcio con la edad.
Los resultados obtenidos corroboran los principales hallazgos encontrados en humano. Los principales efectos observados en los miocitos ventriculares de los ratones progéricos comparados con WT fueron los siguientes:

(i) Disminución del calcio transitorio celular ($p<0.01$) y mayor duración del mismo (FDHM) ($p<0.05$) ;

(ii) Disminución de la corriente de calcio tipo L, aunque existe una tendencia hacia valores más pequeños en ratones envejecidos, esta diferencia no es significativa. Sin embargo sí lo es su inactivación, siendo más lenta en los ratones *Zmpste24*$^{-/-}$ ($p<0.01$ para tau-1);

(iii) Menor capacidad de re-llenado del retículo sarcoplásmico en los ratones progéricos tras 5, 10 y 20 pulsos de estimulación ($p<0.05$), incrementándose esta deficiencia aún más después de 30 o más pulsos de estimulación ($p<0.05$). Esta capacidad también se vio reducida cuando se utilizaron potenciales de membrana entre -40 y 0 mV para llenar el retículo sarcoplásmico ($p<0.05$).

(iv) Disminución de las proteínas SERCA2 ($p<0.01$) y CSQ2 ($p<0.05$) involucradas en la acumulación y tamponamiento del calcio del retículo sarcoplásmico;

(v) Incapacidad de seguir el ritmo de estimulación a frecuencias elevadas, efecto más pronunciado en condiciones de 5mM de calcio extracelular ($p<0.05$);

(vi) Se ralentizó la inactivación rápida de la corriente de calcio (regulado por la liberación de calcio del retículo sarcoplásmico) en ratones progéricos ($p<0.05$);

Estos datos muestras que al igual que en las células auriculares humanas, hay una alteración en el calcio transitorio celular, acompañado de una disfunción en el re-llenado y en la liberación de calcio del RS, que conjuntamente afectarán a la capacidad de seguir un ritmo de estimulación a distintas frecuencias de estimulación.

Sin embargo, de forma similar que en el caso de las miocitos humanos, en los ratones progéricos tampoco se observó una alteración en la liberación espontánea de calcio del retículo sarcoplásmico.

Estos resultados, conjuntamente con los encontrados en las células humanas, apoyan la hipótesis de que la edad conlleva defectos en el procesado de la proteína lamina, lo cual atenúa la expresión y función de proteínas reguladoras del calcio.

III. La propensidad a la fibrilación auricular en pacientes con variantes de riesgo en 4q25 se asociada a alteraciones de la homeostasis del calcio en miocitos auriculares humanos

Puesto que las variantes de riesgo localizadas en el cromosoma 4q25 se han asociado a mayor riesgo de padecer FA y que esta arritmia se asocia a alteraciones en la regulación del calcio, este bloque de resultados analiza el efecto de tres variantes de riesgo sobre los principales mecanismos de regulación del calcio en células auriculares humanas.

Los principales resultados encontrados fueron:

(i) Las variantes de riesgo 4q25 no alteran la amplitud de la corriente de calcio, su constante de inactivación, u otras propiedades del canal de calcio (relación I-V, inactivación de la corriente de calcio voltaje-dependiente);

(ii) Aumento de la frecuencia de corrientes de entrada espontáneas (I_{TI}) en miocitos de pacientes con variantes de riesgo y sin FA ($p<0.001$), que se acentúa en pacientes con variantes de riesgo y FA ($p<0.05$). La amplitud de las ondas fue similar en ambos grupos.

(iii) Mayor frecuencia ($p<0.001$) y amplitud ($p<0.001$) de despolarizaciones espontáneas de la membrana en células de pacientes con variantes de riesgo.

(iv) Incremento en la frecuencia de sparks ($p<0.01$) debido a un aumento de sitios donde se producen ($p<0.01$) en lugar de una mayor frecuencia de sparks en un determinado sitio ($p=0.8$). Las dimensiones y cinéticas de los sparks, sin embargo, no mostraron diferencias entre los diferentes grupos;

(v) Mayor contenido de calcio acumulado en el retículo sarcoplásmico ($p<0.05$) en miocitos de pacientes con variante de riesgo;

(vi) Los niveles de expresión de SERCA2 fueron significativamente más altos ($p<0.05$) en pacientes con variantes de riesgo.

(vii) El análisis de las dos variantes rs2200733 y rs13143308, repetidamente asociados a FA y rs1448818, más próximas al locus de PITX2, mostró que ninguna de las variantes tenía efecto sobre la corriente de calcio. Sin embargo, la presencia de la variante de riesgo rs13143308T sola o con rs2200733 incrementó la frecuencia de $I_{TI}S$, mientras que no lo hacía la variante rs1448818.

Resumiendo, los resultados obtenidos demuestran por primera vez que la variante de riesgo rs13143308T es un marcador genético para mayor riesgo de FA, asociado a un aumento en la liberación de calcio y despolarizaciones de membrana espontáneas que favorecen el inicio de eventos arrítmicos en los pacientes portadores.

IV. La insuficiencia de Pitx2 reproduce los efectos de las variantes de riesgo en 4q25 sobre la homeostasis del calcio

Las variantes de riesgo 4q25 se localizan en la proximidad del factor de transcripción Pitx2, el cual se ha propuesto como mediador entre las variantes riesgo y su efecto en la electrofisiología celular. Teniendo en cuenta los hallazgos que describen una reducción de Pitx2 en pacientes con FA, se utilizó un modelo murino con delección total ($NppaCre^{+}Pitx2^{-/-}$), parcial ($NppaCre^{+}Pitx2^{fl/-}$) o sin delección de Pitx2 ($NppaCre^{-}Pitx2^{fl/fl}$).

Para profundizar en los mecanismos moleculares en los cuales Pitx2 desempeña un papel importante, se hizo un estudio electrofisiológico para conocer si la homeostasis del calcio se altera por la disminución de este factor de transcripción.

El estudio de los principales componentes que regulan el manejo de calcio, realizado a los tres tipos de ratón reveló:

(i) Mayor expresión de los niveles de ARNm de SERCA2 ($p<0.001$), CSQ2 ($p<0.001$) y PLB ($p<0.001$) tanto en aurícula izquierda (AI) como derecha (AD); menor expresión de la subunidad formadora del poro del canal de calcio Cacna1c en AI ($p<0.001$) y aumentada en AD ($p<0.001$), comparando el ratón control $NppaCre^{+}Pitx2^{fl/fl}$ con el deficiente $NppaCre^{+}Pitx2^{-/-}$;

(ii) De acuerdo con los resultados de RT-PCR, los datos electrofisiológicos mostraron que la corriente de calcio tipo L en AI estaba disminuida ($p<0.05$) y el contenido de calcio del retículo sarcoplásmico aumentado tanto en AI ($p<0.01$) como en AD ($p<0.01$);

(iii) Además, el tejido auricular de los ratones con delección parcial de Pitx2 mostraba niveles intermedios de los genes involucrados con el manejo del calcio, demostrándose un efecto dosis-dependiente.

Estos datos indican que la insuficiencia del factor de transcripción Pitx2 induce alteraciones en las proteínas implicadas en la homeostasis del calcio que a la vez provocan alteraciones electrofisiológicas que favorecen la arritmogénesis auricular.

Además se comprobó si las alteraciones del manejo del calcio intracelular vistas en pacientes con variantes de riesgo 4q25, se reproducían en miocitos de la aurícula derecha de ratones con insuficiencia parcial de Pitx2 ($NppaCre^{+}Pitx2^{fl/-}$), y los resultados obtenidos fueron los siguientes:

(iv) No se observaron diferencias en la amplitud de la corriente de calcio tipo L;

(v) Mayor incidencia de sparks de calcio en miocitos auriculares del ratón $NppaCre^{+}Pitx2^{fl/-}$ (comparados con $NppaCre^{-}Pitx2^{fl/fl}$, $p<0.01$). Esta característica no fue única en miocitos de AD, ya que en miocitos de AI fue casi 4 veces mayor ($p<0.001$).

(vi) Mayor contenido del retículo sarcoplásmico en miocitos de ratones $NppaCre^{+}Pitx2^{fl/-}$ en comparación con $NppaCre^{-}Pitx2^{fl/fl}$ ($p<0.05$);

(vii) Incremento de la frecuencia y la amplitud de despolarizaciones de membrana espontaneasen condiciones de reposo ($p<0.05$) en miocitos de ratones NppaCre^{+}Pitx2$^{fl/-}$. Cuando se sometieron a estimulación eléctrica, solo los miocitos de NppaCre^{+}Pitx2$^{fl/-}$ mostraban potenciales de acción espontáneos entre los pulsos de estimulación.

Así, los efectos de la insuficiencia parcial de Pitx2 fueron similares a los efectos de los variantes de riesgo 4q25, apoyando la idea de que la modulación intracelular de calcio por Pitx2 juega un papel importante en procesos electrofisiológicos asociados a la FA.

V. Efecto del envejecimiento sobre pacientes con fibrilación auricular y relación con las variantes del riesgo del cromosoma 4q25

Dado que la fibrilación auricular es la más común de las arritmias cardíacas[7] y provoca un remodelado eléctrico de los miocitos auriculares, es de gran interés estudiar la relación que existe entre alteraciones en la homeostasis del calcio inducido por envejecimiento y las alteraciones observadas en pacientes que padecen fibrilación auricular.

Así, en este capítulo se pretende investigar si el envejecimiento y las variantes de riesgo en el cromosoma 4q25 modifican de forma sinérgica la homeostasis del calcio intracelular en miocitos auriculares humanos de pacientes con y sin fibrilación auricular. Los resultados muestran que:

(i) Existe una disminución de la corriente de calcio de tipo L (I_{Ca}) debido al envejecimiento, tanto en pacientes con FA como sin FA, pero es en los pacientes con FA donde la disminución de I_{Ca} fue más acusada;

(ii) El envejecimiento reduce significativamente el contenido de calcio del retículo sarcoplásmico en pacientes sin FA (ver apartado I de estos resultados y Capítulo I), pero no en pacientes con FA;

(iii) La frecuencia de I_{TI} está aumentada en pacientes con FA, pero no está afectada por la edad. Sin embargo, el grupo formado por los pacientes de mayor edad y con FA presenta una mayor amplitud de la corriente (I_{TI})

provocada por la liberación de calcio espontáneo, aumentando la probabilidad de que estos I_{TI} provoquen eventos arrítmicos (despolarizaciones de la membrana o potenciales de acción espontáneos);

(iv) No se han encontrado evidencias de que la edad modifique los efectos que las variantes de riesgo del cromosoma 4q25 tienen sobre la homeostasis del calcio en células auriculares humanas;

Una problemática recurrente cuando se trabaja con células auriculares humanas para abordar cambios electrofisiológicos asociados con fibrilación auricular, son los posibles factores de confusión que concurren en las enfermedades cardiovasculares, así como el tratamiento farmacológico de los pacientes. Para minimizar estos posibles efectos, los análisis estadísticos tuvieron estos factores en cuenta.

El análisis de potenciales efectos sinérgicos entre variantes 4q25, envejecimiento y la FA revelaba que el envejecimiento *per se* no modifica los efectos de variantes 4q25 sobre la homeostasis del calcio. Sin embargo, dado que el envejecimiento reduce la amplitud de la I_{Ca}, lo cual reduciría el periodo refractario auricular, el envejecimiento podría favorecer la prolongación o el mantenimiento de episodios de arritmia inducidas por actividad eléctrica espontanea. Por lo tanto, es posible que las variantes de riesgo 4q25 constituyan un sustrato electrofisiológico arritmogénico que favorece el inicio de episodios arrítmicos auriculares, y que el envejecimiento actúe prolongando la duración de estos episodios al reducir el periodo refractario auricular a través de la reducción de la amplitud de la I_{Ca}.

Discusión

Siguiendo los objetivos propuestos en esta tesis, primero fue examinado el papel que el envejecimiento tenía sobre la homeostasis del calcio en miocitos auriculares humanos sin aparente patología auricular (Capítulo I). Los datos electrofisiológicos mostraron una disminución de la corriente de calcio (I_{Ca}) asociada a la disminución de la subunidad alfa del canal del calcio (DHPR o Cacnac1c) y una disminución del contenido de calcio del retículo sarcoplásmico (RS) asociado a la disminución de las proteínas SERCA2 y CSQ2. Estos cambios subyacen a la reducción de hasta 3 veces del calcio transitorio intracelular, que junto con su lenta propagación hacia el centro celular, podría favorecer la disminución progresiva de la función contráctil con la edad.

La pérdida de I_{Ca} ha sido también descrita previamente como una característica asociada a FA,[12,13] y a arritmogénesis debido al acortamiento del período refractario del potencial de acción,[13] por lo que nuestros datos de disminución de I_{Ca} sugieren que el envejecimiento podría ser un mecanismo que asocia el envejecimiento a la FA. Por otro lado, otros parámetros descritos como arritmogénicos, como una mayor la liberación espontánea de calcio, frecuencia de I_{TI} [12,14,15] no se vieron afectados con la edad.

Para profundizar en los mecanismos moleculares que subyacen a la alteración del calcio con la edad, se usó el modelo murino de envejecimiento prematuro *Zmpste24*$^{-/-}$ con procesamiento de lamina defectuosa (Capítulo II), afectación también producida durante el envejecimiento fisiológico.[16,17] Los cambios observados en la homeostasis del calcio en los miocitos auriculares humanos debidos al envejecimiento, se confirmaron en este modelo murino que reproduce la rara enfermedad progérica de Hutchinson-Gilford, confirmando el mecanismo que podría subyacer a la reducción de la amplitud de la corriente de calcio, del calcio transitorio intracelular, del calcio acumulado en el RS, así como de la disminución de la expresión de las proteínas SERCA2 y CSQ2, proponiendo el procesado defectuoso de lamina o la acumulación de progerina como nexo mecanístico. De acuerdo con los estudios en miocitos auriculares los I_{TI} no se

encontraron afectados por el envejecimiento en células auriculares humanas ni del ratón *Zmpste24*$^{-/-}$.

Recientes estudios de GWAS han asociado a las variantes genéticas o SNP (single nucleotide polymorphism) en la región cromosómica 4q25 con AF,[7,18] pero su relación con las alteraciones electrofisiológicas que se observan en miocitos auriculares humanas de pacientes con FA no han sido descritas hasta el momento. Por lo tanto, el segundo factor de estudio de esta tesis fueron los efectos que las variantes de riesgo presentes en el cromosoma 4q25 (Capítulo III) ejercen sobre la homeostasis del calcio. Los resultados revelaron que estas variantes de riesgo, en concreto la variante rs13143308T por sí sola o junto con rs2200733T, están asociadas con alteraciones electrofisiológicas ligadas a una elevada tasa de liberación espontánea de calcio, I_{TI}s y despolarizaciones de membrana, características asociadas a la FA.[14,15] Estas alteraciones fueron observadas en pacientes portadores de las variantes de riesgo pero sin FA y acentuados en pacientes portadores con FA. Sin embargo, y a pesar de estar localizado próximo al locus de PITX2, la tercera variante de riesgo estudiada, rs1448818, no presentó ninguno de los efectos descritos para las otras dos. Ninguna de las tres variantes afectó a la reducción de la I_{Ca}, variable también asociada a FA,[13] por lo que se sugiere que las variantes de riesgo en 4q25 no contribuyen a la instauración de la FA reduciendo la I_{Ca}. Por lo tanto, estos datos sugieren que el genotipado para el alelo rs13143308 sería suficiente para identificar pacientes con riesgo de padecer FA asociado a alteraciones en la homeostasis del calcio.

Las variantes de riesgo en el cromosoma 4q25 se ubican cerca del factor de transcripción Pitx2, que desempeña un papel importante durante la embriogénesis,[19] así como en el corazón adulto donde la FA se ha asociado a cambios en su expresión.[8,20–22] Así, Pitx2 se propone como el nexo entre las alteraciones de la homeostasis del calcio y las variantes de riesgo en 4q25.

Para probar esta hipótesis (Capítulo IV), se usó un modelo con delección auricular inducible de Pitx2, comparando los WT o NppaCre-Pitx2$^{fl/fl}$, con los que tenían delección en heterocigosis (NppaCre+Pitx2$^{fl/-}$), y los que tenían delección en homocigosis (NppaCre+Pitx2$^{-/-}$) de Pitx2. Los análisis de qRT-PCR de las

principales proteínas implicadas en el manejo del calcio, realizado en AD y AI en los tres tipos de ratones, reveló unos niveles aumentados de SERCA2, CSQ2 and PLB y disminuidos de Cacna1c en AI, mientras que en AD estaban aumentados. De acuerdo con ello, los datos electrofisiológicos mostraron una disminución de I_{Ca} en AI y un incremento del calcio acumulado en el RS en AD y AI. Además se demostró que los niveles de expresión de estas proteínas eran proporcionales al nivel de delección de Pitx2, demostrando un efecto dosis-dependiente.

El uso del modelo de ratón con delección parcial de Pitx2 (Capítulo IV), mostró que la insuficiencia de Pitx2 en heterocigosis (NppaCre+Pitx2$^{fl/-}$) reproducía las alteraciones en la homeostasis del calcio observadas en pacientes con las variantes de riesgo, como fue un mayor contenido de calcio en el RS, mayor frecuencia de sparks, ondas de calcio, I_{TI} y despolarizaciones espontáneas de la membrana. Sin embargo, estos resultados no demuestran que Pitx2 está reducido en humanos portadores de las variantes de riesgo o con AF, y la bibliografía al respecto no es concluyente.[8,23] Sin embargo, las evidencias que muestran que las variantes de riesgo en 4q25 pueden ejercer una modulación en Pitx2c,[24] combinado con los resultados obtenidos en esta tesis, podrían ser la base para estudios que aborden como las variantes de riesgo afectan a la expresión y actividad de Pitx2 en miocitos auriculares humanos.

Por último, en el Capítulo V se estudió si la edad tenía algún efecto sobre el manejo del calcio en miocitos auriculares de pacientes con previa FA. Los resultados mostraron que la edad ejercía un efecto sumatorio al propio producido por la enfermedad, al reducir aún más la I_{Ca} en los pacientes. Al igual que en pacientes sin FA (Capítulo I), el envejecimiento no se asoció a alteraciones en liberación espontánea de calcio, pero se observó un incremento en la amplitud de I_{TI} en los pacientes más mayores, lo que podría traducirse en una mayor probabilidad de que estos I_{TI} se transformaran en despolarizaciones de membrana o potenciales de acción arritmogénicos.[15,25] La acusada disminución en la I_{Ca} en los pacientes más mayores, podría actuar de forma sinérgica con el incremento de la amplitud de I_{TI} perpetuando los episodios arrítmicos.

No se obtuvo ninguna evidencia de que la edad agravase los efectos negativos de las variantes de riesgo en pacientes con o sin fibrilación auricular. Aun así, podría ser relevante tener en cuenta el envejecimiento en la evaluación del potencial impacto arritmogénico de las variantes de riesgo en 4q25, ya que el efecto en la disminución de I_{Ca} podría actuar de forma sinérgica perpetuando episodios arrítmicos iniciados por una mayor frecuencia en la de despolarizaciones de membrana en pacientes con variantes de riesgo.

Para delimitar el contenido de esta tesis, los efectos sobre la homeostasis del calcio han sido considerados en el contexto de potenciales efectos arritmogénicos en relación con FA. Sin embargo, como se menciona en el Capítulo I, el envejecimiento también conlleva un deterioro de la función contráctil de las células auriculares. Uno de los motivos por el que se ha puesto menor énfasis en este aspecto es que una pérdida significativa de la contractilidad auricular tiene un impacto menor en el llenado ventricular en condiciones normales. No obstante, los efectos negativos del envejecimiento sobre la activación de la contracción auricular pueden tener un impacto más fuerte si se producen en pacientes con patologías como la insuficiencia cardiaca, que reduce la contracción ventricular[2] o la hipertrofia ventricular que reduce la elasticidad del ventrículo.

Conclusiones

1. El envejecimiento desempeña un papel a tener en cuenta en la modulación de la homeostasis del calcio en miocitos auriculares humanos. En concreto se asocia a una disminución de la corriente de calcio tipo L, del calcio transitorio celular y del calcio acumulado en el retículo sarcoplásmico, lo que puede favorecer la disfunción contráctil en la aurícula con la edad. Por otro lado, el envejecimiento no altera la liberación espontánea de calcio que podría inducir a despolarizaciones proarrítmicas.

2. El modelo murino de envejecimiento prematuro *Zmpste24*$^{-/-}$ recapitula los efectos descritos en los cardiomiocitos de pacientes envejecidos: disminución (tendencia) de la corriente de calcio tipo L y del calcio transitorio celular, así como reducción en la capacidad de llenado del retículo sarcoplásmico. Además existe una incapacidad para seguir el ritmo de estimulación a frecuencias elevadas.

3. Las variantes de riesgo asociadas a FA del cromosoma 4q25 (particularmente rs2200733T y rs13143308T) provocan alteraciones en la homeostasis del calcio, favoreciendo las liberaciones espontáneas de calcio del retículo sarcoplásmico y las despolarizaciones de membrana (o potenciales de acción espontáneos), que podrían desencadenar fenómenos arrítmicos en las células cardíacas de los pacientes portadores.

4. El modelo murino con delección parcial de Pitx2 (NppaCre^{+}Pitx2$^{fl/-}$) reproduce los resultados observados en pacientes humanos portadores de las variantes de riesgo en el cromosoma 4q25: una mayor frecuencia de liberación espontánea de calcio (sparks, ondas de calcio, calcio transitorio aumentado) y despolarizaciones de membrana espontáneas que pueden causar eventos arrítmicos.

5. Pitx2 altera el manejo del calcio de una manera dosis-dependiente en el modelo murino con delección parcial de Pitx2. Los ratones con delección de

Pitx2 en heterocigosis ($NppaCre^{+}Pitx2^{fl/-}$) reproducen los resultados encontrados en pacientes humanos que tienen las variantes de riesgo en 4q25, sugiriendo una relación entre insuficiencia de Pitx2 y las alteraciones en la homeostasis del calcio observadas en los pacientes con las variantes de riesgo en 4q25, que podrían ser el preludio de padecer fibrilación auricular.

6. El envejecimiento también tiene efecto sobre el manejo del calcio en pacientes con fibrilación auricular, provocando una mayor disminución de corriente de calcio y una mayor amplitud de la corriente (I_{TI}) provocada por la liberación de calcio espontáneo, aumentando la probabilidad de que estos I_{TI} provoquen eventos arrítmicos. Sin embargo, la edad no parece modular el efecto de las variantes de riesgo sobre la homeostasis del calcio.

7. Los dos factores estudiados, envejecimiento y variantes de riesgo en la región cromosómica 4q25, alteran la homeostasis del calcio en miocitos auriculares humanos, haciendo más propenso el padecimiento de enfermedades con trastorno en el ritmo cardíaco como la fibrilación auricular.

ABSTRACT

ABSTRACT

Background

Ageing is a risk factor that promotes common cardiovascular diseases such as atrial fibrillation (AF) or heart failure (HF), which in turn are associated with pathological changes in intracellular calcium homeostasis. However, the effects that ageing could have on the calcium homeostasis in human atrial cardiomyocytes are not well known. Furthermore, genetic risk variants at single nucleotide polymorphisms (SNPs) associated with a higher incidence of AF have been identified in the chromosomal region 4q25, close to the locus of the Pitx2 transcription factor that plays an important role in cardiac embryonic development. In the adult heart AF has been associated with changes in the expression of Pitx2, but findings are contradictory and the relationship between the 4q25 risk variants and Pitx2 function remain controversial. Moreover, no functional effects of the 4q25 risk variants on the calcium homeostasis have been identified so far. Therefore, in this thesis we investigated how the two risk factors, ageing and risk variants at 4q25, affect the intracellular calcium homeostasis with the intention of identifying mechanisms that underlie potentially arrhythmogenic changes in the calcium homeostasis caused by these risk factors.

Hypothesis

Ageing and 4q25 risk variants produce alterations in the intracellular calcium homeostasis in atrial myocytes that alone or in combination contribute to increase the propensity to atrial fibrillation.

Aims of the thesis

- Analyze the effects of ageing on the mechanisms that regulate the calcium homeostasis in human atrial myocytes.
- Use transgenic murine models of ageing to identify molecular mechanisms underlying ageing-dependent changes in the calcium homeostasis.

- Investigate how risk variants on chromosome 4q25 associated with increased AF risk, affect electrophysiological characteristics of human atrial myocytes and to identify underlying molecular mechanisms.
- Investigate how ageing modulates the effects of 4q25 risk variants in human atrial myocytes.

Methods

Experiments were performed on isolated atrial or ventricular cells from human or murine models. Electrophysiological data were obtained using patch-clamp techniques and confocal microscopy. RT-PCR and western blot techniques were used to determine the expression levels of mRNA and the proteins studied.

Results

The results described in this thesis show that aging decreases the amplitude of the calcium current (I_{Ca}), an electrophysiological parameter that is also reduced by AF, the calcium content of the sarcoplasmic reticulum (SR), and the global calcium transient. These findings are corroborated by comparable changes in the expression of the proteins undertaking the corresponding calcium transport or buffering. Together, these changes likely reduce atrial contraction in the elderly. The results were reproduced in an animal model of premature aging (*Zmpste24*$^{-/-}$) with defective lamin processing, reinforcing the notion that this mechanism may, at least partially, underlie the observed effects of aging on the calcium homeostasis in human atrial myocytes. In addition, ageing accentuated some of the effects of ageing on calcium handling in patients with a previous history of AF. Of particular interest, the I_{Ca} amplitude was further depressed by aging in patients with AF, which might contribute to maintain atrial arrhythmic episodes in these patients.

The study of risk variants on chromosome 4q25 shows that the presence of the rs13143308T risk variant, alone or together with the risk variant rs2200733T, was associated with a higher frequency of spontaneous calcium release, transient inward currents (I_{TI}) and membrane depolarizations, typical of AF. These results

are the first to provide an electrophysiological mechanism that could explain a higher incidence of AF in individuals carrying risk variants at 4q25. Moreover, electrophysiological studies in right atrial myocytes from a mouse model with atrial Pitx2 insufficiency ($NppaCre^{+}Pitx2^{fl/-}$) reproduces all alterations in calcium homeostasis observed in patients with 4q25 risk variants. These results support the notion that modulation of the intracellular calcium handling by Pitx2 plays an important role in electrophysiological processes associated with AF.

Analysis of potential synergies between risk variants at 4q25, ageing, and AF revealed that several effects of ageing were accentuated in patients with AF whereas aging *per se* does not modify the effects of the 4q25 risk variants on calcium homeostasis. However, as aging reduces the amplitude of I_{Ca}, which would reduce the atrial refractory period, this could prolong the duration of atrial arrhythmic episodes favored by the higher frequency and amplitude of spontaneous membrane depolarizations in carriers of 4q25 risk variants.

Conclusions

Ageing modulates calcium homeostasis in human atrial myocytes by decreasing I_{Ca}, calcium transient and SR calcium load. These changes are reproduced in a progeric mouse model, favoring a progressive decline of contractile function with age. Moreover, the observed I_{Ca} reduction is a characteristic feature of AF that may favor its maintenance in elder patients.

Risk variants located on the chromosomal region 4q25, specifically the variant rs13143308T, alone or together with rs2200733T, increases spontaneous calcium release, $I_{TI}s$, and membrane depolarizations. These changes are reproduced in a mouse model of Pitx2 insufficiency, and are all hallmarks of AF that could favor the initiation of arrhythmic events in carriers of the risk variants.

The combined effects of 4q25 risk variants and ageing may work synergistically to promote atrial arrhythmia, with the former constituting an arrhythmogenic electrophysiological substrate that favor initiation of atrial arrhythmic episodes, and with ageing favoring their maintenance.

GENERAL INTRODUCTION

GENERAL INTRODUCTION

Cardiac muscle structure and function

Physiology and heart function

The main function of the heart is to supply the body with oxygen and nutrients by pumping blood through the blood vessels. The systemic circulation provides oxygenated blood to all body tissues that are using oxygen and nutrients to function. The pulmonary circulation returns deoxygenated blood from tissues to the lungs so that it can be reoxygenated.

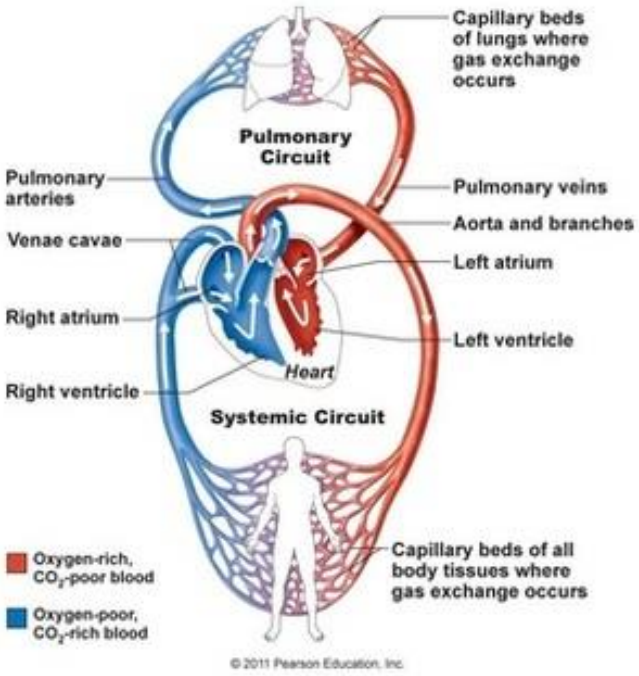

Figure 1. Schematic representation of the circulatory system. Composed by two pumps. On the right side, deoxygenated blood originating from systemic circulation fills the right atrium and is passed through tricuspid valve into right ventricle. From there, blood is directed to pulmonary artery and lungs where exchange of oxygen and carbon dioxide occurs (pulmonary circulation). On the left side, blood rich in oxygen returns to the heart via the pulmonary vein to left atrium and passes to the left ventricle, which pumps the blood to the rest of the body through the aorta (systemic circulation).

Thus, hearts is the pump which maintains both circuits. In humans it is comprised of muscular tissue (myocardium), and, to smaller extent of connective and fibrous tissue (supporting tissue, valves and conduction tissue). It is divided into four chambers. Two are placed on the right side and two on the left side of the heart, and they are separated by the *septum* into two distinctive but functionally and anatomically similar subsystems. The right atrium and the right ventricle pump blood from the systemic veins into pulmonary circulation, and the left atrium and left ventricle, pump blood from the pulmonary circulation into the systemic arteries.

The cardiac cycle

The contraction of the atrial and ventricular chambers occurs in coordinated manner during every heartbeat that is called the cardiac cycle. The cardiac cycle describes the normal rhythmic sequence of contractions of the cardiac chambers, which is coordinated by a series of electrical impulses, produced by specialized heart cells found within the sinoatrial node (SAN) and the atrioventricular node (AVN), the two pacemakers of the cardiac cycle.

The cardiac cycle consists of diastolic and systolic phases. The diastole refers to the period in the cycle where the cardiac chamber is in its relaxed state and is being filled with blood, and the systole refers to the period when contraction occurs and blood is being pumped out of the chamber.

In the course of a typical heartbeat, an electric impulse (action potential or AP) is formed at the junction of the right atrium and the superior vena cava, in the sinoatrial node (SAN) where specialized pacemaker cells are located. The action potential propagates throughout the surrounding cardiac muscle tissue in a synchronized manner; activating the atrial contraction first, and subsequently the atrioventricular node (AVN). The electrical impulse gets delayed at the AVN node before being conducted through the bundles of His and the Purkinje fibers to the apex of the ventricles where it initiates their contraction.

This synchronized contraction of the atria and ventricles allows them to pump blood into the pulmonary and systemic circuits. The amount of blood that needs to be pumped to the body varies greatly, depending on physical activity. Therefore, it is essential that both the cardiac rhythm and contraction are adjusted to meet the physiological needs. The blood supply is adjusted to meet the demand by three mechanisms: 1) Changes in the heart rate, which will change the amount of blood delivered per minute via a change in the number of heart beats per minute. This mechanism is referred to as chronotropy; 2) Adjustments of the stroke volume, which will change the amount of blood that is pumped out of the heart on each beat. This mechanism is referred to as inotropy and 3) Modification of the rate of relaxation that will determine to what extent the heart is relaxed before the next contraction. This mechanism is referred to as lusitropy.

These three mechanisms are regulated by the autonomic nervous system, which modifies the cardiovascular function according to the physiological needs via the sympathetic and parasympathetic nervous system.[26]

Under the influence of the hormone noradrenalin (or norepinephrine), the sympathetic nervous system increases the beating frequency of the sinoatrial node (chronotropic effect). At the same time, noradrenalin increases the permeability of the membranes in cardiac cells for sodium and calcium ions, resulting in increased depolarization of the sinoatrial node and shortening the duration of cardiac cycle. The speed of the electric impulse and the cardiac muscle excitability are increased, leading to stronger contraction of the heart musculature (inotropic effect). The cardiac muscle relaxation phase is also accelerated and muscles recover faster as result of cytosolic calcium re-uptake into the sarcoplasmic reticulum (SR) (lusitropic effect).

Activation of the parasympathetic nervous system leads to acetylcholine production, which has an antagonistic effect to sympathetic nervous system. Acetylcholine increases membrane permeability for potassium ions, which diminishes the depolarization frequency in the SAN and as a result increases the duration of the cardiac cycle. Therefore, the parasympathetic nervous system has

two main effects on the heart muscle: it reduces the frequency of the sinus node and slows the transmission of the cardiac impulse towards the ventricles.

Both the sympathetic and parasympathetic nervous system act simultaneously contributing to modulate the cardiac rhythm and contraction, and variability in cardiac rhythm results from the interaction between these two components of autonomic nervous system.

Cardiac action potential and the ionic currents involved

The cardiac excitation is brought about by the generation of an action potential (AP), which propagates as a wave of depolarization along the cell surface and along the transverse tubules (T-tubules) of the cardiac myocytes and its conduction from cell-to-cell occurs through intercellular gap junctions that allow the heart to function as a syncytium. The AP generation is accomplished through a complex interplay between ionic currents across the cell membrane and the ionic milieu of the cell.[27]

The ionic imbalance across the cell membrane generates a membrane potential (V_m). The V_m influences the conductance of ion channels and transporters and changes in V_m during the AP is the first in a cascade of events, which result in the generation of a Ca^{2+} transient. The V_m of resting myocytes is mainly determined by the K^+ ions, which tend to flow out of the cell due to their concentration gradient, generating a lack of positive charges inside the cell, leading to a negative potential inside the cell at rest. The Na^+/K^+-ATPase, pumping Na^+ out and K^+ into the cell, generates the ionic concentration gradients for Na^+ and K^+, but K^+-channels dictate the negative resting V_m in myocytes because of the higher K^+-conductance in resting cells.

Table 1. Transmembrane ionic gradients (mM)

	Intracellular	Extracellular
Na^+	5-15	145
K^+	140	5
Mg^{++}	30	1-2
Ca^{++}	<0.0001 free	2-5
Cl^-	4	110

For a single cardiac cell, the following equation relates the transmembrane potential (V_m) to the total transmembrane ionic current (I_{ion})

$$dV_m/dt = - 1 / C_m \cdot I_{ion} \qquad (1)$$

where C_m is the membrane capacitance (1 µF/cm2) provided by the charge separation across the lipid bilayer of the cell membrane. [28,29]

Equation 1 simply states that changes in V_m occur due to displacement of charge on the membrane capacitance by the movement of ions across the cell membrane. This movement occurs via voltage-gated ion channels, pumps, and exchangers, and I_{ion} represents their sum.[27] Note that a negative I_{ion} (inward flow of positive ions into the cell) produces a positive dV_m/dt, which elevates (depolarizes) the membrane potential. A positive I_{ion} indicates an outward flow of positive ions and acts to reduce (repolarize) the membrane potential by generating a negative dV_m/dt.

The AP is activated when Na^+ and Ca^{2+}-channels open, causing depolarization of the membrane potential. The AP has different shapes depending on the region of the heart (see Figure 2).

The normal heartbeat initiates in the sino-atrial (SA) nodal cells that normally have the fastest intrinsic pacemaker activity. The maximum diastolic

polarization in these cells is typically about –50 to –60 mV and a gradual pacemaker depolarization leads to an AP with a slow rate of rise and consequently a slow rate of local propagation. Na^+ channels are almost entirely inactivated and do not participate in the rapid depolarization phase (in these cells Ca^{2+} channels serve this role).

In atrial and ventricular muscle cells the resting V_m is near –80 mV and the AP has a very fast upstroke attributable to the Na^+ current, and overshoots 0 mV to reach a peak at +30-50 mV. Repolarization is much faster in atria than in ventricular myocytes and Purkinje fibers. In ventricular cells there is a more prominent action potential plateau. Moreover, the ventricular AP duration (APD) is shortest in epicardial cells, longer in endocardial cells and longest in mid-myocardial cells (reflecting in part differential ion channel expression). The long APD in ventricular myocytes serves two functions. First, it prevents electrical re-excitation, by keeping the membrane depolarized (and thus Na^+ and Ca^{2+} channels inactivated). This inhibits aberrant conduction pathway development. Second, it allows contraction to relax before the next excitation can occur.

From the SA-node the electrical wave passes to atrial muscle (fast propagation 0.1-1 m/s) and the AV node, where conduction slows again progressively from atrial end (AN) to the central node region (0.01-0.05 m/sec), before slightly speeding through the last part of the node (NH). As the wave gets through the His bundle, bundle branches and Purkinje fibers, propagation becomes very rapid (2-4 m/sec) and it remains very fast through ventricular muscle (0.3-1 m/sec).

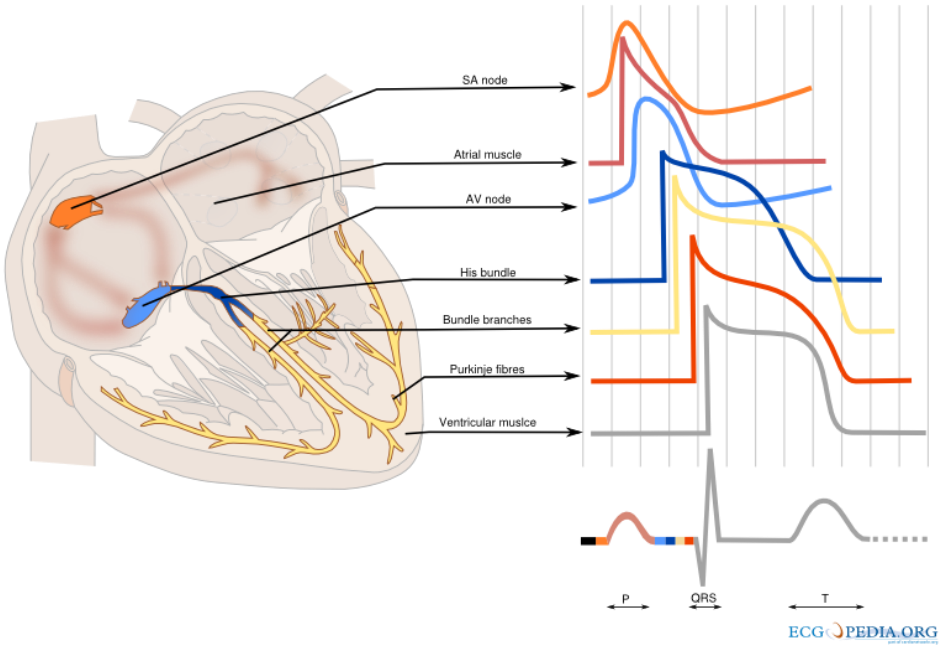

Figure 2. Action potential regional variation and morphology. The APs at right are representative of the different shapes typically observed for the cardiac regions indicated. The position along the time axis for AP upstrokes reflects the different delays from SA node firing. For example, the delay between atrial and Purkinje fiber firing reflects slow transmission through the AV node (and the P-R interval in the ECG). Atrial and ventricular myocyte AP upstrokes are responsible for the P wave and QRS complex in the ECG.

In detail the action potential can be divided into five phases (for ventricular cells):

- Phase 0 - Rapid Depolarization: rapid depolarization is started once the membrane potential reaches a certain threshold (about -70 to -60 mV). This produces activation of sodium channels and a rapid influx of Na^+ and a corresponding rapid upstroke of the action potential (see Figure 3). At higher potentials (-40 to -30) Ca^{2+} influx participates in the upstroke. In the sinus node and AV node a slower upstroke can be observed. This is because Na^+-channels are inactivated during the slow initial depolarization and the subsequent rapid depolarization is mainly mediated by the slower activating Ca^{2+} -channels.
- Phase 1- Early Rapid Repolarization: immediately following rapid depolarization, the inactivation of the Na^+ channel (I_{Na}) and subsequent

activation of the outward K^+ channel (I_{to}) and the Na^+/Ca^{2+} exchanger ($I_{Na,Ca}$), which exchanges 3 Na^+ for 1 Ca^{2+}, produces an early rapid repolarization. Due to the limited role of the Na^+ channel in the upstroke of sinus node and AV node cells and the subsequent slower depolarization, this rapid repolarization is not visible in their action potentials.

- Phase 2 – Plateau: the plateau phase represents an equal influx and efflux of ions, producing a stable membrane potential. This plateau phase is predominantly observed in the ventricular action potential. The inward movement of Ca^{2+} through the open L-type Ca^{2+} channels ($I_{Ca\text{-}L}$) and the exchange of external Na^+ for internal Ca^{2+} by the Na^+/Ca^{2+} exchanger ($I_{Na,Ca}$) are responsible for the influx of ions during the plateau phase. The efflux of ions is the result of outward currents carrying K^+ (I_{Kur} and $_{Ks}$).
- Phase 3 - Final Rapid Repolarization: final repolarization is mainly caused by inactivation of Ca^{2+} channels, reducing the influx of positive ions. Furthermore repolarizing K^+ currents (delayed rectifier current I_{Ks} and I_{Kr} and inwardly rectifying current I_{K1}) are activated which increases the efflux of positive K^+ ions. This results in a repolarization to the resting membrane potential.
- Phase 4 - Resting membrane potential: during phase 4 of the action potential, intracellular and extracellular ion concentrations are restored. Depending on cell type the resting membrane potential is between -50 to -95 mV. Sinus node and AV nodal cells have a higher resting membrane potential (-50 to -60 mV and -60 to -70 respectively) in comparison with atrial and ventricular cardiomyocytes (-80 to -90 mV). Sinus node cells and AV nodal cells (and to a lesser degree Purkinje fibers cells) have a special voltage dependent channel I_f, the funny current. Furthermore they lack I_{K1}, a K^+ ion channel that maintains the resting membrane potential in atrial and ventricular tissue. The I_f channel causes a slow depolarization in diastole, called the phase 4 diastolic depolarization, which results in normal automaticity. The frequency of the sinus node discharges are regulated by the autonomous nerve system and due to the relative high firing frequency

(60-80 beats per minute) the sinus node dominates other potential pacemaker sites.

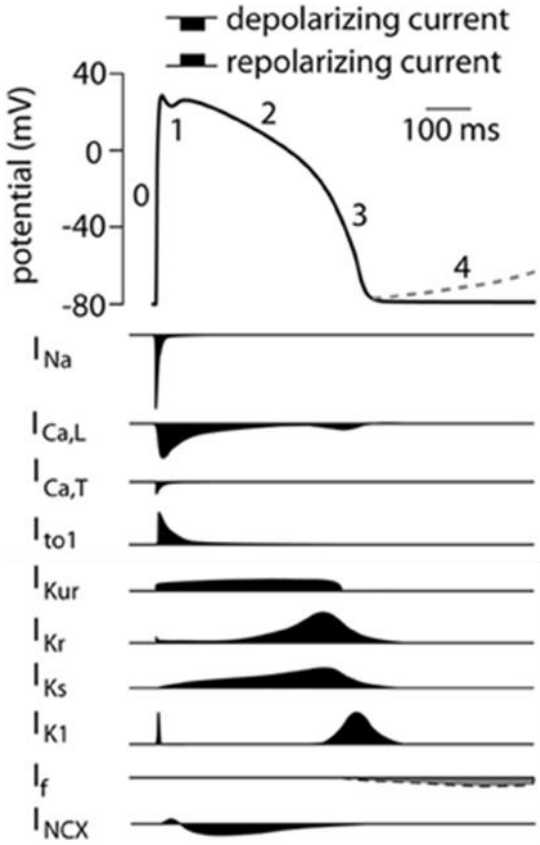

Figure 3. Atrial and ventricular action potential (AP) and the ionic currents involved. Numbers denote the different phases of the ventricular action potential. The dashed line represents phase 4 depolarization normally present in cells from the conduction system. Depolarizing, inward and repolarizing, outward currents that underlie the atrial and ventricular action potential are depicted below. Inward currents: I_{Na} sodium current; $I_{Ca,L}$ L-type calcium current; I_{to} transient outward current; I_{Kur} ultra rapidly activating delayed rectifier current; I_{Kr} and I_{Ks} rapidly and slowly activating delayed rectifier current; I_{K1} inward rectifier current. Phase 0, rapid depolarization; phase 1, rapid early repolarization phase; phase 2, slow repolarization phase ('plateau' phase); phase 3, rapid late repolarization phase; phase 4, resting membrane potential. Adapted from Front. Physiol., 31 August 2012.[30]

Cardiac myocyte

The basic work units of the myocardium are the cardiac myocytes (cardiac muscle cells o cardiomyocytes), which are organized in muscle fibers (myofiber). The myocytes have a cylindrical shape with a length ranging from 50 to 120 μm and a diameter between 5 and 25 μm. The cell's interior is surrounded by the cell membrane. The intracellular space of cardiac myocytes consists mainly of the nucleus, mitochondria, the sarcoplasmic reticulum, and protein networks of the contractile elements. Below, we specify the cellular structures involved in the contractile process, commonly referred to as excitation-contraction coupling (E-C coupling).

Myofilaments

The myofilaments occupy 45-60% of the cell volume in mammalian ventricular myocytes. This fraction is larger in skeletal muscle and smaller in atrial cells and cells specialized for electrical conduction (Purkinje fibers). The myofilaments are the contractile machinery of the cell and represent the end effector responsible for transducing chemical energy into mechanical energy and work. The sarcomere is the fundamental contractile unit in striated muscle and is bounded by the Z-line (Figure 4).

Myofilaments are composed of the thick (myosin) and thin (actin) filaments as well as associated contractile and cytoskeletal components. The I band of the myofilament is composed of the actin fibers. The A band contains myosin fibers, thicker than the actin fibers. During the muscle contraction, both fibers overlap in the A band zone.

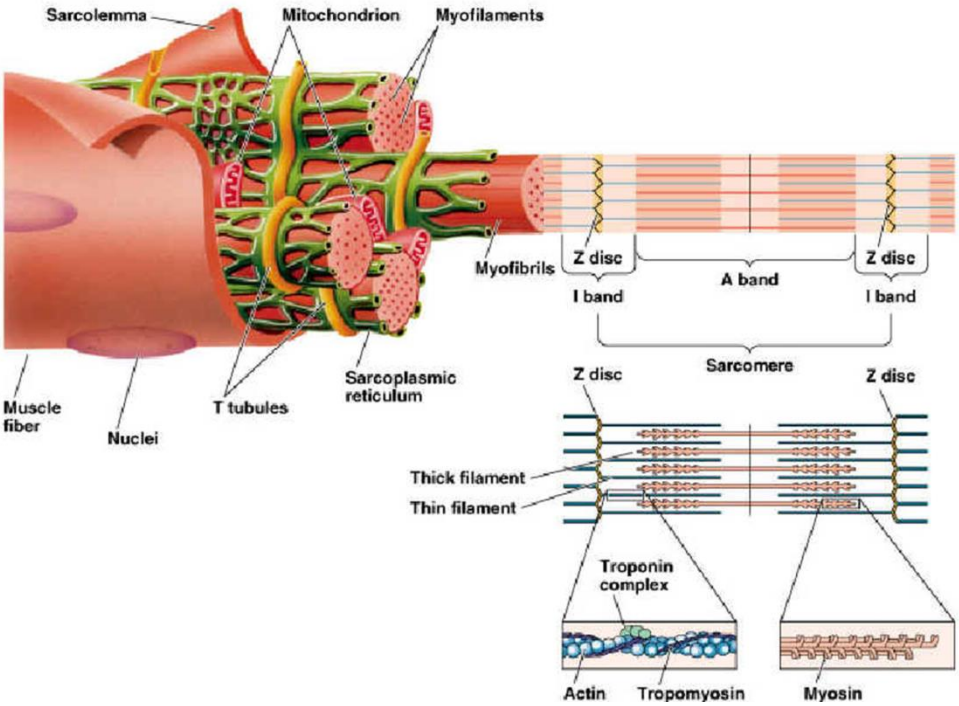

Figure 4. Organization of the cardiac myofilament structures.

Each thick filament is composed of ~300 myosin molecules. The myosin molecule is hexameric, composed of two heavy chains with their tails coiled around each other and two myosin light chains per heavy chain. Each myosin heavy chain (MW ~450,000) has a long (~130 nm) α-helical tail and a globular head (Figure 5). The tails of the myosin heavy chain form the main axis of the thick filament. The heads form the crossbridges to actin on the thin filaments and contain the site of ATP hydrolysis.

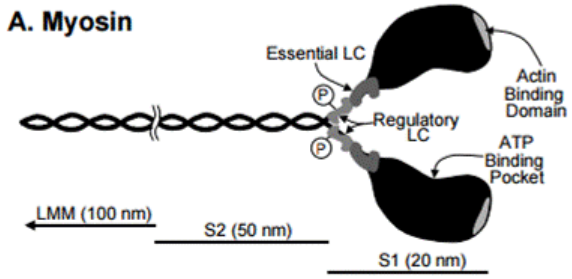

Figure 5. The myosin molecule. The myosin molecule is 170 nm in length with two globular heads (S1) and tails (including LMN and S2). The two light chains (LC) are located on the neck.

The backbone of the thin filament is composed of two chains of the globular protein G-actin, which form a helical doublestranded F-actin polymer.

Tropomyosin (Tm) is a long flexible protein which lies in the groove between the actin strands and spans about 7 actin monomers (Figure 6). Tropomyosin is also double-stranded and mostly α-helical (coiled coil) and the two strands may be connected by a disulfide bridge. The carboxy end also overlaps the amino end of the next tropomyosin. At every seventh actin there is a troponin complex attached to tropomyosin. The troponin complex is made up of three subunits:

- troponin T (TnT, or the tropomyosin binding subunit),
- troponin C (TnC, or the Ca^{2+} binding subunit), and
- troponin I (TnI, or the inhibitory subunit, which also binds to actin)

In the resting state (low $[Ca^{2+}]_i$) TnI binds specifically to actin, and this prevent the myosin head from interacting with actin.

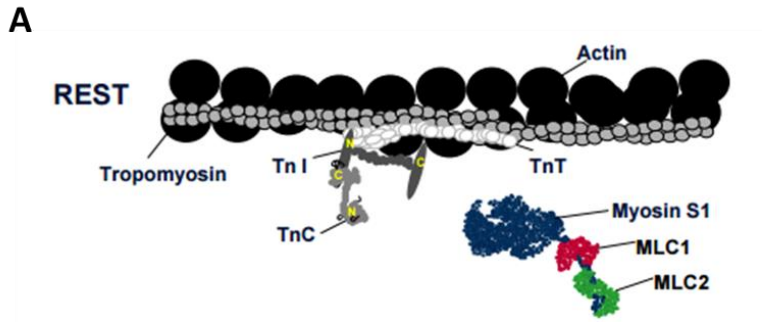

It is well established that the rise in cytoplasmic $[Ca^{2+}]$ is the event which activates the myofilaments. When Ca^{2+} binds to TnC, TnC binds to TnI, causing TnI dissociation from actin. This change in TnC-TnI interaction is sensed by TnT and causes movement of tropomyosin to allow myosin to interact with actin.

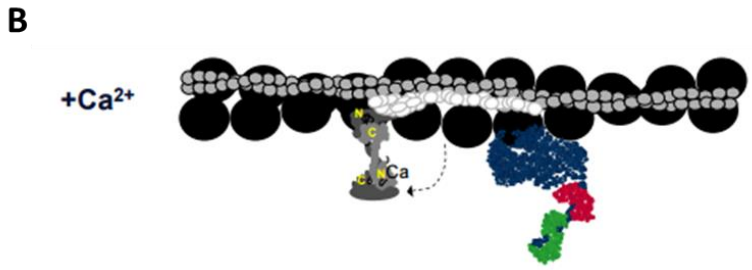

Figure 6. Acto-myosin interaction in cardiac muscle. (A) At rest TnI is bound to actin, thereby anchoring the TnT-tropomyosin complex and prevent the myosin head (S1) from binding to actin.

(B) When Ca binds to TnC, this region binds strongly to TnI, which comes off actin, allowing the TnT-tropomyosin complex to roll deeper into the actin groove and interact with the myosin S1 head.

In the presence of sufficient Ca^{2+}, myosin can interact with actin, which greatly increases the ability of myosin ATPase to hydrolyze ATP and also allows transformation of chemical energy stored in ATP to mechanical energy and work.[31]

Cardiac myofilaments are activated by calcium in a graded manner, so the relationship between the free [Ca^{2+}] and force development is of fundamental importance.

Sarcolemma and Transverse Tubules

The sarcolemma at the cell surface is physically continuous with the membrane of the T-tubules (invaginations of the surface membrane that occur at the Z-lines) and the two combine to form the permeability barrier between the inside of the cell and the extracellular medium. Mammalian ventricular cells contains a clear T-tubular network, but in mammalian atrium this network is not well defined, and atrial myocytes do not possess an extensive T-tubule system or have only a sparse system. The same it has been reported for human atrial cells.[9,32–34]

The ultrastructural organization of the cardiac sarcolemma is important for several reasons. First, it is the site at which Ca^{2+} enters (and leaves) the cell, so the localization of the relevant transport systems is of functional importance. This is particularly important because there is a differential distribution of ion channels, pumps and other membrane specializations.

A major structural specialization of the sarcolemma is its coupling with the SR. In cardiac muscle these junctions are apparent as dyads or triads (coupling of sarcolemma and SR or sarcolemma-SR-sarcolemma) and can occur either at the cell surface or within the T-tubular membrane. The sarcolemma also exhibits caveolae, which are flask-shaped invaginations (50-80 nm in diameter), that

contribute significantly (~10%) to the surface area of both surface and T-tubular sarcolemma.[35,36]

The other major specialization of the sarcolemma is the region where cells are closely apposed end to end, where there are specialized structures for cells connection: i) the gap junction, ii) the fascia adherens or intermediate junction and iii) the macula adherens or desmosome.

Sarcoplasmic reticulum

The SR is an entirely intracellular, membrane-bound compartment, which is not continuous with the sarcolemma. The main function of this organelle in muscle appears to be sequestration and release of Ca^{2+} to the myoplasm via the SR Ca^{2+}-ATPase pump protein and the SR calcium release channel (or ryanodine receptor) respectively. The junctions of the SR with the sarcolemma (surface or T-tubule) are highly specialized and feature bridging structures or proteins that have been called "feet", and are also known as pillars, spanning proteins, bridges and junctional feet.

Based on their distinctive morphology and high affinity for the neutral plant alkaloid, ryanodine, feet were purified and identified as the SR Ca-release channel in skeletal [37,38] and cardiac muscle. [38,39] This ryanodine receptor is a large protein (560 kDa for the monomer) organized in the feet structure in a distinct pattern on the SR underneath the T-tubular membrane and is matched by an organized array of particles in the T-tubular membrane, which are likely to be the sarcolemmal Ca^{2+} channel protein (or DHPR). This arrangement is consistent with a stoichiometry of 1 ryanodine receptor tetramer (RyR) to 2 DHPR as measured in skeletal muscle, whereas in mammalian ventricle the RyR:DHPR ratio is 4-10, depending on species.[31]

Excitation – Contraction coupling and the Ca^{2+} cycle in a cardiac myocyte

Cardiac excitation–contraction coupling (E-C coupling) and relaxation is the physiological basis for the heartbeat, and refers to the mechanisms linking the electrical excitation of the myocyte to the contraction of the heart.[3] In this process, calcium is the secondary messenger essential in cardiac electrical activity and the direct activator of the myofilaments that cause a coordinated contraction of the cardiomyocytes in the atria and ventricles, resulting in the ejection of blood from these chambers.

General scheme of the Ca^{2+} cycle in a cardiac myocyte

During the E-C coupling the cardiac action potential triggers the Ca^{2+} transient, which rapidly rises and decays with each cardiac cycle. This process involves the interaction of a number of cellular proteins to regulate the cytosolic calcium level.[40] A general scheme of E-C coupling (see Figure 7) has been proposed since the work of Ringer,[41] who first suggested a role for Ca^{2+} as activator of cardiac contraction base on the observation that hearts placed in a calcium-free solution ceased to beat. It was proposed by Fabiato[42] that the transsarcolemmal Ca^{2+} influx triggers the release of a greater quantity of Ca^{2+} from the sarcoplasmic reticulum (SR), a process called as calcium-induced calcium release (CICR). Despite the fact that the magnitude of Ca^{2+} influx across the SL is variable amongst mammalian species, most studies indicate that this is inadequate in magnitude to support contraction, and therefore, that Ca^{2+} released from the SR is the major source of Ca^{2+} for contraction in the mammalian heart. Data suggest that 70% to 90% of the Ca^{2+} that activates the myofilaments is from SR release, and the remaining 10% to 30% is derived from Ca^{2+} influx during the cardiac action potential.[31] In this way, transsarcolemmal Ca^{2+} influx and SR Ca^{2+} release play dominant roles in the rise of $[Ca^{2+}]i$ which activates contraction in the heart.

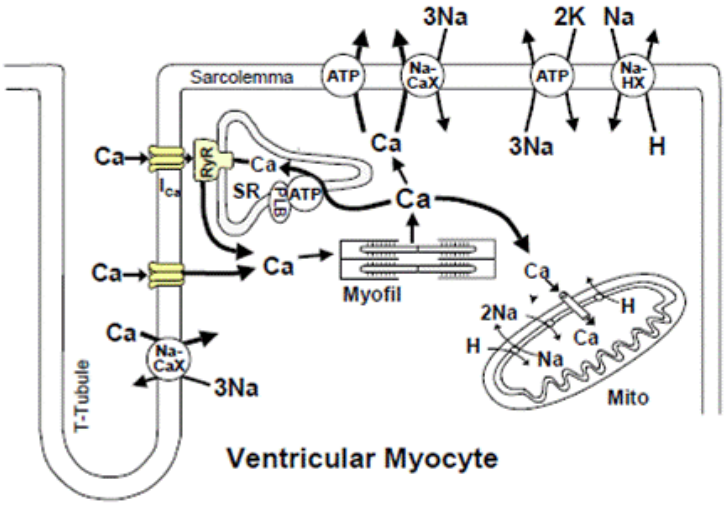

Figure 7. Ca^{2+} transport and requirements for activation of myofilament force. Schematic diagram of cellular Ca^{2+} fluxes. From Donald M. Bers, 'Cardiac fluxes involved in control of cardiac myocyte contraction', 2000.[43]

During the cardiac action potential, Ca^{2+} enters the cell through depolarization-activated Ca^{2+} channels as an inward Ca^{2+} current (I_{Ca}), which contributes to the action potential plateau. This Ca^{2+} contributes directly to the activation of the myofilaments, and it also activates Ca^{2+} release from the SR (calcium induce-calcium release or CICR process). Moreover, a direct electro-mechanical coupling between the sarcolemmal calcium channel protein and the RyR2 may facilitate this process.[44–46] The combination of Ca^{2+} influx and release raises the free intracellular Ca^{2+} concentration ($[Ca^{2+}]_i$), allowing Ca^{2+} to bind to the myofilament protein troponin C, which then switches on the contractile machinery. The degree of contractile activation depends on how much Ca^{2+} is delivered to the myofilaments.

For relaxation to occur, Ca^{2+} must be removed from the cytoplasm, lowering $[Ca^{2+}]_i$ such that Ca^{2+} will dissociate from TnC. Four Ca^{2+} transport processes may be involved in removing Ca^{2+} from the cytoplasm:[47]

1) Ca^{2+} is pumped into the SR by the SR Ca- ATPase pump,

2) Ca^{2+} is pumped out of the cell by the sarcolemmal Ca-ATPase pump,

3) Ca^{2+} is transported out of the cell by the sarcolemmal Na^+/Ca^{2+} exchange or

4) Ca^{2+} is transported into mitochondria via the Ca^{2+} uniporter.

These four calcium transport systems are all in direct competition for cytoplasmic Ca^{2+}. The Ca^{2+} affinities and capacities of each system determine its contribution to the elimination of Ca^{2+} from the cytosol. Table 2 summarizes the relative contribution of each mechanism in rabbit ventricle.

Table 2. Contribution of different Ca transporters to relaxation in rabbit ventricular myocytes.

Transporter	Percent of Ca removal Flux
SL-Ca^{2+}-Pump	0.86 %
Mito. Ca uniport	0.62%
Na^{+}/Ca^{2+} Exchange	30%
SR-Ca^{2+}-Pump	68.5%
All 4 systems	100%

SL is sarcolemmal, Mito is mitochondrial. Table modified from Donald M. Bers, 'Excitation-Contraction Coupling and Cardiac Contractile Force', 2008.[31]

Regulation of the E-C coupling

The cardiac myocyte excitation-contraction coupling is complex process with many regulatory mechanisms involved that interact simultaneously to form varied, but well-tuned, effects that are essential to contractile regulation. Thus, the EC coupling is regulated by signaling cascades operating inside the cardiac myocytes in order to maintain Ca^{2+} homeostasis on a beat-to-beat basis, and in order to continuously adjust to meet the requirements of the body for blood supply to the metabolizing tissues. The autonomic nervous system pays a key role in these processes.

Sources of calcium

There are two main sources of Ca^{2+} involved in the normal activation of cardiac muscle contraction: Ca^{2+} influx from the extracellular space through the voltage-activated L-type calcium channels (LTCCs), followed by further release

from the SR through the SR calcium release channels (ryanodine receptors; RyRs), respectively. Both sarcolemmal Ca^{2+} influx and SR Ca^{2+} release are important elements in E-C coupling and Ca^{2+} from both sources can contribute to the activation of contraction.

Ca^{2+} influx via sarcolemmal Ca^{2+} channels

Since the time of Ringer (1883) it has been known that extracellular [Ca^{2+}] is important in cardiac muscle contraction. The Ca^{2+} current carrying Ca2+ into the myocyte across the sarcolemma was characterized as and inward current.[48,49] There are two types of Ca^{2+} channels in cardiac myocytes (L- and T-type).[31] L-type Ca^{2+} channels are characterized by a large conductance, long lasting openings, sensitivity to 1,4-dihydropyridines (DHPs) and activation at larger depolarizations (i.e. at more positive V_m). T-type channels are characterized by a tiny conductance, transient openings, insensitivity to DHPs, and activation at more negative V_m. The T-type Ca^{2+} channels are low-voltage-activated (LVA) type, while all of the other types (L and other located in neurons and neuroendocrine cells) are referred to as high-voltage-activated (HVA). Both $I_{Ca,L}$ and $I_{Ca,T}$ activate rapidly upon depolarization (though not as strong as I_{Na}) and both show inactivation (not as fast as I_{Na}).

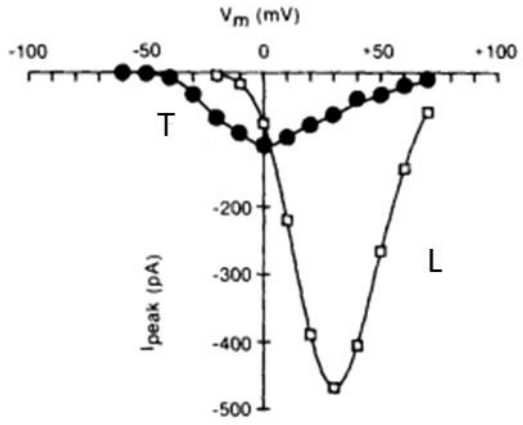

Figure 8. Voltage-dependence of whole cell L- and T-type Ca channel currents. Ba currents (115 mM Ba) induced by V_m steps to test potentials from holding potentials, in dog atrium cells (modified from Donald M. Bers, 'Excitation-Contraction Coupling and Cardiac Contractile Force', 2008.[31]).

$I_{Ca,L}$, the dominant I_{Ca}, is ubiquitous in cardiac myocytes, whereas cardiac $I_{Ca,T}$ was first described in atrial cells[50] and later in canine cardiac Purkinje cells.[51] T-type current is typically small or absent in ventricular myocytes. The relative prominence of $I_{Ca,T}$ in pacemaker and conducting cells, and its activation at V_m in the pacemaker range has led to suggestions and evidence for a role of $I_{Ca,T}$ in atrial pacemaking.[52,53] Because $I_{Ca,T}$ is relatively small and inactivates very rapidly the total amount of Ca^{2+} flux via $I_{Ca,T}$ is small compared to that carried by $I_{Ca,L}$ and negligible in most ventricular myocytes. This may reflect different functional roles, where $I_{Ca,L}$ is more involved in triggering SR Ca^{2+} release and refilling SR Ca stores (see below), rather than in pacemaking.

$I_{Ca,L}$ inactivation is slower than $I_{Ca,T}$ and is both V_m- and Ca^{2+}-dependent. The intrinsic V_m-dependent inactivation is relatively slow, so that with Ca^{2+} influx and SR Ca^{2+} release most of the inactivation is Ca^{2+}-dependent. Indeed, with larger amplitude Ca^{2+} transients and I_{Ca} the inactivation is greatly accelerated. This creates a negative feedback, such that when Ca^{2+} entry and release are large, less total Ca^{2+} entry occurs during the AP.[54] $I_{Ca,L}$ contributes an inward depolarizing current to the cardiac AP. It may not contribute much to the very rapid rising AP phase in myocytes (dictated by I_{Na}), but is the key depolarizing current responsible for the slower rising AP in SA and AV node cells, and it contributes to sustain the plateau phase of the AP. I_{Ca} is also stimulated by PKA, which increases both its amplitude and inactivation rate.[55–57]

SR calcium release through the ryanodine receptor

The Ryanodine receptors are homotetrameric proteins, with each of the 4 subunits having a molecular weight of ~ 560kDa. The Ryanodine receptor family consists of three different isoforms: the skeletal muscle isoform, Ryanodine Receptor type 1 (RyR1); the cardiac muscle isoform, Ryanodine Receptor type 2 (RyR2, also expressed in the brain) and the brain isoform, Ryanodine Receptor type 3 (RyR3).[3]

The cardiac ryanodine receptor (RyR2) is the sarcoplasmic reticulum (SR) Ca^{2+}-release channel, which is centrally involved in the myocyte excitation-

contraction (E-C) coupling process. RyR2 calcium release occurs at junctions between the sarcolemmal and SR membranes, where clusters of RyRs are located (it is estimated that between 10 and 300 RyRs can form a given cluster). These physical junctions are called dyads, and they occur both at the cellular and t-tubular surface. The dyadic microdomain serves to regulate cardiac contractility and signaling. Dyadic Ca^{2+} levels are additionally controlled by influx of Ca^{2+} via L-type calcium channels and removal of Ca^{2+} by the nearby Na^{+}-Ca^{2+} exchanger (NCX).

Since the RyR2 open probability is increased by the cytoplasmic Ca2+ concentration the open probability will be low under resting conditions. It is not, however, zero as shown by the occurrence of Ca2+ “sparks” at rest.58 Thus, the ryanodine receptor also releases Ca2+ during the relaxation phase of the cardiac cycle, giving rise to a diastolic Ca2+ leak. In normal physiological conditions, diastolic Ca2+ leak regulates the proper level of luminal Ca2+ in the SR. Thus, the open probability of the RyR2 is not solely controlled by [Ca2+]i but also by the luminal SR Ca2+ level. Moreover, the RyR2 can be phosphorylated at several sites, and this also affects its opening. In pathological conditions excessive diastolic Ca2+ leak in the form of Ca2+ sparks or waves, caused by elevated luminal calcium levels and/or RyR2 phosphorylation, contribute to the generation of both, acquired and hereditary arrhythmias.[59–62]

While the RyR serves as the SR Ca^{2+} release channel, it is also a scaffolding protein that strategically anchors numerous regulatory proteins to the junctional complex (the critical site where E-C coupling occurs). These regulatory proteins include CaM, Ca-calmodulin dependent protein kinase II (CaMKII), cAMP-dependent protein kinase (PKA, anchored via mAKAP), phosphatase 1 (PP1 anchored via spinophilin), phosphatase 2A (PP2A anchored via PR130), FK-506 binding protein, sorcin, calsequestrin, junctin, triadin, and homer. All of these proteins are anchored to RyR to form a macromolecular complex, and some of them modulate the function of the RyR itself in a highly locally manner.[63]

Calcium removal

The amount of Ca^{2+} which enters the myocyte at each steady state twitch must also be extruded from the cell; otherwise the cell would be gaining or losing Ca^{2+}. There are 3 Ca^{2+} removal systems: the SR Ca-ATPase, the Na^{+}/Ca^{2+} exchange, and the slow systems, that include Ca^{2+} transport by the sarcolemmal Ca-ATPase and the mitochondrial uniporter. Each of these transport systems competes for Ca^{2+} within the cytosol, and the amount of Ca^{2+} gained or lost during cardiac Ca^{2+}-cycling depends upon which of the fluxes is dominant relative to the others.

SR Calcium ATPase

In mammals, three genes (human nomenclature ATP2A1-3) encode three main SERCA proteins. Each of the three transcripts undergoes tissue-dependent alternative splicing. The changes in the expression pattern of the variants during development and tissue differentiation indicate that each isoform is adapted to specific functions. SERCA1a and SERCA1b variants are expressed in adult and neonatal fast-twitch skeletal muscles, respectively. The SERCA2a variant is selectively expressed in heart and slow-twitch skeletal muscles, whereas the SERCA2b variant is expressed nearly ubiquitously and is thus considered the housekeeping isoform. SERCA3 is expressed in a limited number of non muscle cells.[64]

Cardiac SR Calcium ATPases are a key factor in the regulation of intracellular Ca^{2+}. Their main role is to remove cytoplasmic Ca^{2+} ions in order to promote muscle relaxation. They have high affinity for Ca^{2+} and can efficiently regulate it down to very low concentration levels. They are known to transport two Ca^{2+} molecules per hydrolysis of one ATP.

The SR Calcium ATPase recycles released Ca^{2+} back into the SR, which helps maintain low cytosolic resting $[Ca^{2+}]$ (around 100nM) and a high SR Ca^{2+} content (around 1 mM). Thus, there is a large Ca^{2+} gradient from the SR to the cytosol, which is essential for enabling rapid release, but which also results in a constant leak of Ca^{2+} from the SR via the RyRs.

The activity of SERCA depends on various factors: (1) the cytoplasmic Ca^{2+} concentration: the higher this is the greater is the activity of SERCA; (2) the SR Ca^{2+} content: an increase of SR Ca^{2+} increases the gradient against which SERCA must pump and therefore slows its rate. The activity of the SERCA pump is also controlled by the natural inhibitory protein phospholamban (PLB), which is a small transmembrane protein associated with SERCA. Depending on its phosphorylation state, PLB binds to and regulates the activity of SERCA2a. In its dephosphorylated state, PLB binds to SERCA2a at resting Ca^{2+} concentrations and inhibits the Ca^{2+} pump activity. Phosphorylation of PLB alters the PLB–SERCA2a interaction, relieving the Ca^{2+}-pump inhibition and thus enhancing relaxation rates (lusitropic effects) and contractility (ionotropic effects)[65]. Phosphorylation of the hydrophilic portion of PLB by protein kinase A (PKA) at S16 and/or by calmodulin-dependent kinase II, CaMKII on T17 is presumed to detach PLB from the pump, increasing its affinity for cytosolic Ca^{2+} and reactivating Ca^{2+} uptake.[64]

Within the SR exists a Ca^{2+}-binding protein, calsequestrin, which plays a major role in regulating the activity of the Ca^{2+} release channel and E-C coupling. Calsequestrin is the major Ca^{2+}-binding protein in the SR lumen, serving as the Ca^{2+} store of skeletal and cardiac muscle fibers. This regulation of SR calcium loading is thought to regulate the amplitude and rate of Ca^{2+} release from the SR, and thus to optimize Ca^{2+} release while conserving Ca^{2+} within the store. Other potential roles for calsequestrin within the SR lumen that have been suggested include phosphorylation (indicated by its kinase activity), oxidative protein folding (indicated by its thioredoxin structure), and communication of store Ca^{2+} concentrations to store operated Ca^{2+} channels during store operated Ca^{2+} entry.[66]

Na^+/Ca^{2+} exchange (NCX)

The cardiac Na^+/Ca^{2+} exchanger (NCX-1) is the Ca^{2+} transporter in the heart that is largely responsible for extruding the Ca^{2+} that enters via I_{Ca}. The NCX stoichiometry is 3 Na^+:1 Ca^{2+}, such that the NCX transporter is electrogenic (the extrusion of 1 Ca^{2+} is coupled to inward flux of 3 Na^+ and one net charge) and carries a net ionic current (I_{NCX}). I_{NCX} is reversible, and its direction and amplitude

are controlled by the [Na^+] and the [Ca^{2+}] on both sides of the membrane as well as by V_m. At rest V_m is negative to E_{NCX} (typically −50 mV), such that Ca^{2+} extrusion is favored thermodynamically, even though the low $[Ca^{2+}]_i$ limits the absolute rate of Ca extrusion and diastolic inward I_{NCX}. During the AP upstroke, V_m passes E_{NCX} so that Ca^{2+} influx and outward I_{NCX} are favored and can occur briefly.[67] However, this period is very short-lived because as soon as $I_{Ca,L}$ is activated and SR Ca^{2+} release ensues, the very high local $[Ca^{2+}]_i$ near the membrane drives E_{NCX} back above V_m such that I_{NCX} becomes inward and extrudes Ca^{2+} again. Notably, the higher the Ca^{2+} transient is and the further repolarization proceeds, the greater the inward current. Thus, I_{NCX} is an inward current throughout most of the AP under normal conditions, driven by $[Ca]_i$ but tempered by the positive V_m during the AP. However, if I_{Ca} and CICR does not occur in a certain cellular region, Ca^{2+} entry and outward I_{NCX} can continue.[68]

Slower systems: Sarcolemmal Ca^{2+} ATPase and Mitochondria

During relaxation of the Ca^{2+} transient there is a dynamic competition among Na^+/Ca^{2+} exchange, SR Ca^{2+}-pump, sarcolemmal (or plasmalemmal) Ca^{2+}-pump and the mitochondrial Ca^{2+} uniporter. It is well known that the SR Ca^{2+}-pump is the dominant sink of calcium in the cytosol (see Table 2), and the Plasmalemmal Ca^{2+} -ATPase (PMCA) and mitochondria are the slower components.

The plasmalemmal Ca^{2+}-ATPase is involved in Ca^{2+} handling and in the regulation of intracellular signaling pathways in the heart. PMCA is a high-affinity, low-capacity enzyme transporting Ca^{2+} out of the cells in exchange for protons. There are four isoforms of PMCA (PMCA1–4). PMCA1, PMCA4, and, to a lesser extent, PMCA2 were detected in the heart muscle. Since PMCA exhibits high affinity for Ca^{2+} and low transport velocity, it has been proposed to be engaged primarily in subtle regulations of the diastolic $[Ca^{2+}]_i$, while its contribution to outward Ca^{2+} transport has been thought to be of minor importance. However, experiments with a specific PMCA blocker, suggest that PMCA is important not only for the control of the diastolic Ca^{2+} concentration but may also contribute significantly to relaxation in ferret, rabbit, rat, guinea-pig, and sheep ventricular myocytes. PMCA may also

affect sarcoplasmic reticulum (SR) Ca^{2+} content and amplitude of Ca^{2+} transients in rat, ferret, and guinea-pig ventricular myocytes.[69]

The mitochondria are the site of oxidative phosphorylation and the tricarboxylic cycle for energy supplied by aerobic metabolism. Mitochondrial Ca^{2+} plays only a very minor quantitative role in Ca^{2+} fluxes associated with E-C coupling, but may still be important with respect to mitochondrial function and energetics. Ca^{2+} enters mitochondria via a uniport system, down a large electrochemical gradient set up by proton extrusion linked to the passage of electrons down the cytochrome system in the respiratory chain. Ca^{2+} is extruded by a Na^{+}/Ca^{2+} antiport and Na^{+} is extruded by a Na^{+}/H^{+} exchange thereby completing the cycle. The mitochondria can accumulate large amounts of Ca^{2+}, but the Ca^{2+} affinity is low (K_m>30 μM Ca) and under physiological conditions the Ca^{2+} content is probably on the order of 100 μmol/L cytosol. [31]

Sympathetic nervous system and Ca^{2+}-dependent modulation of calcium homeostasis

The calcium homeostasis of the heartbeat is tightly regulated by signaling cascades operating inside the cardiac myocytes. Among these, both the sympathetic nervous system and Ca^{2+}, a critical modulator of its own signaling pathway via Ca^{2+}-dependent proteins, play an important role. Moreover, the two systems are working in concert, as the sympathetic system can interact/enhance the activation of Ca^{2+}-dependent regulatory proteins.

Adrenergic modulation

Activation of the sympathetic nervous system by the transmitters epinephrine (or adrenaline) and norepinephrine (or noradrenaline) increases the heart rate, contractility, and relaxation rate (positive chronotropic, inotropic, and lusitropic effects, respectively), through the adrenergic receptors.

The adrenergic receptors (ARs) belong to the guanine nucleotide binding G protein-coupled receptor (GPCR) superfamily, and are membrane receptors that activate heterotrimeric G proteins. The heterogeneity of the G-protein alpha subunit, of which there are ~ 20 subtypes (Gs, Gi, Gq, Go, and so on), is the central basis of G-protein coupled receptor signaling. G proteins typically stimulate (Gs protein) or inhibit (Gi protein) the enzyme adenylyl-cyclase (AC), or activate (Gq protein) phospholipase C (PLC).

Two classes of ARs have been identified: α and ß. The α-AR receptors are divided into two subtypes: α1 and α2. Within α1-AR receptors we can find at least three subtypes: α1A, α1B and α1D. All subtypes of α1 are expressed in the heart, although the subtype a1A is dominant in humans. α1 receptors are coupled to Gαq proteins and their activation stimulates phospholipase C. This enzyme hydrolyzes phosphatidylinositol 4,5-bisphosphate (PIP2) generating Inositol 1,4,5-for trisphosphate (IP3) which contributes to the regulation of intracellular Ca^{2+} responses (mobilizes Ca^{2+} from the intracellular stores), and diacylglycerol (DAG) that stimulates PKC, related with myofilament Ca^{2+} sensitivity. Thus, α1-AR activation increases both $\Delta[Ca^{2+}]i$ (less than β-AR) and myofilament Ca^{2+} sensitivity, resulting in a positive inotropy, with modest negative lusitropy.[31]

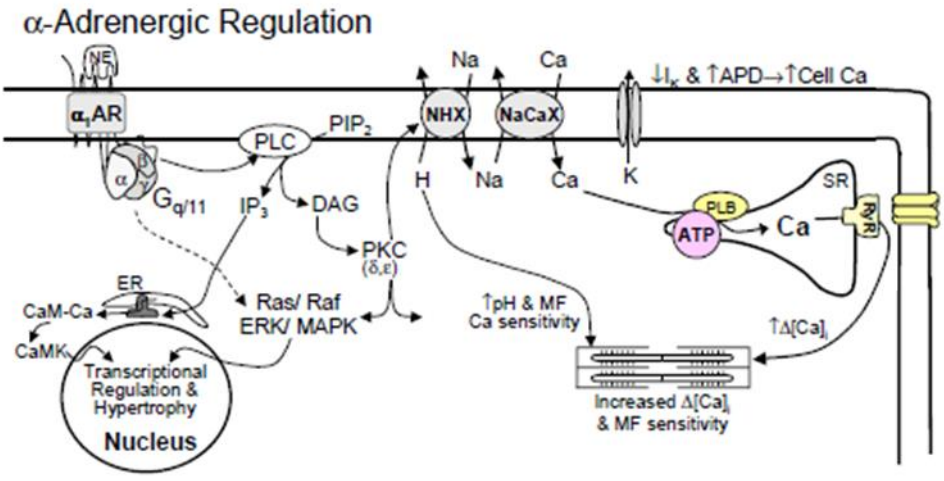

Figure 8. α1-AR transduction pathway in ventricular myocytes. The α1-AR activates the G-protein Gq, which activates phospholipase C (PLC) and D. PLC produces IP3 and diacylglycerol (DAG), and these products have divergent effects leading to positive inotropy and hypertrophy. From Donald M. Bers, 'Excitation-Contraction Coupling and Cardiac Contractile Force', 2008.[31]

The α2-AR subfamily (coupled to Gi) comprises three subtypes: α2A, α2B and α2C-AR. It is now known that in the heart tissue, the α receptors belong exclusively to the type α1. The α2 -AR are present in the vascular smooth muscle, and their stimulation causes a transient vasoconstriction.

Regarding the ß-AR receptor, the human heart contains ß1, ß2 and ß3 receptors.[70] The ß1-AR is highly expressed in the heart, ß2-AR is widely distributed throughout the body, and ß3-AR is primarily found, although not exclusively, in the white and brown adipose tissue.[71]

In the human heart, activation of ß1- and ß2-AR is the most powerful physiologic mechanism to acutely increase cardiac performance. Catecholamine (noradrenaline y adrenaline) binding to β-adrenergic receptors (β-AR), which are G-protein–coupled receptors that trigger GDP–GTP exchange at the stimulatory G-protein subunit Gαs. The activated Gαs-GTP separates from Gβγ and activates adenylyl cyclase (AC), resulting in elevated cyclic AMP (cAMP) levels and activation of the cAMP-dependent protein kinase (protein kinase A [PKA]), which phosphorylates multiple target protein, among them

1) The L-type calcium channels. The increase in Ca^{2+} entry and the synergy with a greater availability of SR Ca^{2+}, both enhance Ca^{2+} transient amplitude (inotropic effect);

2) Phospholamban (at Ser16), the modulator of SERCA2, which accelerates Ca^{2+} reuptake by the SR, reducing $[Ca^{2+}]_i$ and accelerating cardiac relaxation (lusitropic effect);

3) RyR (at Ser2808 and Ser2030),[72,73] increasing its open probability.

4) Troponin I and myosin binding protein-C, which reduce myofilament sensitivity to Ca^{2+} accelerating the relaxation of myofilaments (lusitropic effect together with PLB phosphorylation, although phosphorylation of phospholamban is by far the dominant mechanism).[74]

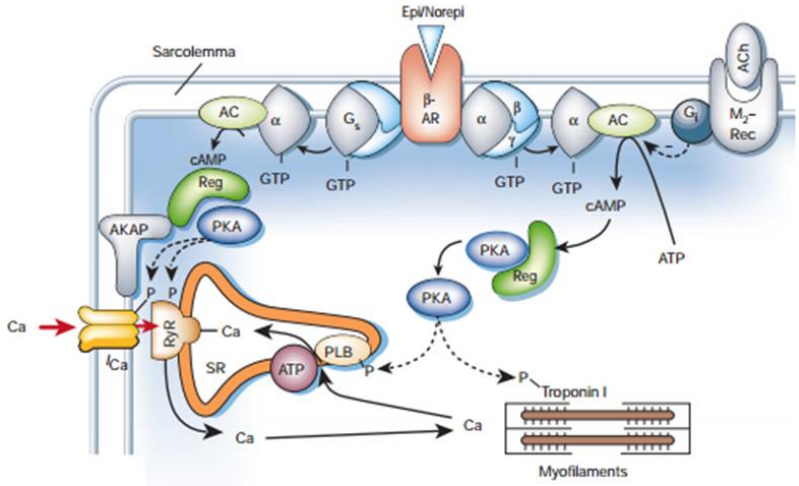

Figure 9. β-adrenergic receptor activation and phosphorylation targets relevant to excitation-contraction coupling. AC, adenylyl cyclase; ACh, acetylcholine; AKAP, A kinase anchoring protein; b-AR, b-adrenergic receptor; M2-Rec, M2-muscarinic receptor; PLB, phospholamban; Reg, PKA regulatory subunit; SR, sarcoplasmic reticulum. From Donald M. Bers, 'Cardiac fluxes involved in control of cardiac myocyte contraction', 2000.[43]

Ca^{2+}-dependent modulation

Other important modulation of E-C coupling can be carried out by its own ion effector: Ca^{2+}. In addition to the direct effects of Ca^{2+} on the myofilaments, Ca^{2+} plays a pivotal role in activation of a number of Ca^{2+}-dependent proteins or second messengers, which can modulate E-C coupling. Of these proteins, calmodulin (CaM) and Ca-CaM-dependent kinase II (CaMKII) are of special interest in the heart because of their role in modulating Ca^{2+} influx, SR Ca^{2+} release, and SR Ca^{2+} uptake during E-C coupling.

CaM and CaMKII can associate with some ion channels and Ca^{2+} transporters and both can modulate cellular calcium handling. CaMKII is one of the targets for CaM binding. CaMKII is a multifunctional CaMK, because it can phosphorylate and alter the function of a variety of substrates. CaMKII phosphorylates several proteins in the heart in response to Ca^{2+} signals, including Ca^{2+} transport proteins such as RyR and phospholamban (PLB).[75]

I_{Ca} inactivation is highly Ca^{2+}-dependent and influenced by both Ca^{2+} influx through the L-type Ca^{2+} channel and SR Ca^{2+} release. Since Ca^{2+}-dependent inactivation also occurs in the presence of cytosolic Ca^{2+}-buffers it is likely that

Ca^{2+} entry through the channel itself exerts a very local inactivation signal directly at the channel. This Ca^{2+}-dependent inactivation provides a feedback mechanism to limit the amount of Ca^{2+} entry via I_{Ca}. In addition, CaMKII phosphorylates the L-type Ca^{2+} channel increasing the I_{Ca} amplitude and slowing inactivation (Ca^{2+}-dependent I_{Ca} facilitation). I_{Ca} inactivation is a rapid negative feedback limiting the Ca^{2+} entry at a single heart beat, while I_{Ca} facilitation is manifest as longer single channel openings that may limit the decrease of Ca^{2+} channel availability from beat to beat at higher heart rates.

Ca^{2+}/calmodulin dependent protein kinase II (CaMKII) can phosphorylate RyR2 at Ser2814[72] and modulate its activity. This phosphorylation positively modulates cardiac inotropy, but in extreme situations such as heart failure, elevated CaMKII activity can adversely increase Ca^{2+} release from the SR and lead to arrhythmogenesis.[76]

CaMKII also phosphorylate PLB at Thr-17, which releases the inhibition of SERCA that PLB exerts in its unphosphorylated state.[75]

The carboxy-terminal region of cardiac Troponin T (TnT), which is important in Ca^{2+}-dependent control of the actin myosin reaction, contains most of the sites phosphorylated by protein kinase C (PKC) and CaMKII.

NCX can be regulated by $[Ca^{2+}]i$ by binding to an allosteric regulatory site, but there are no reports that CaM or CaMKII directly modulate NCX in the heart.

In situations of adrenergic stimulation or cellular Ca^{2+} overloading, protein kinase A and Ca^{2+}-calmodulin kinase type 2 (CaMKII) become activated, phosphorylating RyR2s (increasing its open probability) and PLB (causing it to dissociate from and relieve inhibition SERCA2a). While this system is adaptive under conditions of acute stress-related increases in demand for cardiac work, sustained Ca^{2+} overloading and CaMKII activation cause abnormal diastolic Ca^{2+} releases via the RyR2. The released Ca^{2+} is extruded from the cell by the Na^{+}/Ca^{2+} exchanger (NCX), which carries an inward current that causes phase 4 membrane depolarizations known as delayed afterdepolarizations (DADs).

Pathological changes in Ca^{2+} homeostasis

Defective intracellular Ca^{2+} homeostasis plays and important role in the development of cardiac disease, is a central cause of contractile dysfunction and arrhythmias in failing myocardium. Impaired Ca^{2+} homeostasis in heart failure (HF) and atrial fibrillation (AF), among others, can result from pathological alteration in the expression and activity of Ca^{2+} homeostatic binding proteins, ion channels and enzymes.

Calcium handling dysfunction and ageing

The most common sustained arrhythmia and the major cause of cardiovascular morbidity and mortality is atrial fibrillation (AF). Advanced age is a potent risk factor since AF increases gradually with age, reaching an incidence of 10% in octogenarians.[77] The propensity of older subjects to develop episodes of AF could be favored by an age-related intrinsic dysfunction of atrial intracellular calcium homeostasis.

AF is a final endpoint of atrial remodeling caused by a variety of cardiac diseases and conditions and AF itself causes important remodeling that contributes to the progression of the arrhythmia. There are four principal pathophysiological mechanisms contributing to AF: electrical remodeling, structural remodeling, autonomic nervous system alterations, and Ca^{2+} handling abnormalities.[6]

1) Electrical remodeling: atrial electrophysiological properties are governed by ion channels, pumps, and exchangers, any of which can be altered by atrial remodeling. Atrial electrical remodeling identified to date include decreased L-type Ca^{2+} current (I_{Ca}, carried by L-type Ca2+ channels). During AF, the high atrial rate causes accumulation of intracellular Ca^{2+}, engaging homeostatic defense mechanisms against chronic Ca^{2+} overload. The Ca^{2+} dependent calcineurin/nuclear factor of activated T cells (NFAT) system is then activated. NFAT translocates into the nucleus and suppresses transcription of the gene encoding Cav1.2 (CACNA1C), decreasing I_{Ca}. Reduced I_{Ca} decreases the inward

Ca^{2+} current, shortening the AP duration (APD), and thereby promoting re-entry.

Other components involved in the electrical remodeling are, rectifier background K^+ current (I_{K1}), and constitutive acetylcholine-regulated K^+ current (I_{KACh}). I_{K1} is the principal cardiac inwardly rectifying K^+- current, which determines the resting potential and the terminal phase 3 of repolarization. I_{K1} is up-regulated in AF. I_{KACh}, is activated by acetylcholine and underlies the ability of vagal activation to promote AF by causing heterogeneous increases in the inward rectifier current and reductions in APD. AF suppresses agonist-induced I_{KACh} but enhances a constitutive form (I_{KAChc}), promoting maintenance of AF.

Alterations in gap junction ion channels, such as connexin 40 and connexin 43, which mediate cardiomyocyte-to-cardiomyocyte electrical coupling, contribute significantly to AF-induced remodeling.[78]

2) Structural remodeling: is characterized by atrial enlargement and tissue fibrosis. Fibrosis promotes AF by interrupting fiber bundle continuity and causing local conduction disturbances.[79] Atrial fibrosis appears to be a common endpoint of a wide range of AF-promoting conditions and may predict recurrences. Furthermore, AF appears to promote atrial fibrosis, which contributes importantly to therapeutic resistance in patients with long-standing arrhythmia. [80–82]

3) Autonomic nervous system alterations: autonomic nervous system control regulates atrial bioelectricity and contributes to the initiation and maintenance of AF. Adrenergic activation increases I_{Ca}, RyR2 open probability, and SR Ca^{2+} load via phosphorylation by CaMKII and protein kinase A. The risk of DADs is consequently enhanced, and adrenergic activation may play a critical role in AF by promoting ectopic activity. Autonomic hyperinnervation is a consequence of AF-related remodeling and contributes to the vulnerable AF substrate.[6]

4) Ca^{2+} handling abnormalities: a direct atrial profibrillatory consequence of Ca^{2+} handling abnormalities is the induction of DAD-related spontaneous atrial ectopic activity. Patients with long-standing persistent AF have an increased risk of arrhythmogenic DADs/triggered activity. They show hyperphosphorylation and increased open probability of RyR2.[15] In addition, some studies show that NCX is up-regulated, increasing the size of DAD-generating inward currents for any given amount of aberrant Ca^{2+} release.[6] These abnormalities appear to be caused by AF-induced remodeling, with CaMKII activation resulting from Ca^{2+} overloading due to sustained very rapid atrial activation. While long-standing persistent AF is likely maintained by complex multiple circuit reentry,[83,84] ectopic activity may contribute by reinitiating AF should it terminate spontaneously or via medical intervention.

Since advanced age is a potent risk factor in cardiovascular diseases associated with altered intracellular calcium homeostasis, it is vitally important to explore the molecular mechanisms underlying age-related disorders. Extensive evidence demonstrates that age-related changes in the expression and function of various ion channels, receptors, enzymes and signaling pathways play a key role in the pathophysiological basis of ageing in the heart and have the potential to alter both mechanical and electrical properties of the myocardium. However, knowledge of the intrinsic effects of ageing on the intracellular calcium homeostasis in the human heart is sparse. Therefore, this study aimed to analyze how ageing affects key mechanisms that regulate intracellular calcium levels in human atrial myocytes.

Most of the studies analyzing the effects of ageing on cardiomyocyte function have been performed in ventricular myocytes from rodents, reproducing some of the pathological alterations described in the AF, such as enlargement of myocyte size[85] and focal proliferation of the matrix linked to an altered cardiac fibroblast number or function. Moreover, the number of cardiac myocytes becomes reduced because of necrosis and apoptosis.[2] The alterations lead to the hypertrophy of remaining cells and to pathologic remodeling, with the consequent

reactive fibrosis that increases cardiac stiffness and reduces the cardiac compliance.

Several studies in aged rodents have reported that ageing alter E-C coupling process due to prolongation of the AP, Ca^{2+} transient and contraction, and blunt force-and relaxation-frequency responses (inotropic and lusitropic responses), consequent to changes in the expression and function of Ca^{2+} transport proteins and in sarcolemmal K^{+} currents. Nevertheless, knowledge of the intrinsic effects of ageing on atrial intracellular calcium handling in humans is lacking and data from experimental animal models are sparse and often inconsistent.[2]

Genetic variants and alteration of calcium homeostasis that could predispose to atrial fibrillation

In addition to the complex aging-related mechanism that could predispose to contractile dysfunction and arrhythmias, some genes have been associated to the development of atrial fibrillation. The road towards discovering the genetic basis of AF has progressed from identification of genes associated with familial AF to clinical observational studies demonstrating hereditability of common AF and to genome wide association studies (GWAS) that have identified to date several genetic loci associated with AF risk.

In familial AF several ion channel gene mutations have been identified, including potassium channels (e.g. in KCNQ1, KCNE2, KCNH2, KCNJ2, KCNA5), sodium channel mutations (in SCN5A and SCN4B), the RyR2 and several non-ion channel genes (see Table 3).

Although familial AF studies have contributed much to our understanding of the genes associated with monogenic forms of AF, they represent only a small fraction of the overall burden of disease. Overall, the genetics of common AF pathogenesis is complex, involving modest contributions to the risk of disease from genetic variations in many genes. The genetic architecture of a disease depends on the number of variants that influence a given pathology, the effect size of each variant on the phenotype, and the frequency of the variant. Complex

diseases such as AF follow the "common disease common variant" hypothesis of genetic architecture where common variants with small effects appear to be responsible for a majority of the heritability of the trait.[86] In alignment with this hypothesis, the first GWAS for AF identified a common susceptibility locus at chromosome 4q25.[7] And subsequent studies has identified an additional number of loci associated with risk of AF (see table 3). The association between AF and 4q25 has been further replicated in all GWAS to date.[18,87,88] Furthermore, this locus has been associated with recurrence of AF after ablation and new onset AF in the postoperative period after coronary bypass surgery.[87,89]

Genetics variants at 4q25 are located close to the paired-like homeodomain 2 PITX2 gene, suggesting a role for Pitx2 in cardiac arrhythmias. PITX2 encodes 3 different isoforms of the protein by alternative splicing. Importantly, the major isoform Pitx2c is involved in embryogenesis and left-right differentiation of the heart[90] and in the formation of pulmonary veins that are the putative site of AF initiation.[91] Thus, Pitx2 is a biologically attractive causative candidate gene in the region, as it appears to be involved in the regulation of several ion channel genes that plausibly may predispose to atrial arrhythmia.[8,92]

Given this pivotal role, it was postulated that Pitx2 dysfunction might be the molecular link between risk variants at 4q25 and AF. In this thesis we have studied how these mentioned risk variants affect calcium homeostasis in cardiac cells and the potential key with AF, and how Pitx2 modulate this interaction.

Table 3. Gene loci associated with atrial fibrillation (from Gutierrez & Chung, 2016).[93]

Gene	Function
Familial studies	
KCNQ1	Gain of function of potassium channel contributing to I_{ks}
KCNE2	Gain of function mutation of the potassium channel responsible for the I_{Ks} current
KCNH2	Encodes for the channel responsible for the rapidly depolarizing current I_{kr}
KCNJ2	Encodes for the inward rectifier potassium channel Kir 2.1
KCNA5	Modulation of ultrarapid depolarizing current I_{Kur}
SCN5A	Nav 1.5 responsible for upstroke of action potential
SCN4B	β subunit of the voltage gated sodium channel
PRKAG2	ϒ2 subunit of AMP-activated protein kinase which regulates ATP generation and use.
NPPA	Frameshift mutation causes ANP to be resistant to breakdown increasing its half life
ABCC9	ATP binding cassette leads to loss of function of I_{KATP}
RYR	Alteration of ryanodine receptor leading to imbalance of calcium homeostasis
NUP155	Nucleoporin 155, a component of the nucleopore formation reducing nuclear envelope permeability
LMNA	Laminin A/C in inner nuclear membrane
GATA 4,5	Zinc finger transcription factor involved in cardiac development
Candidate gene studies	
KCNE 1,3,4 and *5*	Mutation of the β subunit of voltage gated potassium channel leading to altered function of I_{Ks}
KCNJ 5 and *8*	α subunits of inwardly rectifying potassium channels
KCND3	$K_v4.3$ α subunit causing increase in the transient outward potassium current I_{to}
SCN1B,2B,3B	Mutation in the β subunits of the sodium channel leading to decreased sodium current
SCN10A	Nav 1.8 which participates in the late sodium current
GJA5	Connexin 40 in gap junctions altering action potential propagation
NKX2.5	Homeobox transcription factor involved in cardiogenesis
RAAS	Angiotensin conversion enzyme inhibitor, angiotensin gene promoter and angiotensinogen polymorphisms
Genome wide association studies	
PITX2	Right-left asymmetry, atrial cardiomyocyte and SA node development, intercalated disk
ZFHX3	Zinc finger homeobox 3; regulation of growth and differentiation of skeletal muscle and neuronal tissue.
PRRX1	A homeodomain transcription factor expressed in connective tissue in the developing heart
KCNN3	Intronic variant in the gene encoding for the calcium activated potassium channel SK3
HCN4	Hyperpolarization-activated cyclic nucleotide-gated 4 channel of the I_f
CAV1	Caveolin-1, a structural component of caveolae
SYNE2	Intronic SNP encoding for nespirin 2; anchors the nucleus to the cytoskeleton
MYOZ1/SYNPO2L	Intergenic variant. *MYOZ1* encodes for myozenin 1 a protein involved in stabilizing the sarcomere
C9orf3	Opening reading frame of chromosome 9, potential causal gene is still unclear
GJA1	Connexin 43 in gap junctions altering action potential propagation
NEURL	E3 ubiquitin ligase- interacts with *PITX2* and leads to increased AP duration
CAND2	TBP- interacting protein involved in myogenesis
TBX5	Transcription factor involved in the development of cardiac conduction system
CUX2	Cut-like homebox 2 a transcription factor involved in neural development

HYPOTHESIS

HYPOTHESIS AND OUTLINE OF THE THESIS

Ageing and disturbances in the intracellular calcium homeostasis are both associated with an increase in the incidence in several common heart diseases such as AF and IC. However, little is known about the effect of ageing on the intracellular calcium homeostasis in the human atrium. Moreover, common single nucleotide polymorphisms on chromosome 4q25 have recently been associated with increased risk of AF, but it is not known whether 4q25 risk variants affect the calcium homeostasis and/or aging increase their penetrance.

Therefore, this thesis aims to test the hypothesis that ageing and 4q25 risk variants produce alterations in the intracellular calcium homeostasis in atrial myocytes that alone or in combination contribute to increase the propensity to atrial fibrillation.

To test the hypothesis, cardiomyocytes were isolated from human right atrial samples, and from different transgenic mouse models, and subjected to specific electrophysiological protocols designed to address the following aims:

- Analyze the effects of ageing on the mechanisms that regulate the calcium homeostasis in human atrial myocytes.
- Use a transgenic murine model of ageing to identify molecular mechanisms underlying ageing-dependent changes in the calcium homeostasis.
- Investigate how risk variants on chromosome 4q25 associated with increased AF risk, affect electrophysiological characteristics of human atrial myocytes and to identify underlying molecular mechanisms.
- Investigate how age modulate the effects of 4q25 risk variants in human atrial myocytes.

GENERAL METHODOLOGIES

EXPERIMENTAL DESIGN AND GENERAL METHODOLOGIES

This chapter describes the methodology common to most of the investigation carried out in this thesis. The methodology specific to particular subjects is given in the respective chapters.

ISOLATION OF MYOCYTES

Obtaining human atrial tissue

Atrial tissue samples were obtained previously to the cannulation of the right atrial appendage in operations requiring cardiopulmonary bypass surgery in the Unit of Cardiology and Cardiac Surgery at Hospital de la Santa Creu i Sant Pau in Barcelona. Although the atrial tissue samples consisted of tissue that would normally be discarded during surgery, permission to study this tissue was obtained from each patient. The study was approved by the ethics committee of our institution.

To preserve the quality of the samples, these were transported immediately to the laboratory (it normally took less than 5 minutes to the start the isolation of cardiomyocytes) in a Tyrode solution without Ca^{2+}, oxygenated and cold, to which we added monoxime butanedione (BDM) 30 mM. The calcium-free Tyrode solution composition is described below in Table 1.

Isolation of human right atrial myocytes

Tissue samples were carefully obtained and immediately taken to the laboratory in cold and oxygenated calcium-free Tyrode solution containing 30 mmol/L butanedione monoxime. It was cleaned and cut into small pieces (1 x 1 mm) that were introduced into a calcium-free Tyrode solution with collagenase 1.2mg/ml (Worthington type2, 298U/mg); proteinase 0.45mg/ml (Sigma type XXIV, 11U/mg) and bovine fatty acid-free serum albumin (BSA) (2 mg/ml) and

incubated at 35 ºC for 30 minutes. Cells were dissociated from the tissue removing gently the pieces in calcium-free Tyrode solution with 50 mg/ml BSA using a Pasteur pipette. The remaining tissue was incubated again 3-4 times for 15 minutes in fresh enzyme solution containing collagenase 0.7mg/ml at 35 °C for further digestion. Isolated cells were resuspended in Ca^{2+}-free solution, and Ca^{2+} was gradually increased to 1 mmol/L. After this process, only elongated cells with clear striations and without granulation will be used to perform the experiments.

Isolation of mouse ventricular and atrial cardiomyocyte

In order to obtain a good yield and a high quality of mouse cardiomyocytes for subsequent experiments, Langendorff perfusion of the whole heart was used. The mouse was injected with heparin (5000 IU/kg, i.p.) and anestesthisized (medetomidine 1 mg/kg and ketamine 75 mg/kg) 15 minutes before starting the experimental protocol and sacrificed by cervical dislocation. This protocol is in accordance with the animal care committee at our institution.

The heart was quickly removed and cannulated via the aorta. The cannulated heart was mounted on the Langendorff perfusion system with a constant flow rate of 3 ml/min at 37°C; first with a calcium-free Tyrode solution with EDTA 0.1M, for 3 minutes to wash residual blood. Then with an enzyme containing solution (collagenase Type 2, 298U/mg, 0.4 mg/ml, proteinase 0.04 mg/ml and 0.1% albumin) for 8 minutes.

After perfusion, the heart was removed from the cannula and cut to separte atria and ventricle. The atrial and/or ventricular tissue was cut into small pieces (1 x 1 mm, approx.) and the digestion was continued with the enzyme solution for 5 min followed by gentle agitation of the tissue fragments in calcium free Tyrode solution. This process was repeated three times (or more to achieve optimal quality and yield of myocytes). Myocytes from each cycle were then pooled in a solution in which extracellular calcium concentration was increased stepwise to 0.2, 0.4, and 0.8 mM. Myocytes were then stored at room temperature and those showing elongated and striated features were used for electrophysiological,

calcium imaging and immunofluorescent labelling studies. All solutions used were oxygenated throughout the isolation protocol.

Experimental solutions

Table 1. Composition of the different solutions used in the experimental protocols.

SOLUTION	COMPOSITION
Ca^{2+}-free Tyrode for cell isolation (Human, mice)	88 mM Sucrose, 88 mM NaCl, 5.4 mM KCl, 4 mM $NaHCO_3$, 0.3 mM NaH_2PO_4, 1.1 mM $MgCl_2$, 10 mM HEPES, 20 mM Taurine, 10 mM Glucose, 5 mM Na-Pyruvate. pH adjusted to 7.40 with NaOH 1N at room temperature.
External medium for voltage-clamp (Human)	127 mM NaCl, 5 mM TEA, 4 mM $NaHCO_3$, 0.33 mM NaH_2PO_4, 2 mM $CaCl_2$, 1.8 mM $MgCl_2$, 10 mM HEPES, 10 mM glucose, 5 mM pyruvic acid. pH adjusted to 7.40 with NaOH 1N at room temperature.
Internal medium for voltage-clamp (Human, perforated patch)	109.2 mM DL-Aspartatic Acid (no K^+ salt), CsOH until disolution, 46.8 mM CsCl, 3 mM Mg_2ATP, 1mM $MgCl_2$, 5 mM Na_2PC, 0.42 mM LiGTP, 10 mM HEPES. pH adjusted to 7.20 with CsOH 1N at room temperature.
External medium for current-clamp (Human, mice)	136 mM NaCl, 4 mM KCl, 4 mM $NaHCO_3$, 0.33 mM NaH_2PO_4, 2 mM $CaCl_2$, 1.6 mM $MgCl_2$, 10 mM HEPES, 5 mM Glucose, 5 mM pyruvic acid. pH adjusted to 7.40 with NaOH 1N at room temperature.

Internal medium for current-clamp (Human and mice, perforated patch)	109.2 mM DL-Aspartatic Acid (no K^+ salt), 47 mM KCl, 3 mM Mg_2ATP, 1mM $MgCl_2$, 5 mM Na_2PC, 0.42 mM LiGTP, 10 mM HEPES. pH adjusted to 7.20 with KOH 1N at room temperature.
Physiological external solution for calcium imaging (Human)	132 mM NaCl, 4 mM KCl, 0.33 mM NaH_2PO_4, 4 mM $NaHCO_3$, 2 mM $CaCl_2$, 1.6 mM $MgCl_2$, 10 mM HEPES, 5 mM Glucose, 5 mM Na-Pyruvate. pH adjusted to 7.40 with NaOH 1N at room temperature.
External medium for voltage-clamp (Mice)	127 mM NaCl, 5.4 mM CsCl, 4 mM $NaHCO_3$, 0.33 mM NaH_2PO_4, 10 mM HEPES. pH adjusted to 7.40 with NaOH 1N at room temperature.
Internal medium for voltage-clamp (Mice, perforated patch)	90 mM DL-Aspartatic Acid (no K^+ salt), CsOH until disolution, 50 mM CsCl, 1mM $MgCl_2$, 10 mM HEPES. pH adjusted to 7.20 with CsOH 1N at room temperature.
Physiological external solution for calcium imaging in Mice	132 mM NaCl, 5.4 mM KCl, 0.33 mM NaH_2PO_4, 4 mM $NaHCO_3$, 1 mM $CaCl_2$, 1 mM $MgCl_2$, 10 mM HEPES, 10 mM Glucose. pH adjusted to 7.40 with NaOH 1N at room temperature.

ELECTROPHYSIOLOGICAL MEASUREMENTS

Ionic currents were measured with patch-clamp technique in the whole cell configuration, using an EPC-10 amplifier (HEKA Elektronik, Germany). First, some drops of the cell suspension were added to a Petri dish with BSA coating on the bottom that contained the extracellular patch solution (see composition at Table

1). A glass patch-pipette, containing the intracellular patch solution (see composition at Table 1), was introduced in the bath and placed close to a cell. Aplication of a small negative pressure was used to attach the myocyte to the patch pipette, which caused the resistance to increase from 2-5 MΩ to 2-20 GΩ (seal formation). Then, the cell was lifted up from the bottom of the Petri dish and placed in front of one of three adjacent capillaries containing the extracellular solution.

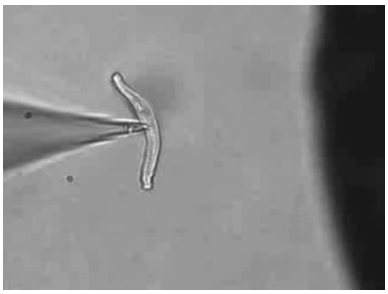

Figure 1. Representative images of a human atrial myocyte subjected to whole cell patch-clamp during experimental protocols. Dark shade on right is part of one of the capillaries of the perfusion system.

Amphotericine (250 μg/ml) was added to the pippete solution before starting the experiments using perforated configuration. The patch-clamp experiments were carried out at room temperature.

Determination of the L-type calcium current (I_{Ca})

The Ca^{2+} entry through the L-type calcium channels was measured, in steady-state conditions, using a stimulation protocol with a 50 ms prepulse (from -80 mV to -45 mV to inactivate sodium current, I_{Na}) followed by 200 ms depolarizing to 0 mV to activate I_{Ca} (see figure 2). The inward current elicited by the 200 ms depolarization was the L-type Ca^{2+} current (I_{Ca}), and its amplitude was determined as the difference between the peak inward current and the current measured at the end of a 200 ms depolatization. Moreover, the stimulation pulse allowed examination of the tail current (I_{tail}) elicited by repolarizing the cell to -80 mV. The time-integral of this inward tail current was used as a measure of the total

amount of Ca^{2+} extruded from the cell through the activity of the Na^{+}/Ca^{2+} exchanger.

These two inward currents (I_{Ca} and I_{Tail}) represent the amount of Ca^{2+}flowing across the sarcolemma. For Ica two charges are carried per Ca^{2+} ion, whereas the Na^{+}/Ca^{2+} exchanger carries one net charge por Ca^{2+}, assuming a stoichiometry exchange of 3 Na^{+} per 1 Ca^{2+}.

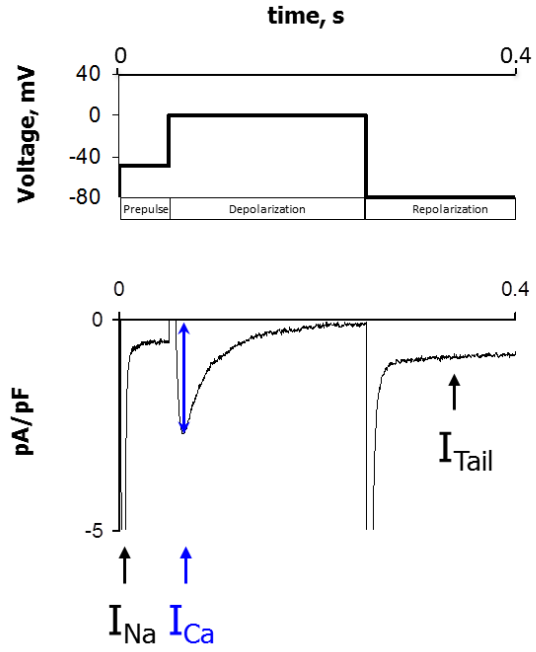

Figura 2. Representative estimulation protocol indicating the membrane potencial to be applied to the myocyte and its corresponding membrane current recording. The currents that are activated in each segment of the protocol are indicated: I_{Na} (sodium current), I_{Ca} (L-type c alcium current), I_{tail} (Ca^{2+} extruded from the cell through the activity of the Na^{+}/Ca^{2+} exchanger.

The beat-to-beat stability of intracellular calcium handling was evaluated by measuring the calcium current and intracellular calcium transient at increasing stimulation frequencies (0.2 to 2Hz).

Determination of the current-voltage (I-V) relationship for I_{Ca}

The relationship between I_{Ca} intensity and voltage, was measured using different membrane potential depolarizations (between -40 and +50 mV) with a 50 ms prepulse at -45 mV to inactivate I_{Na}.

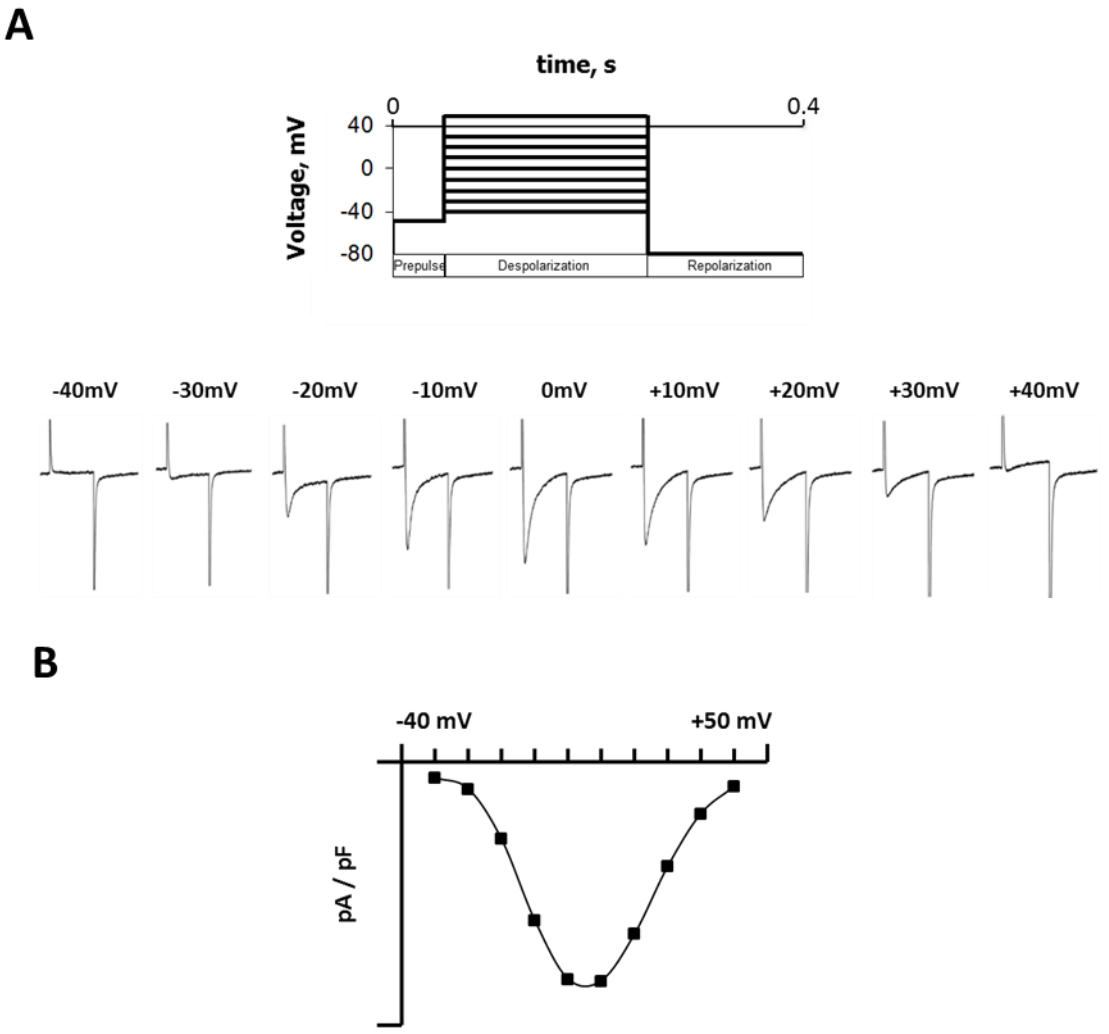

Figura 3. Current-voltage relationship for Ica (A) Representative estimulation protocol indicating the membrane potential (from -40 mV to +50 mV) and the calcium currents recordings at the different membrane potentials, and (B) the resulting graph showing the relation between current intensity and voltage applied.

Determination of I_{Ca} inactivation

To measure how fast calcium channels are inactivated, that is the disappearance of I_{Ca} after ativation, the time constants for its disappearance (with steady-state stimulation) were calculated, adjusting the decaying phase with a double exponential to obtain the time constants for fast (tau-1) and slow inactivation (tau-2):

$$y(x) = y_0 + ampl_1 * \exp(-x / tau_1) + ampl_2 * \exp(-x / tau_2)$$

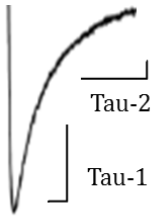

Figure 4. I_{Ca} inactivation. Calcium current inactivation with indication of the inactivation time constants Tau-1 (fast) and Tau-2 (slow) of the decaying phase of I_{Ca}.

In adition, the voltage dependecy of the inactivation of calcium channels was determined by measuring how the I_{Ca} amplitude changes when a pre-pulse to different membrane potential was applied prior to the stimulation pulse. A Boltzman equation was then used to determinate the voltage for half-maximal I_{Ca} inactivation.

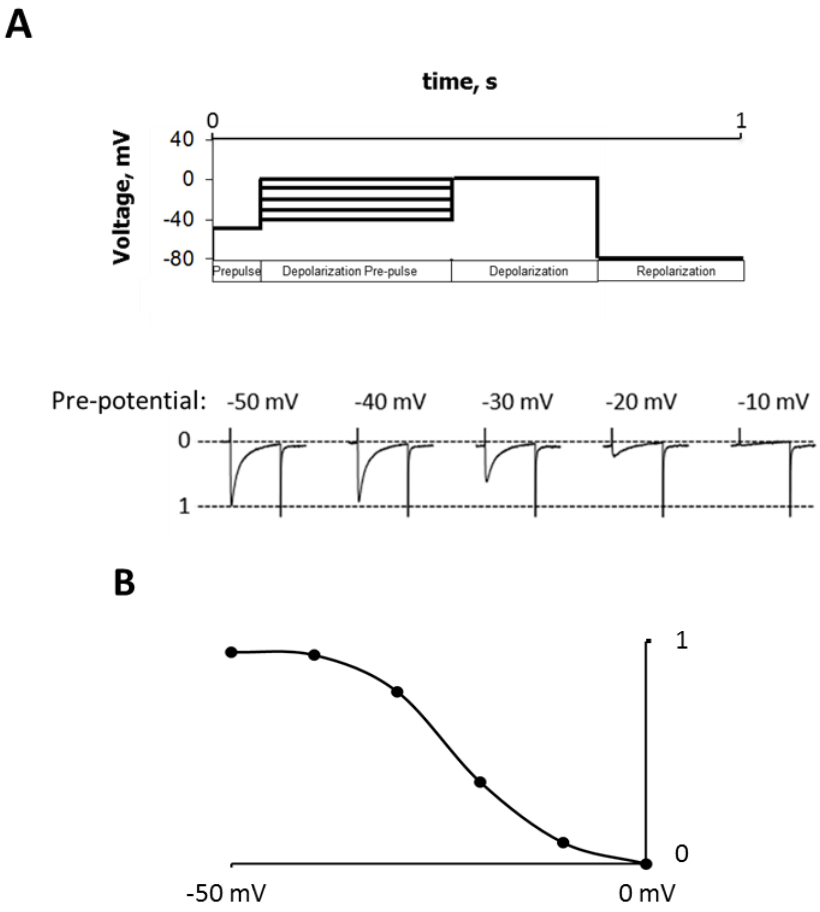

Figura 5. Voltage dependent I_{Ca} inactivation. (A) Representative stimulation protocol indicating the membrane protential (up). The representative I_{Ca} traces were obtained after a prepulse to different membrane

potential indicated in the protocol (given above traces). Current traces were normalized to the I_{Ca} amplitude at -50 mV. (B) Graph of voltage-dependent I_{Ca} inactivation normalized to the maximal peak (-50 mV).

Determination of I_{Ca} recovery for inactivation

To stimate the time needed for a total recovery of the calcium channels from inactivation after a depolarization pulse (0 mV), we used a protocol with increasing time intervals (100 ms) before a second depolarization pulse used to elicit I_{Ca}.

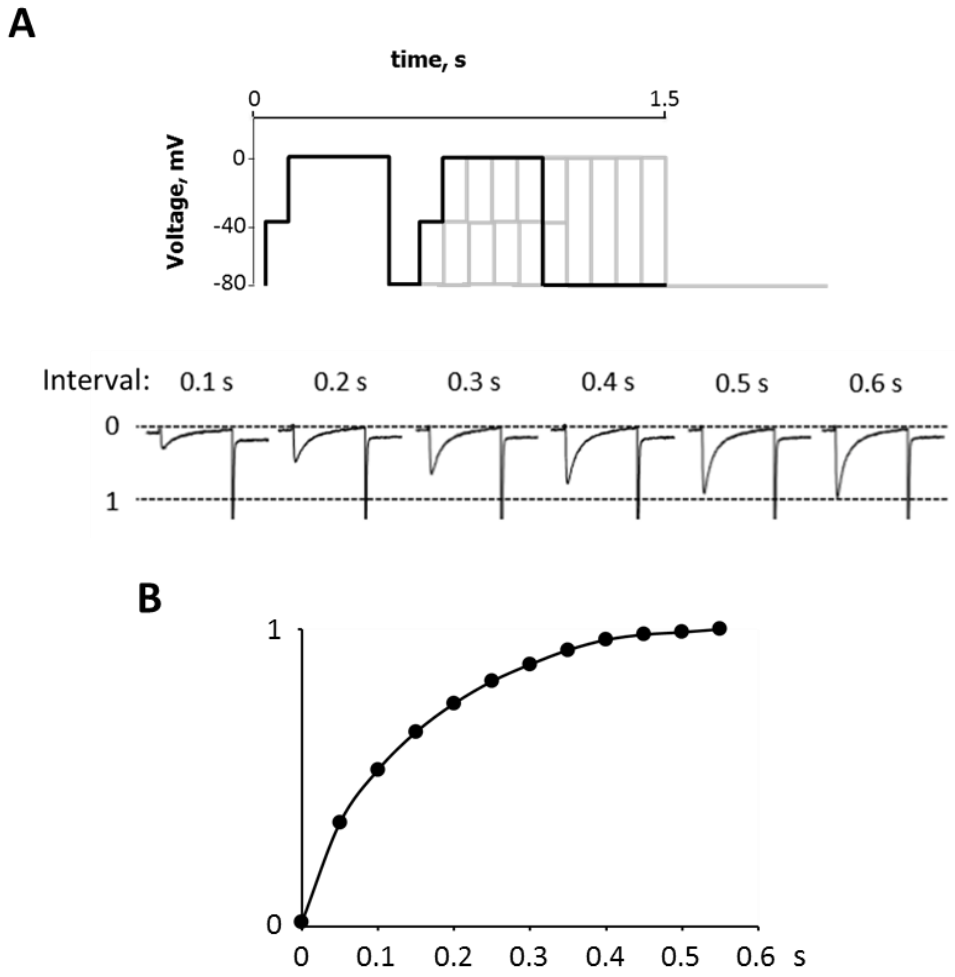

Figura 6. I_{Ca} recovery from inactivation. (A) Representative stimulation protocol indicating the membrane potential (up) and the ICa traces elicited at diferent times (given above traces) after the preceding stimulation pulse were normalized to the I_{Ca} amplitude at 0.6 s. (B) Graph of I_{Ca} recovery for inactivation normalized to the maximal peak (0.6 s).

Determination of the SR Ca^{2+} Content and spontaneous Ca^{2+} release

To stimate the SR Ca^{2+} content in intact cardiac myocytes, we used the time-integral of the inward Na^+/Ca^{2+} exchange current (I_{NCX}) elicited by exposure of the cell rapidly and transiently (5 seconds) to 10 mM caffeine (see Figure 7A). The integral of the resulting from extrusion of the calcium released from the SR by caffeine by the Na^+/Ca^{2+} exchanger was converted to amoles (10^{-18} mol) of calcium, assuming a stoichiometry of 3 Na^+: 1 Ca^{2+} the Na^+/Ca^{2+} exchanger.

The transient inward current (I_{TI}) elicited by spontaneous calcium realese from the SR was also detected in myocytes with the membrane potential clamped to -80 or -50 mV [10] during 30 seconds.

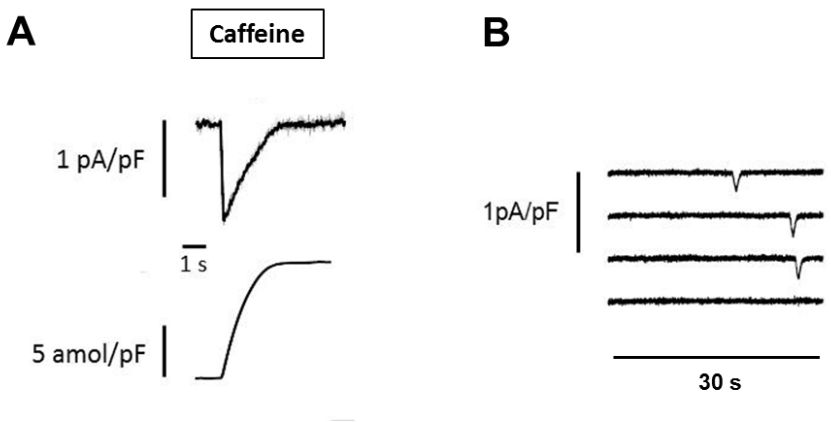

Figure 7. Caffeine (CAF) induces an inward ionic current. A) Exposure of cell to 10 mM caffeine induces a transient inward ionic current (top). The integral of the inward current is shown below. B) Spontaneous inward currents recorded with the membrane potential clamped to -80 mV.

Determination of spontaneous membrane depolarizations

Membrane potentials were measured in the current-clamp configuration using K^+-containing intra and extracellular media (see composition on Table 2). The holding current was varied in order to assess the amplitude and frequency of spontaneous membrane depolarizations at different resting membrane potentials (between -80 and -60 mV).

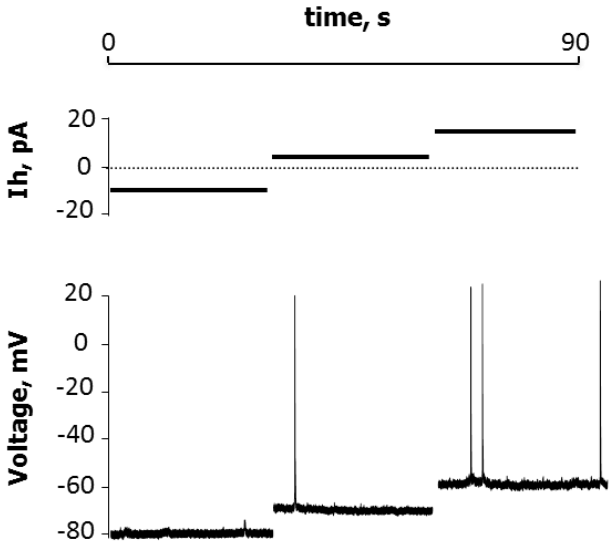

Figure 8. Representative protocol for measuring of spontaneous membrane depolarizations. Indicated holding current (I_h) (up) to maintain the membrane potential at different voltage. Recordings of spontaneosus membrane depolarizations are shown (bottom).

CONFOCAL MICROSCOPY AND CALCIUM IMAGING

Determination of the intracellular calcium by confocal microscopy

A confocal microscope with high-speed resonance scanning (Leica TCS SP5 AOBS) was used to visualize changes in cytosolic calcium level (calcium transient) induced by each stimulation pulse. For visualization and measurement of intracellular calcium, cardiomyocytes were loaded with a fluorescent calcium indicator.

To measure green fluorescence emission fluo-4 AM or CAL-520 AM was used. For red fluorescence emission CAL-590 AM or Rhod-2 AM was used. The incubation time for the myocytes was different dependent on the calcium indicator and cell type used:

Fluo-4: 2.5 μM for 20 minutes at room temperature. After incubation, cells were washed with a physiological external solution and left for 30 minutes at room

temperature (for de-esterification of the fluorophore) before starting the experiments.

CAL-520 and CAL-590: 2μM for 20 minutes at room temperature. Washed and left for 30 minutes with a physiological external solution.

Rhod-2: 5 μM for 40 minutes at room temperature. Washed and left for 30 minutes with a physiological external solution.

Fluo-4 / CAL-520 were excited at 488 nm and fluorescence emission was collected between 500 and 650 nm. CAL-590 and Rhod-2 were excited at 543 nm and the fluorescence emission was collected at 580-750 nm. When using patch-clamp and calcium imaging simultaneously, the synchronization of the confocal images and the recorded ionic currents was achieved using a Leica DAQ box (National Instruments) and HEKA patch-master software (HEKA Elektronik, Lambrecht / Pfalz, Germany). The calcium transient measured represents the fluorescence emitted in the confocal plane of the cell. The solution used for confocal experiments is described in Table 1.

Field stimulation for measuring intracellular calcium handling

Isolated myocytes are loaded with any of the fluorescent calcium indicator mentioned and the excitation and fluorescence emission was collected as indicated before. Calcium transients were recorded at room temperature (20-22ºC) and elicited by subjecting myocytes to electrical field stimulation (5 ms pulses, 5-15 V) at increasing stimulation frequency (0.5 to 4 Hz). Calcium transients and spontaneous calcium waves were automatically detected and quantified using custom-made programs.[94]

The calcium transient measured represents the fluorescence emitted in the confocal plane of the cell. The solution used for confocal experiments is described in Table 1.

Calcium sparks detection

Isolated myocytes were loaded, excitated and the emission was collected as mentioned before. Experiments were performed at room temperature and calcium sparks were detected using custom made algorithms (colaboration with department of Automatic Control, UPC) using MATLAB (The Mathworks Inc., Boston, MA). Briefly, a wavelet-based detection method was applied to the normalized time-dependent fluorescence signal zi(t) at every pixel in order to detect candidates for Ca2+ release events. More specifically, gaussian wavelet of order 2 with scales from 5 to 10 were used in order to enhance Ca2+ release events with a duration of 20 to 300ms. Candidate event regions were detected by thresholding the wavelet signals at 3.5σ. The noise variance of the wavelet signal σ was robustly estimated using the median absolute deviation of the fluorescence signal of a pixel at the center of the cell. Subsequently, spark candidates were filtered based on a relative intensity threshold of 0.4, a full duration at half maximal between 10 and 150 ms, a spark decay constant between 15 to 150 ms and a minimal R2 for the exponential fit of the decay of 0.5. To eliminate sparks occurring within a calcium wave, events with an elevated baseline (1.5x or higher) were eliminated. The program allowed visual inspection of the calcium signal and consecutive images with indication of the detected spark in order to manually validate or reject doubtful events and it allowed to merge consecutive recordings from the same cell. After supervised validation and merging, sparks that coincided spatially (within a radius of 2 μm) were pooled into a common spark site and calcium traces were generated for each spark site. Each spark was characterized by its amplitude, its duration characterized as the Full Duration at Half Maximum (FDHM) and its width characterized as the Full Width at Half Maximun (FWHM). The spark frequency was calculated as the number of sparks/cell/min or normalized to the cell area within the confocal plane and expressed as sparks/μm^2/min. Additionally, the number of spark sites were given as sites/cell or normalized to the cell area and given as sites/μm^2. The average spark frequency per site was given as sparks/site/min.

Determination of T-tubular structures

The presence of T-tubular structures was assessed by incubation of isolated myocytes with one of the fluorescent dyes Di-4-ANEPPS or RH-237 (both 2 μM for 5 minutes at room temperature). Di-ANEPPS was exited at 488 nm and fluorescent emission collected between 500 and 650 nm. RH-237 was excited at 543 nm and fluorescence emission collected between 580 and 750 nm.

Immunohistochemistry

The main protein studied by inmunolabeling was the RyR2 in isolated cardiac cells. Prior to the inmunolabelling, the cardiomyocytes were fixed with paraformaldehyde 4% (formalin 10%) for 5 minutes at room temperature and washed gentenly 2 times with PBS. Next, cells were incubated with PBS / Glycine 0.1 M during 10 minutes at RT and with PBS / Triton X-100 0.2% for at least 30 minutes to permeabilize the cells and then washed with PBS. To block the non specific sites, we used PBS / Tween 20, 0.2% / Horse serum, 10% for 30 minutes at RT. To visualize RyR2 clusters, myocytes were inmunofluorescently labelled using a primary anti-RyR2 antibody (Calbiochem) diluted in PBS / Tween 20 0.2% / Horse serum 5% (1:300) for at least 1 hour or overnight. After that, cells were washed gentenly with PBS. The secondary antibody used was AlexaFluor 488 or 594 diluted int PBS / Tween 20, 0.2% / Horse serum 5% (1:1000) and incubated for at least 1 hour. Finally, the cells were washed again and stored with PBS-Azide, 0.2 % at 4ºC until visualization.

To analyze the RyR clusters in the confocal images, an automatic custom-made algorithm (colaboration with department of Automatic Control, UPC) was used. The algorithm first enhanced the contrast of images using a histogram stretching intensity transformation. Subsequently, it removed background noise by using an adaptive median filter that estimated the noise level, and enhanced the location of all labelled RyRs with a 2D Gaussian filter with a standard deviation of 0.5 μm followed by segmentation using a multilevel watershed algorithm. Non-specific staining was eliminated by setting the maximal RyR diameter to 1.2 μm.

Protein expression

Protein expression was determined with western blot techniques and is detailed in the methods presented in the results section.

DATA ANALYSIS AND STATISTIC

Results are given as mean ± SEM, and data sets were tested for normality. Statistical significance was evaluated using a Student's t-test and ANOVA was used for comparison of multiple effects. Bonferroni post-test was used to evaluate the significance of specific effects. Differences were considered statistically significant when $p<0.05$. Other specific test are detalled in the corresponding results section.

ETHICAL CONSIDERATIONS

These studies were approved by the ethics committee of the Hospital de la Santa Creu i Sant Pau, Barcelona, and were conducted in accordance with the principles of the Declaration of Helsinki. The informed consent were requested to the patients for use of the auricular samples, although this tissue normally be discarded during.

In addition, animal experimentation were approved by the animal care committee.

RESULTS

RESULTS

The results of this thesis are structured in independent chapters, attempting to identify mechanisms that can afford an explanation for the age-dependent increase in the incidence of atrial fibrillation and to association of this arrhythmia with alterations in the intracellular calcium handling. Most of the results presented here are included in manuscripts in preparation, submitted for publication, or already published.

The first chapter is dedicated to the first and main aim of the thesis, trying to elucidate the mechanisms involved in changes in the intracellular calcium handling with age in human atrial myocytes and the potential contribution of such changes to increase the risk of atrial fibrillation in the eledrly. The reults of this chapter are published.[9]

The second chapter uses the progeric mouse model Zmpste24$^{-/-}$ to investigate whether defective lamin processing, previously associated to natural and premature ageing processes, reproduces the effects of ageing in the human atrial myocytes. This chapter contains results included in a second publication entitled "Cardiac electrical defects in progeroid mice and Hutchinson-Gilford progeria syndrome patients with nuclear lamina alterations",[10] and additional experimentation not included in this paper.

In the third chapter we investigate if and how common single nucleotide polymorphisms on chromosome 4q25, associated to a higher risk for AF, affect arrhythmogenic calcium release in human atrial myocytes. The results of this paper form part of a publication currently submitted for publication.

The fourth chapter investigates how the transcription factor Pitx2, thought to be a primary target for 4q25 risk variants, modulate the calcium homeostasis and whether Pitx2 insufficiency can reproduce the effects of 4q25 risk variants in human atrial myocytes. For this purpose we used a transgenic mouse model with atrial-specific deletion of Pitx2. Some of these results are part of a published paper

investigating mechanisms underlying Pitx2 mediated changes in the expression and function of calcium regulatory proteins[11] and the results addressing the effects of partial Pitx2 insufficiency are included in the manuscript on the effects of 4q25 risk variants in human atrial myocytes.

Finally chapter five integrates the effects of ageing and 4q25 risk variants on calcium homeostasis in human atrial myocytes, in order to determine whether ageing modulate the effect of 4q25 risk variants on intracellular calcium homeostasis. These results form part of a manuscript under preparation.

I. AGEING IS ASSOCIATED WITH DETERIORATION OF CALCIUM HOMEOSTASIS IN ISOLATED HUMAN RIGHT ATRIAL MYOCYTES

INTRODUCTION

As a result of the progressive increase in life span in highly developed countries, knowledge of the effects of ageing on human pathophysiology is of great relevance. Coronary atherosclerosis, heart failure, and atrial fibrillation (AF) are among others, prevalent cardiovascular diseases closely linked to ageing.[1]

Left atrial enlargement with impaired mechanical function is often observed in healthy humans after the eight decade.[95–97] Since older age is frequently associated with diastolic left-ventricular (LV) dysfunction,[95] enlargement of the left atrium in older subjects could merely result from the increased LV filling pressure. However, an intrinsic derangement of atrial cellular calcium homeostasis induced by age could theoretically impair the mechanical atrial function in subjects with otherwise normal LV function. Moreover, the propensity of older subjects to develop episodes of AF[98] could also be favored by an age-related intrinsic dysfunction of atrial intracellular calcium homeostasis. Nevertheless, knowledge of intrinsic effects of ageing on atrial intracellular calcium handling in humans is lacking and data from experimental animal models are sparse and often inconsistent.[2]

Therefore, this study aimed to analyze the effect of ageing on calcium handling in isolated human right atrial myocytes to gain insight into the pathophysiology of prevalent age-associated derangements of atrial function and atrial disease in humans.

METHODS

Human atrial tissue

A total of 159 isolated right atrial myocytes obtained from 80 patients submitted to elective cardiac surgery were analyzed. The tissue samples were collected as described before (General Methodologies) and permission was given from the patients for the study.

None of the patients had a previous history of AF and all presented with normal left-atrial size at echocardiography (reference range for normal indexed left-atrial diameter: <2.3 cm/m^2). Patients were divided into three age categories: (i) young (<55 years, 49 myocytes, n=21); (ii) middle aged (55 to 74 years, 60 myocytes, n=42); and (iii) old (≥75 years, 50 myocytes, n=11).

Patch-clamp technique

The experimental solutions used for this study had the following composition. Extracellular solution (mM): NaCl 127, TEA 5, HEPES 10, $NaHCO_3$ 4, NaH_2PO_4 0.33, glucose 10, pyruvic acid 5, $CaCl_2$ 2, $MgCl_2$ 1.8 (pH 7.4). The pipette solution contained (mM): aspartatic acid 109, CsCl 47, Mg_2ATP 3, $MgCl_2$ 1, Na_2-phosphocreatine 5, Li_2GTP 0.42, HEPES 10 (pH 7.2 with CsOH). Amphorericin (250 μg/ml) was added to the pipette solution before starting the experiment. Chemicals were from Sigma-Aldrich.

Whole membrane currents were measured in the perforated patch configuration with an EPC-10 amplifier (HEKA Elektronik). The L-type calcium current (I_{Ca}), the current-voltage relationship (IV) for I_{Ca}, the voltage-dependent inactivation, the time constants for fast (tau-1) and slow (tau-2) steady-state I_{Ca} inactivation, recovery of I_{Ca} from inactivation, SR calcium content and spontaneous calcium release were measured as indicated in the General Methodologies.

Confocal calcium imaging

A resonance-scanning confocal microscope (Leica TCS SP5 AOBS) was used to visualize intracellular calcium levels in the frame-scanning mode as previously described in General Methodologies. The cross-sectional area of the cells was measured from the transmission images using Image J software. For calcium imaging, myocytes were loaded with 2.5 µmol/L fluo-4 (Invitrogen). Fluo-4 was excited at 488 nm with laser power set to 20% of maximum and attenuation to 4%. Fluorescence emission was collected between 500 and 650 nm. Calcium transients and waves were measured from the whole cell fluorescence (see Figure 1). For comparison of the maximal and mean fluorescence was measured in a 5 x 10 µm rectangle covering the peak of the calcium transient and the mean fluorescence was measured in the whole cell area.

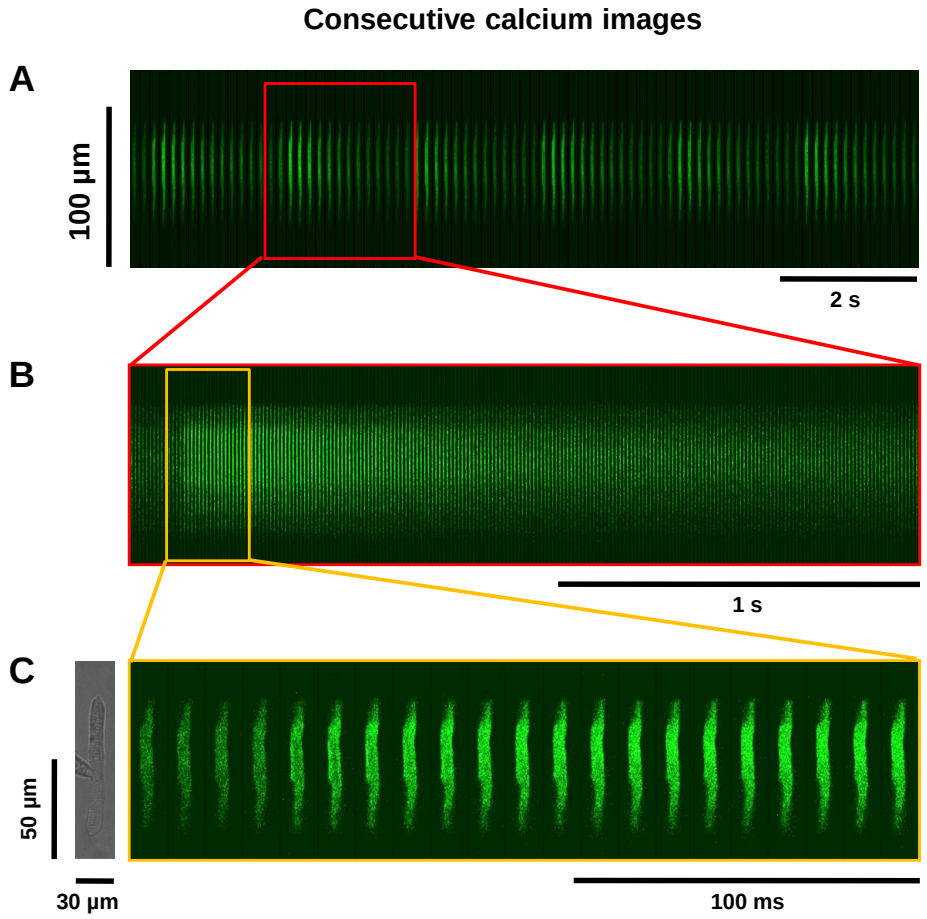

Figure 1. Calcium imaging in isolated human atrial myocytes. (A) Sequence of consecutive time-averaged calcium images from a human atrial myocyte. These images were generated by averaging 15 consecutive original calcium images recorded at a frame rate of 90 Hz (shown in panels B and C). (B) Sequence of calcium images recorded at 90 Hz used to generate the time-

averaged calcium images shown in A. These images are also used to measure the intracellular calcium transient. (C) Amplified segment of calcium images recoded at 90 Hz during the upstroke of the calcium transient. The transmission image of the cell attached to the patch-pipette is shown on the left with indication of the dimensions of the images.

The presence of T-tubular structure was assessed by incubating isolated myocytes with one of the fluorescent dyes Di-4-ANEPPS or RH-237 (2μM) as described before.

To visualize RyR2 clusters, human atrial myocytes were immunofluorescently labelled using a primary anti-RyR2 antibody (Calbiochem). Clusters were detected automatically using a custom-made algorithm (collaboration) previously mentioned.

Analysis of protein levels

Right-atrial tissue samples of about 20 mg were pulverized in liquid nitrogen and 'homogenized' in 200 μl of ice-cold lysis buffer containing 50 mM HEPES pH 7.4, 0.1% (v/v) Tween 20, 100 mM NaCl, 2.5 mM EGTA, 10 mM glycerol-2-phosphate, 10 % (v/v) glycerol and 1 mM DTT supplemented with a cocktail of protease inhibitors (Roche). Proteins were separated by SDS-PAGE (10% acrylamide: bisacrylamide) and electrotransferred onto Immobilon polyvinylidene diflouride membranes (Millipore). Membranes were incubated with primary and secondary antibodies diluted in 5% non-fat dry milk except for DHPR blots, for which SuperBlock™ Blocking Buffer (Thermo Scientific) was used. Antibodies against SERCA (#9580, Cell Signaling Technology), calsequestrin-2 (ab3516, Abcam), DHPR (ab81980, Abcam) and NCX1 (ab135735, Abcam) were used. After a standard washing protocol, detection was performed using the appropriate horseradish peroxidase-labeled IgG and the Supersignal™ detection system (Supersignal West Dura™, Pierce). Molecular-mass standards (Bioline) were used to estimate protein size and glyceraldehyde-3-phosphate dehydrogenase (GAPDH; MAB374, Millipore) was used as a loading control. Immunoblots were digitized (GS-800 Calibrated Densitometer; Bio-Rad) and analyzed with the Quantity One 4.6.3 software (Bio-Rad).

Data Analysis

Statistical analysis was performed using SPSS software. Unless otherwise stated, values were expressed as mean ± SEM. Data sets were tested for normality. Statistical significance was evaluated using Student's t-test and ANOVA was used for comparison of multiple effects. Age, sex, LV ejection fraction, valvular heart disease, ischaemic heart disease and treatment with ACE inhibitors, beta-blockers, angiotensin receptor blockers, and calcium channel antagonists were evaluated and taken into account as potential confounding factors using a general linear model. Bonferroni post-test was used to evaluate the significance of specific effects. Data were also analysed as a continuum and correlations were reported using the Pearson Correlation (r), the slope and the significance (p) for a two-tailed analysis. Differences were considered statistically significant when $p<0.05$.

RESULTS

Study population

Table 1 summarizes the clinical characteristics of the 80 patients included in the study. Older patients had a higher incidence of combined valvular and ischaemic heart disease and greater percentage of coronary bypass surgery than young and middle-aged patients. There were not statistically significant differences in sex, left atrial size, and LV ejection fraction among the 3 age groups. ACE-inhibitors and beta-blockers were administered in nearly 30% of instances and only about 17.5% of patients were on angiotensin receptor blockers.

Table 1: Clinical data of the study patients

	Total (n=80)	< 55 years (n=21)	55-75 years (n=42)	≥75 years (n=17)	p value
Anthropometrics characteristics					
Male *n (%)*	59 (73.8%)	16 (76.2%)	33 (78.6 %)	10 (58.8 %)	ns
BMI Kg/m^2	28.3±5.7	24.9±4.0	29.1±5.0	28.2±4.1	0.004
Echocardiographic characteristics					
LA diameter *mm*	37±5	36±5	38±5	38±4	ns
Indexed LA cm/m^2	2.0±0.2	1.9±0.2	2.0±0.2	2.1±0.2	ns
LVEF *%*	59±13	60±13	59±12	53±16	ns
Heart disease					
Valvular heart disease *n (%)*	33 (41.3%)	10 (47.6%)	17 (40.5%)	6 (35.3%)	ns
Ischaemic heart disease *n (%)*	23 (28.8%)	4 (19.0%)	13 (31%)	6 (35.3%)	ns
Valvular + ischaemic heart disease *n (%)*	11 (13.8%)	2 (9.5%)	5 (11.9%)	4 (23.5%)	0.023
Surgical treatment					
Aortic valve replacement *n(%)*	40 (50%)	10 (47.6%)	20 (47.6%)	10 (58.8%)	ns
Mitral valve replacement *n (%)*	3 (3.8%)	1 (4.8%)	2 (4.8%)	0	ns
Tricuspid valve surgery *n(%)*	6 (8.1%)	4 (19.0%)	2 (4.8%)	0	ns
CABG *n (%)*	35 (43.8%)	3 (14.3%)	20 (47.6%)	12 (70.6%)	0.002
CABG + valve replacement *n (%)*	16 (20.0%)	1 (4.8%)	8 (19%)	7 (41.2%)	0.020
Pharmacological treatment					
ACE-inhibitors n *%*	24 (30.0%)	6 (28.6%)	11 (26.2%)	7 (41.2%)	ns
Angiotensin receptor blocker n *%*	14 (17.5%)	1 (4.8%)	9 (21.4%)	4 (23.5%)	ns
Beta-blockers n *%*	23 (28.8%)	6 (28.6%)	11 (26.2%)	6 (35.3%)	ns
Calcium channels antagonists n *%*	15 (18.8%)	1 (4.8%)	9 (21.4%)	5 (29.4%)	ns

p values are from ANOVA analysis.
Abbreviations: BMI: body mass index; LA: left atrium; LVEF: left ventricular ejection fraction; CABG: coronary artery bypass grafting; ACE: angiotensin conveter enzyme.

Measurements of cross sectional area of the myocytes (Figure 2A) and cell membrane capacitance (Figure 2B) revealed no significant differences between the three age groups, suggesting that ageing does not affect cell surface area or cell size. Moreover, T-tubular structures were not detectable in myocytes from any of the three age groups (Figure 2C).

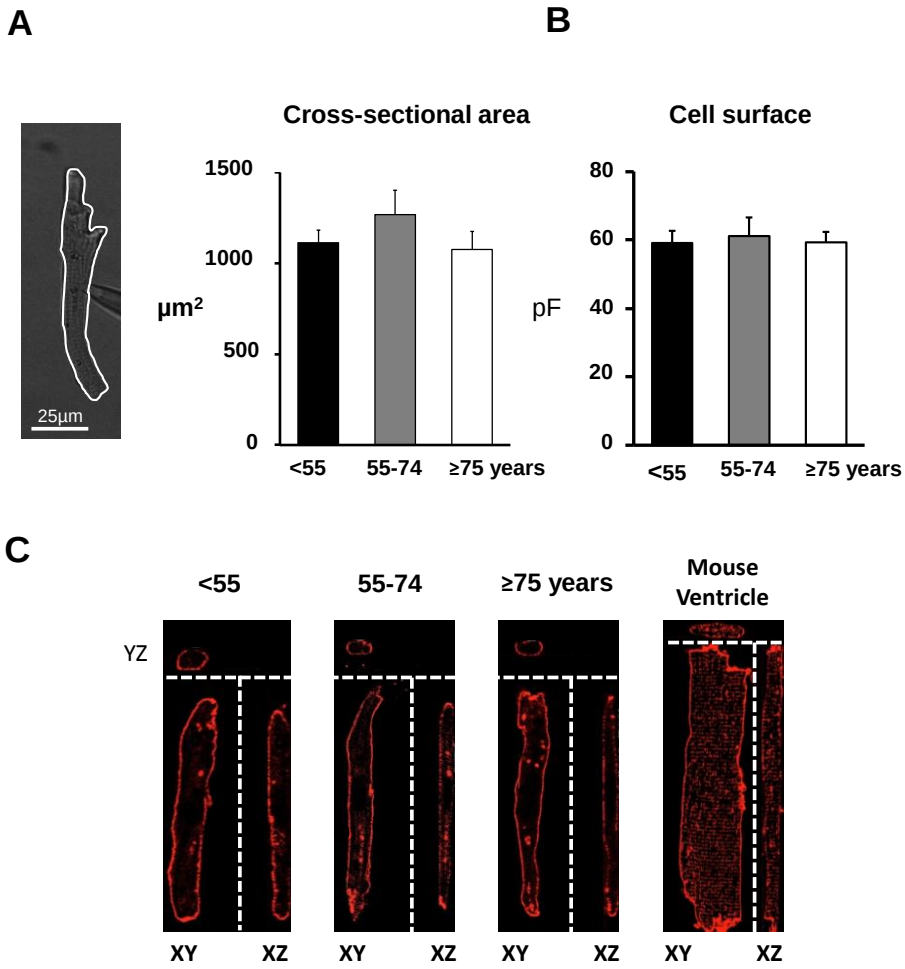

Figure 2. Effect of ageing on human atrial myocyte size and structure. (A) Left panel shows a transmission image of a human atrial myocyte. The cross sectional area was measured as the area delimited by the white line. The average cross-sectional areas of myocytes from young (<55 years), middle aged (55-74 years), and old (≥75 years) patients are shown in the right panel. (B) Cell capacitance measured in 21 young, 42 middle aged and 17 old patients. (C) Staining of the sarcolemma with RH-237 in atrial myocytes from a young (<55), middle aged (55-74) and an old (≥75) patient. T-tubular structures were not observed in any of 36 myocytes from 6 patients covering an age-range from 37 to 79 years. Staining of a mouse ventricular myocyte is shown on the right as a positive control for T-tubular staining. XY, XZ and YZ indicate the scan direction.

Ageing reduces the intracellular calcium transient amplitude and decay

Confocal calcium imaging was used to compare the amplitude and kinetics of intracellular calcium transients between the three age groups. Figure 3A shows contact sheets of consecutive time-averaged calcium images and the resulting calcium transient recorded in right-atrial myocytes from a young (top panel) and an old patient (bottom panel). As shown in Figure 3B, the calcium transient amplitude decreased gradually with age and was 3.2-fold smaller in myocytes from patients 75 years or older than in those younger than 55 years ($p<0.01$).

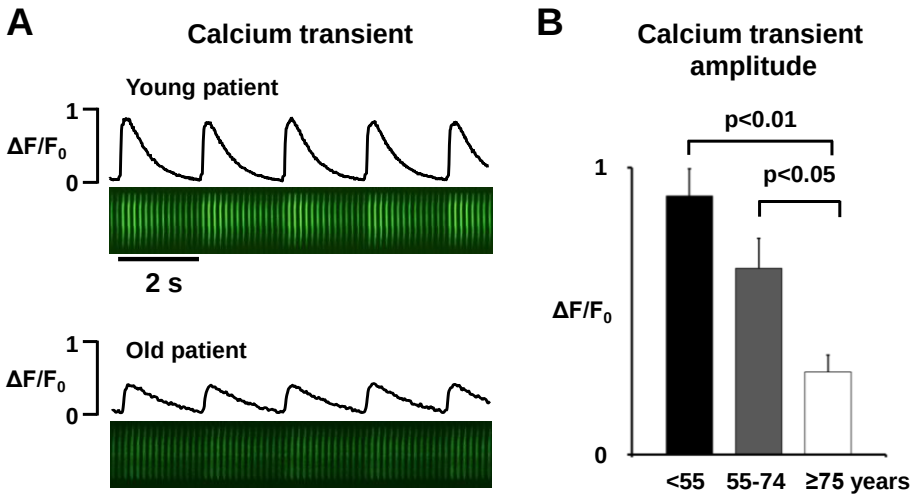

Figure 3. Effects of ageing on the intracellular calcium transient. (A) Calcium transient traces and the corresponding sequence of 68 consecutive time-averaged calcium images, recorded in myocytes from a young and an old patient. (B) Average calcium transient amplitude in myocytes from young (8 cells; n=7) middle age (10 cells; n=7), and old (6 cells; n=5) patients.

Segmentation of the cells in three concentric layers, extending from the sarcolemma to the centre of the cell (Figure 4A), also revealed that there was an age-related delay in the propagation of the calcium transient from the sarcolemma to the cell centre (Figure 4B). This delay was apparently not attributable to the presence of T-tubular structures, as they were not detected in any of the human atrial myocytes analysed (Figure 2C).

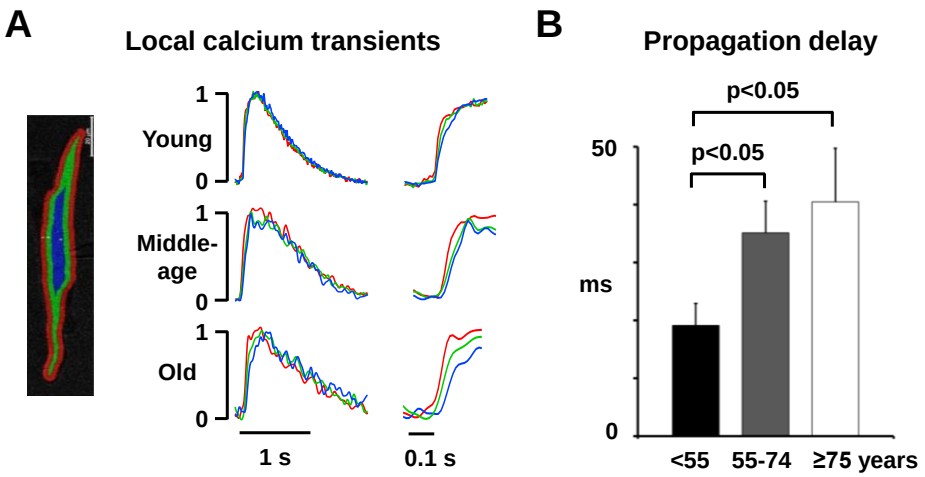

Figure 4. Age-related delay in the propagation of the calcium transient. (A) Calcium transients measured in three concentric rings (shown on the left). Transients were normalized to their peak values in a young, middle aged, and an old patient. The upstroke of the calcium transient is amplified on the right. Notice the delay between the calcium transient near the sarcolema (SL; red) and the cell centre (CC; blue) in the old patient. (B) Average time-delay between the calcium transient in the SL and CC for the three patient groups.

The decay of the calcium transient also became slower with increasing age (Figure 5A), as reflected by a significantly longer duration at the half maximal amplitude (FDHM) in the oldest patient group (Figure 5B).

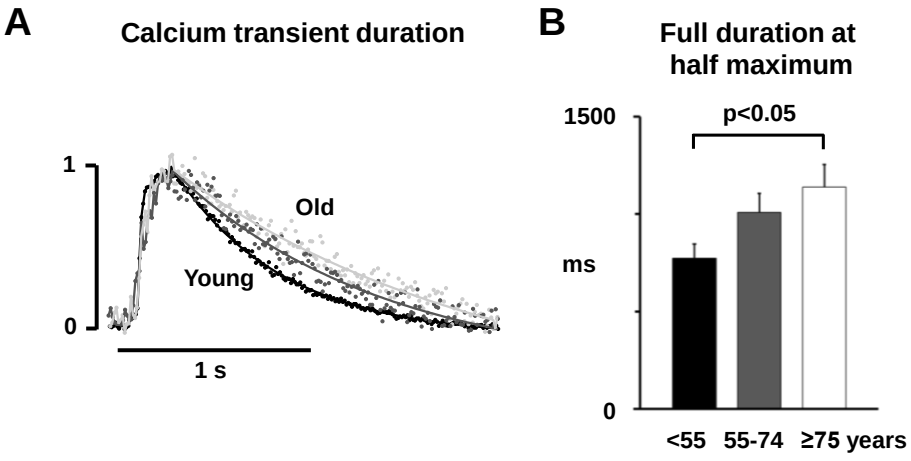

Figure 5. Effects of ageing on the decay of the calcium transient. (A) Superimposed calcium transients normalized to their peak amplitude. (B) Average duration of the calcium transient at half maximal amplitude. P-values for significant differences are indicated above the corresponding bars.

Ageing reduces the L-type calcium current (I_{Ca})

To identify the mechanisms underlying the age-dependent depression of the calcium transient, we examined the effects of age on sarcolemmal calcium entry. Figure 6A shows recordings of I_{Ca} elicited at different membrane potentials in a young and an old patient demonstrating that ageing was associated with depressed I_{Ca} amplitude without changes in the shape of the current-voltage relationship (Figure 6B). Accordingly, continuous stimulation at 0.5 Hz revealed an age-dependent decrease in the I_{Ca} amplitude at steady state from 2.4±0.3 pA/pF in young to 2.1 ± 0.2 pA/pF in middle aged and 1.4±0.2 pA/pF in old patients ($p<0.001$, young vs. old patients, Figure 6C). The effect was independent of confounding clinical factors included in the statistical analysis.

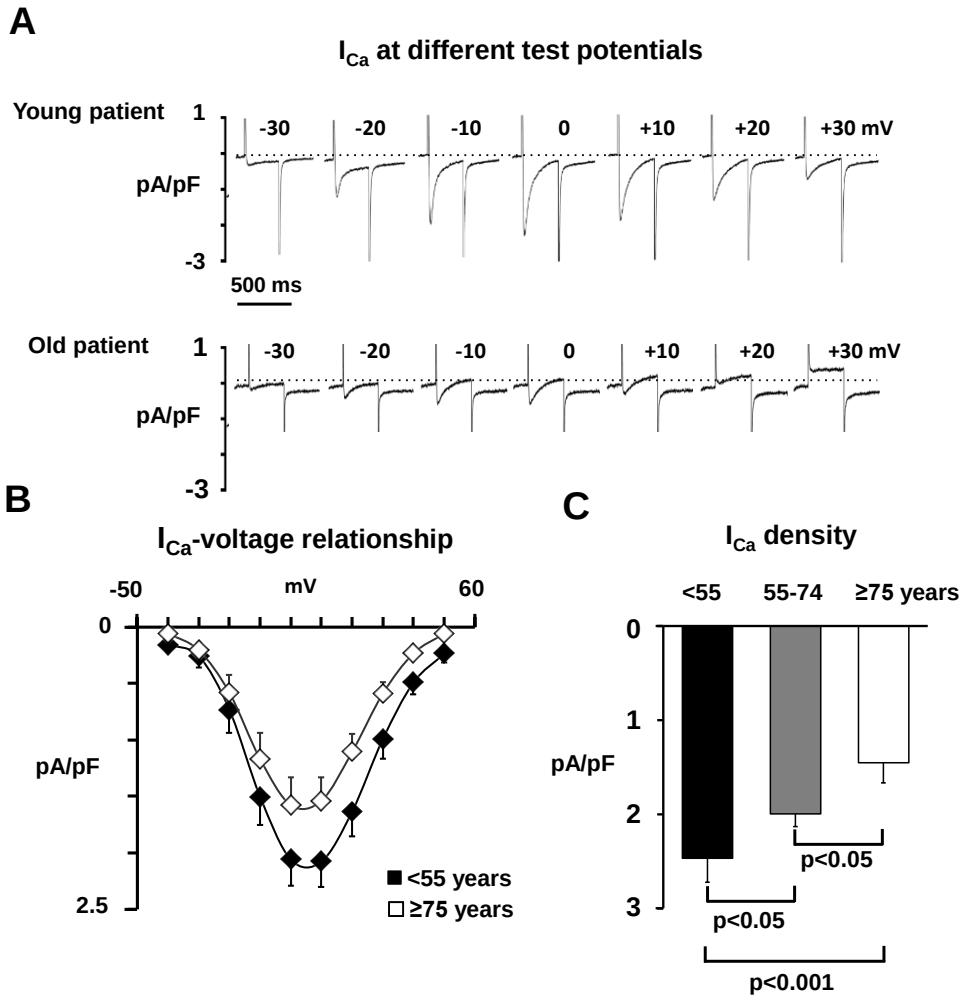

Figure 6. Effects of ageing on the L-type calcium current. (A) Representative L-type calcium currents elicited by depolarization to different membrane potentials (indicated above traces) in a

young (20 years) and an old patient (77 years). (B) The I_{Ca}-voltage relationship in 21 young (<55) and 17 old (≥75) patients. (C) Peak I_{Ca} density in 21 young (<55), 42 middle aged (55-74) and 17 old (≥75) patients.

Western blot analysis revealed a concurrent age-related reduction in the expression of the L-type calcium channel alpha-subunits in patients (Figure 7A).

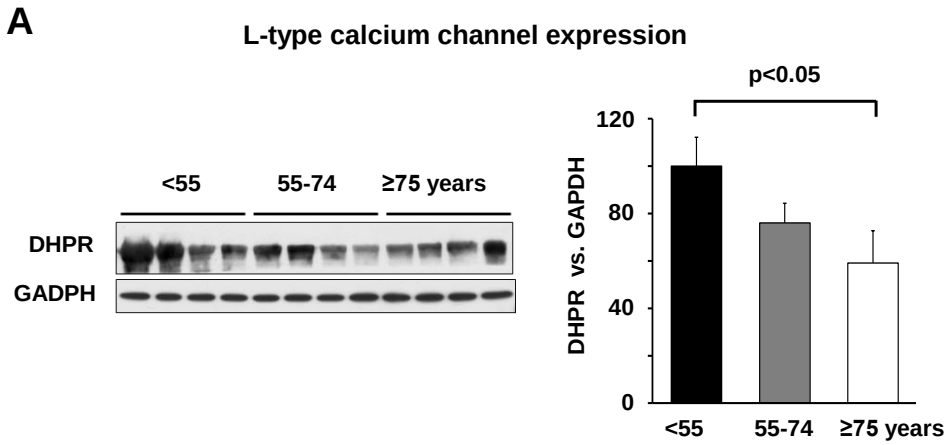

Figure 7. Effects of ageing on L-type calcium channel expression. (A) Representative western blot of the L-type calcium channel alpha subunit (DHPR) in young (<55 years), middle aged, and old (≥75 years) patients. Average DHPR levels from seven young, eight middle aged, and seven old patients are expressed as percentage of the GAPDH level in the right panel. P-values for significant differences are indicated above the corresponding bars.

Moreover, analysis of the data as a continuum confirmed that there is a significant correlation between age and the I_{Ca} density (r=0.419; p<0.001; see Figure 8).

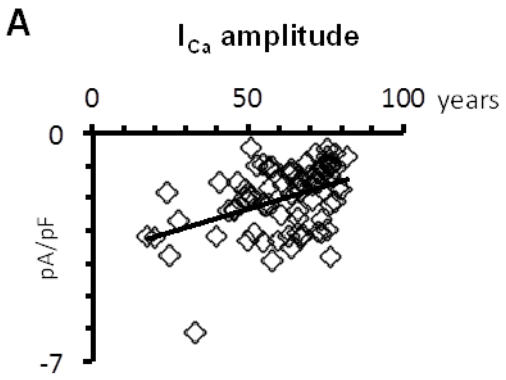

Figure 8. Analysis of I_{Ca} amplitude data as a continuum. (A) Age-dependency of I_{Ca} (r=0.419, p<0.001).

Analysis of intrinsic I_{Ca} properties in the older and younger patients showed no significant differences in voltage-dependent inactivation (Figure 9A-C) or in recovery of I_{Ca} from inactivation (Figure 9D-F).

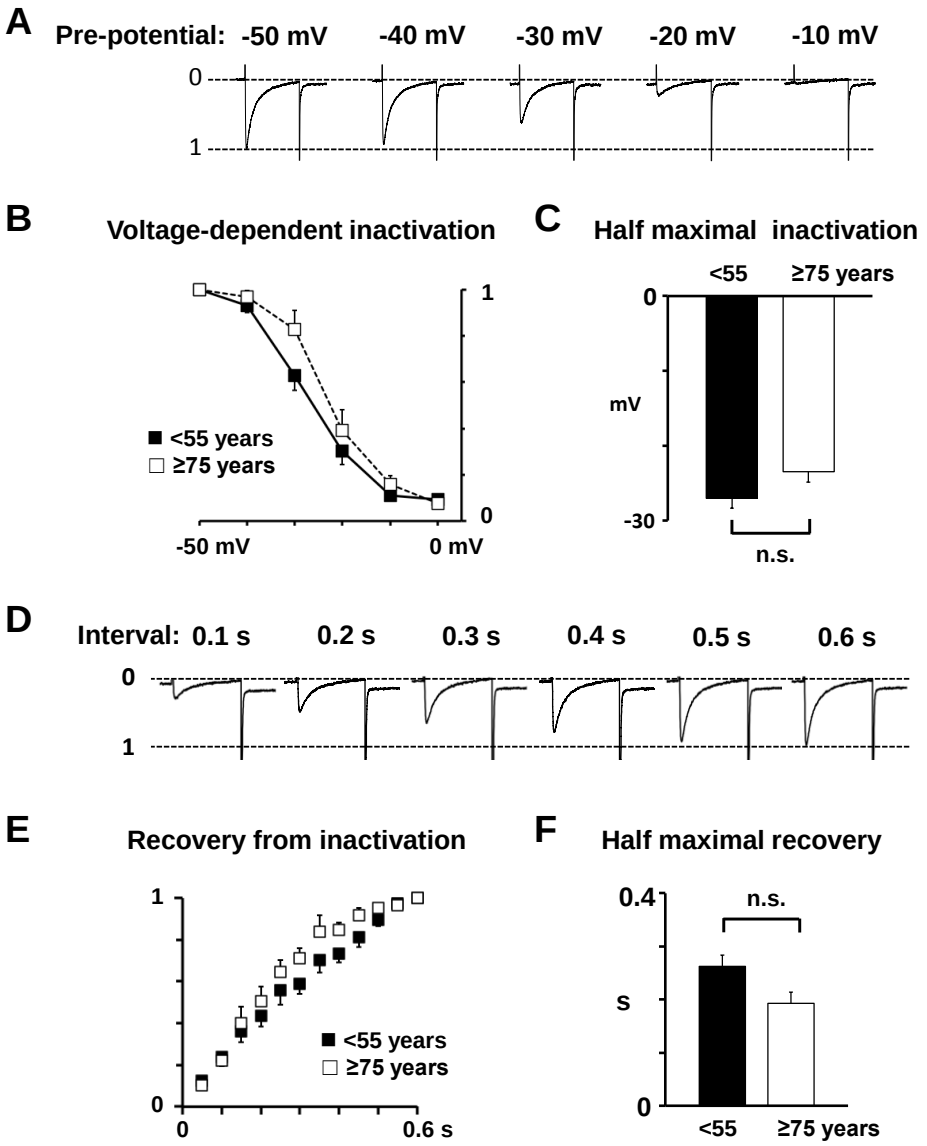

Figure 9. Effects of ageing on intrinsic L-type calcium channel properties (A) Representative I_{Ca} traces obtained after a prepulse to different membrane potentials (given above traces). Current traces are normalized to the I_{Ca} amplitude at -50 mV. (B) Relationship between the prepulse potential and the I_{Ca} amplitude. (C) Bar diagram of the voltage for half-maximal I_{Ca} inactivation. Values were obtained by fitting data in (B) with a Boltzmann equation. (D) Representative I_{Ca} traces elicited at different times (given above traces) after the preceding stimulation pulse. (E) Relationship between pulse interval and the recovery of the I_{Ca} amplitude. Values were normalized to the I_{Ca} amplitude at 0.6s. (F) Bar diagram of the time for half-maximal recovery of I_{Ca}. Values

were obtained by fitting data in (E) with an exponentially decaying function (n.s. indicates a non-significant difference).

However, both fast and slow steady-state I_{Ca}-inactivation were significantly slower in patients 75 years or older when compared to the patients younger than 55 years (Figure 10A). Thus, the time constant (tau-1) for fast I_{Ca} inactivation increased by 44% from 14.5±0.9 ms in young to 20.9±1.9 ms in old patients ($p<0.01$). Similarly the tau-2 for slow I_{Ca} inactivation was 73±3 ms in young vs. 120±12 ms in old patients ($p<0.001$).

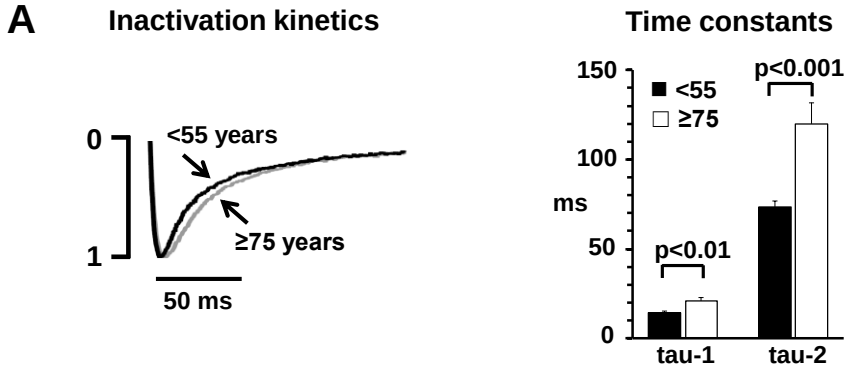

Figure 10. Effects of ageing on I_{Ca}-inactivation. (A) Normalized I_{Ca} traces from a young and an old patient. Average fast (tau-1) and slow (tau-2) time constants are shown in the right panel. P-values for significant differences are indicated for corresponding bars. All values are from 21 young (<55) and 17 old (≥75) patients (n.s. indicates a non-significant difference).

Ageing reduces sarcoplasmic reticulum calcium content

Since ageing concurred with slowing of the decay of the calcium transient and with down-regulation of sarcolemmal calcium entry through the L-type calcium channel, we also examined whether age affected removal of calcium from the cytosol by the SR during cell relaxation. Indeed, as shown in Figure 11A, we observed and age-related decrease in the caffeine releasable SR calcium content [from 10.1±0.8 amol/pF in the younger patients to 6.5±0.4 amol/pF in the middle aged patients ($p<0.01$) and 6.4±0.6 amol/pF in the older group ($p<0.05$)]. Western blot analysis revealed that not only SERCA2 (Figure 11B) but also Calsequestrin-2 (CSQ-2. Figure 11C) protein levels decreased with age.

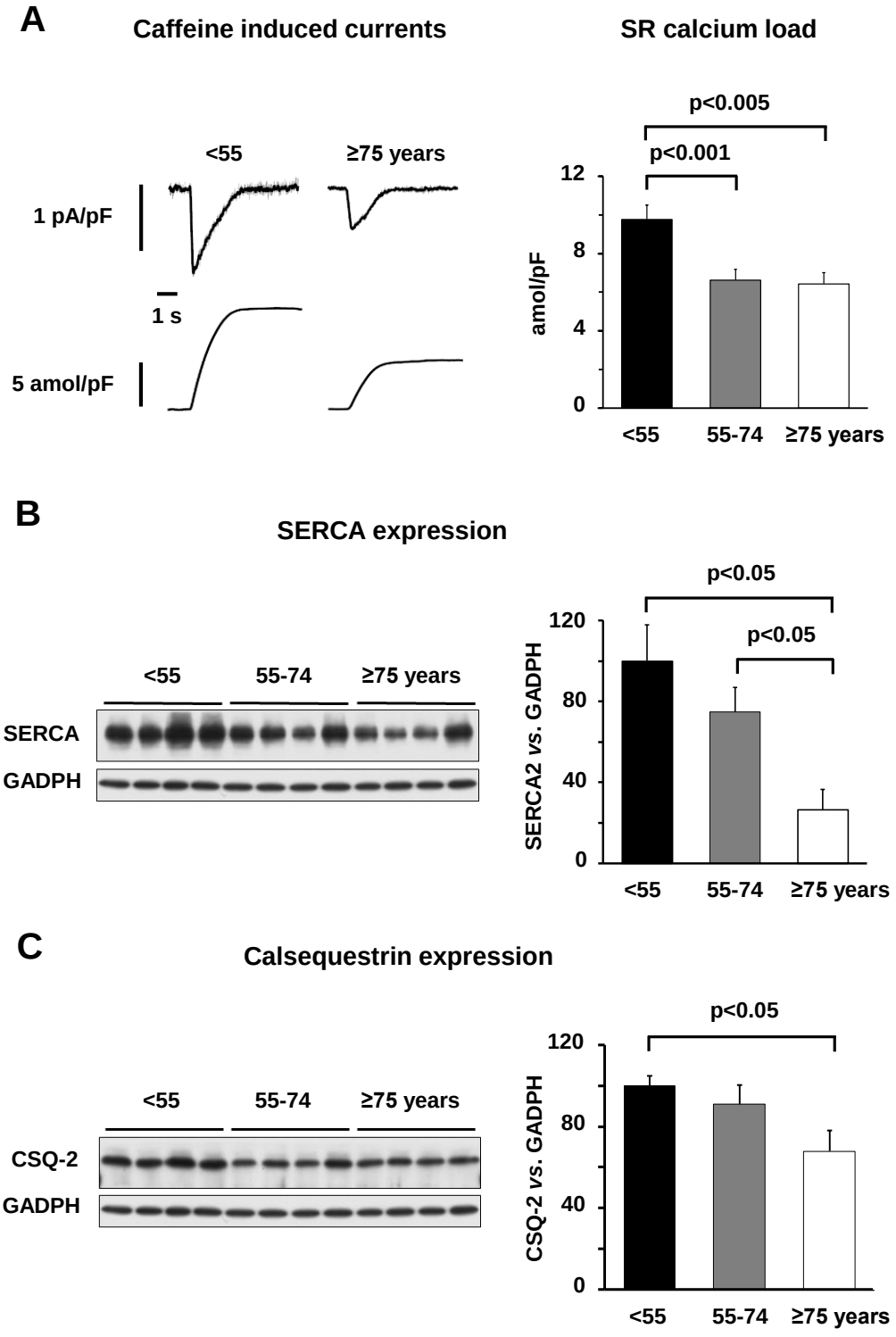

Figure 11. Effects of ageing on sarcoplasmic reticulum calcium uptake (A) Traces of the transient inward current elicited by caffeine (top traces) and its time integral (bottom traces) in a young and an old patient. Average time integrals are shown on the right. (B) Representative western blot of SERCA2 in young (<55 years), middle aged, and old (≥75 years) patients. Average SERCA2 levels from seven young, eight middle aged, and seven old patients are expressed as percentage of the GAPDH level on the right. (C) Representative western blot of CSQ-2 in young,

middle-aged, and old patients. Average CSQ-2 levels from seven young, eight middle aged, and seven old patients are expressed as percentage of the GAPDH level on the right.

The effect of ageing on SR calcium load was independent of confounding clinical factors, and analysis of the data as a continuum confirmed a significant correlation between age and SR calcium content (r= -0.366; p<0.001; see Figure 12).

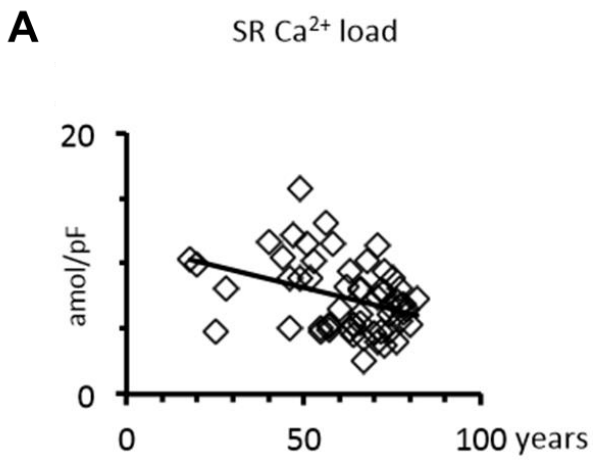

Figure 12. Analysis of SR Ca^{2+} load data as a continuum. (A) Age-dependency of the caffeine releasable SR Ca^{2+} content (r=-0.366, p<0.001).

In contrast, ageing was not associated with significant changes in the expression of the cardiac Na-Ca exchanger nor with its ability to extrude calcium across the sarcolemma (see Figure 13).

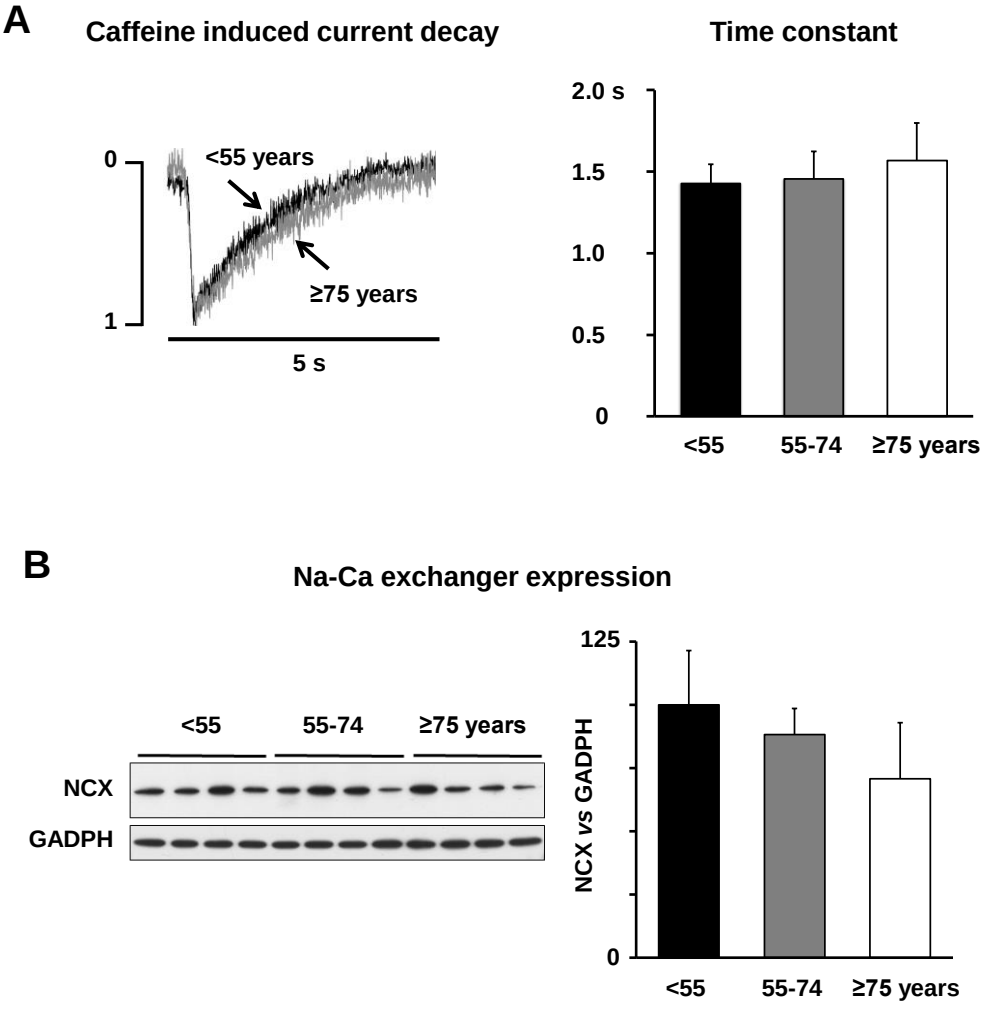

Figure 13. Effect of ageing on the expression and activity of the Na-Ca exchanger. (A) Normalized caffeine induced NCX currents recorded in myocytes from a young (black trace) and an old patient (grey trace). The time constant for the decay of the caffeine induced NCX current is shown on the right for 21 young, 42 middle aged and 17 old patients. (B) Representative western blot of atrial samples from young (<55), middle aged (55-74) and old (>75) patients. Average Na^+-Ca^{2+} exchange (NCX) levels from seven young, eight middle aged, and seven old patients are shown as percentage of the GADPH level on the right.

Ageing does not alter spontaneous calcium release

To assess whether ageing could favour a potentially arrhythmogenic release of calcium from the SR, we measured the frequency of spontaneous calcium waves (Figure 14A) and/or the associated transient inward currents (I_{TI}) in myocytes from the three age groups. Figure 14B demonstrates that the I_{TI} amplitude was proportional to the amplitude of the calcium wave (slope= 0.48; r= 0.54, $p<0.05$).

Similarly, 2D analysis of the calcium image sequences showed that there was a linear relationship between the maximal amplitude of the calcium wave with the mean calcium wave amplitude (slope= 1.6; r= 0.86, p<0.05). However, no age-related differences were observed in these two parameters.

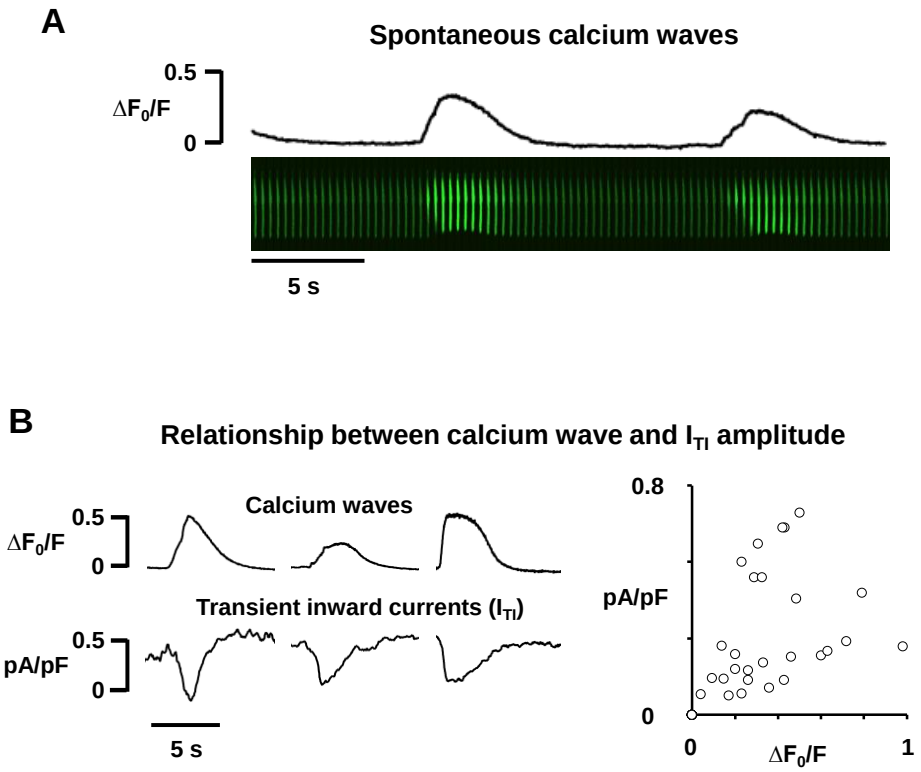

Figure 14. Effects of ageing on spontaneous SR calcium release. (A) Sequence of consecutive time-averaged calcium images with two spontaneous calcium waves. The whole cell calcium signal is shown above images. (B) Simultaneous recordings of calcium waves and concurrent I_{TI}. The relationship between the I_{TI} amplitude and the calcium wave amplitude is shown on the right.

The I_{TI} frequency and the I_{TI} amplitude were comparable among the three age groups (Figure 15C-E) at holding potentials of -80 or -50 mV. Analysis of these data as a continuum confirmed the lack of linear correlation between age and I_{TI} frequency (r= -0.118; P= n.s.) or amplitude (r= -0.237; P= n.s. see Figure 16).

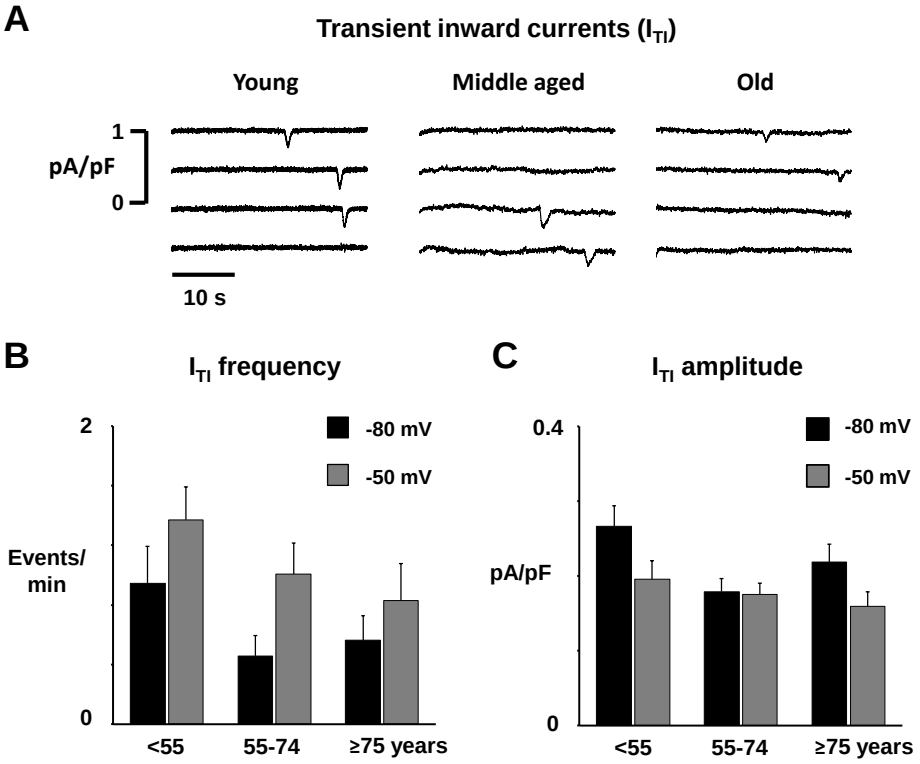

Figure 15. Effects of ageing on spontaneous SR calcium release. (A) Spontaneous inward currents recorded in myocytes from a young (<55 years), a middle aged (55-74 years), and an old (≥75 years) patient. (B) Average transient inward current (I_{TI}) frequency. (C) Average I_{TI} amplitude. Values are from 21 young, 42 middle aged and 17 old patients.

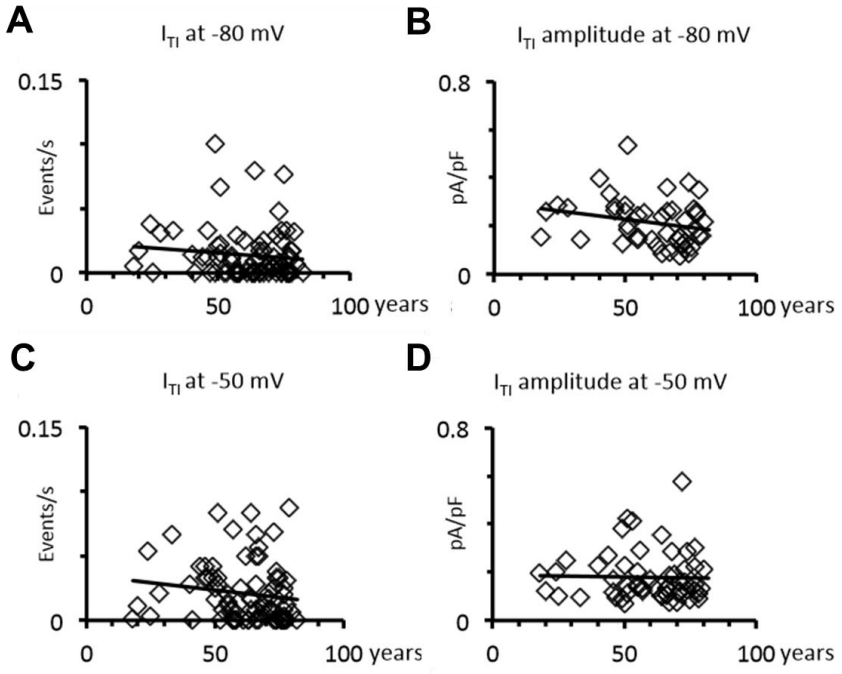

Figure 16. Analysis of data as a continuum. (A) Age-dependency of the I_{TI} frequency at -80 mV (r=-0.118, p=0.30). (B) Age-dependency of the I_{TI} amplitude at -80 mV (r=-0.237, p=0.11). (C) Age-

dependency of the I_{TI} frequency at -50 mV (r=-0.149, p=0.18). (D) Age-dependency of I_{TI} amplitude at -50 mV (r=-0.03, p=0.85).

In line with this, the RyR2 density was not different in a total of 96 myocytes from the three patient groups (Figure 17).

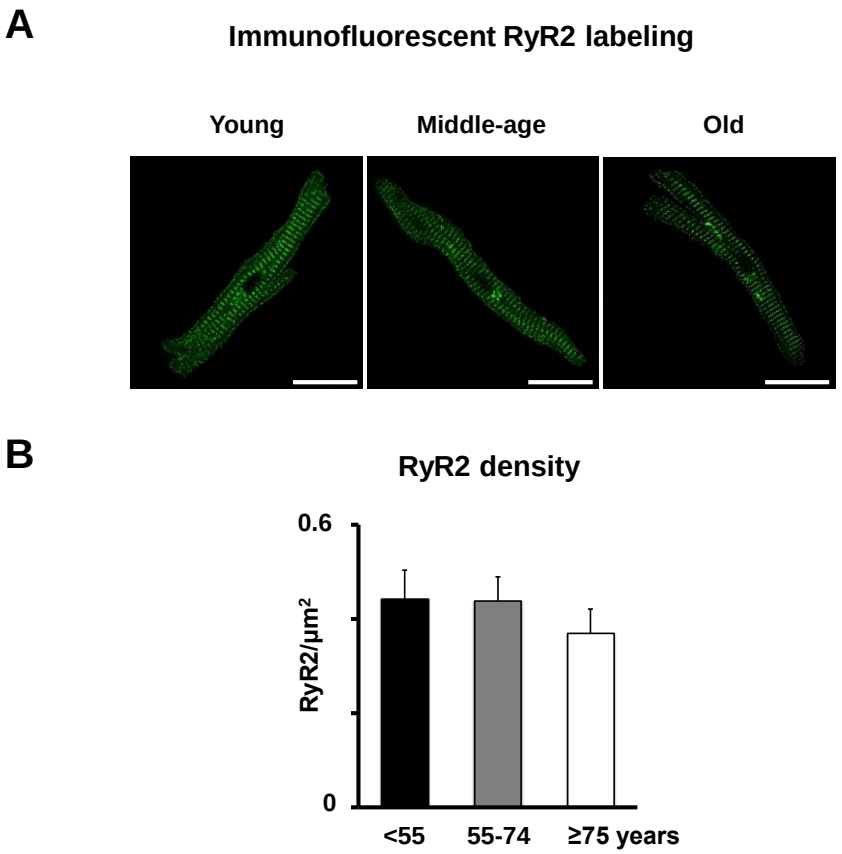

Figure 17. Effect of ageing on the RyR2 density. (A) Representative images of immunofluorescent labeling of the RyR2 in human atrial myocytes froma a young (<55), middle aged (55-74) and an old (≥75) patient. (B) average RyR2 density in 11 myocytes from 3 young, 53 myocytes from 11 middle aged, and 32 myocytes from 7 old patients. There were no significant differences among the three age groups and no correlation between age and RyR2 density (density = 0.0001 x age +0.436, R=0.006). White scale bars represent 20 µm.

DISCUSSION

Main findings.

To our knowledge, this is the first study reporting age-dependent changes in intracellular calcium homeostasis in isolated human right atrial myocytes. We observed a reduction in the expression of several key calcium regulatory proteins with age that lead to coherent concurrent functional alterations in the intracellular calcium homeostasis. Specifically we found: (i) reduction in the expression of the alpha sub unit of the L-type calcium channel and decreased I_{Ca} density; (ii) reduction in SERCA2 and CSQ-2 expression associated with lower caffeine releasable SR calcium content; (iii) slower propagation of calcium transient towards the cell centre.

These observations, likely account for the observed three-fold reduction of the calcium transient amplitude and slowing of its decay in patents older than 75 years, which may favor a progressive decline in atrial contractile function with age.

Effects of ageing on intracellular calcium homeostasis

Most of the studies analyzing the effects of ageing on cardiomyocyte function have been performed in ventricular myocytes from small rodents and have provided inconsistent results. Indeed, some studies found increased calcium transients and high I_{Ca} density in rodents[2] and in sheep,[99] whereas others failed to detect changes in I_{Ca} or SR calcium handling proteins[100] or even found depressed levels of I_{Ca} density or SR calcium handling proteins.[101–104]

Here we report for the first time on age-dependent changes in humans using isolated atrial myocytes and tissue samples. The findings revealed a gradual decay in the peak I_{Ca} density with age, which is linked to a reduction in the expression of the alpha subunit of the L-type calcium channel. Ageing has also been associated with increased levels of reactive oxygen species (ROS) in rabbit hearts [105], and in humans with AF, elevation of ROS caused by reduced glutathione levels have been proposed to underlie reduced $I_{Ca.}$[106] Thus, increased ROS could be a possible mechanism underlying age-related I_{Ca} reduction.

Similarly, the SERCA2 and CSQ-2 expression was significantly reduced in patients aged 75 years or older and concurred with significantly lower caffeine releasable SR calcium content and a reduction in the calcium release-induced I_{Ca} inactivation. These observations, likely account for the observation of a three-fold smaller calcium transient amplitude and a 50% slowing of its decay in the older patients. However, we cannot rule out additional modulation of SR calcium homeostasis caused by concurrent age-dependent changes in phospholamban expression and/or phosphorylation. The lower SR calcium content in the old age group might also contribute to the observed slowing of the propagation of the calcium transient from the sarcolemma to the cell centre, especially since t-tubular structures were not detected in any of the three age groups.

While the reduction in SERCA and CSQ-2 expression is expected to contribute to the observed reduction of SR calcium loading in the oldest patients, low CSQ-levels have also been reported to favor spontaneous calcium release and arrhythmia in transgenic mouse models.[107–109] However, the I_{TI} frequency was not different among the three age groups examined suggesting that the concurrent lowering of SERCA and L-type calcium channels may reduce the amount of calcium available for binding to CSQ-2 sufficiently to prevent an increase in spontaneous SR calcium release events.[110] The lack of significant age-dependent changes in the amplitude of the calcium-wave front or the global calcium wave, and in the I_{TI} frequency also suggests that ageing *per se* is likely not responsible for a higher rate of spontaneous calcium release events reported in myocytes from AF-patients.[12,14,15]

Considerations on the model

Human right-atrial tissue is currently accessible in vivo during pump-on cardiac surgery because cannulation of the right atrium is always required to set-up the extracorporeal circulation. In contrast, extraction of left-atrial tissue samples would only be justifiable in patients undergoing mitral valve surgery, but in these cases usually the left atrium is diseased and the cavity dilated. Thus, analysis of atrial cellular electrophysiology in nearly normal human atrial myocytes is more feasible in the right than in the left atrium.

Cell viability is a common challenge when using isolated human cardiomyocytes. Therefore, only elongated cells with a clear striation were included in this study. Moreover, myocytes with spontaneous I_{TI} were only accepted for further study if the I_{TI} frequency remained stable for at least 5 minutes in control conditions. Finally, experiments were performed in the amphotericin perforated patch configuration. This technique avoids dialysis of the cytosol through the patch pipette, renders the current recordings stable for more than 30 minutes, and has yielded reproducible recordings of I_{Ca}, SR calcium loading, and I_{TI} in human atrial myocytes.[12,14,111–114]

Another source of potential concern is the heterogeneous clinical profile of patients undergoing cardiac surgery and their individualized pharmacological treatments. To deal with this issue, we included only patients with normal left-atrial size and no previous history of AF. Moreover, possible confounding effects of sex, the presence of valvular or ischaemic heart disease, the treatment of patients with ACE-inhibitors, beta-blockers, angiotensin receptor blockers, calcium antagonists as well as the LV ejection fraction were taken into account in the statistical analysis of the electrophysiological data.

Interestingly, we did not observe any differences in cross sectional area or myocyte capacitance among the three patient groups, suggesting that the observed effects of ageing on calcium handling are not secondary to myocyte hypertrophy.

Clinical implications

The age-related changes in cellular calcium homeostasis observed in our patients may have mechanical and electrophysiological implications.

First, as a result of the reduction of I_{Ca}, the SR calcium content and the calcium transient amplitude, it is conceivable that the mechanical efficiency of the atria will decline over age. In this regard, information on the intrinsic atrial contractility in elderly subjects based on invasive atrial hemodynamic recordings is not available. However, echocardiographic studies analyzing atrial dynamics and volumes have found left-atrial dilation and reduced atrial mechanical function with ageing, especially in subjects older than 80.[95,96,115] Likewise, older age has been associated with reduced atrial functional response to pharmacological adrenergic

stress using 3D cardiovascular magnetic resonance.[116] This indirect evidence combined with the present data, suggest that further invasive assessment of the intrinsic atrial contractile properties is warranted, to establish the concept that ageing can directly blunt atrial mechanical function.

Secondly, the present study shows that ageing *per se* causes changes in intracellular calcium homeostasis that have previously been related to the genesis of AF [98]. Specifically, the reduction of the I_{Ca} density and the calcium transient observed in our old patients are hallmarks of myocytes from patients with AF [12,13] or from patients at high risk for this arrhythmia;[117] suggesting that these age-dependent changes could contribute to increase the risk of AF in the elderly. Possibly, the electrophysiological derangements reported here work in concert with concurrent age-related structural alterations such as increased atrial fibrosis and amyloid deposition[118], or arrhythmogenic conduction abnormalities and local microreentry linked to non-uniform cellular connectivity of structural origin.[119] On the other hand, an increased frequency of spontaneous calcium release, another characteristic feature of myocytes from patients with AF,[12,14,15] was not observed in the old patient group. This lack of frequent SR calcium release could in part be interpreted as a protective effect of the reduced I_{Ca} density and SR calcium content in the ederly.

In summary, we report ageing-associated depression of L-type calcium channel expression and current, SERCA-2, CSQ-2 and SR calcium content. These electrophysiological derangements likely underlie a 3.5-fold reduction of the calcium transient amplitude and slowing of its decay in myocytes from the older patients and may blunt contraction and relaxation in ageing human atria. Moreover, reduced I_{Ca} and calcium transient are hallmarks of atrial myocytes from patients with AF, which could contribute to increase the risk of this arrhythmia in the elderly.

II. PROGEROID *ZMPSTE 24*$^{-/-}$ MICE RECAPITULATE AGE-DEPENDENT ALTERATIONS OF THE CALCIUM HOMEOSTASIS IN HUMAN ATRIAL MYOCYTES

INTRODUCTION

The LMNA gene encodes A-type lamins (lamin A and lamin C), key components of the mammalian nuclear envelope with important structural and regulatory functions affecting signaling, transcription, and chromatin organization, among other processes.[120] To yield mature lamin A, the precursor prelamin A undergoes a series of posttranslational modifications, including sequential farnesylation at the cysteine in the CSIM (cysteine-serine-isoleucine-methionine) motif, cleavage of the SIM residues, carboxymethylation of the newly accessible cysteine, and a final proteolytic cleavage by the zinc metalloprotease ZMPSTE24/FACE-1.[17] Mutations in the LMNA gene or defective processing of prelamin A cause a group of human diseases termed laminopathies, including the premature aging disorder Hutchinson-Gilford progeria syndrome (HGPS, OMIM #176670), a very rare genetic disorder with an estimated prevalence of 1 in 21 million people.[121] HGPS patients exhibit accelerated atherosclerosis and arterial stiffness, leading to premature death at an average age of 14.6 years, predominantly from myocardial infarction, heart failure or stroke.[122,123] Most HGPS patients carry a non-inherited de novo heterozygous synonymous mutation at codon 608 in LMNA (c.1824C>T:GGC>GGT; p.G608G), which activates the use of an internal 5' splicing site in exon 11 that causes the synthesis of progerin. This unprocessed form of prelamin A lacks 50 aminoacids encompassing the ZMPSTE24 cleavage site and therefore remains permanently farnesylated.[17] ZMPSTE24 mutations have also been linked to several other human progeroid syndromes,[124,125] reinforcing the notion that accumulation of either progerin or prelamin A accelerates cellular aging. Moreover, progerin and prelamin A are both expressed in cells and tissues of normally aging non-HGPS individuals, suggesting their involvement in physiological aging.[16,17]

Genetically-modified mice expressing prelamin A or progerin have enabled the study of mechanisms underlying progeria[126] and testing of the efficacy of various therapies.[127,128] Here, we examined age-related cardiac electrical abnormalities and the underlying molecular mechanisms in *Zmpste24*-null mice (*Zmpste24*$^{-/-}$) in order to investigate how this progeria model affects the intracellular calcium homeostasis in isolated ventricular myocytes and whether the model reproduces the age-dependent changes observed in human atrial myocytes.

METHODS

Mouse cardiomyocyte isolation and intracellular calcium measurements

Ventricular myocytes were isolated from mouse hearts by enzymatic digestion as described in General Methodologies.

Confocal calcium imaging was performed in fluo-4 loaded ventricular myocytes using a Leica TCS AOBS SP5 resonance scanning confocal microscope equipped with a 63X 1.3 NA glycerol objective. Fluo-4 was excited at 488 nm and fluorescence emission was measured between 500 and 650 nm in the frame scanning mode.[112] Calcium transients were recorded at room temperature (20-22ºC) and elicited by subjecting myocytes to electrical field stimulation (5 ms pulses, 5-15 V) at increasing stimulation frequency (0.5 to 4 Hz). Calcium transients and spontaneous calcium waves were automatically detected and quantified using custom-made programs.[94]

Perforated patch-clamp in ventricular myocytes

Ionic currents in ventricular myocytes were measured with the perforated patch-clamp technique.[14] L-type calcium currents were elicited by a 100 ms depolarization to 0 mV from a holding potential of -80 mV. Na^+- currents were eliminated by inclusion of 30 μM tetrodotoxin in the bath solution and a 50-ms

prepulse from -80 to -50 mV. Transient inward currents and the amount of calcium released from the SR were measured as described in General Methodologies.

Statistical analysis

Data are presented as mean±SEM. Statistical significance was assessed by unpaired two-tailed t-test for paired comparisons, or one-way ANOVA followed by Newman–Keuls post-hoc test for multiple comparisons. Statistical significance was assigned at $p<0.05$.

RESULTS

Based on the effects of ageing in human atrial myocytes (see chapter I), we investigated the intracellular calcium homeostais properties in the *Zmpste24*-/- mice, in order to determine if this model reproduces the observations in aged human cardiomyocytes.

Effect of *Zmpste 24*$^{-/-}$ on the intracellular calcium transient

Intracellular Ca^{2+} transients recorded with confocal mycroscopy in isolated cardiomyocytes from WT and *Zmpste24*$^{-/-}$ mice, were paced at 0.5 Hz showing a significantly smaller calcium transient amplitude (Figure 1A) and a longer duration of the transient (at half maximal amplitude) (FDHM) in Zmpste24$^{-/-}$ cells (Figure 1B).

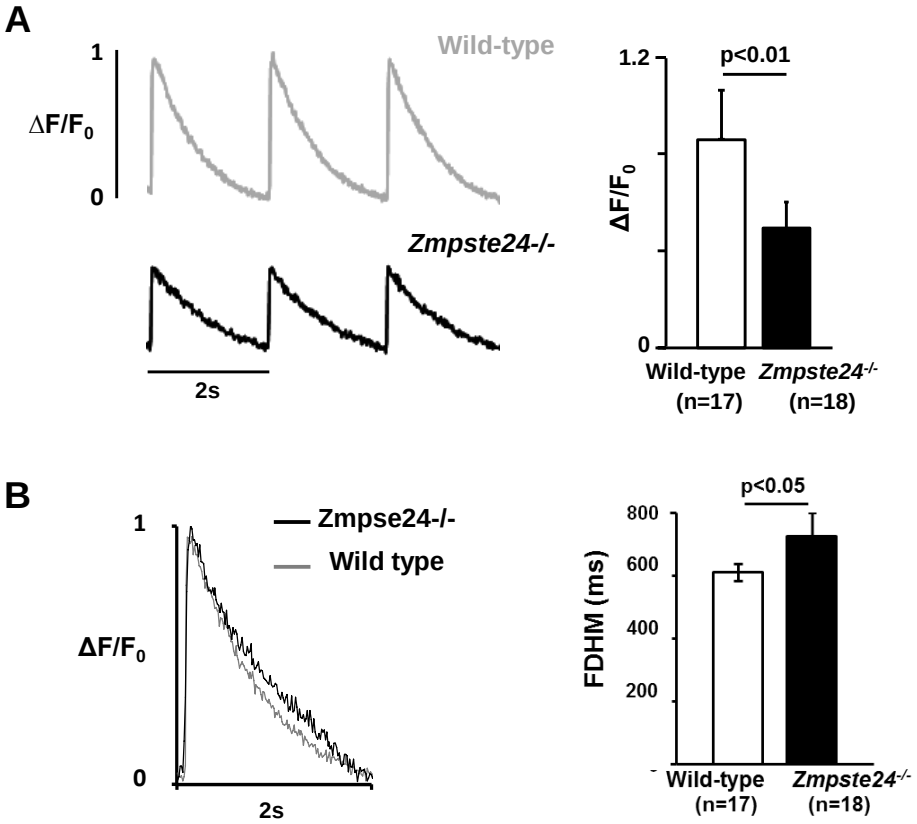

Figure 1. Effect of *Zmpste24*$^{-/-}$ on calcium transient duration and amplitude. (A) Representative calcium transient (ΔF/F0) recordings from myocytes paced at 0.5 Hz (left) and calcium transient amplitude quantification (right). Indicated cardiomyocytes are from n=6 mice/genotype. (C) Superimposed normalized calcium transient recordings (left). Mean calcium transient duration at half maximal amplitude (FDHM) recorded in myocytes paced at 0.5 Hz (right) (17 wild-type and 18 *Zmpste24*$^{-/-}$ myocytes from n=6 mice per group).

To identify the mechanisms underlying depression of the calcium transient, we examined first the effects on sarcolemmal calcium entry and next the amount of calcium release from SR.

Effect of *Zmpste 24*$^{-/-}$ on the L-type calcium current

Data showed a decrease in the I_{Ca} density in *Zmpste24*$^{-/-}$ cardiocyocytes (-2,15 ± 0,36 pA/pF), but did not differ significantly from the WT cardiomyocytes (-2,78 ± 0.46 pA/PF) (Figure 2). This effect was not overcome by increasing the extracelluar calcium concentration to 5 mM as I_{Ca} was increased proportionally in *Zmpste 24*$^{-/-}$ (by 38,84%) and WT (by 42,27%).

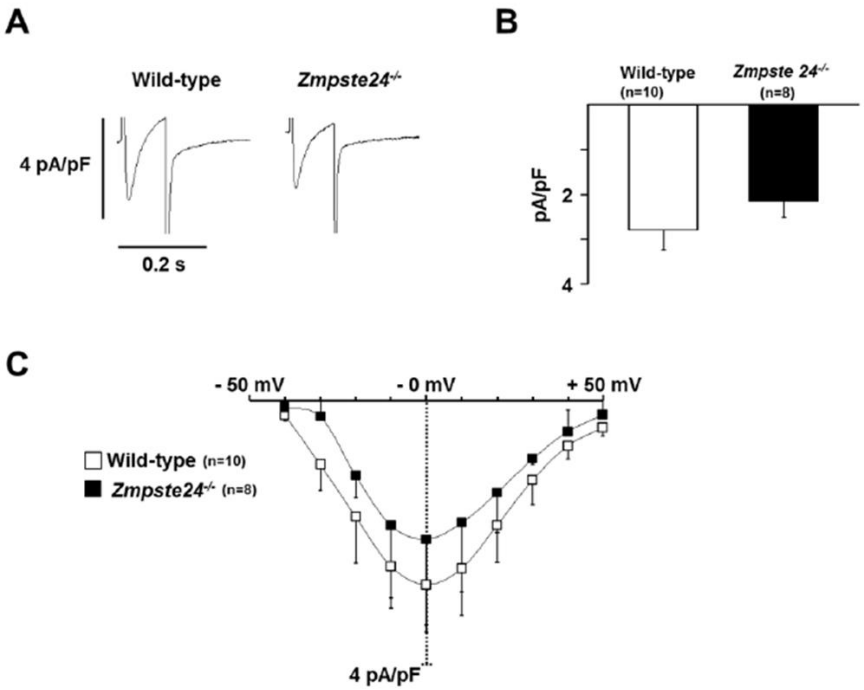

Figure 2. Effect of *Zmptse24*$^{-/-}$ on L-type calcium current. (A) L-type calcium current traces recorded in myocytes stimulated at 0.5 Hz. (B) Average I_{Ca} amplitude in isolated myocytes stimulated continuously at 0.5 Hz (WT, n=6; Zmpste24-/-, n=10). (C) I_{Ca}-voltage relationship in the same myocytes.

In agreement with a smaller I_{Ca} amplitude in *Zmptse24*$^{-/-}$ myocytes, steady-state I_{Ca}-inactivation was significantly slower in *Zmpste24*$^{-/-}$ cells compared with WT. This was true both for the fast (19,49 ± 2,58 ms; n=7; for *Zmpste24*$^{-/-}$ vs. 14.16 ± 1,32 ms, n=6; for WT) and the slow component of I_{Ca} inactivation (60,41 ± 11,58 ms; n=7; for *Zmpste24*$^{-/-}$ vs. 44.54 ± 2,70 ms, n=7; for WT) (Figure 3).

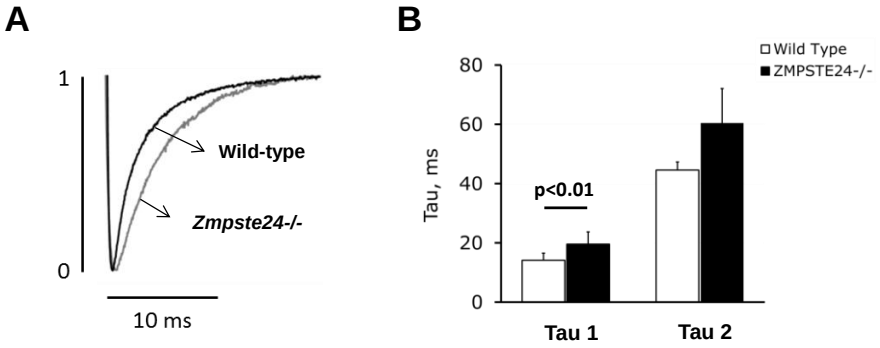

Figure 3. Effect of *Zmptse24*$^{-/-}$ on steady-state I_{Ca}-inactivation. (A) Superimposed normalized I_{Ca} traces from WT and *Zmpste24*$^{-/-}$ recordings. (B) Average time constants for fast (tau-1) and slow (tau-2) inactivation.

Effect of *Zmpste 24*$^{-/-}$ on SR calcium load

To determine the SR Ca^{2+} reloading capacity in ventricular myocytes, we loaded the SR by exposing cells to a train of stimulation pulses and estimated the resulting Ca^{2+} load from the time-integral of the caffeine-induced inward current traces (Figure 4A). SR reloading was significantly weaker in *Zmpste24*$^{-/-}$ myocytes than in wild-type cells after 5, 10, and 20 stimulation pulses (Figure 4B), and the defective response was still more apparent after ≥30 stimulation pulses (Figure 4C). Moreover, elevation of the extracellular calcium concentration only increased SR calcium loading in myocytes from WT mice (Figure 4B-C).

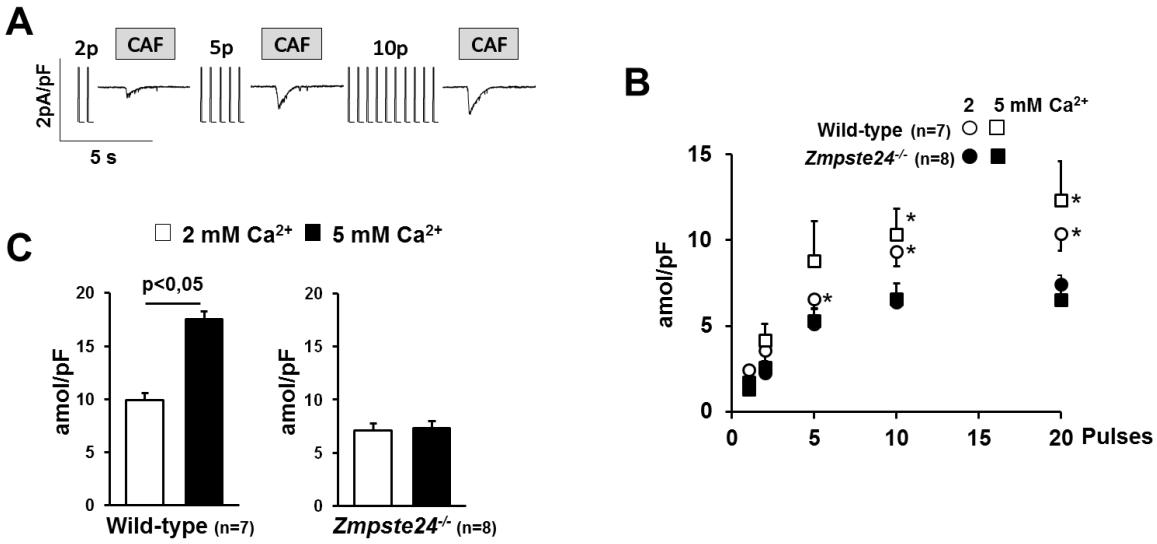

Figure 4. EFfect of *Zmpste24*$^{-/-}$ on the SR Ca^{2+} loading capacity. (A) Representative caffeine-induced currents recorded after SR reloading with the indicated number of stimulation pulses (p). Transient exposure to caffeine (CAF) was used to release SR calcium content before reloading and to measure loading after the train of stimulation pulses. (B) Time integral of caffeine-induced currents recorded after SR reloading with the indicated stimulation pulses. Data were obtained from 7 *Zmpste24*$^{-/-}$ and 8 wild-type myocytes (from n=5 mice) exposed consecutively to 2 and 5 mM extracellular Ca^{2+}. Time integrals were converted to amoles of Ca^{2+} and normalized to the cellular capacitance (in pF). (C) Effect of the extracellular calcium concentration on the time integral of the caffeine-induced current at steady-state (after ≥30 stimulation pulses). *, $p<0.05$

Significantly lower SR Ca^{2+} loading in *Zmpste24*$^{-/-}$ myocytes was also measured when the caffeine-induced currents were recorded after loading the SR by depolarizing the membrane potential to -40, -30, -20 or 0 mV for 5s (Figure 5A-B).

In line with impared SR calcium loading in *Zmpste24*$^{-/-}$ mice, western blot analysis revealed that both SERCA2 mRNA and protein levels were significantly lower in these mice (Figure 5C-D). Expression of cardiac CSQ-2, the protein acting as luminal calcium buffer in the SR, was also significantly lower (Figure 5C-D), providing a mechanistic explanation for a reduced SR loading capacity in the *Zmpste24*$^{-/-}$ mice. Interestingly, mRNA leves for the RyR2 was not significantly different in *Zmpste24*$^{-/-}$ and WT (Figure 5C).

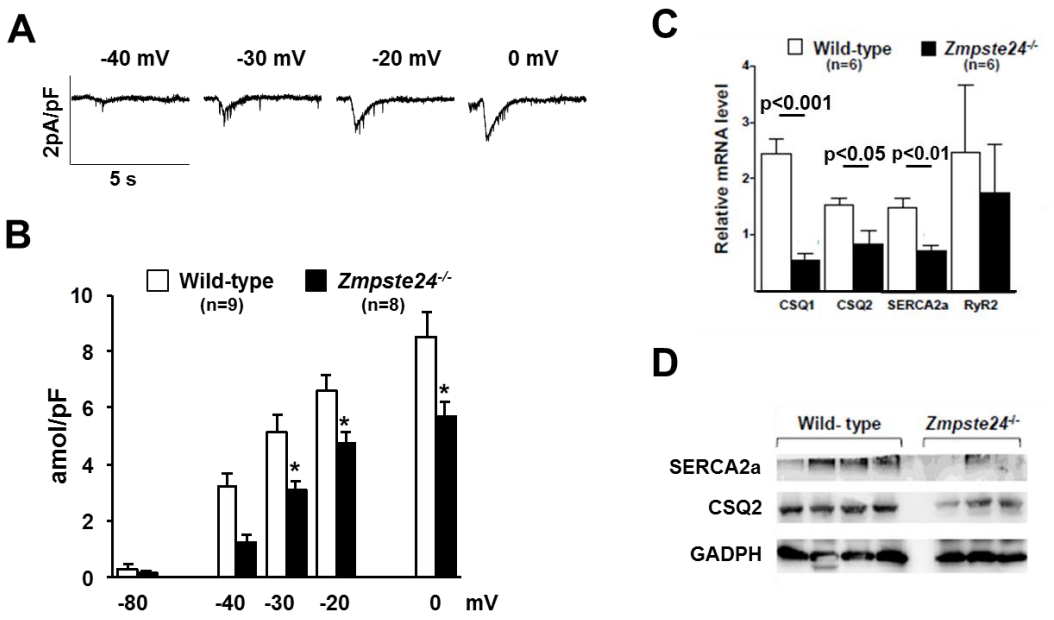

Figure 5. Effect of *Zmpste24*$^{-/-}$ on voltage-dependent SR calcium loading. (A) Representative caffeine-induced currents recorded after SR loading with a 5s depolarization to the indicated membrane potentials. (B) Mean time integral of the caffeine-induced current recorded in the presence of 2 mM extracellular Ca^{2+} after SR reloading at rest (-80 mV) and after depolarizing to the indicated potential (in mV). Data were obtained from 8 *Zmpste24*$^{-/-}$ myocytes (n=5 mice) and 9 wild-type myocytes (n=6 mice). (C) qPCR and (D) western blot analysis of heart tissue. *, p<0.05; **, p<0.01; ***, p<0.001.

Zmpste 24$^{-/-}$ does not alter spontaneous calcium release

To check whether the reduced SR calcium load in *Zmpste24*$^{-/-}$ affected the frequency of spontaneous calcium release, we performed confocal calcium imaging experiments in isolated Fluo-4 loaded myocytes. Figure 6 shows that there was no significant between-genotype differences in the frequency of spontaneous Ca^{2+} waves. As expected, elevation of the extracellular [Ca^{2+}] increased the calcium wave frequency. However, the wave frequency was comparable in *Zmpste24*$^{-/-}$ and

wild-type ventricular myocytes at all extracellular Ca^{2+} concentrations tested (1, 2, or 5 mM) (Figure 6A, B).

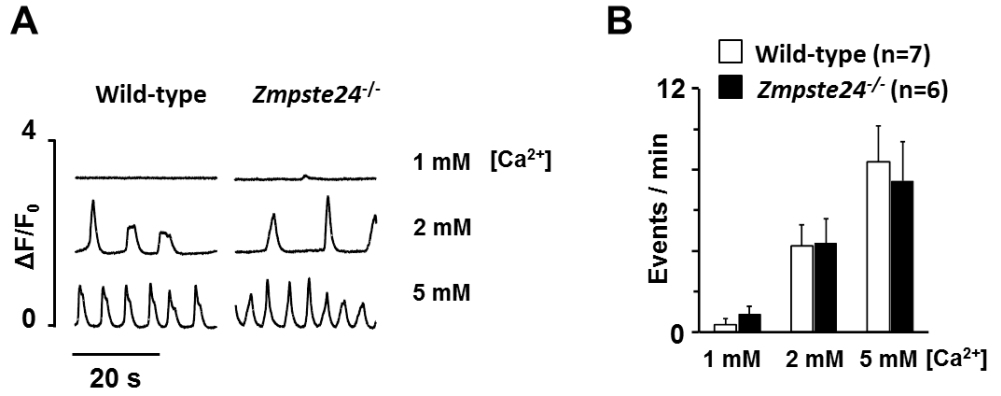

Figure 6. *Zmpste24*$^{-/-}$ does not affect the frequency of spontaneous inward currents. (A) Transient inward current (I_{TI}) recordings of WT and *Zmpste24*$^{-/-}$ myocytes at different calcium concentrations. (B) Average transients inward current (I_{TI}) frequency.

Zmpste 24$^{-/-}$ impairs stability of the calcium transient at different stimulation frequencies

When subjected electric field stimulation *Zmpste24*$^{-/-}$ myocytes responded poorer when the stimulation frequency was increased, causing instability in the Ca^{2+} transients at lower stimulation frequencies, an effect that was particularly prominent at 5 mM extracellular Ca^{2+} (Figure 7A).

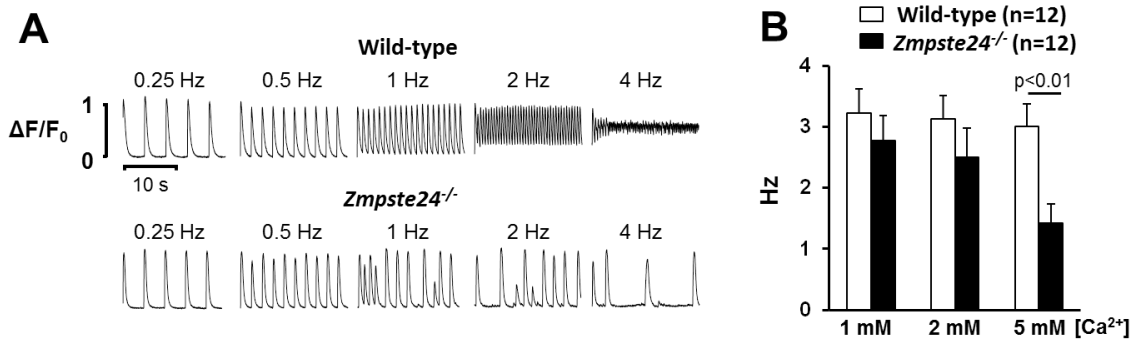

Figure 7. Effect of *Zmpste24*$^{-/-}$ on the beat-to-beat stability of Ca^{2+} transients. (A) Analysis of the beat-to-beat stability of Ca^{2+} transient in isolated ventricular myocytes subjected to increasing stimulation frequencies. Representative calcium transients were recorded in the presence of 5 mM extracellular Ca^{2+}. (B) The graph shows threshold frequencies for the induction of non-uniform beat-to-beat responses at the indicated Ca^{2+} concentrations. Responses were recorded in myocytes isolated from wild-type and *Zmpste24*$^{-/-}$ mice (12 cells from 6 mice of each genotype). Statistical significance was analyzed by ANOVA test followed by post-hoc analyses.

Zmpste 24$^{-/-}$ mice show defective SR calcium release-dependent inactivation

To test if impaired SR calcium loading in *Zmpste24*$^{-/-}$ affected SR Ca^{2+} release-dependent I_{Ca} inactivation, I_{Ca} inactivation was measured at each consecutive stimulation pulse given after clearance of SR Ca^{2+} content with caffeine. The experimental protocol is shown in Figure 8A. In agreement with a fast SR calcium loading in WT myocytes, I_{Ca} inactivation became increasingly faster as the number of pulses used for SR reloading increased from 1 (p1) to 30 (p30). By contrast, the effect of SR loading on the I_{Ca} inactivation rate in *Zmpste24*$^{-/-}$ myocytes was very modest (Figure 8B). Accordingly, the time constant for I_{Ca} inactivation decreased progressively with an increasing pulse number in WT but not in *Zmpste24*$^{-/-}$ myocytes (Figure 8C). Together these findings indicate that both SR Ca^{2+} uptake and triggered SR Ca^{2+} release are blunted in *Zmpste24*$^{-/-}$ myocytes.

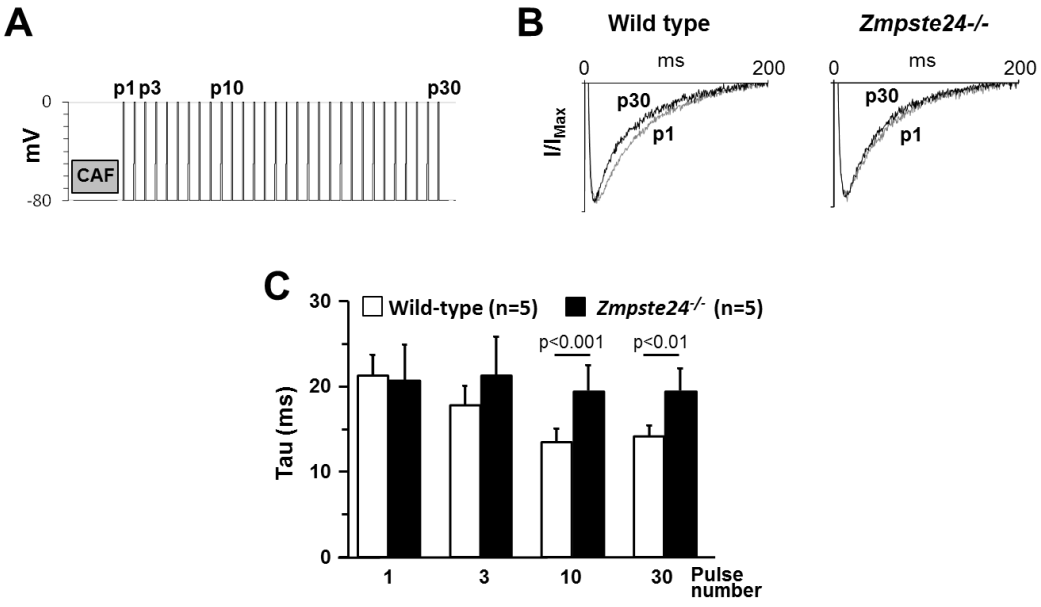

Figure 8. Effect of *Zmpste24*$^{-/-}$ on SR calcium release-dependent I_{Ca} inactivation. (A) Protocol used to measure the effect of SR calcium loading on I_{Ca} inactivation. The SR calcium content was first cleared with caffeine (CAF) and then reloaded with a train of 30 stimulation pulses (p1-p30). (B) Representative superimposed I_{Ca} recordings on p1 and p30. Currents were normalized to their respective peak values and fitted to a double exponential equation. (C) Dependency of the time constant (tau) for fast I_{Ca} inactivation on the number of pulses (indicated below bars) used to reload the SR in *Zmpste24*$^{-/-}$ and WT myocytes.

DISCUSSION

Main findings

HGPS is a devastating disease characterized by premature cardiovascular disease and death caused by defective lamin processing. Here, we provide evidence of altered calcium homeostasis in a progeric *Zmptse24*$^{-/-}$ mouse model for this disease. Specifically we find that ventricular myocytes from *Zmptse24*$^{-/-}$ mice reproduce the main effects of normal aging on the calcium homeostasis in human atrial myocytes (see Chapter I of the Results), suggesting that deficient lamin processing might be an underlying cause of age-dependent alterations of intracellular calcium handling in cardiac myocytes.

Resemblance of pathological cardiovascular changes in HGPS patients and *Zmpste24*$^{-/-}$ mice

Animal models resembling the clinical phenotype of HGPS patients are an important tool to understand the underlying mechanism of the disease and to identify possible mechanism of normal ageing. Our analysis of the well-established *Zmpste24*$^{-/-}$ mouse model of progeria caused by prelamin A accumulation[127,129] revealed progressive development of cardiac rhythm disturbances that concurred with alterations in the calcium homeostasis. Specifically, we found in *Zmpste24*$^{-/-}$ cardiomyocytes a significantly weakened I_{Ca} inactivation and reduced amplitude of the intracellular Ca^{2+} transient, together with an impaired SR calcium handling.

Some of the cardiac abnormalities we found in progeroid *Zmpste24*$^{-/-}$ mice also occur in HGPS patients and during normal aging. Thus, it has been described that alterations of the heart and the cardiovascular system in this mouse model include extensive fibrosis and loss of smooth muscle cells in coronary arteries, impaired calcium homeostasis, and the progressive development of cardiac rhythm abnormalities and ST-T-wave repolarization defects. The progressive development of bradycardia and deteriorating cardiac conduction in the progeriod mice resemble clinical rhythm abnormalities observed in the elderly.[130,131]

Some of the nuclear envelope alterations in the heart associated with altered prelamin A or progerin expression also occur during normal aging,[130,131] suggesting that shared mechanisms might cause cardiac alterations in HGPS patients and in the geriatric population. Consistent with this idea, prelamin A and progerin are both produced in the cells of normally aging individuals, raising the possibility that altered lamin A processing contributes to normal aging and associated cardiovascular disease.[16,17] Much like in normal human aging, progeroid *Zmpste24*$^{-/-}$ mice develop coronary fibrosis, bradycardia and severe conduction abnormalities.

Differences in cardiac rhythm disturbances and calcium homeostasis in *Zmpste24*$^{-/-}$ and normally ageing mice.

Cardiac conduction abnormalities also arise during the aging of wild-type mice, and are associated with an increased incidence of arrhythmias.[132] However, there are noticable differences in the calcium homeostasis in myocytes from normally ageing WT and *Zmpste24*$^{-/-}$ mice. In this regard, Ca^{2+} transients are smaller in older than in younger mice from WT[133] smaller and in *Zmpste24*$^{-/-}$ than in young WT. However, myocytes from *Zmpste24*$^{-/-}$ were unable to maintain stable Ca^{2+} transients at 4 Hz, mainly at high Ca^{2+} concentración on the bath solution. Secondly, ventricular myocytes from aged wild-type mice also present a significantly higher incidence of spontaneous Ca^{2+} sparks than cells from young animals.[133] In contrast to this, we did not observe significant differences in spontaneous calcium release between progeroid mice and age-matched controls.

Resemblance of calcium handling disturbances in myocytes from *Zmpste24*$^{-/-}$ mice and from elderly human atria.

Interestingly, changes in the calcium homeostasis in *Zmpste24*$^{-/-}$ myocytes, resembled closely the diffrences observed between human atrial myocytes from younger and elderly patients, showing 1) reduced calcium transient, 2) no change in the rate of spontaneous calcium release 3) defective SR Ca^{2+} uptake and 4) smaller negative feedback of triggerd calcium release on I_{Ca} inactivation, all

features observed in aging human atrial myocytes (See results Chapter I). Common to the progeric mice (Figure 7), aged WT mice,[133] and aged human atrial myocytes,[9] the Ca^{2+} transient amplitude was significantly reduced by ageing, suggesting that ageing is always associated with diminished calcium transients and consequently reduced force of contraction. However, the underlying defects in the calcium regalutory mechanisms may be different.

Conclusions

While ion channels are highly conserved between humans and mice, important electrophysiological differences also exist between men and mice,[134] making it complicated to translate findings from mouse models of disease to the clinical arena. In spite of this, the present findings show that the progeric mouse model *Zmpste24*$^{-/-}$ reproduce important pathological alterations of cardiac function in patients with the Hutchington-Gilford Progeria Syndrome and that concurrent alterations in the calcium homeostasis of myocytes from the *Zmpste24*$^{-/-}$ model essentially reproduce changes observed in atrial myocytes from elderly patients. This, on one hand suggests that deficient lamin processing might be an underlying cause of age-dependent alterations of intracellular calcium handling in cardiac myocytes. On the other hand these findings also suggest that *Zmpste24*$^{-/-}$ mice might be a suitable model to identify the molecular mechanisms that translate deficient lamin processing into defective calcium homeostasis in aged cardiac myocytes.

III. PREDISPOSAL TO ATRIAL FIBRILLATION IN PATIENTS WITH 4q25 RISK VARIANTS IS LINKED TO DEFECTIVE CALCIUM HOMEOSTASIS

INTRODUCTION

Atrial fibrillation (AF) is the most common cardiac arrhythmia, which affects 1-2% of the general population and increases gradually with age, attaining an incidence of 9% in octogenarians. Even though AF duplicates the mortality rate and increases by 5-fold the risk of cerebrovascular embolism,[77] the current treatment is quite often ineffective.

A number of electrophysiological, molecular, and structural alterations take place in the fibrillating atria favoring the maintenance and self-perpetuation of the arrhythmia.[135] Among the electrophysiological alterations, several studies have reported disturbances in the intracellular calcium homeostasis[12–14,136] and malfunctioning of the sarcoplasmic reticulum (SR).[12,14,15,136–138] Indeed, myocytes from patients with AF depict a high spontaneous SR calcium release[14] likely linked to an increased protein-kinase A (PKA)-dependent phosphorylation of ryanodine receptor type 2 (RyR2) at ser-2808.[12,138] The RyR2 phosphorylation can be also activated by Calmodulin Kinase II (CaMKII), thus contributing to increase the diastolic SR calcium leak in patients with AF.[15,137] Importantly, the spontaneous calcium waves can induce arrhythmogenic membrane depolarizations in atrial myocytes from patients with AF,[15] and occur both in resting and electrically stimulated human atrial myocytes.[112,139] Moreover, transgenic mouse models with high rates of spontaneous calcium release are more prone to present spontaneous or induced arrhythmia;[15,140–142] supporting the notion that spontaneous SR calcium release plays a central role in arrhythmogenic processes.

While electrophysiological mechanistic analysis is shedding new light on the molecular mechanisms underlying AF, the genetic bases of this disease remain elusive. Mutations in a variety of ion channels have been associated to familial

AF,[143–145] but these account in a minority of the patients. Genome-wide association studies (GWAS), revealed distinct genetic loci on chromosomes 4q25, 1q21 and 16q22 that have been associated with AF[18] and additional loci have subsequently been associated with this arrhythmia.[146] Recent GWAS meta-analyses have further increased the number of risk variants, but the most striking arrhythmogenic variants remain those located at 4q25.[147] Considering that the bicoid-related homeodomain transcription factor Pitx2 is located in the vicinity of the 4q25 SNPs and the pivotal role of Pitx2 during cardiac and pulmonary vein development,[148] Gudbjartsson et al.[7] postulated that Pitx2 dysfunction might be the molecular link between risk variants at 4q25 and AF. In support of this concept, Chinchilla et al.[8] demonstrated that Pitx2c expression decreases in patients with sustained AF, providing a molecular connection between loss of Pitx2 function and AF. However, other studies found increased Pitx2 transcripts in patients with AF[23] and unchanged Pitx2c expression or even increased Pitx2a expression in patients with 4q25 risk variants,[149,150] making the functional relationship between 4q25 risk variants, Pitx2 function and AF uncertain. On the other hand, no studies have so far investigated if the 4q25 risk variants are associated with electrophysiological disturbances commonly associated to functional alterations in the intracellular calcium homeostasis AF. Therefore, we here tested the hypothesis that 4q25 risk variants are associated with potentially arrhythmogenic alterations in the intracellular calcium homeostasis that have previously been linked to AF in myocytes from patients with this arrhythmia.

METHODS

Human atrial samples and myocyte isolation

A total of 543 blood samples were genotyped for the presence of the normal 4q25 variants rs2200733C, rs13143308G and rs1448818T or for the corresponding AF risk variants rs2200733T, rs13143308T and rs1448818G. Right atrial myocardial samples were collected simultaneously from 280 of the genotyped patients undergoing cardiac surgery at Hospital de la Santa Creu i Sant Pau in Barcelona and used for cell isolation and molecular biological analysis.

Table 1 summarizes the clinical, echocardiographic, and therapeutical data of these patients. Myocytes were isolated from the atrial samples as previously described [14] and detailed in General Methodologies. Each patient gave written consent to obtain blood and tissue samples. The latter would otherwise have been discarded during the surgical intervention. The study was approved by the Ethical Committee at Hospital de la Santa Creu i Sant Pau and conducted in accordance with the Declaration of Helsinki principles.

Table 1. Clinical characterization of the patients included in the study.

	Normal n=174	**Risk n=106**	**p-value**
Age (years)	68.0 ± 0.8	66.7± 0.8	ns
Height (cm)	164 ± 1	164 ± 1	ns
Weight (kg)	76 ± 1	75 ± 1	ns
Cardiovascular disease			
Arterial hypertension	117 (67%)	78 (74%)	ns
Diabetes	69 (40%)	32 (30%)	ns
Pulmonary pressure (mm Hg)	45.1 ± 2.2	46.4 ± 2.6	ns
Aortic valve disease	85 (49%)	60 (57%)	ns
Mitral valve disease	45 (26%)	23 (22%)	ns
Tricuspid valve disease	23 (13%)	10 (9%)	ns
Ischaemic heart disease	108 (62%)	56 (53%)	ns
Echocardiography			
Left atrial diameter (mm)	46.6 ± 1.0	44.6 ± 1.2	ns
Left atrial diameter index	2.61 ± 0.07	2.47 ± 0.08	ns
LVEF (%)	55.2 ± 1.1	58.0 ± 1.3	ns
Pharmacological treatment			
ACE-inhibitors	72 (41%)	38 (35%)	ns
ARB	34 (20%)	23 (21%)	ns
β-Blockers	90 (52%)	59 (56%)	ns
Calcium antagonists	38 (21%)	27 (25%)	ns
Nitrates	44 (25%)	26 (25%)	ns
Dicoumarin	35 (20%)	31 (29%)	ns
Acetyl salicylic acid	72 (41%)	46 (43%)	ns
Statins	105 (60%)	72 (68%)	ns

LVEF, left ventricular ejection fraction; ACE-inhibitors, angiotensin converting enzyme inhibitors; ARB angiotensin receptor blockers; Values are given as mean ± standard deviation, number of

patients and percentage (%). * indicates a significant difference ($p<0.05$) between patients with and without AF.

SNP Genotyping

Genomic DNA samples from 174 patients with AF and 369 patients with no reported episodes of AF were included and analyzed. Samples from the 174 patients with AF were collected as follows: 75 at the Spanish National DNA Bank (BNADN, Salamanca), 68 at the Cardiology Service at Hospital de la Santa Creu i Sant Pau, Barcelona, and 31 at the Cardiology Unit of the Hospital Regional Ciudad de Jaén. Samples from the 371 patients free of AF were obtained from the Spanish National DNA Bank (BNADN, Salamanca) in 157 cases, and from Hospital de la Santa Creu i Sant Pau (Barcelona) in 212 cases. Polymerase chain reaction (PCR) amplification of single nucleotide polymorphisms (SNPs) rs2200733, rs13143308 and rs1448818 were carried out using flanking oligonucleotides as outlined in Table 2, followed by direct sequencing.

This study was approved by the Ethics Committees of the Spanish National DNA Bank (BNADN, Salamanca), Hospital de la Santa Creu i Sant Pau (Barcelona) and of the University of Jaén, and the investigation conforms to the principles outlined in the Declaration of Helsinki.

Table 2. SNP Genotyping

SNP	Sequence
rs1448818 forward	5´AAAATCGCAATGCTTCAAATG 3´
rs1448818 reverse	5´TGTGGCGTTTTGTTTTATTAAAGT 3´
rs2200733 forward	5´ TCAGAAGACTCCAGCTCATTCA 3´
rs2200733 reverse	5´ GTGGAGGCCAGATGAGGA 3´
rs13143308 forward	5´ TGGGGGATGGACCAGTATAA 3´
rs13143308 reverse	5´ CCTACTTGGGGAGTTGAAACA 3´

Flanking nucleotides used for polymerase chain reaction amplification of the single nucleotide polymorphisms rs1448818, rs2200733 and rs13143308.

Western blot

Protein expression was determined with western blot technique. Approximately 20 mg of right atrial sample was pulverized in liquid nitrogen and homogenized in 200 µl of ice-cold lysis buffer containing (in mM): 50 HEPES, 100 NaCl, 2.5 EGTA, 10 glycerol-2-phosphate 1 DTT supplemented with a cocktail of protease inhibitors (Roche) and with 0.1% (v/v) Tween 20 and 10 % (v/v) glycerol at pH=7.4. Proteins were separated by SDS-PAGE (10% acrylamide:bisacrylamide) and electrotransferred onto Immobilon polyvinylidene diflouride membranes (Millipore). Membranes were incubated with primary and secondary antibodies diluted in 5% non-fat dry milk. Antibodies against SERCA (#9580, Cell Signalling Technology), CSQ-2 (ab3516, Abcam) and NCX1 (ab135735, Abcam) were used. Detection was performed using the appropriate horseradish peroxidase-labeled IgG and the SupersignalTM detection system (Supersignal West DuraTM, Pierce). Molecular-mass standards (Bioline) were used to estimate protein size and glyceraldehyde-3-phosphate dehydrogenase (GAPDH; MAB374, Millipore) was used as a loading control. Immunoblots were digitized (GS-800 Calibrated Densitometer; Bio-Rad) and analyzed with the Quantity One 4.6.3 software (Bio-Rad).

Patch-clamp technique

Electrophysiological recordings were performed using perforated patch-clamp technique in isolated human atrial myocytes as described in General Methodologies. Briefly, L-type calcium current, spontaneous transient inward calcium release induced Na-Ca exchange (NCX) currents (I_{TI}), and the caffeine releasable SR calcium content was measured using the whole cell voltage-clamp configuration. Membrane potentials were recorded in the current-clamp configuration.

Confocal calcium imaging

To visualize changes in the intracellular calcium concentration, myocytes were loaded with 2.5 µM fluo-4 AM for 15 minutes, followed by wash and de-

esterification for 30 min or more. Confocal calcium images (512x140 pixels) were recorded at frame rates of 90 Hz, using a resonance-scanning confocal microscope with a 63x glycerol-immersion objective (Leica SP5 AOBS, Wetzlar, Germany). The excitation wavelength was 488 nm and fluorescence emission was collected between 500 and 650nm with a Leica Hybrid Detector. Laser power was set to 20% of 100 mW and then attenuated to 4%. Experiments were performed at room temperature and calcium sparks were detected using custom made algorithms implemented using MATLAB (The Mathworks Inc., Boston, MA) as described in General Methodologies.

Data analysis

Experiments were performed without knowledge about clinical data and clinicians did not know the experimental results. Statistical analysis was performed using SPSS software. Unless otherwise stated, values were averaged for each patient or mouse and expressed as mean±SEM. Data sets were tested for normality. Statistical significance was evaluated using Fishers exact test for categorical data. Student's t-test was used for paired or unpaired comparisons, and ANOVA was used for comparison of multiple effects where appropriate. The statistical significance is indicated with the p-value and differences were considered statistically significant at the 95% confidence interval.

RESULTS

Frequency of 4q25 risk variants

Genotyping of 543 patients confirmed the association of the rs13143308T risk variant to AF, as the frequency of this variant was significantly higher in patients with AF (p=0.005). Moreover, the frequency of the risk variants rs2200733T and rs1448818G tended to be higher in patients with AF (see Figure 1).

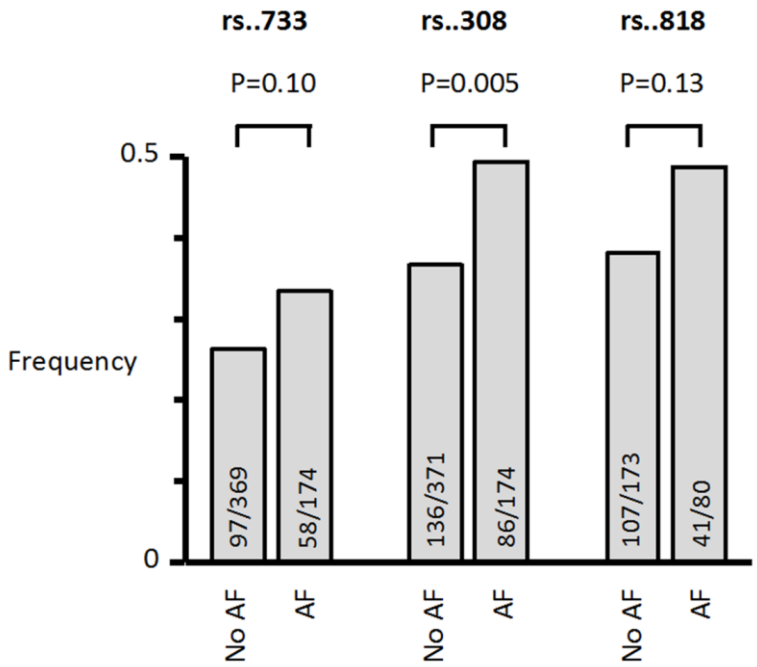

Figure 1. Frequency of 4q25 risk variants in patients with and without AF. The frequency of the rs2200733T (rs..733), rs13143308T (rs..308) and rs1448818G (rs..818) risk variants on chromosome 4q25. Number of patients genotyped are given for each risk variant in patients without (No AF) and with AF.

Further analysis showed that there were almost no genotypes with a rs2200733 risk variant (T) and a normal rs13143308 variant (GG), while genotypes containing a risk variant at both loci (T-T combination) were more than twice as frequent as expected; indicating that rs2200733T co-segregates with rs13143308T ($p<0.001$; Figure 2A). On the other hand, the segregation of the rs2200733 and rs1448818 loci as well as rs13143308 and rs1448818 loci was in accordance with the allele frequencies (Figure 2B-C).

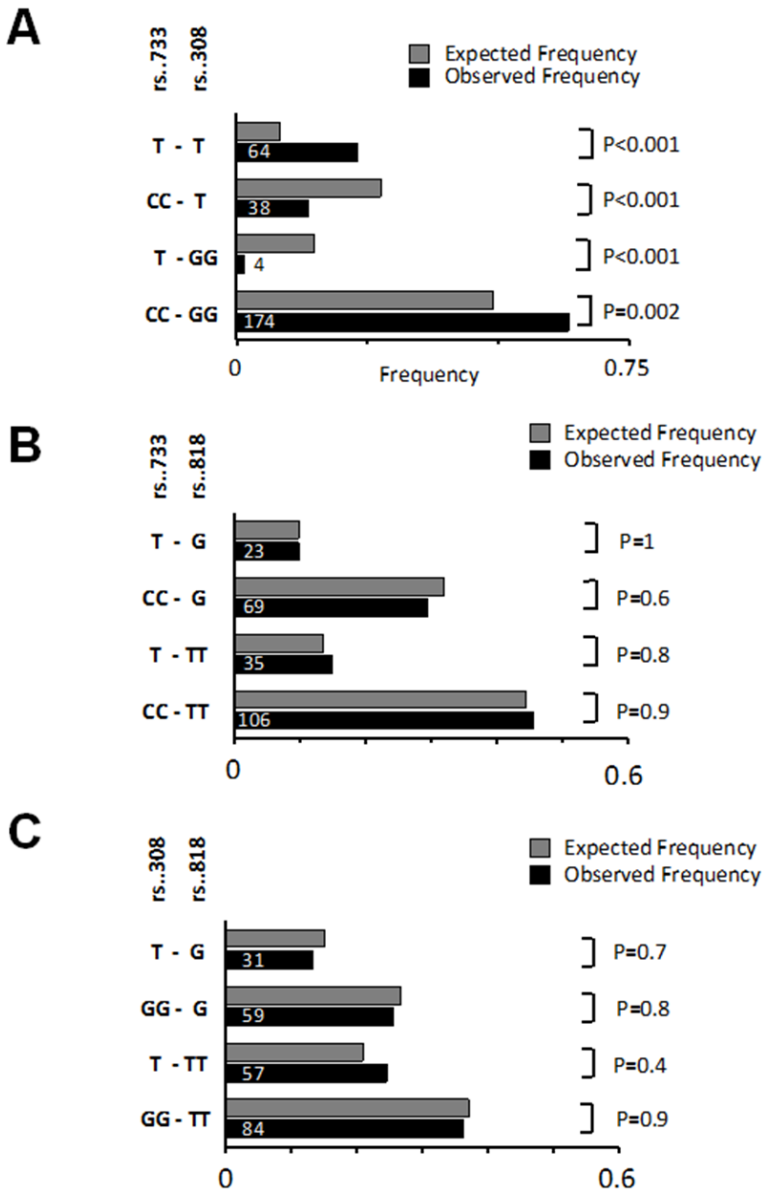

Figure 2. Segregation of the 4q25 loci rs2200733, rs13143308 and rs1448818. (A) Relative frequency of rs…733 and rs..308 genotypes in 280 patients donating right atrial tissue (black bars). T at rs..733 indicates the presence of at least one risk allele and T at rs..308 indicates the presence of at least one risk allele at this locus. (B) Relative frequency of rs2200733 (rs..733) and rs1448818 (rs..818) genotypes in patients donating right atrial tissue. Black bars are from a total of 233 patients. T indicates the presence of at least one risk allele at rs..733 and G indicates the presence of at least one risk allele at rs..818. (C) Relative frequency of 13143308 (rs..308) and rs1448818 (rs..818) genotypes. Black bars are from a total of 231 patients and the number of patients is given for each bar. T indicates the presence of at least one risk allele at rs..308 and G indicates the presence of at least one risk allele at rs..818. Grey bars indicate the expected frequency of the same genotypes based on the allele frequencies. P-value for difference between observed and expected frequencies are given on the right.

4q25 risk variants do not alter L-type calcium current.

Since one of the hallmarks of atrial fibrillation is a prominent reduction of the L-type calcium current (I_{Ca}) density,[13] we first analyzed how the presence of 4q25 risk variants affected I_{Ca} density and properties. Initially, we analyzed the effects of the risk variants rs2200733T and rs13143308T that have repeatedly been associated with AF. In line with previous studies on AF, the I_{Ca} amplitude was significantly smaller ($p<0.01$) in myocytes from patients with AF than without AF. However, I_{Ca} was not different in myocytes from patients with and without a risk variant at 4q25 (Figure 3A). Moreover, the decay of I_{Ca} was significantly slower in myocytes from patients with AF independently of the genotype at 4q25 (Figure 3B).

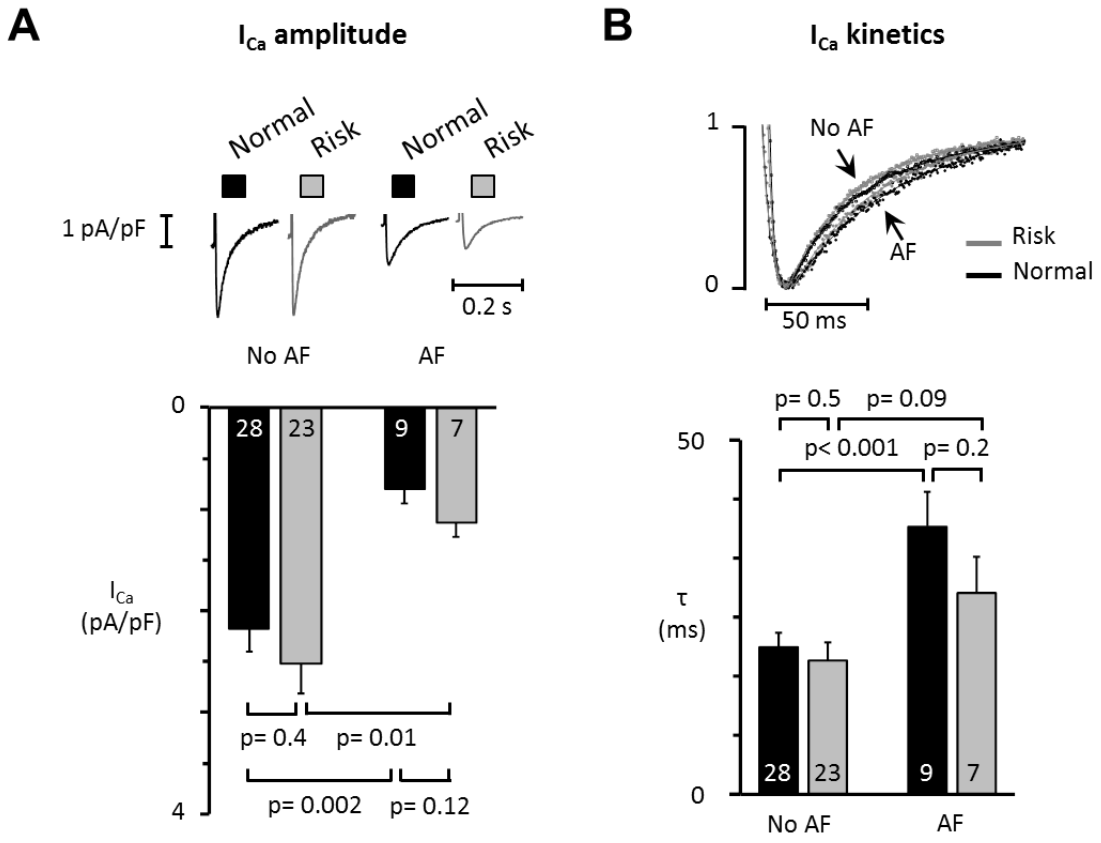

Figure 3. Risk variants at 4q25 do not modify the L-type calcium current. (A) Representative I_{Ca} recordings from four patient groups that had a normal (black traces) or a risk variant (grey traces) in the absence of presence of AF. The mean I_{Ca} amplitude is shown below each trace. (B) Superimposed normalized I_{Ca} traces (top panel) and the fast time constant for I_{Ca} inactivation (bottom).

Comparison of the gating properties of the L-type calcium channel for the normal genotype and for the risk variants revealed that neither the presence of risk variants at 4q25 nor AF affected the shape of the current-voltage (I-V) relationship (Figure 4A) or the voltage dependent inactivation (Figure 4B).

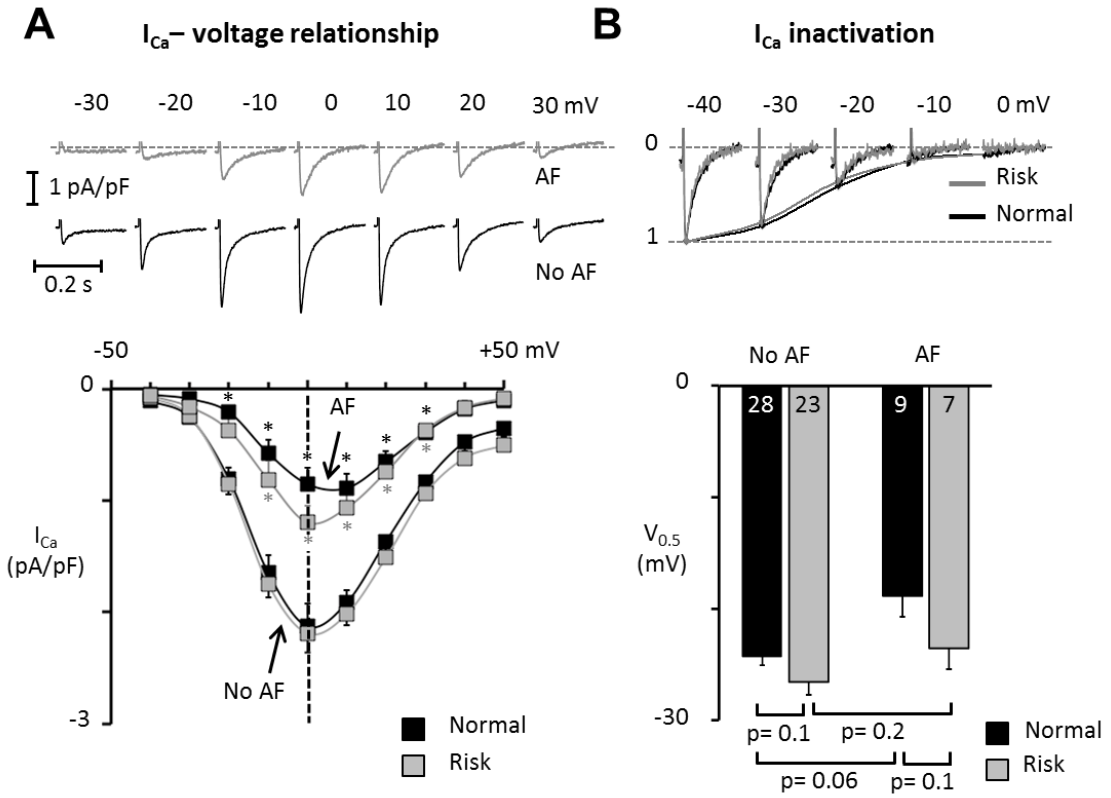

Figure 4. Risk variants at 4q25 do not alter the L-type calcium current properties. (A) I_{Ca} recordings at different test potentials (top) in myocytes from a patient with and without AF (no AF). Current-voltage curves are given for each of the four patient groups below. (B) I_{Ca}-traces recorded with different pre-potentials (top) in a myocytes from patients without AF with a normal or a risk variant at 4q25. The voltage for half-maximal I_{Ca}-inactivation is shown for the four patient groups below. The number of patients in each group is indicated and the p-values for statistical significance for comparisons are given.

4q25 risk variants have a higher frequency of transient inward currents and spontaneous membrane depolarizations.

Subsequently, we tested if risk variants at 4q25 promoted calcium release-induced transient inward currents (I_{Ti}) or membrane depolarizations; another hallmark of AF.[14,15] As shown in Figure 5A-B, the I_{Ti} frequency was significantly higher in myocytes from patients with risk variants. This was true even in patients

without AF and was observed both at normal (-80 mV) and depolarized membrane potentials reported in patients with diseased atria [151] (-50 mV, Figure 5C).

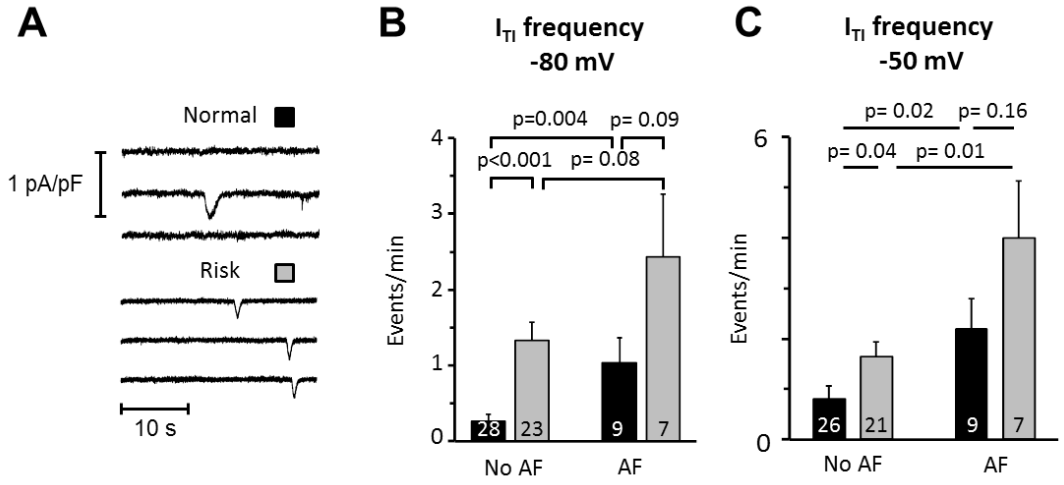

Figure 5. 4q25 risk variants increase calcium release-induced currents. (A) Transient inward currents (I_{TI}) recorded in myocytes from patients with normal variant and with a 4q25 risk variant. (B) Mean I_{TI}-frequency in myocytes from with or without 4q25 risk variants at -80 mV, and (C) -50 mV. Number of patients is given for each bar. P-values for differences are given above bars.

The I_{TI}-amplitude was similar for myocytes from patients without AF and no risk variant and for myocytes from patients with a risk variant and/or AF (Figure 6A) at membrane potentials of either -80 or -50 mV, suggesting that the membrane depolarizations produced by a spontaneous I_{TI} would be similar for the four groups.

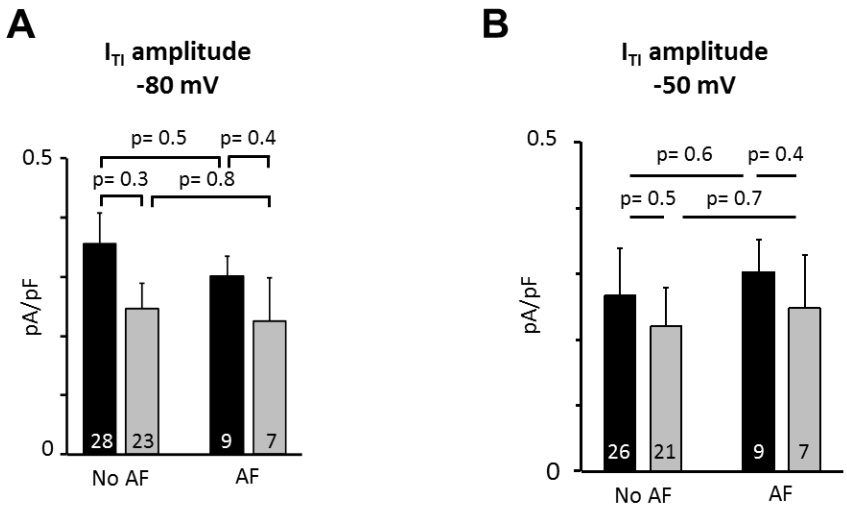

Figure 6. 4q25 risk variants do not modify the I_{TI} amplitude. (A) Mean I_{TI} amplitude in myocytes from the same patients as in Figure 5 B-C for -80 mV and (B) -50 mV.

To determine the real impact of calcium-release induced Na^{+}-Ca^{2+} exchange on the membrane potential, we performed current-clamp experiments in myocytes from a subset of patients. Figure 7A-B shows that myocytes from patients with a risk variant at 4q25 had a significantly higher frequency of spontaneous membrane depolarizations at a normal (-80 mV) resting membrane potential and the amplitude of the depolarizations was larger in the risk variants (Figure 7C).

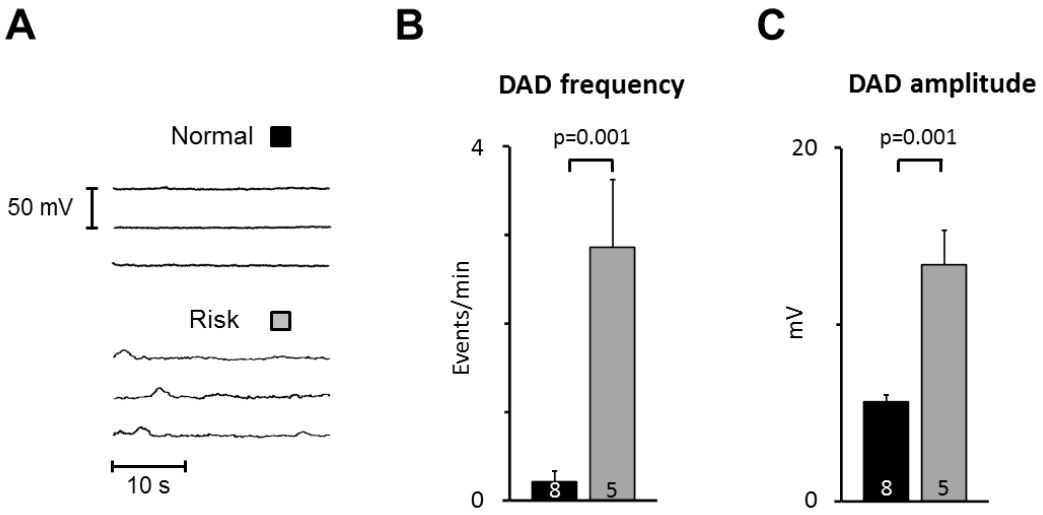

Figure 7. 4q25 risk variants increase spontaneous membrane depolarizations. (A) Membrane potential recordings at -80 mV in myocytes from a patient with a normal and one with a risk variant at 4q25. Traces are displaced by 50 mV for clarity. (B) Average frequency of spontaneous membrane depolarizations (DAD) recorded at -80 mV in myocytes from patients with and without a 4q25 risk variant. (C) Average amplitude of the spontaneous membrane depolarizations recorded at -80 mV in the same myocytes as in panel B. Number of patients is given for each bar. P-values for significant differences are given above bars.

Arrhythmogenic calcium release in 4q25 risk variants is linked to higher calcium spark frequency and SR calcium loading

To determine if the higher I_{Ti} frequency in myocytes from patients with 4q25 risk variants was linked to a higher activity of the SR calcium release channel (also referred to as ryanodine receptor or RyR2) we used frame-scanning confocal calcium imaging to visualize local calcium release from RyR2 clusters in a longitudinal section of the myocyte. Analysis of the spark dimensions and kinetics, in patients without AF, revealed no differences in spark amplitude (Figure 8A-B),

duration (Figure 8C) or width (Figure 8D-E) among myocytes from patients with a normal or a risk variant.

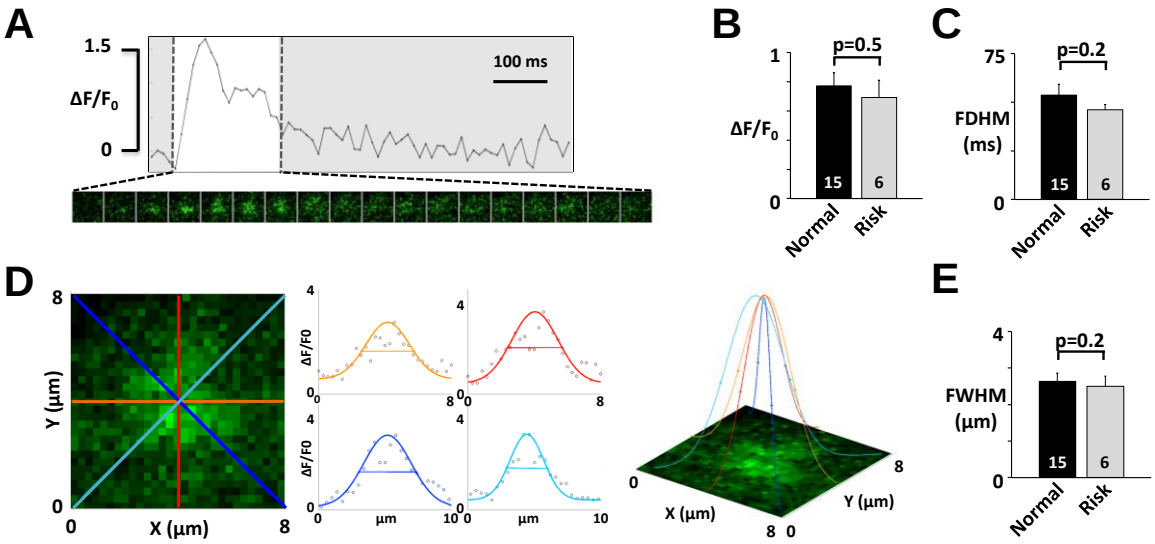

Figure 8. Risk variants at 4q25 do not modify the sparks properties (A) Ca^{2+} transient from a single spark site. Consecutive 8 x 8 µm images of the calcium spark are shown below the Ca^{2+} transient during its rise and decay (white area). (B) Calcium spark amplitude. (C) Calcium spark duration. (D) Enlarged image of the calcium spark in panel A, recorded at its maximal amplitude. The profile of the calcium spark is shown for each of the four axes outlined in the image on the left and the profiles are overlaid in the 3D representation on the right. (E) Width of the calcium spark at half maximum (FWHM). Values in panels B, C and E are means of 41 myocytes from 15 patients with the normal variant and 22 myocytes from 6 patients with risk variants b. P-values for differences are given above bars.

By contrast, the presence of a risk variant was associated with a significantly higher spark frequency (Figure 9A-B), which in turn was due to a higher density of spark sites (Figure 9C) rather than a higher frequency of sparks per site (Figure 9D).

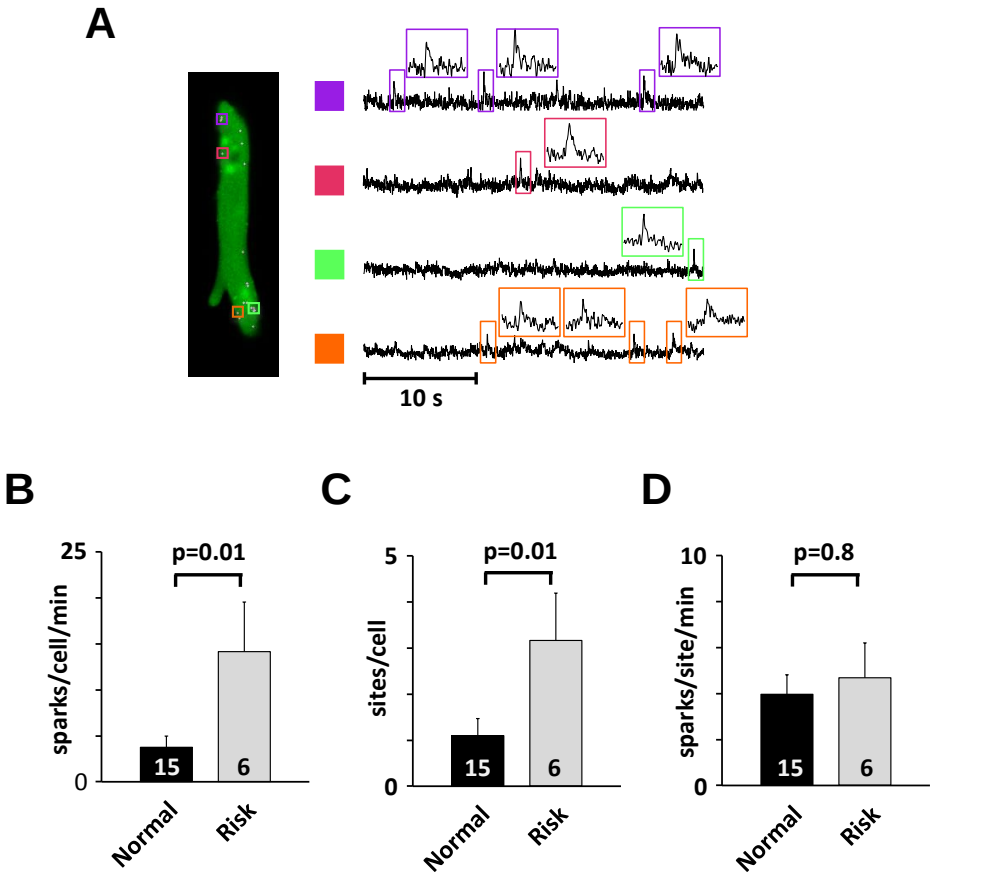

Figure 9. Risk variants at 4q25 increase the calcium spark density. (A) Image of a human atrial myocyte, from a patients with a 4q25 risk variant, with indication of four spark sites on the left. Calcium signals are shown for each spark site on the right. Insets show calcium signals for individual sparks. (B) Spark frequency. (C) Sparks sites per cell. (D) Spark frequency per site. Values in panels B, C and D are means of the same cells and patients mentioned before in Figure 8, panels B, C and D. P-values for differences are given above bars.

The higher density of calcium spark sites in the risk variants is expected to result from a higher density of RyR2 clusters that have reached the threshold for store-overload induced calcium release. Measurements of the SR calcium load from the time-integral of the caffeine induced NCX current showed that atrial myocytes from patients without a previous history of AF had a significantly higher caffeine releasable calcium load when a 4q25 risk variant was present (Figure 10A). This difference was not present in myocytes from patients with AF, suggesting that instauration of the arrhythmia may cause additional remodeling of the calcium homeostasis.

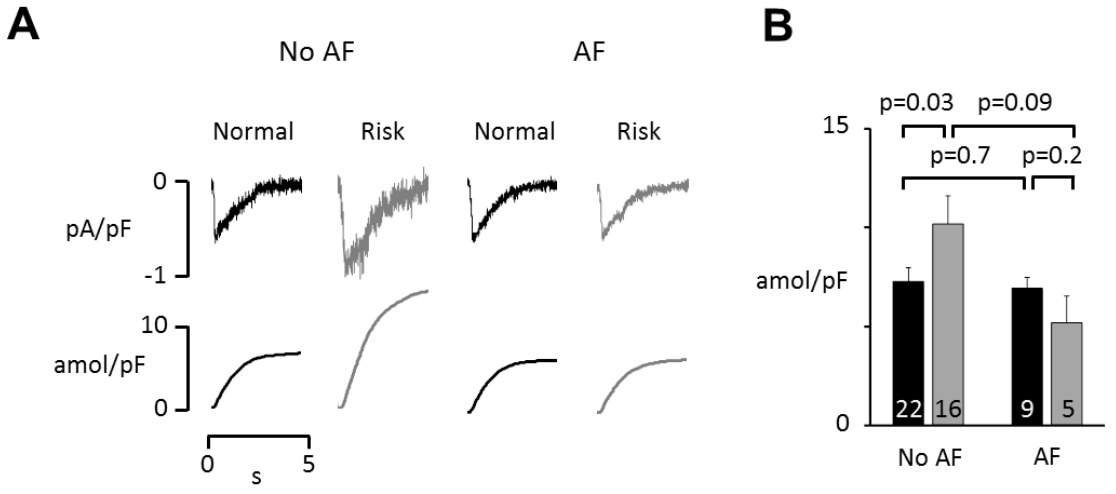

Figure 10. 4q25 risk variants increase SR calcium loading. (A) Caffeine-induced transient inward currents (top) and their time integral (bottom) in myocytes from patients with 4q25 risk variants or with normal variants. (B) Average of SR calcium load of the number of patients given in each bar.

Potentially, the larger I_{TI} amplitude observed in myocytes from patients without any risk variant (see Figure 6A) could be due to a higher activity of the NCX. However, when the NCX rate was plotted against the calcium available for extrusion by the NCX, there were no differences in the resulting slope among the four patient groups (Figure 11A) suggesting that there are no differences in the NCX-activity among patients with and without risk variants.

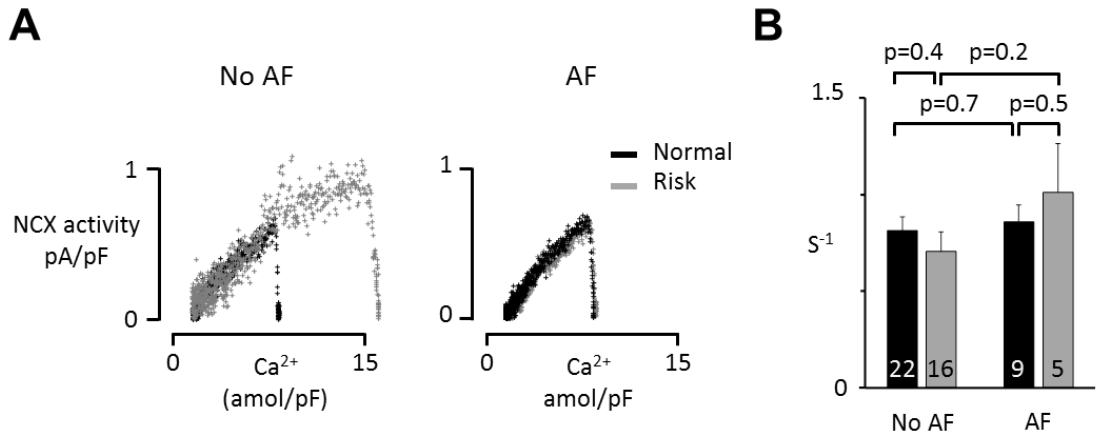

Figure 11. 4q25 risk variants don´t alter the NCX activity. (A) Relationship between the activity of the NCX (given in pA/pF) and the calcium available for extrusion (given in pC/pF) in a myocyte from a patient with a normal and one with a risk variant. (B) Average slope of the relationships for normal and risk variants from patients without (No AF) or with AF.

To determine if the electrophysiological measurements of SR calcium loading and NCX activity were caused by changes in protein expression, we performed western blot analysis in samples from patients without AF. The results revealed that CSQ-2 expression tended to increase and that SERCA2 expression was significantly higher in patients with a 4q25 risk variant (Figure 12A-B), which may account for the higher SR calcium load in patients with a risk variant. In accordance with the electrophysiological data, analysis of the NCX expression showed no difference between patients with and without risk variants (Figure 12A-B).

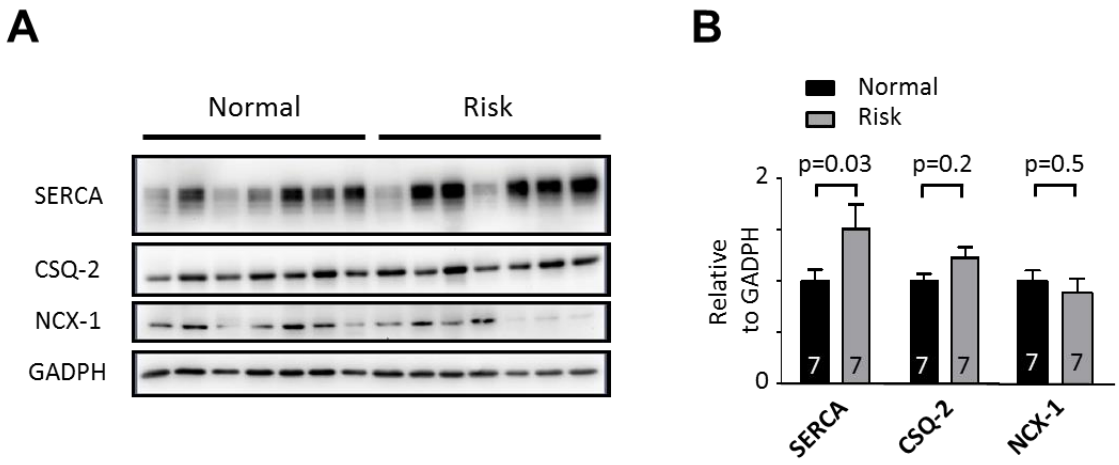

Figure 12. 4q25 risk variants increase SR calcium loading and SERCA expression. (A) Immunoblots of SERCA2, CSQ-2, NCX-1 and GADPH in human right atrial samples from patients without AF, with normal or risk variants at 4q25. GADPH served as reference. (B) Mean SERCA2, CSQ-2 and NCX-1 expression levels. Values were normalized to the mean expression level in the normal variant. P-values are given above bars and the number of patients is given for each bar.

Differential effects of individual 4q25 risk variants on the intracellular calcium homeostasis.

To assess if different 4q25 variants had distinct effects on calcium handling, we compared the effects of three different variants at rs2200733, rs13143308 and rs1448818, the latter being a variant that is closer to the PITX2 locus.[152] Comparison of the I_{TI} frequency for each risk allele showed that the presence of a risk allele at rs220073 or rs13143308 was associated with a significantly higher I_{TI} frequency (Figure 13A). Moreover, the spontaneous I_{TI} frequency increased with the number of loci with a risk variant (Figure 13B). Of notice, the presence of a

single rs13143308T allele (without risk at rs2200733 and rs1448818) strongly increased the I_{TI} frequency (TT-GT-CC combination in figure 13C). The I_{TI} frequency was increased to a similar degree in patients with a risk allele at both rs2200733 and rs13143308, but without risk at rs1448818 (TT-GT-CT combination in Figure 13C). However, the rs1448818G risk allele (without risk at rs2200733 and rs13143308) did not modify the I_{TI} frequency (TT-GG-CC and GT-GG-CC combinations in Figure 13C).

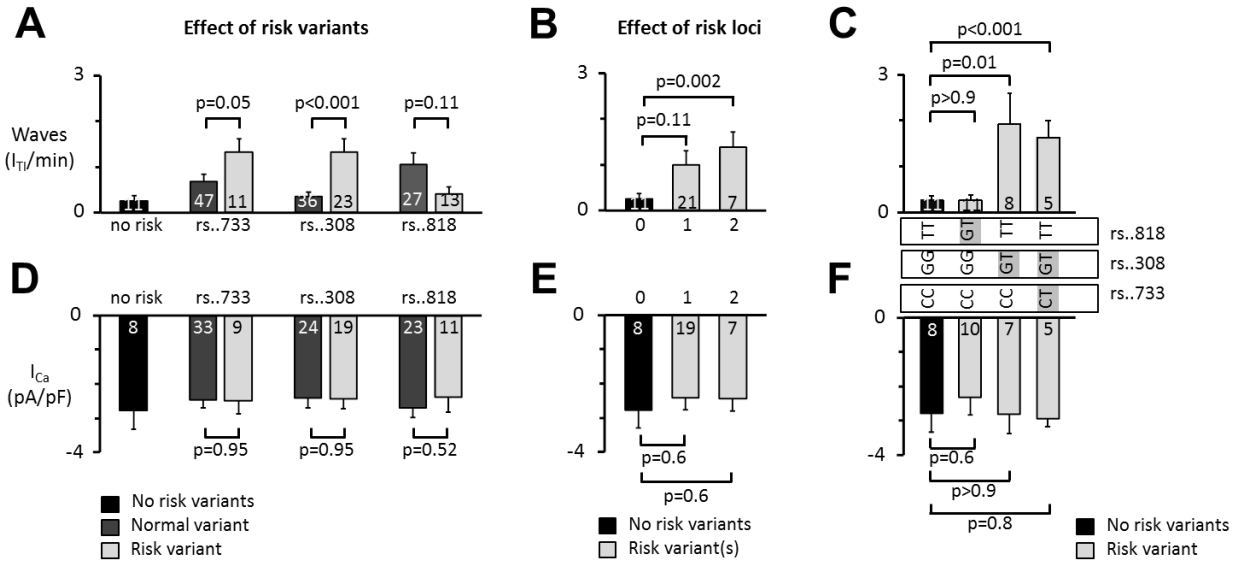

Figure 13. The risk variant rs13143308T increases the frequency of calcium release-induced I_{TI} currents. (A) Effect of the risk variants at rs2200733 (rs..733), rs13143308 (rs..308) and rs1448818 (rs..818) on the I_{TI}-frequency. The risk allele is specified below each bar. Patients without risk variants (no risk) are given for reference. (B) Effect of the number of risk loci on the I_{TI}-frequency. (C) Dependency of the I_{TI}-frequency on predominant genotypes (indicated below bars). (D) I_{Ca}-amplitude in patients with the allele specified above each bar. (E) Effect of the number of risk loci on the I_{Ca}-amplitude. (F) Dependency of the I_{Ca}-amplitude on predominant genotypes (given above bars). Patients are the same as in panels A-C and D-F. The number of patients is given for each bar. P-values are given for the comparisons indicated.

In contrast to the pronounced effects of the rs13143308T variants on I_{TI}, the presence of a risk variant at any of the three examined loci had no significant effect on the I_{Ca} density (Figure 13D), nor did the number of loci where a patient was carrying a risk variant (Figure 13E) or specific genotypes combination (Figure 13F) modify the I_{Ca} density.

DISCUSSION

Main findings

This study is the first affording an electrophysiological mechanism to explain the association between single nucleotide polymorphisms on chromosome 4q25 and the incidence of AF. By analyzing human right atrial myocytes we demonstrate that the presence of the risk variant rs13143308T alone or together with the risk variant rs2200733T is associated with a higher incidence of calcium release-induced transient inward currents and spontaneous membrane depolarizations. These features are hallmarks of myocytes from patients with AF [14,15] and have been reported to contribute to the initiation of this arrhythmia [15,136,153]. Moreover, alterations in the calcium homeostasis linked to the 4q25 risk variants were observed even in myocytes from patients with no recorded episodes of AF, and they were exacerbated in the patients that had AF; thus suggesting that the higher incidence of spontaneous calcium release as a risk factor for AF by favoring the initiation and occurrence of this arrhythmia.

Association between 4q25 risk variants and spontaneous SR calcium release

Confocal calcium imaging in human atrial myocytes revealed that 4q25 risk variants promote spontaneous SR calcium release by increasing the calcium spark frequency through an elevation of the number of calcium spark sites. The higher incidence of spontaneous arrhythmogenic calcium release events have been linked to a higher RyR2 open probability,[154,155] and inhibition of RyR2 opening[156,157] especially by reducing the duration of the RyR2 opening[157] can prevent arrhythmia. Mechanistically, increased RyR2 opening has been attributed to several factors, including luminal calcium activation,[158,159,60] hyperphosphorylation of the RyR2[12,15,137,138,59] and/or increased SR calcium loading.[136,160] In accordance with the latter, we found a significantly higher SERCA2 expression and SR calcium loading in patients without AF but who carried 4q25 risk variants. This finding, combined with the lack of apparent changes in the CSQ-2 level in the same patients is expected to favor that more RyR2 clusters reach the threshold for store-overload

induced calcium release[161] thus explaining the observed increase the calcium spark density. Interestingly risk variants increased SR calcium loading only in patients without AF, suggesting that the 4q25 mediated increase in SR calcium loading may precede the occurrence of AF and contribute to the initiation of the arrhythmia but not to its maintenance. Indeed, a higher incidence of spontaneous calcium release has been associated with higher SR calcium load in patients with paroxysmal AF[136] but not in patients with permanent AF.[12,14,15,136,137]

The 4q25 risk variant rs13143308T is a genetic marker for risk of atrial fibrillation linked to spontaneous SR calcium release

Analysis of the effects of specific 4q25 genotype combinations at the loci rs2200733, rs13143308 and rs1448818 revealed that the rs1448818 variant did not modify the I_{TI} frequency when normal variants were present at the other loci. By contrast a single rs13143308T risk allele combined with normal variants at the other loci increased the I_{TI} frequency 7-fold. In agreement with previous findings,[7] we found that rs2200733T co-segregates with rs13143308T, precluding analysis of the effect of the rs2200733T allele alone. However when rs2200733T was present together with rs13143308T the effect was similar to that of the rs13143308T variant alone. Thus, genotyping for the rs13143308 allele would be sufficient to identify patients at risk of AF associated with arrhythmogenic calcium release.

Functionally, the presence of a single rs13143308T risk variant increased both the frequency of spontaneous calcium release-induced membrane depolarizations and their amplitude (Figure 7A-C). Interestingly, the I_{TI} amplitude was similar in patients with and without the risk variant (Figure 6A-B), suggesting that the larger amplitude of the membrane depolarizations observed in the rs13143308T variants might be caused by concomitant changes in other ionic currents such as a reduction in the inwardly rectifying potassium current $K_{v1.5}$ and/or the acetyl choline activated potassium current ($I_{K,Ach}$), previously reported to occur in patients with AF;[162,163] and the present results warrants a thorough

analysis of the expression and activity of potassium currents in patients with 4q25 risk variants.

A prominent reduction in the I_{Ca} density is another characteristic feature of atrial myocytes from patients with AF.[12,13,23] However, analysis of I_{Ca} recordings revealed that I_{Ca} was reduced to the same extent in patients with AF independently of the genetic variant present at 4q25. Indeed, neither of the three risk variants examined here had any effect on the amplitude or properties of I_{Ca} in patients with or without AF; suggesting no role for L-type channels as a functional link between 4q25 risk variants and AF.

Study limitations

A limitation of the present study is that it only used human right atrial specimens. However, extraction of left atrial tissue samples for myocyte isolation is only ethically justifiable in the fraction of patients undergoing mitral valve surgery, and in these cases the left atrium is usually diseased and the cavity dilated, which in itself has been reported to affect calcium homeostasis.[117] Thus, electrophysiological analysis of human atrial myocytes from patients with diseased and nearly normal human atrial myocytes is feasible in the right but hardly in the left atrium. Another concern when working with human atrial samples is potentially confounding effects of underlying cardiovascular disease or pharmacological treatments of the patients donating the tissue samples. However, in the present study there were no significant differences in the incidence of concurrent diseases or in the drug prescription among patients with and without 4q25 risk variants (see Table 1).

Clinical relevance and conclusions

In summary, our findings identify the rs13143308T risk allele as a new genetic marker for AF risk linked to arrhythmogenic calcium release. Clinically, this should provide novel means for 1) Identification of patients at risk or with AF that is specifically linked to defective calcium homeostasis and 2) Improved stratification and treatment of patients with AF. Specifically, the abnormally high

incidence of calcium release events observed in patients with a rs13143308T allele predict that pharmacological therapies aiming to control calcium release from the sarcoplasmic reticulum might be much more efficient in AF patients with this risk allele than in those with the normal rs13143308G allele.

In addition, our results point to the rs13143308 risk variant on chromosome 4q25 as a new key to understand the array of molecular mechanisms that link AF to perturbations in the calcium homeostasis.

IV. PITX2 INSUFFICIENCY IN AN ATRIAL-SPECIFIC TRANSGENIC MOUSE MODEL REPLICATE THE EFFECTS OF 4q25 RISK VARIANTS ON THE INTRACELLULAR CALCIUM HOMEOSTASIS

INTRODUCTION

Several cardiovascular risk factors are associated with an increased incidence of AF, including hypertension, obesity, previous records of cardiovascular disease, and familial history of AF.[164] Different mechanisms have been proposed to underlie AF, including the generation of ectopic electrical foci at the pulmonary veins and the formation of electrical rotors.[165] In addition, structural remodeling, involving atrial fibrosis as well as atrial dilation, have been widely associated with AF onset.[166,167] At the molecular level, AF has been linked to impaired calcium handling such as reduced calcium influx through L-type calcium channels,[13,168] increased calcium release from the sarcoplasmic reticulum (SR)[12,14,15,137,168] and calcium release-induced afterdepolarizations.[15] Atrial electrical remodeling by shortening of atrial refractoriness and action potential duration are also causative mechanisms linked to AF onset.[169]

Importantly, although AF prevalence is high, the genetic bases of AF are still not well settled. Rare mutations in a variety of ion channels have been associated to familial AF,[145] but they only account for a minority of cases. Recent genome-wide association studies (GWAS) have identified common risk variants associated with AF in four distinct genetic loci; 4q25, located in the vecinity of the transcripion factor Pitx2, 1q21 which is intronic to KCNN3, 16q22 linked to ZFHX3 and 16q13 to IL6R.[7,170–173] Meta-GWAS studies have further implicated six other loci in AF (CAV1, HCN4, SYNE2, SYNPO2L, PRRX1, and WNT8A).[147,152,174] So far, relevant functional links to atrial arrhythmogenesis have only being provided for PITX2 [8,20,21] and more recently for KCNN3.[175,176]

Experimental evidences in distinct laboratories, including ours, have demonstrated that Pitx2 loss of function in a transgenic mouse model reproduce features of atrial arrhythmogenesis.[8,20,21] Thus, Wang et al.[20] demonstrated that Pitx2 haploinsufficiency predisposes to AF in electrically stimulated adult mice and Kirchhof et al.[21] reported increased predisposition to AF in electrically stimulated Pitx2c deficient adult mice and evidenced dysregulation of distinct ion channels. It should be highlighted that both of these Pitx2 haploinsufficient mouse models display normal basal ECG recordings and no atrial structural remodeling. On the contrary, atrium-specific conditional Pitx2 mouse mutants, in whom right-sided sinus node formation is intact, displayed abnormal ECG features such as absence of P waves and atrioventricular block as well as atrial dilation in the absence of fibrosis[8]. In this model, voltage-gated sodium and inward rectifying potassium channels are abnormally expressed in the atrial myocardium at both fetal and adult stages, indicating that Pitx2 impairment caused the onset of left-sided electrophysiological defects that are substrates predisposing to AF. More recently, Tao et al.[22] developed a post-natal Pitx2 deficient mouse model, which displayed variable RR intervals and spontaneous P-wave alterations, characteristics of sinus node dysfunction. In addition ChIP-seq and quantitative PCR (qPCR) analyses revealed that Pitx2 regulates distinct cell junctional proteins, ion channels, and also distinct transcriptional regulators. Overall, these data support a pivotal role of Pitx2 in the regulation of gene expression that, if impaired, increases the vulnerability to develop atrial arrhythmias. It does, nevertheless, remain to be elucidated why some Pitx2 deficient mice display spontaneous atrial arrhythmias whereas a trigger is needed in others.

Here, we investigated the effects of atrium-specific conditional deletion of Pitx2 on the intracellular calcium homeostasis and the electrical activity in isolated atrial myoccytes to test the hypothesis that this model of PITX2 insufuciency can reproduce the effects of 4q25 risk variants on Ca^{2+} homeostasis in human atrial myocytes.

METHODS

Transgenic mouse lines and breeding strategy

The Pitx2floxed and NppaCre transgenic mouse lines have been described previously.[177,178] Generation of conditional atrial (NppaCre) mutant mice has been described previously.[8] Three different conditions were used for the NppaCrePitx2 mice: wild type Cre- controls (NppaCre-Pitx2$^{fl/fl}$), atrial-specific heterozygous (NppaCre+Pitx2$^{fl/-}$) and atrial-specific homozygous (NppaCre+Pitx2$^{-/-}$). This investigation conforms the Guide for the Care and Use of Laboratory Animals published by the US National Institutes of Health. The transgenic mice were generously provided by Dr. D. Franco at University of Jaén, and this study was approved by the Bioethics Committees at University of Jaén and at Hospital de la Santa Creu I Sant Pau.

Tissue samples, mRNA isolation, and reverse transcription

Mice were sacrificed by cervical dislocation. Adult hearts were carefully dissected and briefly rinsed in Ringer´s solution. Tissue samples corresponding to the right atrium (RA) and left atrium (LA) were collected for each experimental condition, immediately snap-frozen in liquid nitrogen and stored at -80ºC until used. Pooled samples of at least three independent mice were processed for each condition, respectively. Three independent pooled samples were further processed for RNA isolation and qPCR analyses At University of Jaén.

qRT-PCR (mRNA)

RT-PCR was performed in Mx3005Tm QPCR System with a MxPro QPCR Software 3.00 (Stratagene) and SYBR Green detection system. Three internal controls, mouse β-actin, Gusb and Gapdh, were used in parallel for each run. Each PCR reaction was performed at least three times to obtain representative average. The Livak method was used to analyze the relative quantification RT-PCR data[179] and normalized in all cases taking as 100% the wild-type (control) value, as previously described.[180]

Atrial myocyte dissociation

Cardiomyocytes were isolated from 3-6 months-old NppaCre^{-}Pitx2$^{fl/fl}$ and NppaCre^{+}Pitx2$^{-/-}$ and NppaCre^{+}Pitx2$^{-/-}$ mice as detailed in General Methodologies.

Patch-clamp recordings

The properties and current-volatage relationship of I_{Ca} , the frequency and amplitude of transient inward currents (I_{Ti}) and the SR Ca^{2+} content, measured as the time integral of the current eleicited by transient exposure to 10 mM caffeine, were recorded in the perforated patch configuration with a software-controlled patch-clamp amplifier (EPC 10, HEKA) at room temperate as detailed in General Methodologies. Membrane potentials were measured in the current-clamp configuration using K^{+}-containing intra and extracellular media. The bath solution and the pipette solution composition are described in General Methodologies. The holding current was varied in order to assess the amplitude and frequency of spontaneous membrane depolarizations at different resting membrane potentials.

Data analysis

The properties, time-integral or frequency of ionic currents recorded in cells from the same animal were averaged. Unless otherwise stated, average values from each animal were used for statistical analysis and expressed as mean ± SEM. Student's t-test or two-way analysis of variance and Holm-Sidak test were used as indicated to assess significant differences. Differences were considered statistically significant when $p<0.05$.

RESULTS

Calcium handling is impaired in atrial-specific Pitx2 mutants in a dose-dependent manner

The expression level of major components of the cardiac calcium-regulatory system was analyzed by qRT-PCR in the LA chamber of NppaCre^{+}Pitx2$^{-/-}$,

NppaCre^{+}Pitx2$^{fl/-}$ and NppaCre^{-}Pitx2$^{fl/fl}$ control mice that display distinct Pitx2 expression levels (Figure 1A).

These experiments revealed that the L-type calcium channel pore-forming subunit Cacna1c is significantly down-regulated, whereas ancillary subunits Cacnb1 and Cacnb3, but not Cacn4b, are up-regulated in the LA of NppaCre^{+}Pitx2$^{-/-}$ compared with NppaCre^{-}Pitx2$^{fl/fl}$ controls (Figure 1B). Regulators of the sarcoplasmic reticulum calcium content such as Atp2a2, Casq2, and Pln all displayed a strong up-regulation, and RyR2 a minor but significant up-regulation in the LA of NppaCre^{+}Pitx2$^{-/-}$ mice (Figure 1B). Moreover, NppaCre^{+}Pitx2$^{fl/-}$ mice displayed intermediate levels for theses genes, demonstrating a dose-dependent effect of Pitx2 deficiency (Figure 1C).

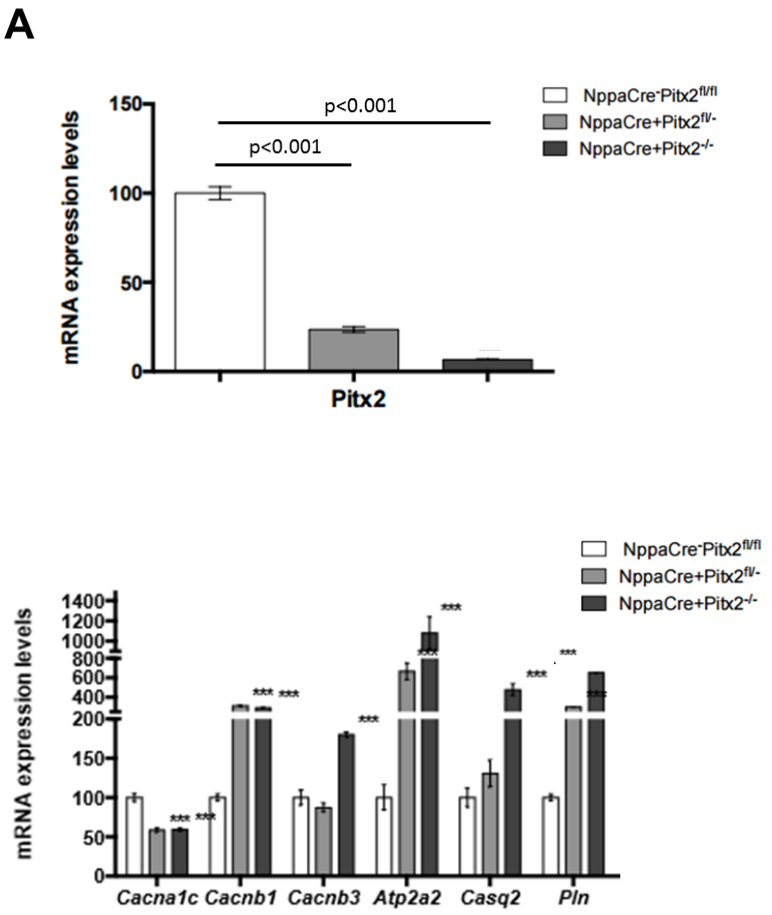

Figure 1. mRNA expression of Pitx2 and main proteins of cardiac calcium-regulatory system. (A) qPCR analyses of Pitx2 in the left atrial chamber of NppaCre^{+}Pitx2$^{-/-}$, NppaCre^{+}Pitx2$^{fl/-}$ and NppsCre^{-}Pitx2$^{fl/fl}$ mice. (B) Calcium handling gene expression in the left atrial chambers of NppaCre^{+}Pitx2$^{-/-}$, NppaCre^{+}Pitx2$^{+/-}$ and NppaCre^{-}Pitx2$^{fl/fl}$. *Cacna1c* and *Ppp1r12* are severely down-

regulated while *Cacnb1, Cacnb3, Atp2a2, Casq2 and Pln,* are up-regulated, n=3 animals *p<0.01; **p<0.05; ***p<0.001.

In line with these findings, electrophysiological analyses demonstrated a significant decrease in I_{Ca} amplitude in the LA of atrial-specific NppaCre^{+}Pitx2$^{-/-}$ mutants compared with controls (Figure 2A-B). Deletion of Pitx2 did not affect the kinetics of I_{Ca} inactivation (Figure 2C) or the shape of the current-voltage (I-V) relationship (Figure 2D).

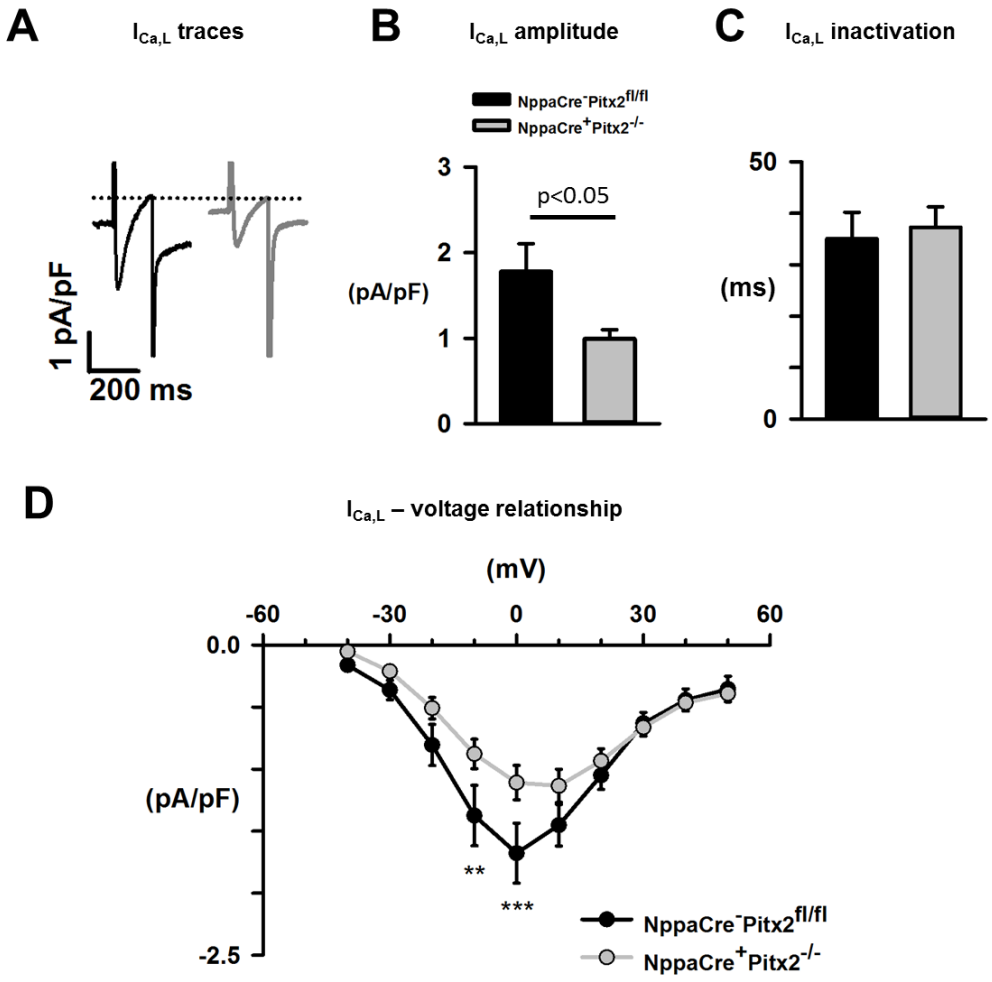

Figure 2. I_{Ca} amplitude and properties. (A) Representative L-type calcium current traces in myocytes from LA. (B) Averaged data for normalized I_{Ca} current density showing that the I_{Ca} amplitude was lower in LA myocytes from NppaCre^{+}Pitx2$^{-/-}$ than from NppaCre^{-}Pitx2$^{fl/fl}$. NppaCre^{-}Pitx2$^{fl/fl}$, n=7 animals, NppaCre^{+}Pitx2$^{-/-}$, n=9 animals. *p< 0.05. (C) Averaged data for the time-dependent inactivation of $I_{Ca.}$ Time constants are given for NppaCre^{-}Pitx2$^{fl/fl}$ (black bars) and for NppaCre^{+}Pitx2$^{-/-}$ (grey bars). (D) Current-voltage relationship for I_{Ca} in LA myocytes. Values are normalized to the cell capacitance. Significant differences between NppaCre^{+}Pitx2$^{-/-}$ and NppaCre^{-}Pitx2$^{fl/fl}$ are indicated with ** (p<0.01) or *** (p<0.001).

Also in line with the RT-qPCR analyses, the SR calcium load was increased in NppaCre^{+}Pitx2$^{-/-}$ compared to NppaCre^{-}Pitx2$^{fl/fl}$ control mice (Figure 3A-B).

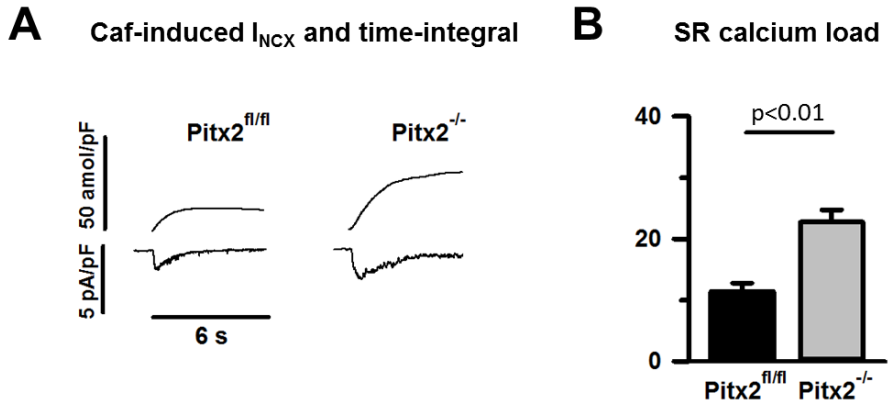

Figure 3. Determination of sarcoplasmic reticulum calcium load. (A) Representative traces of caffeine-induced Na^{+}-Ca^{2+} exchange currents and their corresponding time integrals converted to amol Ca^{2+}/pF. (B) Average time integrals of the Na^{+}-Ca^{2+} exchange currents, showing larger time integrals in LA myocytes from NppaCre^{+}Pitx2$^{-/-}$ mice. NppaCre^{-}Pitx2$^{fl/fl}$, n=6 animals, NppaCre^{+}Pitx2$^{-/-}$, n=7 animals.

Thus, the alteration of calcium regulatory protein expression is paralleled by functional changes in calcium handling in the left atria of NppaCre^{+}Pitx2$^{-/-}$ mice.

Calcium handling is altered in atrial-specific Pitx2 mutants in a chamber-specific manner

Since the contribution of the right and left atrium to atrial arrhytmogenesis is distinct, and because myocyte isolation and patch-clamp analysis in humans is feasible for the right atrium but less so for the left atrium, we explored whether changes observed in the LA also occurred in the RA chamber. qPCR analyses revealed that Cacna1c display up-regulation in the RA and down-regulation in the LA of NppaCre^{+}Pitx2$^{-/-}$ mice (Figure 4A). In contrast, up-regulation of Cacnb1, Cacnb3, Atp2a2, Casq2, and Pln was observed in both RA and LA chambers,. Functional analysis confirmed that down-regulation of Cacna1c in LA myocytes of

NppaCre^{+}Pitx2$^{-/-}$ mice was accompanied by a significant decrease I_{Ca} in LA (Figure 4B) and up-regulation of Atp2a2 and Casq2 in both RA and LA of NppaCre^{+}Pitx2$^{-/-}$ mice was associated with higher SR calcium content in both LA and RA (Figure 4C).

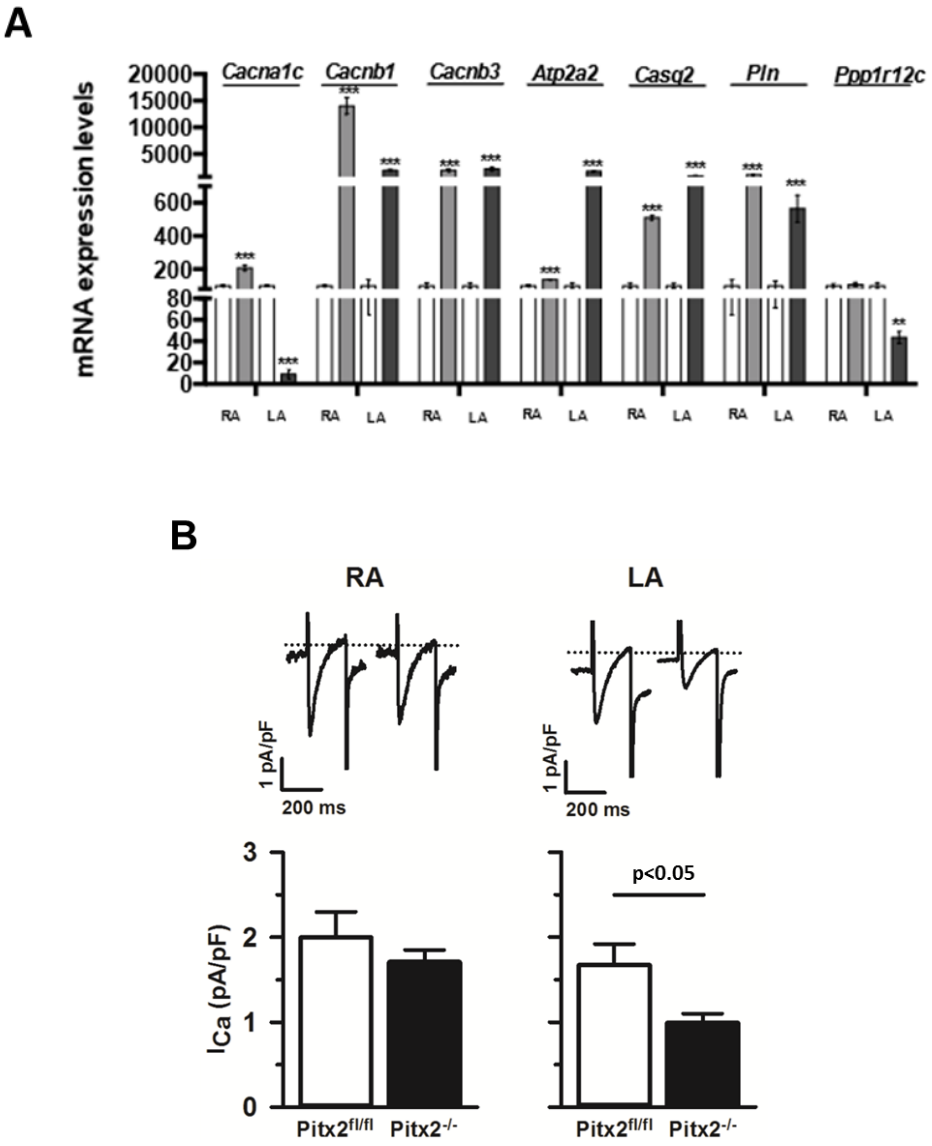

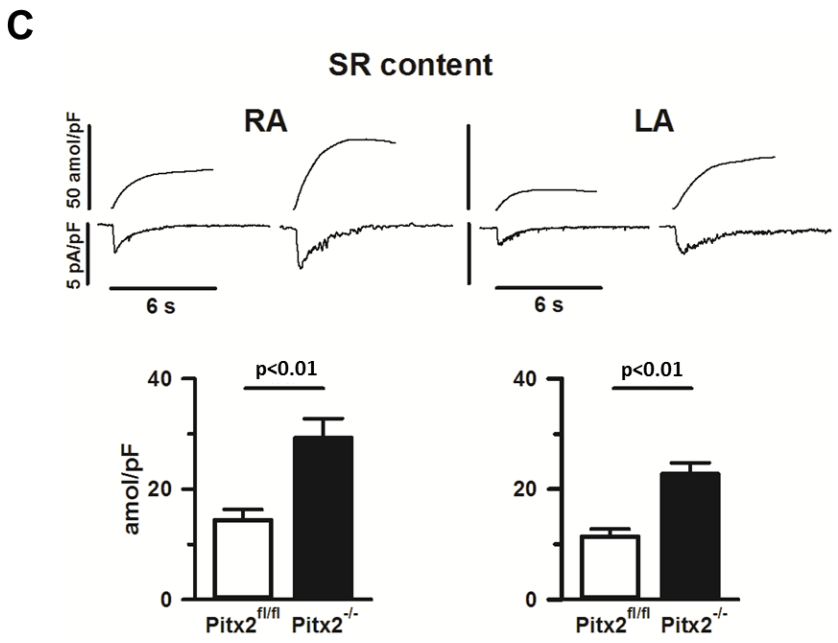

Figure 4. Differences in I_{Ca} and SR calcium content in cells from right and left atria chambers of NppaCre^{+}Pitx2$^{-/-}$ and NppaCre^{-}Pitx2$^{fl/fl}$ mice. (A) qPCR analyses in RA and LA chambers of NppaCre^{+}Pitx2$^{-/-}$ and NppaCre^{-}Pitx2$^{fl/fl}$ hearts. Differential left/right regulation was observed for *Pp12r12c*, whereas similar up-regulation in both atrial chambers is observed for *Cacnb1, Cacnb3, Atp2a2, Casq2, Pln* and *Ppp1r12c*. *Cacna1c* display up-regulation in the RA and down-regulated in the LA, n=3 pooled samples. (B) Representative L-type calcium current traces in myocytes from RA and LA of NppaCre^{+}Pitx2$^{-/-}$ and NppaCre^{-}Pitx2$^{fl/fl}$ and their correspondent averaged data for normalized I_{Ca} current density showing that the I_{Ca} amplitude was lower in LA myocytes from NppaCre^{+}Pitx2$^{-/-}$ than from NppaCre-Pitx2$^{fl/fl}$ and from RA myocytes from both NppaCre^{+}Pitx2$^{-/-}$ and NppaCre^{-}Pitx2$^{fl/fl}$. (C) Representative SR calcium load traces in RA and LA atrial myocytes, of caffeine-inuded Na^{+}-Ca^{2+} exchange currents and their corresponding time integrals (converted to amol).

Atrial specific heterozygous Pitx2 knockout recapitulate calcium-handling disturbances observed in patients with 4q25 risk variants

Since the transcription factor Pitx2 has been proposed as a molecular link between 4q25 risk variants and atrial fibrillation,[7] we tested if partial deletion of Pitx2 expression, could reproduce the alterations in the intracellular calcium homeostasis observed in right atrial myocytes from patients with 4q25 risk variants (chapter III). For this purpose, we used right atrial myocytes from the conditional heterozygous atrial-specific NppaCre^{+}Pitx2$^{fl/-}$ mutant mouse model.

Electrophysiological analysis with perforated patch-clamp technique revealed no differences in the L-type calcium current amplitude among right atrial

myocytes from NppaCre^{-}Pitx2$^{fl/fl}$ and NppaCre^{+}Pitx2$^{fl/-}$ mice (-1.62±0.34 vs. -1.66±0.30 pA/pF). By contrast, right atrial myocytes from NppaCre^{+}Pitx2$^{fl/-}$ mice had a higher incidence of calcium sparks (Figure 5A) and this feature was not unique to right atrial myocytes since the calcium spark frequency was 3.9 fold higher in 22 left atrial myocytes from 6 NppaCre^{+}Pitx2$^{fl/-}$ mice than in 25 left atrial myocytes from 8 NppaCre^{-}Pitx2$^{fl/fl}$ mice (52.7±9.2 vs. 13.5±3.5 sparks/min/1000µm^2; p<0.001). The frequency of calcium waves and spontaneous calcium transients was also elevated in right atrial myocytes from NppaCre^{+}Pitx2$^{fl/-}$ mice (Figure 5B). Moreover, spontaneous calcium waves were able to elicit spontaneous calcium transients (see Figure 5B). In line with this, the frequency of spontaneous I_{TI}s was higher in myocytes from NppaCre^{+}Pitx2$^{fl/-}$ than from NppaCre^{-}Pitx2$^{fl/fl}$ mice (Figure 5C); similar to the difference between human right atrial myocytes from patients with normal and risk variants at 4q25 (Chapter III, Figure 3). Also in line with the human data, the caffeine releasable SR calcium content was significantly higher in right atrial myocytes from NppaCre^{+}Pitx2$^{fl/-}$ than NppaCre^{-}Pitx2$^{fl/fl}$ mice (Figure 5D).

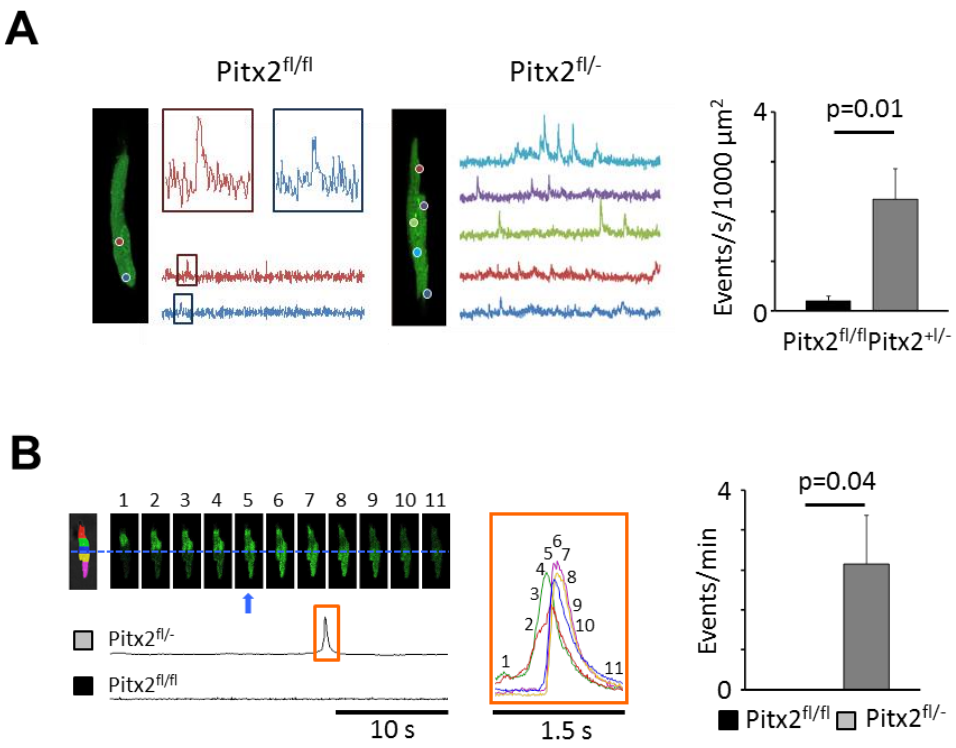

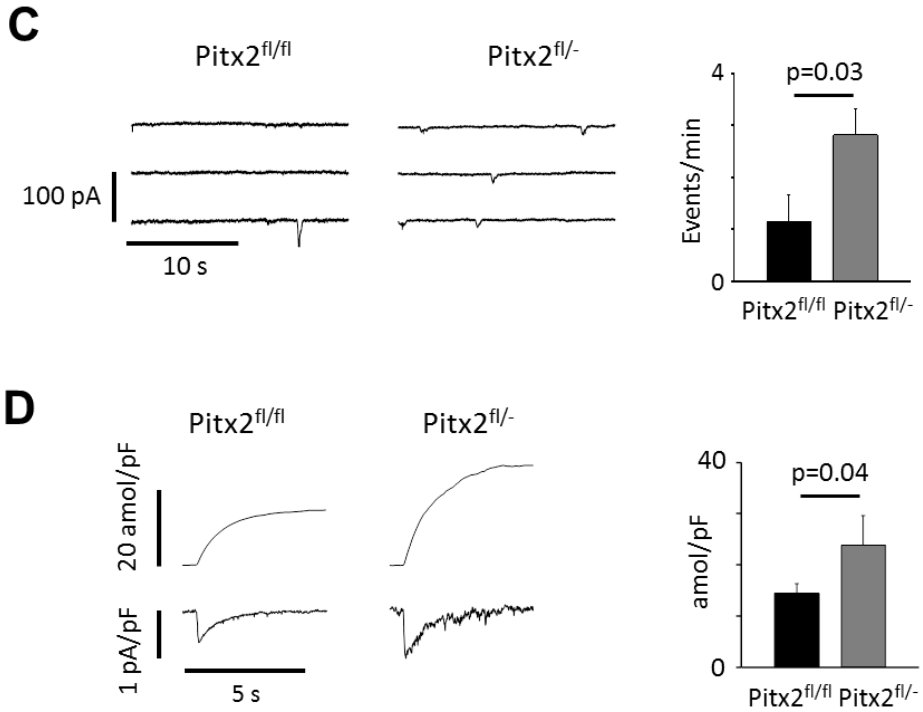

Figure 5. Atrial specific deletion of Pitx2 recapitulates the effects of 4q25 risk variants on calcium homeostasis in isolated atrial myocytes. (A) Right atrial myocytes from a NppaCre^{-}Pitx2$^{fl/fl}$ and a NppaCre^{+}Pitx2$^{fl/-}$ mouse with indication of spark sites. Calcium traces from each site are shown to the right of each cell and insets show details of the calcium sparks. Mean spark frequencies are shown on the right. (B) Consecutive images of a calcium wave from a NppaCre^{+}Pitx2$^{fl/-}$ mouse. The blue line and arrow indicates the point where the calcium wave triggers a spontaneous calcium transient. The corresponding calcium trace is shown below for the NppaCre^{+}Pitx2$^{fl/-}$ mouse and for a NppaCre-Pitx2$^{fl/fl}$ mouse. The calcium signal is shown for 5 adjacent regions in the inset on the right. The color of each trace corresponds to the region of the myocyte (on the left) with the same color. The wave frequency is shown on the far right. NppaCre^{-}Pitx2$^{fl/fl}$ mice had no calcium waves. (C) Transient inward current recordings (left) and frequency (right). (D) Caffeine induced currents (top) and their time integral (bottom). The caffeine releasable SR calcium content is shown on the right.

Importantly, when subjected to current-clamp technique the same myocytes from wild type mice primarily had modest membrane depolarizations at rest and rarely had any spontaneous action potentials, whereas the heterozygous NppaCre^{+}Pitx2$^{fl/-}$ mice often showed spontaneous action potentials (Figure 6A). Overall, the incidence of spontaneous action potentials recorded at resting membrane potentials between -80 and -60 mV was significantly higher ($p<0.05$) in atrial myocytes from the NppaCre^{+}Pitx2$^{fl/-}$ mice (Figure 6B). Moreover, when subjected to electrical stimulation, only atrial myocytes from NppaCre^{+}Pitx2$^{fl/-}$

mice displayed spontaneous action potentials between stimulation pulses (Figure 6C).

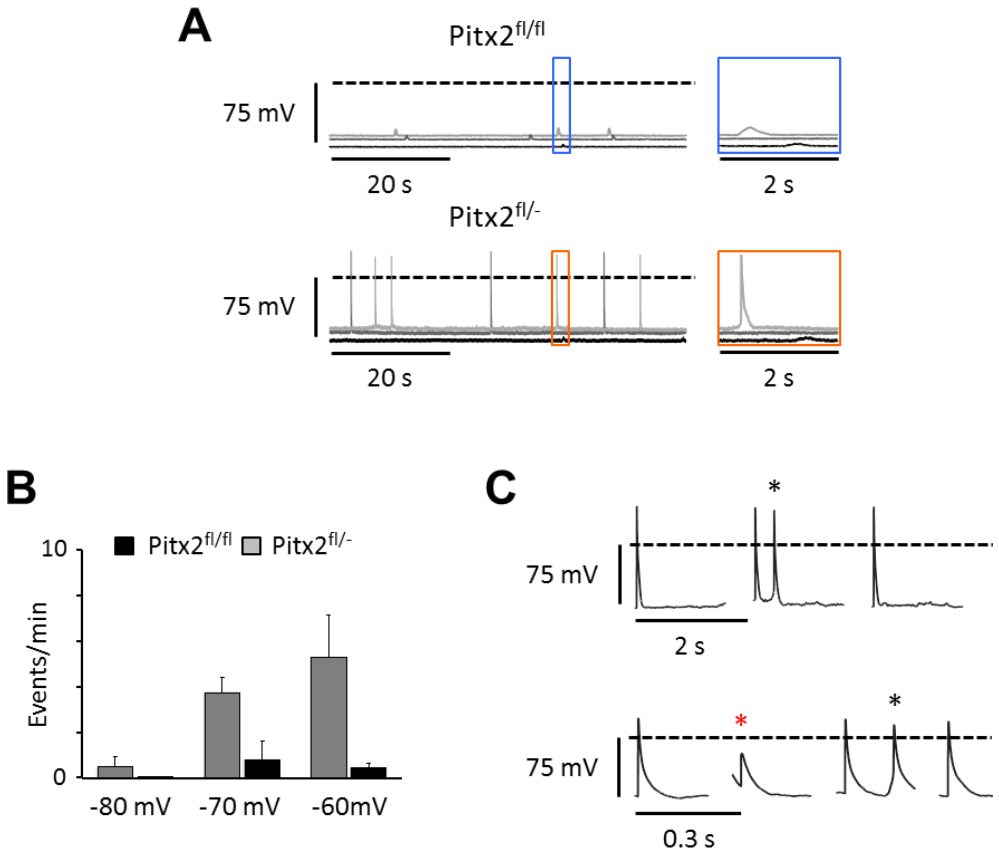

Figure 6. Atrial specific deletion of Pitx2 promote spontaneous membrane potentials. (A) Membrane potential recordings in NppaCre^{-}Pitx2$^{fl/fl}$ (top) and NppaCre^{+}Pitx2$^{fl/-}$ mice (bottom). Membrane depolarizations and action potentials are amplified on the right.(B) Frequency of spontaneous action potentials (events·min^{-1}) at different resting potentials (given below bars). Values are from 8 NppaCre^{+}Pitx2$^{fl/-}$ (grey bars) and 8 NppaCre^{-}Pitx2$^{fl/fl}$ mice (black bars). (C) Recordings of afterdepolarizations (*) in myocytes paced at 0.5 and 3 Hz in myocytes from NppaCre^{+}Pitx2$^{fl/-}$ mice. The red asterisk (*) indicates an action potential diminished by a preceding afterdepolarization (only the tail was recorded). Dashed lines indicate 0 mV. Afterdepolarizations were not recorded at any stimulation frequency between 0.5 and 4 Hz in any of 4 NppaCre^{-}Pitx2$^{fl/fl}$ mice.

DISCUSSION

Main findings

The present study is the first to undertake a systematic analysis of the effects of Pitx2 insufficiency on the expression and function of key calcium regulatory proteints. For this pupose we used an inducibe atrial-specific Pitx2-insufficient transgenic mouse model NppaCrePitx2. Our findings show that Pitx2 insuficiency affect the expression and funcion of key calcium regulatory proteins in a dose-dependent and chamber specific manner. Importantly, right atrial myocytes from mice with heterozygous Pitx2 deletion display alterations in the calcium homeostasis and calcium regulatory proteins similar to those observed in right atrial myocytes from patients with a 4q25 risk variant at rs13143308, supporting the notion that Pitx2 mediates the effects of the rs13143308 risk variant on the calcium homeostasis.

Effect of Pitx2 insufficiency on the expression and function of multiple calcium regulatory genes

Analysis of the effect of Pitx2 insufficiency on the expression profile of calcium regulatory proteins revealed a strong upregulation of proteins involved in the regulation of SR calcium homeostasis such as Atp2a2, Casq-2 and Pln. This effect was dependent on the degree of Pitx2 insufficiency, being stronger in mice with homozygous than heterozygous Pitx2 deletion. Moreover, upregulation of the calcium regulatory proteins was accompanied by a parallel increase in the SR calcium content in atrial myocytes from $NppaCre^{+}Pitx2^{-/-}$ mice. Comparison of the right and left atria revealed that the changes in both expression and function were similar for the two chambers. Interestingly, the observed increase in Atp2a2 and Casq-2 increases SR calcium loading in $NppaCre^{+}Pitx2^{-/-}$ left atrial myocytes in spite of a concurrent reduction of Cacna1c expression and I_{Ca} density. This finding is also in line with findings in human atrial myocytes from patients with AF where a two-fold reduction in the I_{Ca} density has no negative impact on the SR calcium content.[12,15]

The effct of Pitx2 insufficeincy on sarcolemmal calcium fluxes was more heterogeneous. Thus, there were no significant effects on the NCX in any of the atrial chambers, and I_{Ca} was only down-regulated in left atrial myocytes. Such left/right differences were observed for other Pitx2-regulated genes also, which were previously reported associated to left-to-right differences in Pitx2 expression.[21,181]

The observed downregulation of the L-type calcium channels in the left atrium is in line with a reported loss of I_{Ca} in atrial myocycets from patients at high risk of AF[117] or with AF.[12,13] However, Pitx2 deficiency is associated with loss of I_{Ca} in the left but not the right atrium while most observations in humans are from the right atrial appendix, suggesting that several mechanisms contribute to I_{Ca} remodelling in humans. Moreover, measurements of Pitx2 expression in human atria from patients with atrial fibrillation are divergent,[8,20,23,149,150,182] making the association between Pitx2 levels and alterations in the calcium homeostasis less clear.

Pitx2-insufficient mice NppaCre^{+}Pitx2$^{fl/-}$ model recapitulates the effect of 4q25 risk variants on calcium homeostasis in humans

Since the genetic variants at 4q25 are located in the vicinity of the transcription factor Pitx2, and AF has been associated with Pitx2 insufficiency in some studies[8] we considered it important to test the effect of Pitx2 insufficiency in the transgenic mouse model under conditions that most closely imitates the conditions expected to be found in patients with a 4q25 risk variant. Since most patients will be heterozygous carriers of 4q25 risk variants we used right atrial myocytes from heterozygous NppaCre^{+}Pitx2$^{fl/-}$ mice to test the hypothesis that partial Pitx2 insufficiency mimics the effects of the 4q25 risk variant rs13143308. In accordance with this hypothesis, right atrial myocytes from the heterozygous NppaCre^{+}Pitx2$^{fl/-}$ mice faithfully recapitulated the observed calcium handling disturbances in carriers of 4q25 risk variants, including unchanged I_{Ca} density, higher calcium spark frequency and SR calcium load, associated with increased I_{TI} and action potential frequency. Together, these findings support the notion that

Pitx2-mediated modulation of intracellular calcium handling plays an important role in electrophysiological processes associated with AF. The findings would seem to be of particular relevance to the understanding of electrophysiological processes preceding the chronification of AF, since the observed lack of changes in I_{Ca} combined with increased SR calcium load and spontaneous calcium release is similar to changes in the intracellular calcium homeostasis reported in patients with paroxysmal AF.[136]

Limitations and translation of the findings

While the present findings demonstrate that Pitx2 deficiency in the transgenic mouse model faithfully recapitulate the effects of 4q25 risk variants on intracellular calcium homeostasis in human atrial myocytes, the present study does not provide direct evidence that Pitx2 is in fact reduced carriers of 4q25 risk variants. Avialable reports on Pitx2 expression in atrial samples from patients with 4q25 risk variants are not conclusive,[8,23,149] but circumstantial evidence have documented that 4q25 can exert long-range modulation of PITX2C and ENPEP.[24] Moreover, downregulation of Pitx2 has been reported in right and left atrial samples from patients with AF,[8] but another study has reported increased Pitx2 mRNA levels in right atrial samples from AF patients.[23] Thus the role of Pitx2 as a mediator of calcium handling disturbances in patients with 4q25 risk variants remain uncertian and will have to await further studies setteling how risk variants at 4q25 affect the expression and activity of Pitx2.

In summary, here we show that Pitx2 alter calcium handling in a dose-dependent manner in a transgenic inducible atrial-specific Pitx2 knock out mouse model. Moreover, atrial specific heterozygous Pitx2 knockout mice recapitulate calcium-handling disturbances observed in patients with 4q25 risk variants, confirming a relationship between partial insufficiency of Pitx2, 4q25 risk variants and alterations in calcium homeostasis which, could be the prelude to AF.

V. EFFECTS OF AGEING AND 4q25 RISK VARIANTS ON THE CALCIUM HOMEOSTASIS IN ATRIAL MYOCYTES FROM PATIENTS WITH ATRIAL FIBRILLATION

INTRODUCTION

As a result of the progressive increase in life span in highly developed countries and the well-known association between age and the incidence of prevalent cardiovascular diseases, understanding of the underlying molecular and electrophysiological mechanisms is essential for the development of new strategies to prevent and treat cardiovascular diseases such as atrial fibrillation whose incidence is expected to triplicate by 2050.[183]

New knowledge on the mechanism of ageing affecting atrial intracellular calcium handling in humans has been proposed in the first chapter of this thesis, where we demonstrate that a reduction in the expression of several key calcium regulatory proteins with age lead to concurrent functional alterations in the intracellular calcium homeostasis such as decreased I_{Ca} density, lower caffeine releasable SR calcium content, reduction of the calcium transient amplitude, and slowing of its decay. Some of these changes such as reduced I_{Ca} density and calcium transient amplitude are also observed in myocytes from patients with AF,[13,184] but it has not been examined how ageing affect the calcium homeostasis in atrial myocytes from patients with AF.

On the other hand we have in Chapters III and IV examined the effects of 4q25 risk variants and Pitx2 insufficiency on atrial myocyte calcium homeostasis and presented evidence that 4q25 risk variants and Pitx2 insufficiency produce alterations in the calcium homeostasis, which could contribute to trigger episodes of atrial arrhythmia. These findings include, a higher incidence of calcium release-induced transient inward NCX currents and spontaneous membrane depolarizations, features that are hallmarks of myocytes from patients with AF[14,15]

and have been reported to contribute to the initiation of this arrhythmia.[15,153] These effects were found in myocytes from patients with 4q25 risk variants but without AF, and the effects of the 4q25 risk variant was higher in patients with AF (see Chapter III).

Thus, we have documented alterations in the calcium homeostasis that could lead to atrial fibrillation both in the studies of ageing (Chapters I and II) and the studies of 4q25 risk variants and Pitx2 insufficiency (Chapters III and IV). Therefore, we here we aimed to investigate how ageing and 4q25 risk variants affect the calcium homeostasis in patients with atrial fibrillation and whether these factors have a summatory effect on calcium homeostasis and electrophysiological parameters in patients with AF. For this purpose we used patch-clamp technique in human atrial myocytes isolated from patients with and without AF to test the hypothesis that ageing synergistically exacerbates calcium handling disturbances in patients with 4q25 risk variants.

METHODS

Human atrial tissue

A total of 217 isolated right atrial myocytes obtained from 106 patients submitted to elective cardiac surgery were analyzed. Tissue samples from the right atrial appendix were collected as described before (General Methodologies) and each patient gave informed consent to use the tissue sample for the study.

All the patients had a previous history of AF, most of them had chronic AF (n=67) and the rest had paroxysmal AF (n=39). Following the same classification as used in the first chapter of this thesis, patients were divided into three age categories: (i) young (<55 years, 25 myocytes, n=9); (ii) middle aged (55 to 74 years, 120 myocytes, n=60); and (iii) old (≥75 years, 72 myocytes, n=37). When analyzing the combined effects of age and 4q25 risk variants, patients were divided into two groups: younger (≤65; n=26) and older (>65 years; n=43) patients.

Patch-clamp technique

The experimental solutions used for this study had the composition indicated in General Methodologies for external and internal media for voltage-clamp. Amphotericin (250 μg/ml) was added to the pipette solution before starting the experiment. Chemicals were from Sigma-Aldrich.

Whole membrane currents were measured in the perforated patch configuration with an EPC-10 amplifier (HEKA Elektronik). The L-type calcium current (I_{Ca}), current-voltage (I-V) relationship for I_{Ca}, voltage-dependent inactivation, time constants for fast (tau-1) and slow (tau-2) steady-state I_{Ca} inactivation, SR calcium content, and spontaneous calcium release-induced transient inward currents (I_{TI}) were measured as indicated in the General Methodologies.

RESULTS

Study population

Table 1 summarizes the clinical characteristics of the 106 patients included in the study. Older patients had a higher incidence of combined aortic valve replacement surgery and treatment with calcium channels antagonist than young and middle-aged patients. There were not statistically significant differences in the anthropometrics and echocardiographic characteristics among the 3 age groups.

Table 1. Clinical data of the study patients

	Total (n=106)	< 55 years (n=9)	55-75 years (n=60)	≥75 years (n=37)	p value
Anthropometrics characteristics					
Male *n (%)*	51 (48.1%)	6 (66.7%)	26 (43.3 %)	19 (51.4 %)	ns
BMI Kg/m^2	31.1±3.7	27.1±1.8	27.7±0.5	37.5±10.6	ns
Echocardiographic characteristics					
LA diameter *mm*	50.7±1	49.1±4.4	50.1±1.5	51.9±1.4	ns
Indexed LA cm/m^2	2.9±0.1	2.3±0.2	2.8±0.1	3.1±0.1	ns
LVEF *%*	59.7±1.4	57.6±6.4	58.6±1.7	62.1±2.3	ns
Heart disease					
Valvular heart disease *n (%)*	78 (73.6%)	7 (77.8%)	44 (73.3%)	27 (73.6%)	ns
Ischaemic heart disease *n (%)*	35 (33%)	1 (11.1%)	20 (33.3%)	14 (37.8%)	ns
Valvular + ischaemic heart disease *n (%)*	27 (25.5%)	0 (0%)	14 (23.3%)	13 (35.1%)	ns
Surgical treatment					
Aortic valve replacement *n(%)*	58 (54.7%)	3 (33.3%)	29 (48.3%)	26 (70.3%)	0.044
Mitral valve replacement *n (%)*	51 (48.1%)	3 (33.3%)	30 (50%)	18 (48.6%)	ns
Tricuspid valve surgery *n(%)*	1 (0.9%)	0 (0%)	1 (1.7%)	0 (0%)	ns
CABG *n (%)*	32 (30.2%)	2 (22.2%)	18 (30%)	12 (32.4%)	ns
CABG + valve replacement *n (%)*	23 (21.7%)	1 (11.1%)	12 (20%)	10 (27%)	ns
Pharmacological treatment					
ACE-inhibitors n *%*	44 (41.5%)	3 (33.3%)	25 (41.7%)	16 (43.2%)	ns
Angiotensin receptor blocker n *%*	14 (13.2%)	0 (0%)	7 (11.7%)	7 (18.9%)	ns
Beta-blockers n *%*	43 (40.6%)	4 (44.4%)	28 (46.7%)	11 (29.7%)	ns
Calcium channels antagonists n *%*	13 (12.3%)	2 (22.2%)	3 (5%)	8 (21.6%)	0.034

p value corresponding from ANOVA analysis.
Abbreviations: BMI: body mass index; LA: left atrium; LVEF: left ventricular ejection fraction; CABG: coronary artery bypass grafting; ACE: angiotensin conveting enzyme.

Measurements of cell membrane capacitance of the myocytes (Figure 1) revealed no significant differences between the three age groups, but cell capacitance is higher in patients with AF (≤55: 73.6±6.4; 55-74: 71.6±4.0; ≥75: 66.4±4.0 pF), than in patients without the arrhythmia (≤55: 59.2±3.6; 55-74: 61.1±3.0; ≥75: 57.4±4.3 pF).

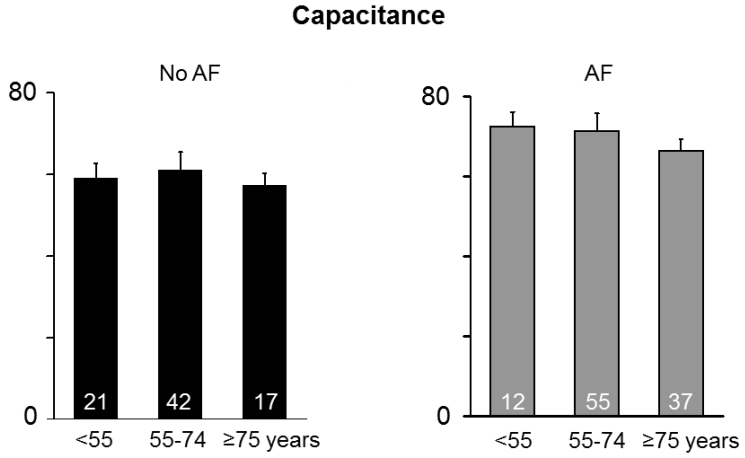

Figure 1. Age does not affect the cell capacitance. Average cell membrane capacitance measured in patients without AF (NO AF patients included in the study of Chapter I) and in patients with AF. The age of the tree patient groups is given below bars. Number of patients are indicated on each bar.

Effect on I_{Ca} of ageing in AF patients

Patch-clamp recordings of the I_{Ca} showed an age-dependent decrease in the steady-state I_{Ca} amplitude in patients with AF from 2.2 ± 0.5 pA/pF in young (n=11) to 1.4 ± 0.1 in middle aged (n=54) and 1 ± 0.1 in old patients (n=37). This effect was similar to the effect of aging observed in patients without AF (Figure 2B) but overall, the I_{Ca}-density was lower in patients with than without AF (1.36 ± 0.1 vs 2.06 ± 0.12, $p<0.001$). The effects of ageing were independent of confounding clinical factors (LA diameter, LVEF % and pharmacological treatment: ACE-inhibitors, angiotensin receptor blocker, beta-blockers, calcium channels antagonist).

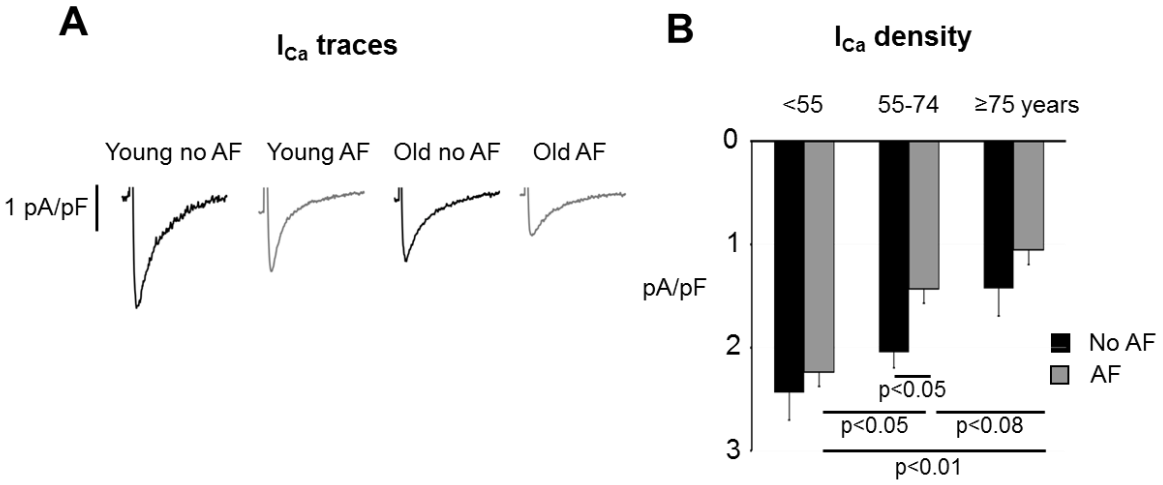

Figure 2. Effect of ageing on I_{Ca} in patients with AF. (A) Representative I_{Ca} traces from different patient groups. (B) Mean I_{Ca} density (pA/pF) in the patients with AF (gray bars), stratificated by age. The effect of ageing in patients is shown for reference (black bars). P-values for significant differences between bars are indicated below the respective bars.

Analysis of the intrinsic I_{Ca} properties showed no significant differences in the shape of the current-volatge relationship when myocytes from patients with AF were divided into the three age groups (Figure 3A). Steady state I_{Ca}-incactivation studied in the AF patients, showed that most of these patients only had one time constant (tau-1), while almost all of the no AF patients had a fast; tau-1 and a slow; tau-2 time constant. Data show that in the AF group, old patients have a slower tau-1 than the young patients. Moreover, tau-1 is significantly slower in AF patients compared with the no AF group, and this was true both in the groups younger and older than 65 years. (Figure 3B).

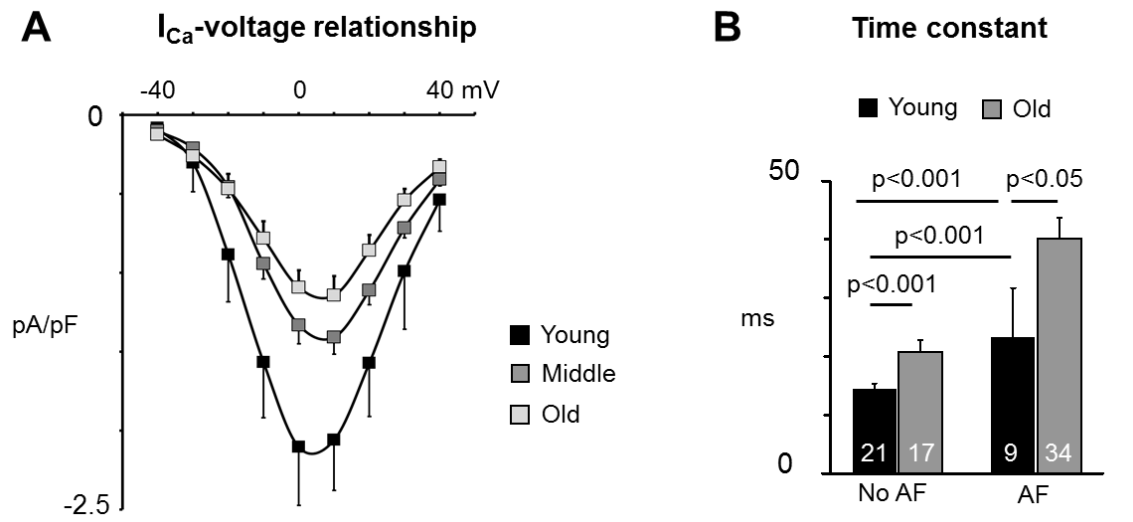

Figure 3. Effect of ageing on intrinsic I_{Ca} properties in patients with AF. (A) I_{Ca}-voltage relationship in the three age group of AF patients (young n=7, middle aged n=48, and old n=32 patients). (B) Average time constant for I_{Ca} inactivation (tau-1) in younger and older patients with AF and without AF (no AF). P-values for significant differences are indicated above bars. Number of patients is given for each bar.

Effect of ageing on SR calcium content and transinet inward currents in patients with AF

To assess if ageing in patients with AF affected the SR calcium content, this was measured from the time integral of the current elicited by exposure of the cell rapidly and transiently (5 seconds) to 10 mM caffeine. Figure 3 shows that the SR calcium content was not modified by ageing in patients with AF. Moreover the effect of ageing in patients with AF was comparable to the effect observed in the no AF group.

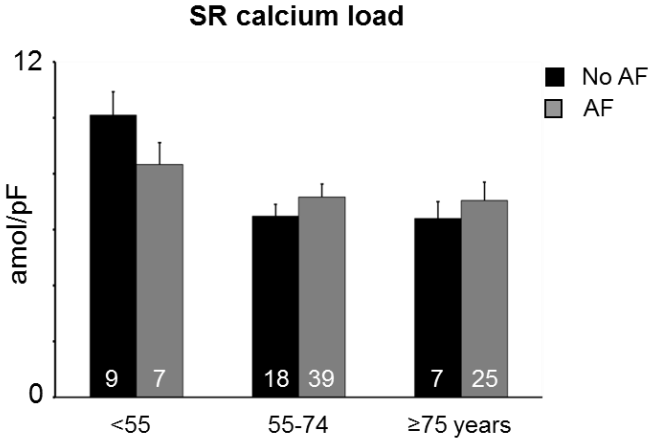

Figure 3. Effect of ageing on the SR calcium load in AF patients. Average time integrals of the current generated when calcium is released by caffeine and ejected by the Na^+/Ca^{2+} exchanger. Integrals are converted to amoles (10^{-18} mol) of calcium released. The age for the three patient groups is given below bars. Number of patients are indicated on each bar.

Analysis of the incidence of calcium release induced I_{TI}s for the three age groups revealed that the incidence was significantly higher in patients with than without AF (no AF) but that ageing had no effect on the I_{TI} frequency. Interestingly, the I_{TI} amplitude did not change with age in patients without AF whereas the amplitude increased with age in AF patients, being significantly larger in middle ($p<0.05$) and old patients (trend) with AF than in old patients without AF.

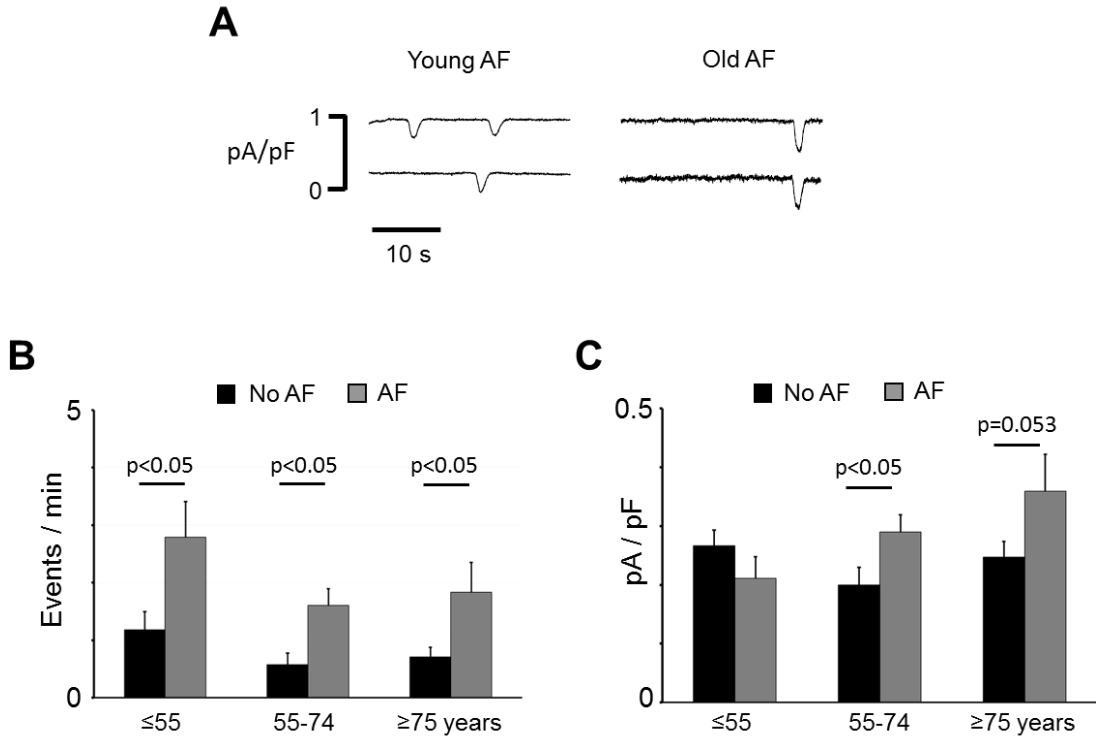

Figure 4. Effect of ageing on spontaneous SR calcium release in AF patients. (A) Representative I_{TI} recordings in a young and an old patient with AF. (B) Average transient inward current (I_{TI}) frequency and (C) average I_{TI} amplitude measured at a resting membrane potential of -80mV in the three age groups (indicated below bars), from patients with and without AF (No AF). Values are from 21 young, 42 middle aged and 17 old patients for No AF, and 9 young, 56 middle aged and 36 old patients for AF. Statistically significant differences are indicated above the corresponding bars.

Effect of 4q25 risk variants and age on electrophysiological properties

Since both ageing and risk variants at 4q25, have been demonstrated to have affect some electrophysiological properties, we investigated the their combined effect on calcium handling. Patients were clasified according to the presence of risk variants at 4q25 and age in eight groups. Due to the reduced number of genotyped young patients with AF, classification by age was limited to those ≤ 65 years (younger) and those >65 years (older).

One of the hallmarks of AF is a reduction of the L-type calcium current (I_{Ca}) density,[13] and we therefore studied how the combination of age and 4q25 risk variants affected the I_{Ca} density. As shown in chapter I, ageing decreases the I_{Ca} density (Chapter I, Figure 2) whereas 4q25 had no effect (Chapter III, Figure 1). Table 2 shows that 4q25 risk variants did neither affect the I_{Ca} density in the older nor in the younger patients.

Table 2. Effect of age and 4q25 risk variants on the I_{Ca} density.

	Ica					
	Young (<65y)			**Old (>65y)**		
	Normal	Risk	**p**	Normal	Risk	**p**
No AF	-2,15 ± 0,31 (n=13)	-2,32 ± 0,53 (n=7)	n.s.	-2,19 ± 0,35 (n=15)	-2,62 ± 0,35 (n=16)	n.s.
AF	-2,60 ± 1,36 (n=2)	-0,99 ± 0,13 (n=3)	n.s.	-0,74 ± 0,15 (n=8)	-1,24 ± 0,22 (n=4)	n.s.
p	n.s.	n.s.		p<0.01	n.s.	

Mean ± SEM I_{Ca} amplitude for the different groups, indicating n and p. No differences were found due to ageing or 4q25 risk variants.

As to the I_{Ti} frequency, it was shown in Chapter I (Figure 5) that ageing *per se* had no effect on spontaneous calcium release from SR, while Chapter III (Figure 2) showed that the I_{Ti} frequency was higher in myocytes from patients with risk variants. Figure 5 shows that the presence of a risk variant increases the I_{TI} frequency in both younger and older patients with No AF. This is also true in older patients with AF, but not in the younger patients with AF.

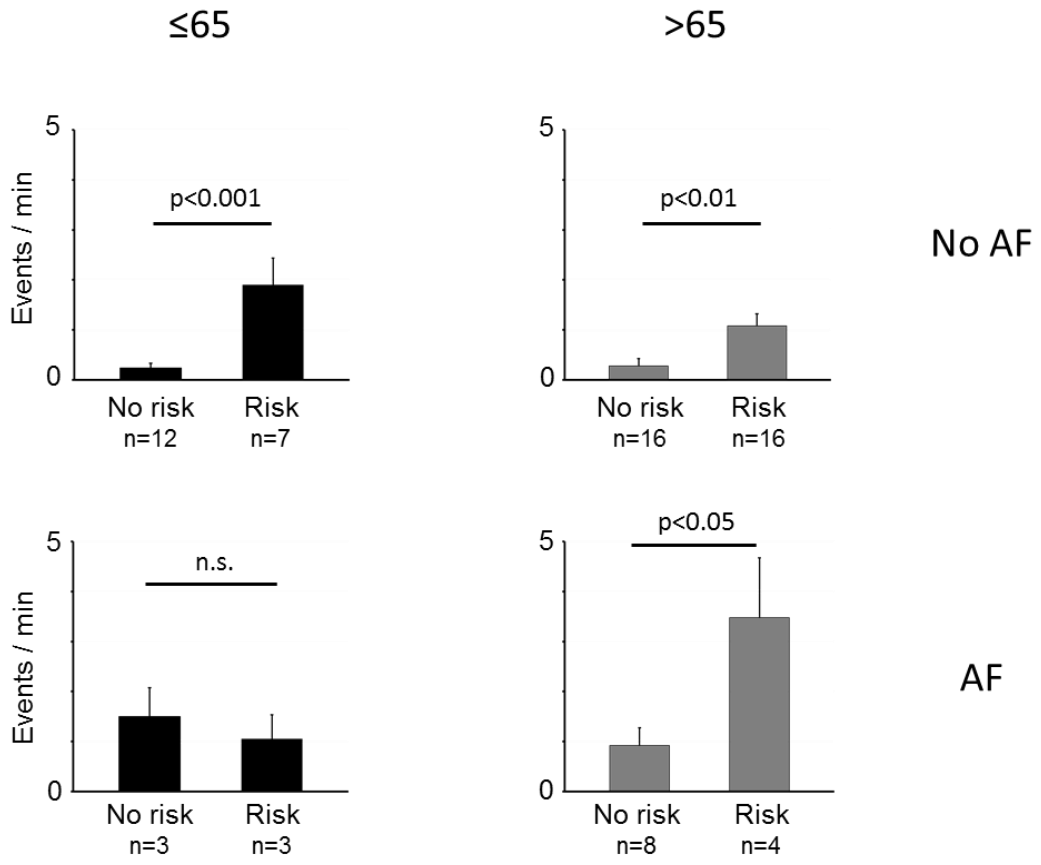

Figure 5. Effect of ageing and 4q25 risk variant on spontaneous calcium release. Average of I_{Ti} frequency on the different groups, young patients (black bars) or ≤65 years, old patients (grey bars) or >65 years, with or without AF and compared by 4q25 risk variants.

When analyzing the caffeine releasable calcium load, the presence of a risk variant had no effect on SR calcium loading in younger or older patients with or without AF (Figure 6).

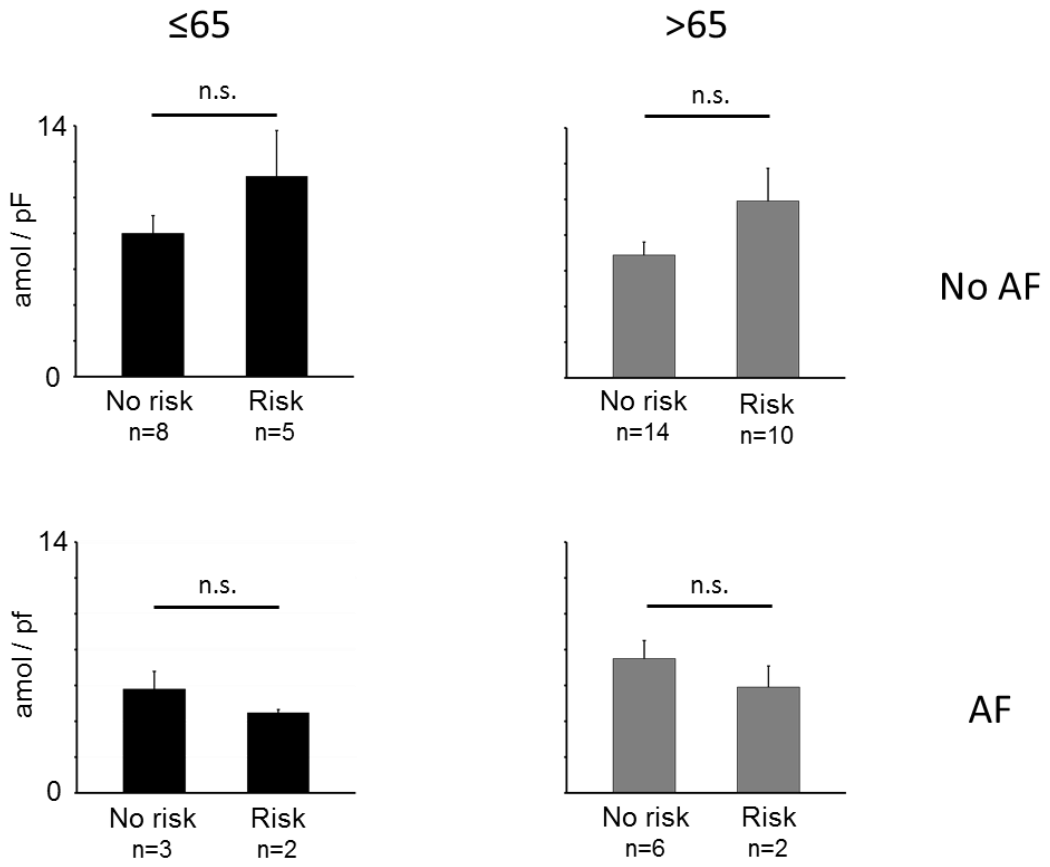

Figure 6. Effect of ageing and 4q25 risk variants on SR calcium load. Mean SR calcium load for patients ≤65 years (black bars) and patients >65 years (grey bars), without AF (No AF, top panels) or with AF (lower panels). The absence (no risk) or presence of a risk variant at 4q25 is indicated below bars.

DISCUSSION

Main Findings

This study aimed to investigate whether ageing and 4q25 risk variants synergistically modify the intracellular calcium homeostasis in human atrial myocytes from patients with AF. Our results show that 1) Age-dependent depression of I_{Ca} occured both in patients with and without AF, but in absolute terms, the I_{Ca} density was more severely depressed in AF-patients; 2) Ageing significantly reduced SR calcium loading in patients without AF (see also Chapter I)

but not in patients with AF; 3) Old age differentially increased the I_{TI} amplitude in patients with AF, increasing the potential of each I_{TI} to induce arrhythmogenic membrane depolatizations or action potentials. Together, these differential effects of ageing on calcium handling might facilitate the reinitiation and maintenance of arrhythmic episodes in patients with AF. By contrast, our results do not support the notion that ageing modifies the effects of 4q25 risk variants on the calcium homeostasis.

Effect of ageing on the calcium homeostasis in patients with atrial fibrillation

We previously described that ageing *per se* depresses the amplitude of the intracellular calcium transient, the I_{Ca} density, and the SR calcium loading[9] (see Chapter I). The present findings show that ageing also depresses I_{Ca} in patients with AF. By contrast, there is no significant effect of age on SR calcium loading in patients with AF, and most importantly, the I_{TI} amplitude increases with age in patients with AF, reaching an amplitude in the old patients that is twice as big in the AF than the no AF group ($p<0.001$).

Since the I_{TI} results from electrogenic calcium extrusion by the NCX[3], its amplitude is expected to determine the amplitude of the resulting membrane depolarization and hence the risk of triggering spontaneous action potential.[15,25] Therefore, the differential increase in the I_{TI} amplitude in old patients with AF might contribute to facilitate triggered activity[185] and the reinition of arrhythmic episodes in patients with AF. Moreover, I_{Ca} depression has previsously been proposed to contribute to AP shortening and electrical reentry in patients with AF, [186–188] suggesting that the stronger I_{Ca} depression in older patients with AF may act in synergy with the larger I_{TI} density in these patients to initiate and perpetuate atrial arrhythmic episodes in these patients.

Combined effects of ageing and 4q25 risk variants on calcium homeostasis

The division of pateints into 8 groups according to age (≤65 and >65 years), the presence of 4q25 risk variants (normal and risk), and the presence of AF (NoAF

and AF) revealed that a higher I_{TI} frequency, the primary calcium handling disturbance in 4q25 risk variants (see Chapter III), was observed in patients with a risk variant independently of the age group. The notion that old age does not aggravate effects of 4q25 risk variants is in accordance a study showing that the 4q25 risk variant rs2200733 is associated with early-onset lone AF in patients younger than 40 years.[189]

Limitations and translation of the findings

A recurrent issue when working with human atrial myocytes to address electrophysiological alterations associated with AF is potentially confounding effects of concurrent cardiovascular disease and pharmacological treatments of the patients. To minimize such effects, regression analysis that includes potentially confounders was normally performed. However, this requires larger sample sizes and/or it puts constraints on the number of confounding factors that can be included in the statistical analysis for a given sample size. Moreover, in order to evaluate how age modulate alterations in the calcium homeostasis by 4q25 risk variants in patients with and without AF, it was necessary to limit the age groups to two. Even so, at this time the number of younger genotyped patients with AF (n=6) is limited, precluding a rigourous statistical analysis of the effect of 4q25 risk variants in this group.

GENERAL DISCUSSION

GENERAL DISCUSSION

Main findings

Following the objectives proposed in this thesis, I first examined the role of ageing on calcium homeostasis in human atrial myocytes in Chapter I. The use of a transgenic mouse model of premature ageing in Chapter II corroborated a potential role for lamin deficiency as a mechanism that could potentially underlie the observed reductions in I_{Ca} amplitude, SERCA2 expression, and SR calcium loading associated with ageing in humans reported in Chapter I. Secondly, investigation of common genetic SNP on chromosome 4q25 in Chapter III revealed for the first time that the risk variant rs13143308T is linked to excessive spontaneous calcium release and membrane depolarizations, providing a new criteria for risk stratification and treatment of patients with AF. Further research (Chapter IV) using a transgenic mouse model with atrial-specific deletion of the transcription factor Pitx2, thought to be regulated by the 4q25 risk variants, showed that heterozygous Pitx2 insufficiency reproduces all the observed calcium disturbances in patients with 4q25 risk variants. Finally in Chapter V, taking into account the combined effect of these three parameters (age, atrial fibrillation and 4q25 risk variants) did not provide evidence that ageing aggravate the negative effects of the risk variants on calcium handling. On the other hand, ageing decreased the I_{Ca} amplitude even more in patients with AF and differentially increased the amplitude of I_{TI} in older patients with AF, increasing the potential of each I_{TI} to induce arrhythmogenic membrane depolarizations or action potentials. Thus, the risk variant rs13143308T on chromosome 4q25 may favor the initiation of AF by inducing spontaneous calcium release-induced atrial electrical activity. Ageing does not modify this phenomenon, but by reducing the I_{Ca} amplitude it may contribute the higher incidence of AF in the ageing population by reducing the atrial refractory period. This effect of ageing could also work in concert with the 4q25 risk variant by favoring the maintenance of spontaneous electrical activity, increasing further the risk of AF in carriers of the risk variant.

Ageing *per se* blunts calcium homeostasis in human atrial myocytes

The electrophysiological and calcium imaging studies carried out in isolated human atrial myocytes from patients with no apparent atrial pathologies revealed several alterations in the calcium homeostasis due to ageing that may impact atrial contraction and rhythm.

First, there was a decrease in key calcium handling proteins with age that was accompanied by concurrent functional changes: 1) the alpha subunit of the L-type calcium channel accompanied a decreased I_{Ca} density 2) reduction in the expression of SERCA2 and CSQ-2 was associated with lower caffeine releasable SR calcium content. These changes were associated with a three-fold reduction of the calcium transient amplitude and a slowing of its decay. Together with the slower propagation of the calcium transient towards the cell center, these alterations may favor a progressive decline in atrial contractile function with age.

Loss of I_{Ca} has also previously been reported as a distinct feature of AF [12,13] and claimed to promote atrial arrhythmogenesis by reducing the action potential duration and refractory period.[186–188] Therefore, our observation of a similar loss of I_{Ca} with age suggests that this could represent an electrophysiological mechanism that contributes to increase the risk of AF in the elderly.

On the other hand, spontaneous calcium release, I_{TI} frequency or I_{TI} amplitude were not different among the three age groups, suggesting that ageing *per se* is not responsible for a higher rate of spontaneous calcium release, also reported as a potentially arrhythmogenic feature of myocytes from AF patients.[12,14,15]

In summary, ageing is associated with depression of SR calcium content, L-type calcium current, and calcium transient amplitude that may favor a progressive decline in human right atrial contractile function. Moreover, the reduction in I_{Ca} and calcium transient amplitude are hallmarks of AF suggesting that these features could also make the elderly more prone to suffer from AF.

The progeric mouse model *Zmpste 24*$^{-/-}$ reproduces the effects of ageing on calcium handling in humans

At the molecular level ageing processes have, among others, been linked to defective lamin processing[16,17] and shortening of the telomeres.[190,191] Therefore, to achieve further insight into the molecular mechanisms underlying altered calcium handling with age, we used the well-established *Zmpste24*$^{-/-}$ progeric mouse model that reproduces essential features of the Hutchinson-Gilford progeria syndrome (HGPS), a disease that entails several cardiovascular disorders like atherosclerosis, arterial stiffness, leading to myocardial infarction, heart failure or stroke and early death.[122,123] This rare genetic disease is caused by defective prelamin-A processing leading to prelamin A accumulation.[129] A comparable phenomenon, resulting in progerin accumulation[16,17] occurs during physiological aging but on a slower time scale.

In line with this, changes in the calcium homeostasis in ageing human atrial myocytes were largely reproduced by the *Zmpste24*$^{-/-}$ mouse model. Thus, when compared with wild type mice, *Zmpste 24*$^{-/-}$ mice showed slower I_{Ca} inactivation, defective SR Ca^{2+} uptake and release, and reduced calcium transient amplitude, which was associated to the lower levels of SERCA2 and CSQ-2. Together, these parallel changes in calcium handling in the *Zmpste24*$^{-/-}$ model and in ageing human atrial myocytes provide an experimental basis for testing whether the changes in calcium handling observed in humans occur in parallel with an age-dependent accumulation of progerin or other products of defective lamin processing.

Propensity to atrial fibrillation in patients with 4q25 risk variants is linked to defective calcium homeostasis

Atrial fibrillation has also been associated with an elevated rate of spontaneous calcium release, I_{TI}, and membrane depolarizations,[14,15] but none of these variables were modified by ageing in human atrial myocytes or in myocytes from the *Zmpste24*$^{-/-}$ model. Recently, common genetic variants on chromosome

4q25 have been associated to AF,[7,146,174] but the relationship between these genetic risk variants and functional electrophysiological alterations associated to AF remain elusive. We therefore tested whether the risk variants were associated with alterations in the SR function, and subsequently if ageing affects such alterations.

This thesis describes for the first time functional electrophysiological changes caused by 4q25 risk variants in human atrial myocytes. Thus, the presence of a single 4q25 risk variant at the rs13143308 locus was associated with an increase in the frequency of spontaneous calcium release, I_{TI}, and membrane depolarizations; all hallmarks of atrial fibrillation.[14,15] These alterations were present in myocytes from patients carrying the risk variants but without AF and they were exacerbated in patients with risk variants and AF. The higher I_{TI} frequency in patients with 4q25 risk variants was linked to a higher calcium spark frequency due to an elevation on the number of calcium sparks sites. This in turn may result from higher SR calcium loading for the risk variants, which concurred with a higher SERCA2 but not CSQ-2 expression, leading to an increase in the number of RyR clusters that reach the threshold for store-overload induced calcium release.[161]

Analysis of the fine structure of the 4q25 site associated with increased risk of AF have revealed different risk loci within this site that independently are associated with risk of AF.[192] In this thesis we have focused on two inter-dependent risk loci, rs2200733 and rs13143308 that have been most strongly and consistently associated with AF[7,89,192] as well as the rs1448818 locus that is closer to the PITX2 locus, thought to mediate functional effects of the risk variants. Analysis of the individual effects of these three risk loci revealed that the presence of a single rs13143308T risk variant increased the I_{TI} frequency 7-fold. Moreover, the rs2200733T risk variant, when present, was found to co-migrate with rs13143308T and the effect of these two risk variants was similar to the effect of rs13143308T alone. By contrast, the presence of a risk variant at rs1448818 alone had no effect on the I_{TI} frequency. Thus, our findings suggest that genotyping for

the rs13143308 allele alone is sufficient to identify patients at risk of AF that is associated with excessive calcium release in human atrial myocytes.

While a strong I_{Ca} density reduction is another prominent feature of myocytes from patients with AF, our analysis showed that none of the three risk variants at 4q25 had any effect on the I_{Ca} amplitude, suggesting that 4q25 risk variants are not contributing to reduce the I_{Ca} amplitude in AF.

In summary, the results in Chapter 3 identify the rs13143308 risk variant on chromosome 4q25 as a new key to understand the complex molecular mechanisms that link AF to perturbations in the calcium homeostasis. Clinically, our findings should provide novel means to identify patients at risk or with AF that is specifically linked to defective calcium homeostasis and predict that pharmacological therapies aiming to control calcium release from the SR would be more efficient in patients with a rs13143308T risk allele than in those with normal rs13143308G alleles.

Atrial specific Pitx2 insufficiency in a heterozygous mouse model recapitulates the effects of 4q25 risk variants on the calcium homeostasis

It has been described that 4q25 risk variants are located close to Pitx2, a homeobox transcription factor that plays essential roles during embryogenesis.[19] Recent studies have provided evidences that Pitx2 also play a pivotal role in the adult heart, predisposing to atrial arrhythmias.[8,20–22] In this way, Pitx2 located in the proximity of the 4q25 risk variants, is proposed to be the link between altered calcium homeostasis and the 4q25 risk variants.

To test the proposed role of Pitx2, we used a transgenic mouse model with inducible atrial-specific deletion of Pitx2 comparing WT Cre- controls ($NppaCre^{-}Pitx2^{fl/fl}$), atrial-specific heterozygous ($NppaCre^{+}Pitx2^{fl/-}$), and atrial-specific homozygous ($NppaCre^{+}Pitx2^{-/-}$) Pitx2 deletion. qRT-PCR analysis of the major components of the cardiac calcium-handling system, performed in the LA and RA

chamber in the three types of mice (NppaCre^{+}Pitx2$^{-/-}$, NppaCre^{+}Pitx2$^{+/-}$ and NppaCre^{+}Pitx2$^{fl/fl}$ control mice), revealed an up-regulation of the SERCA2, CSQ2 and PLB mRNA levels, and a down-regulation on the L-type calcium channel pore-forming subunit Cacna1c in LA, whereas in the RA Cacna1c was up-regulated. In line with these findings, electrophysiological analyses demonstrated that the dramatic down-regulation of Cacna1c in LA myocytes of NppaCre^{+}Pitx2$^{-/-}$ mice was accompanied by a significant decrease I_{Ca} in LA and that up-regulation of Atp2a2 and Casq2 in both RA and LA of NppaCre^{+}Pitx2$^{-/-}$ mice concurred with enhanced SR calcium content in both LA and RA. Importantly, it was shown that NppaCre^{+}Pitx2$^{fl/-}$ mice displayed intermediate expression levels for multiple genes involved in calcium handling, demonstrating a dose-dependent effect. Thus, our data demonstrate that alteration of calcium regulatory protein expression is accompanied by functional changes in calcium handling in NppaCre^{+}Pitx2$^{-/-}$ mice that might lead to atrial arrhythmogenesis.

Since the transcription factor Pitx2 has been proposed as a molecular link between 4q25 risk variants and atrial fibrillation,[7] and the above results show that the effects of Pitx2 insufficiency are chamber and dose-dependent, we tested whether heterozygous deletion of Pitx2 expression in the NppaCre+Pitx2$^{fl/-}$ mouse model could reproduce the alterations in the intracellular calcium homeostasis observed in human right atrial myocytes from patients with 4q25 risk variants. The results from right atrial myocytes show that the NppaCre^{+}Pitx2$^{fl/-}$ mice recapitulate all the calcium-handling disturbances caused by the 4q25 risk variants, i.e. higher SR calcium content, incidence of calcium sparks, calcium waves, I_{TI}, and spontaneous membrane depolarizations.

Together, these findings demonstrate that Pitx2 deficiency in the transgenic mouse model can faithfully reproduce the effects of 4q25 risk variants on intracellular calcium homeostasis in human atrial myocytes. However, the findings do not provide direct evidence that Pitx2 is in fact reduced in carriers of 4q25 risk variants, and available reports on Pitx2 expression in patients with 4q25 risk variants[193,194] or with AF[8,23] are not conclusive. Nevertheless, circumstantial evidence show that 4q25 can exert long-range modulation of PITX2C and ENPEP,[24]

and this, combined with the present findings, settles the bases for future studies addressing how risk variants at 4q25 affect the expression and activity of Pitx2 in the human left and right atrium.

Distinct effects of ageing and 4q25 risk variants on calcium homeostasis may synergistically increase the risk of AF in the elderly

Once analyzed the effect on aging *per se* in patients without AF and normal atrial size (Chapter I), the effect of ageing was studied in patients with a previous history of AF in order to test if there were any additional effects of ageing on the intracellular calcium homeostasis in this group. Data from this study show that the deteriorating effects of ageing go in the same direction as the findings in the patient group without AF and normal atrial size, but that AF accentuates several effects. Thus, the age-dependent decrease in I_{Ca} amplitude and increase in fast I_{Ca} inactivation constant (tau 1) were more prominent in patients with AF, suggesting that the negative effects of ageing and AF on I_{Ca} are complementary. Moreover, even though ageing had no effect on the I_{TI} frequency, it did differentially increase the I_{TI} amplitude in patients with AF, which would increase the ability of an I_{TI} to trigger spontaneous action potentials[15,25] and induce triggered electrical activity.[185] Combined with the higher I_{TI} frequency in the elder patients with AF, it is plausible that this potentiates re-initiation of arrhythmic episodes in patients with AF. Moreover, the stronger I_{Ca} depression in older patients with AF may act in synergy with their larger I_{TI} frequency and amplitude by perpetuating arrhythmic episodes initiated by the larger I_{TI}s.

Finally, we tested whether ageing synergistically modified alterations in the intracellular calcium homeostasis in human atrial myocytes from patients carrying risk variants at 4q25. However, ageing was not found to alter any of the effects of the risk variants in patients with or without AF. Even so, it may still be relevant taking ageing into account when evaluating the potential arrhythmogenic impact of 4q25 risk variants. Thus, the age-dependent I_{Ca} depression could synergically

perpetuate arrhythmic episodes initiated by the more frequent and larger spontaneous membrane depolarizations in risk carriers.

Crosstalk between ageing, 4q25 risk variants, and atrial fibrillation in human atrial myocytes

When evaluating the individual and combined effects of the results from each of the chapters in this thesis, the effects on the calcium homeostasis have primarily been considered in the context of potential arrhythmogenic effect in relation to AF. However, as mentioned in Chapter I, ageing is also expected to have a strong negative impact on atrial contractility as both I_{Ca}, SR calcium loading and the calcium transient are rather strongly depressed in the older patient group.[9] A similar effect is expected in patients with AF, as it is associated with smaller I_{Ca} [13] and calcium transient amplitude.[12] To delimit the focus of this thesis, less emphasis has been put on these aspects of the experimental results of the thesis. However, even though a significant loss of atrial contractility has a minor impact on ventricular filling under normal conditions, the negative effects of ageing on calcium homeostasis may have a stronger impact if occurring in patients with pathologies that reduce ventricular contraction[2] or compliance.[195,196] Moreover, the age-dependent alterations of the calcium homeostasis in human atrial myocytes will presumably occur in ventricular myocytes also (see Chapter II) and affect ventricular contraction. Thus, our findings may also be of relevance to identify cellular electrophysiological alterations that contribute to the higher incidence of heart failure in the elderly.

As stated above, the main focus of this thesis has been on age-dependent alterations in the calcium homeostasis that could provide mechanistic clues to explain the strong increase in the incidence of AF in the ageing population. As outlined in the schematic representation below, this thesis consists of two main branches and their contribution to alterations in the calcium homeostasis and AF. The first branch examines the effects of ageing on the intracellular calcium homeostasis either directly (Chapter I) or via defective lamin processing (Chapter

II), which leads to age-dependent progerin accumulation[16,17] and premature progeria syndromes.[122,123] The findings of these studies show that defective lamin processing in the transgenic mouse model *Zmpste24*$^{-/-}$ largely recapitulates the effects of ageing on the calcium handling in human atrial myocytes. The key change that could potentially contribute to promote atrial arrhythmia in the elderly is the observed age-dependent reduction in the I_{Ca} amplitude that may favor the maintenance of atrial arrhythmia by shortening the refractory period.[6,13,186–188] Interestingly, ageing generally accentuates the deteriorating effects of AF on calcium handling. In particular, the effect of ageing on I_{Ca} adds to the inhibitory effect of AF on the I_{Ca} amplitude, resulting in a stronger total I_{Ca} depression in the elderly with AF, facilitating further the maintenance of atrial arrhythmia in this group.

The second branch of the thesis examines how common single nucleotide polymorphisms, associated with an increased risk of AF, affect the calcium homeostasis either directly (Chapter III) or via reduction of Pitx2 function (Chapter IV). These studies demonstrate for the first time that the 4q25 risk variant rs13143308T is associated with an excess of calcium sparks, waves and I_{TI}s, responsible for a higher incidence and amplitude of spontaneous membrane depolarizations. This in turn, may favor initiation of atrial arrhythmic episodes, providing a mechanistic basis for a higher incidence of AF in individuals with 4q25 this risk variant. Moreover, we show that a transgenic mouse model of heterozygous atrial-specific Pitx2 insufficiency replicate the effects of 4q25 risk variants on calcium handling in human atrial myocytes. This points to Pitx2 as a key molecular link between 4q25 risk variants and pro-arrhythmic alterations in the calcium homeostasis, even though it remains to be established whether the 4q25 risk variants affect Pitx2 function. While ageing generally accentuated the effects of AF on calcium homeostasis, we found no evidence that ageing modulates any effect of the 4q25 risk variants on calcium handling. This, however, does not necessarily imply that ageing has no impact on the penetrance of the 4q25 risk variants. Thus, it is possible that the 4q25 risk variants constitute an arrhythmogenic electrophysiological substrate that favor ectopic activity, which

initiates atrial arrhythmic episodes, and that ageing prolongs the duration of these episodes by reducing the atrial refractory period via reduction of the I_{Ca} amplitude.

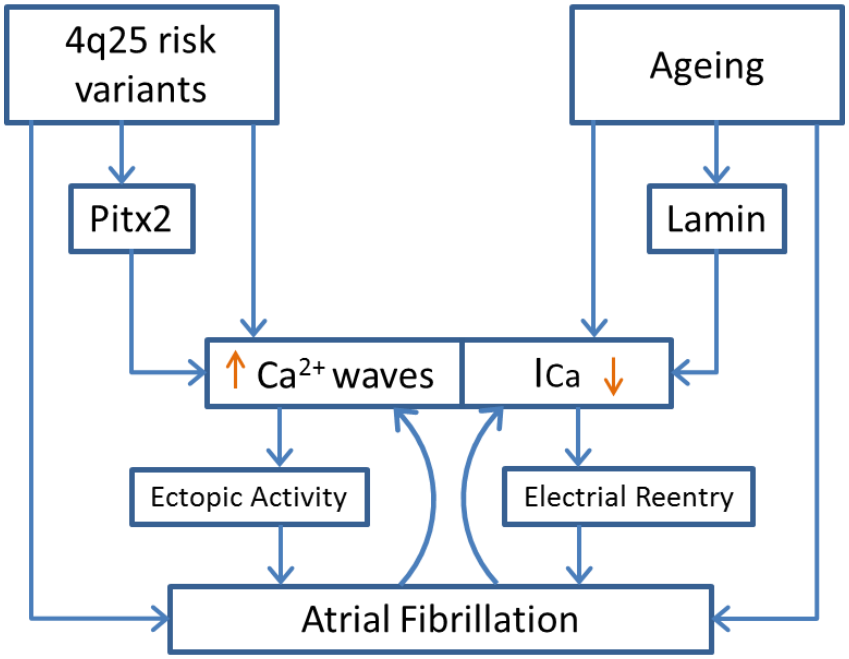

Figure 1. Diagram integrating the effects of risk variants at the chromosomal region 4q25 and ageing on the intracellular calcium homeostasis in human atrial myocytes and the mechanisms that we have identified in this thesis as functional links between 4q25 risk variants, ageing, and atrial fibrillation.

CONCLUSIONS

CONCLUSIONS

1. Ageing modulates the calcium homeostasis in human atrial myocytes. Specifically it decreases the L-type calcium current, the calcium transient and the SR calcium load. These changes favor 1) Progressive decline in atrial contractile function with age and 2) Shortening of the refractory period via reduction of the I_{Ca} amplitude.

2. The progeric transgenic mouse model *Zmpste 24*$^{-/-}$ recapitulates the effects of ageing on calcium homeostasis observed in humans, suggesting that deficient lamin processing might be an underlying cause of age-dependent alterations of intracellular calcium handling in cardiac myocytes.

3. Risk variants on chromosome 4q25 (specifically rs13143308 alone or together with rs2200733) increase spontaneous SR calcium release and the resulting I_{TI}s, key features of atrial myocytes from patients with AF, that increases the frequency and amplitude of spontaneous membrane depolarizations and thereby the likelihood that they can trigger arrhythmic events in patients carrying a risk variant.

4. A transgenic mouse model of atrial specific Pitx2 deletion ($NppaCre^{+}Pitx2^{fl/fl}$) $NppaCre^{+}Pitx2^{fl/-}$, $NppaCre^{+}Pitx2^{-/-}$) reveal that Pitx2 insufficiency alters the expression and function of several calcium handling proteins in a dose- and chamber dependent manner.

5. Right atrial myocytes from heterozygous $NppaCre^{+}Pitx2^{fl/-}$ mice reproduce the results found in human patients with the risk variant rs13143308T at 4q25, i.e. higher frequency of calcium sparks, calcium waves, I_{TI}, and membrane depolarizations. This supports the notion that Pitx2-mediated modulation of intracellular calcium handling plays an important role in electrophysiological processes associated with human AF.

6. The effect of aging on the calcium handling is accentuated in patients with AF, resulting in a greater decrease in I_{Ca}, which is expected to decrease the refractory period further and thereby increase the likelihood that electrical reentry can prolong or maintain arrhythmic episodes.

7. Ageing *per se* does not modify the effects of 4q25 risk variants on calcium handling. However, by reducing the I_{Ca} amplitude, ageing may act synergistically with the increased likelihood of calcium release-induced arrhythmic episodes in carriers of the rs13143308 4q25 risk variant, by increasing the likelihood that electrical reentry can prolong or maintain the arrhythmic episodes.

REFERENCES

REFERENCES

1. World health statistics 2013. (2013). Available at: http://www.who.int.

2. Janczewski, A. M. & Lakatta, E. G. Modulation of sarcoplasmic reticulum Ca(2+) cycling in systolic and diastolic heart failure associated with aging. *Heart Fail. Rev.* **15,** 431–45 (2010).

3. Bers, D. M. Cardiac excitation-contraction coupling. *Nature* **415,** 198–205 (2002).

4. Broers, J. L. V, Ramaekers, F. C. S., Bonne, G., Yaou, R. Ben & Hutchison, C. J. Nuclear lamins: laminopathies and their role in premature ageing. *Physiol. Rev.* **86,** 967–1008 (2006).

5. Merideth, M. A. *et al.* Phenotype and course of Hutchinson-Gilford progeria syndrome. *N. Engl. J. Med.* **358,** 592–604 (2008).

6. Nattel, S. & Harada, M. Atrial Remodeling and Atrial Fibrillation: Recent Advances and Translational Perspectives. *J. Am. Coll. Cardiol.* **63,** 2335–2345 (2014).

7. Gudbjartsson, D. F. *et al.* Variants conferring risk of atrial fibrillation on chromosome 4q25. *Nature* **448,** 353–7 (2007).

8. Chinchilla, A. *et al.* PITX2 Insufficiency Leads to Atrial Electrical and Structural Remodeling Linked to Arrhythmogenesis. *Circ. Cardiovasc. Genet.* **4,** 269–279 (2011).

9. Herraiz-Martinez, A. *et al.* Ageing is associated with deterioration of calcium homeostasis in isolated human right atrial myocytes. *Cardiovasc. Res.* **106,** 76–86 (2015).

10. Rivera-Torres, J. *et al.* Cardiac electrical defects in progeroid mice and Hutchinson–Gilford progeria syndrome patients with nuclear lamina alterations. *Proc. Natl. Acad. Sci.* 201603754 (2016). doi:10.1073/pnas.1603754113

11. Lozano-Velasco, E. *et al.* Pitx2 impairs calcium handling in a dose-dependent manner by modulating Wnt signalling. *Cardiovasc. Res.* **109,** 55–66 (2016).

12. Llach, A. *et al.* Abnormal calcium handling in atrial fibrillation is linked to up-

regulation of adenosine A2A receptors. *Eur. Heart J.* **32,** 721–9 (2011).

13. Van Wagoner, D. R. *et al.* Atrial L-type Ca2+ currents and human atrial fibrillation. *Circ. Res.* **85,** 428–36 (1999).

14. Hove-Madsen, L. *et al.* Atrial fibrillation is associated with increased spontaneous calcium release from the sarcoplasmic reticulum in human atrial myocytes. *Circulation* **110,** 1358–63 (2004).

15. Voigt, N. *et al.* Enhanced sarcoplasmic reticulum Ca2+ leak and increased Na+-Ca2+ exchanger function underlie delayed afterdepolarizations in patients with chronic atrial fibrillation. *Circulation* **125,** 2059–70 (2012).

16. Gordon, L. B., Rothman, F. G., López-Otín, C. & Misteli, T. Progeria: a paradigm for translational medicine. *Cell* **156,** 400–7 (2014).

17. Trigueros-Motos, L., Gonzalez, J. M., Rivera, J. & Andres, V. Hutchinson-Gilford progeria syndrome, cardiovascular disease and oxidative stress. *Front. Biosci. (Schol. Ed).* **3,** 1285–97 (2011).

18. Liu, X., Wang, F., Knight, A. C., Zhao, J. & Xiao, J. Common variants for atrial fibrillation: results from genome-wide association studies. *Hum. Genet.* **131,** 33–9 (2012).

19. Franco, D., Christoffels, V. M. & Campione, M. Homeobox transcription factor Pitx2: The rise of an asymmetry gene in cardiogenesis and arrhythmogenesis. *Trends Cardiovasc. Med.* **24,** 23–31 (2014).

20. Wang, J. *et al.* Pitx2 prevents susceptibility to atrial arrhythmias by inhibiting left-sided pacemaker specification. *Proc. Natl. Acad. Sci. U. S. A.* **107,** 9753 (2010).

21. Kirchhof, P. *et al.* PITX2c is expressed in the adult left atrium, and reducing Pitx2c expression promotes atrial fibrillation inducibility and complex changes in gene expression. *Circ. Cardiovasc. Genet.* **4,** 123–33 (2011).

22. Tao, Y. *et al.* Pitx2, an atrial fibrillation predisposition gene, directly regulates ion transport and intercalated disc genes. *Circ. Cardiovasc. Genet.* **7,** 23–32 (2014).

23. Pérez-Hernández, M. *et al.* Pitx2c increases in atrial myocytes from chronic atrial fibrillation patients enhancing IKs and decreasing ICa,L. *Cardiovasc. Res.* **109,** (2016).

24. Aguirre, L. A. *et al.* Long-range regulatory interactions at the 4q25 atrial fibrillation risk locus involve PITX2c and ENPEP. *BMC Biol.* **13,** (2015).

25. Schlotthauer, K. & Bers, D. M. Sarcoplasmic Reticulum Ca2+ Release Causes Myocyte Depolarization. *Circ. Res.* **87,** (2000).

26. Hall, J. E. & Guyton, A. *Tratado de fisiología médica*. (Elsevier, 2011).

27. Kléber, A. G. & Rudy, Y. Basic mechanisms of cardiac impulse propagation and associated arrhythmias. *Physiol. Rev.* **84,** 431–88 (2004).

28. Fozzard, H. A. Membrane capacity of the cardiac Purkinje fibre. *J. Physiol.* **182,** 255–67 (1966).

29. Hodgking, A. The ionic basis of electrical activity in nerve and muscle. *Biol Rev* **26,** 339–409 (1951).

30. Hoekstra, M., Mummery, C. L., Wilde, A. A. M., Bezzina, C. R. & Verkerk, A. O. Induced pluripotent stem cell derived cardiomyocytes as models for cardiac arrhythmias. *Front. Physiol.* **3,** 346 (2012).

31. Bers, D. M. Excitation-contraction coupling and cardiac contractile force. 427 (2008).

32. Gadeberg, H. C. *et al.* Heterogeneity of T-Tubules in Pig Hearts. *PLoS One* **11,** e0156862 (2016).

33. Brette, F. & Orchard, C. T-Tubule Function in Mammalian Cardiac Myocytes. *Circ. Res.* **92,** 1182–1192 (2003).

34. Brandenburg, S. *et al.* Axial tubule junctions control rapid calcium signaling in atria. *J. Clin. Invest.* (2016). doi:10.1172/JCI88241

35. Levin, K. R. & Page, E. Quantitative studies on plasmalemmal folds and caveolae of rabbit ventricular myocardial cells. *Circ. Res.* **46,** 244–55 (1980).

36. Anderson, R. G. Caveolae: where incoming and outgoing messengers meet. *Proc. Natl. Acad. Sci. U. S. A.* **90,** 10909–13 (1993).

37. Inui, M., Saito, A. & Fleischer, S. Purification of the ryanodine receptor and identity

with feet structures of junctional terminal cisternae of sarcoplasmic reticulum from fast skeletal muscle. *J. Biol. Chem.* **262,** 1740–7 (1987).

38. Lai, F. A., Erickson, H., Block, B. A. & Meissner, G. Evidence for a junctional feet-ryanodine receptor complex from sarcoplasmic reticulum. *Biochem. Biophys. Res. Commun.* **143,** 704–9 (1987).

39. Inui, M., Saito, A. & Fleischer, S. Isolation of the ryanodine receptor from cardiac sarcoplasmic reticulum and identity with the feet structures. *J. Biol. Chem.* **262,** 15637–42 (1987).

40. Bers, D. M. Calcium fluxes involved in control of cardiac myocyte contraction. *Circ. Res.* **87,** 275–281 (2000).

41. Ringer, S. A further Contribution regarding the influence of the different Constituents of the Blood on the Contraction of the Heart. *J. Physiol.* **4,** 29–42.3 (1883).

42. Fabiato, A. Calcium-induced release of calcium from the cardiac sarcoplasmic reticulum. *Am. J. Physiol.* **245,** C1-14 (1983).

43. Bers, D. M. Calcium fluxes involved in control of cardiac myocyte contraction. *Circ. Res.* **87,** 275–281 (2000).

44. Bers, D. M. & Stiffel, V. M. Ratio of ryanodine to dihydropyridine receptors in cardiac and skeletal muscle and implications for E-C coupling. *Am. J. Physiol.* **264,** C1587-93 (1993).

45. Franzini-Armstrong, C. & Protasi, F. Ryanodine receptors of striated muscles: a complex channel capable of multiple interactions. *Physiol. Rev.* **77,** 699–729 (1997).

46. Franzini-Armstrong, C., Protasi, F. & Ramesh, V. Shape, size, and distribution of Ca(2+) release units and couplons in skeletal and cardiac muscles. *Biophys. J.* **77,** 1528–39 (1999).

47. Bassani, R. A., Bassani, J. W. & Bers, D. M. Mitochondrial and sarcolemmal Ca2+ transport reduce [Ca2+]i during caffeine contractures in rabbit cardiac myocytes. *J. Physiol.* **453,** 591–608 (1992).

48. Mascher, D. & Peper, K. Two components of inward current in myocardial muscle fibers. *Pflugers Arch.* **307,** 190–203 (1969).

49. Beeler, G. W. & Reuter, H. The relation between membrane potential, membrane currents and activation of contraction in ventricular myocardial fibres. *J. Physiol.* **207,** 211–29 (1970).

50. Bean, B. P. Two kinds of calcium channels in canine atrial cells. Differences in kinetics, selectivity, and pharmacology. *J. Gen. Physiol.* **86,** 1–30 (1985).

51. Hirano, Y., Fozzard, H. A. & January, C. T. Characteristics of L- and T-type Ca2+ currents in canine cardiac Purkinje cells. *Am. J. Physiol.* **256,** H1478-92 (1989).

52. Hagiwara, N., Irisawa, H. & Kameyama, M. Contribution of two types of calcium currents to the pacemaker potentials of rabbit sino-atrial node cells. *J. Physiol.* **395,** 233–53 (1988).

53. Wu, J. Y. & Lipsius, S. L. Effects of extracellular Mg2+ on T- and L-type Ca2+ currents in single atrial myocytes. *Am. J. Physiol.* **259,** H1842-50 (1990).

54. Puglisi, J. L., Yuan, W., Bassani, J. W. & Bers, D. M. Ca(2+) influx through Ca(2+) channels in rabbit ventricular myocytes during action potential clamp: influence of temperature. *Circ. Res.* **85,** e7–e16 (1999).

55. Tsien, R. W. *et al.* Mechanisms of calcium channel modulation by beta-adrenergic agents and dihydropyridine calcium agonists. *J. Mol. Cell. Cardiol.* **18,** 691–710 (1986).

56. Hartzell, H. C. Regulation of cardiac ion channels by catecholamines, acetylcholine and second messenger systems. *Prog. Biophys. Mol. Biol.* **52,** 165–247 (1988).

57. McDonald, T. F., Pelzer, S., Trautwein, W. & Pelzer, D. J. Regulation and modulation of calcium channels in cardiac, skeletal, and smooth muscle cells. *Physiol. Rev.* **74,** 365–507 (1994).

58. Díaz, M. E., Graham, H. K., O'neill, S. C., Trafford, A. W. & Eisner, D. A. The control of sarcoplasmic reticulum Ca content in cardiac muscle. *Cell Calcium* **38,** 391–6

59. Reiken, S. *et al.* Beta-blockers restore calcium release channel function and improve cardiac muscle performance in human heart failure. *Circulation* **107,** 2459–66 (2003).

60. Jiang, D. *et al.* Enhanced store overload-induced Ca2+ release and channel sensitivity to luminal Ca2+ activation are common defects of RyR2 mutations linked to ventricular tachycardia and sudden death. *Circ. Res.* **97,** 1173–81 (2005).

61. Terentyev, D. *et al.* Abnormal interactions of calsequestrin with the ryanodine receptor calcium release channel complex linked to exercise-induced sudden cardiac death. *Circ. Res.* **98,** 1151–8 (2006).

62. Priori, S. G. & Chen, S. R. W. Inherited dysfunction of sarcoplasmic reticulum Ca2+ handling and arrhythmogenesis. *Circ. Res.* **108,** 871–83 (2011).

63. Bers, D. M. & Guo, T. Calcium signaling in cardiac ventricular myocytes. *Ann. N. Y. Acad. Sci.* **1047,** 86–98 (2005).

64. Brini, M. & Carafoli, E. Calcium pumps in health and disease. *Physiol. Rev.* **89,** 1341–78 (2009).

65. MacLennan, D. H. & Kranias, E. G. Phospholamban: a crucial regulator of cardiac contractility. *Nat. Rev. Mol. Cell Biol.* **4,** 566–77 (2003).

66. Beard, N. ., Laver, D. . & Dulhunty, A. . Calsequestrin and the calcium release channel of skeletal and cardiac muscle. *Prog. Biophys. Mol. Biol.* **85,** 33–69 (2004).

67. Weber, C. R., Piacentino, V., Ginsburg, K. S., Houser, S. R. & Bers, D. M. Na(+)-Ca(2+) exchange current and submembrane [Ca(2+)] during the cardiac action potential. *Circ. Res.* **90,** 182–9 (2002).

68. Bers, D. M. Calcium Cycling and Signaling in Cardiac Myocytes. *Annu. Rev. Physiol* **70,** 23–49 (2008).

69. Mackiewicz, U. *et al.* Sarcolemmal Ca2+-ATPase ability to transport Ca2+ gradually diminishes after myocardial infarction in the rat. *Cardiovasc. Res.* **81,** 546–54 (2009).

70. Bylund, D. B. *et al.* International Union of Pharmacology Nomenclature of Adrenoreceptors. *Pharmacol. Rev.* **46,** 121–136 (1994).

71. Santulli, G. & Iaccarino, G. Adrenergic signaling in heart failure and cardiovascular aging. *Maturitas* **93,** 65–72 (2016).

72. Marx, S. O. & Marks, A. R. Dysfunctional ryanodine receptors in the heart: New

insights into complex cardiovascular diseases. *J. Mol. Cell. Cardiol.* **58,** 225–231 (2013).

73. Xiao, B. *et al.* Characterization of a novel PKA phosphorylation site, serine-2030, reveals no PKA hyperphosphorylation of the cardiac ryanodine receptor in canine heart failure. *Circ. Res.* **96,** 847–55 (2005).

74. Triposkiadis, F. *et al.* The Sympathetic Nervous System in Heart Failure: Physiology, Pathophysiology, and Clinical Implications. *J. Am. Coll. Cardiol.* **54,** 1747–1762 (2009).

75. Maier, L. S. & Bers, D. M. Calcium, Calmodulin, and Calcium-Calmodulin Kinase II: Heartbeat to Heartbeat and Beyond. *J. Mol. Cell. Cardiol.* **34,** 919–939 (2002).

76. Currie, S. Cardiac ryanodine receptor phosphorylation by CaM Kinase II: keeping the balance right. *Front. Biosci. (Landmark Ed.* **14,** 5134–56 (2009).

77. Camm, A. J. *et al.* 2012 focused update of the ESC Guidelines for the management of atrial fibrillation: an update of the 2010 ESC Guidelines for the management of atrial fibrillation--developed with the special contribution of the European Heart Rhythm Association. *Europace* **14,** 1385–413 (2012).

78. Igarashi, T. *et al.* Connexin gene transfer preserves conduction velocity and prevents atrial fibrillation. *Circulation* **125,** 216–25 (2012).

79. Burstein, B. *et al.* Changes in Connexin Expression and the Atrial Fibrillation Substrate in Congestive Heart Failure. *Circ. Res.* **105,** 1213–1222 (2009).

80. Oakes, R. S. *et al.* Detection and Quantification of Left Atrial Structural Remodeling With Delayed-Enhancement Magnetic Resonance Imaging in Patients With Atrial Fibrillation. *Circulation* **119,** 1758–1767 (2009).

81. Burstein, B., Qi, X.-Y., Yeh, Y.-H., Calderone, A. & Nattel, S. Atrial cardiomyocyte tachycardia alters cardiac fibroblast function: a novel consideration in atrial remodeling. *Cardiovasc. Res.* **76,** 442–52 (2007).

82. Verheule, S. *et al.* Loss of Continuity in the Thin Epicardial Layer Because of Endomysial Fibrosis Increases the Complexity of Atrial Fibrillatory Conduction. *Circ. Arrhythmia Electrophysiol.* **6,** 202–211 (2013).

83. Wakili, R., Voigt, N., Kääb, S., Dobrev, D. & Nattel, S. Recent advances in the

molecular pathophysiology of atrial fibrillation. *J. Clin. Invest.* **121,** 2955–68 (2011).

84. Nattel, S. New ideas about atrial fibrillation 50 years on. *Nature* **415,** 219–26 (2002).

85. Fraticelli, A., Josephson, R., Danziger, R., Lakatta, E. & Spurgeon, H. Morphological and contractile characteristics of rat cardiac myocytes from maturation to senescence. *Am. J. Physiol.* **257,** H259-65 (1989).

86. Manolio, T. A. *et al.* Finding the missing heritability of complex diseases. *Nature* **461,** 747–753 (2009).

87. Husser, D., Adams, V., Piorkowski, C., Hindricks, G. & Bollmann, A. Chromosome 4q25 variants and atrial fibrillation recurrence after catheter ablation. *J. Am. Coll. Cardiol.* **55,** 747–53 (2010).

88. Lubitz, S. A. *et al.* Genetics of atrial fibrillation: implications for future research directions and personalized medicine. *Circ. Arrhythm. Electrophysiol.* **3,** 291–9 (2010).

89. Body, S. C. *et al.* Variation in the 4q25 chromosomal locus predicts atrial fibrillation after coronary artery bypass graft surgery. *Circ. Cardiovasc. Genet.* **2,** 499–506 (2009).

90. Liu, C., Liu, W., Lu, M. F., Brown, N. A. & Martin, J. F. Regulation of left-right asymmetry by thresholds of Pitx2c activity. *Development* **128,** 2039–48 (2001).

91. Haïssaguerre, M. *et al.* Spontaneous initiation of atrial fibrillation by ectopic beats originating in the pulmonary veins. *N. Engl. J. Med.* **339,** 659–66 (1998).

92. Franco, D., Chinchilla, A., Daimi, H., Dominguez, J. N. & Aránega, A. Modulation of conductive elements by Pitx2 and their impact on atrial arrhythmogenesis. *Cardiovasc. Res.* **91,** 223–31 (2011).

93. Gutierrez, A. & Chung, M. K. Genomics of Atrial Fibrillation. *Curr. Cardiol. Rep.* **18,** 55 (2016).

94. Barriga, M. *et al.* Low density lipoproteins promote unstable calcium handling accompanied by reduced SERCA2 and connexin-40 expression in cardiomyocytes. *PLoS One* **8,** e58128 (2013).

95. Boyd, A. C., Richards, D. A. B., Marwick, T. & Thomas, L. Atrial strain rate is a sensitive measure of alterations in atrial phasic function in healthy ageing. *Heart* **97,** 1513–9 (2011).

96. Boyd, A. C., Schiller, N. B., Leung, D., Ross, D. L. & Thomas, L. Atrial dilation and altered function are mediated by age and diastolic function but not before the eighth decade. *JACC. Cardiovasc. Imaging* **4,** 234–42 (2011).

97. Gardin, J. M. *et al.* Echocardiographic measurements in normal subjects: evaluation of an adult population without clinically apparent heart disease. *J. Clin. Ultrasound* **7,** 439–47 (1979).

98. Kannel, W. B. & Benjamin, E. J. Current perceptions of the epidemiology of atrial fibrillation. *Cardiol. Clin.* **27,** 13–24, vii (2009).

99. Dibb, K. M., Rueckschloss, U., Eisner, D. A., Isenberg, G. & Trafford, A. W. Mechanisms underlying enhanced cardiac excitation contraction coupling observed in the senescent sheep myocardium. (2004). doi:10.1016/j.yjmcc.2004.09.005

100. Xu, A. & Narayanan, N. Effects of aging on sarcoplasmic reticulum Ca2+-cycling proteins and their phosphorylation in rat myocardium. *Am. J. Physiol.* **275,** H2087-94 (1998).

101. Dun, W., Yagi, T., Rosen, M. R. & Boyden, P. A. Calcium and potassium currents in cells from adult and aged canine right atria. *Cardiovasc. Res.* **58,** 526–34 (2003).

102. Guo, K. K. & Ren, J. Cardiac overexpression of alcohol dehydrogenase (ADH) alleviates aging-associated cardiomyocyte contractile dysfunction: role of intracellular Ca2+ cycling proteins. *Aging Cell* **5,** 259–65 (2006).

103. Lompré, A. M., Lambert, F., Lakatta, E. G. & Schwartz, K. Expression of sarcoplasmic reticulum Ca(2+)-ATPase and calsequestrin genes in rat heart during ontogenic development and aging. *Circ. Res.* **69,** 1380–8 (1991).

104. Ren, J., Li, Q., Wu, S., Li, S.-Y. & Babcock, S. A. Cardiac overexpression of antioxidant catalase attenuates aging-induced cardiomyocyte relaxation dysfunction. *Mech. Ageing Dev.* **128,** 276–85 (2007).

105. Cooper, L. L. *et al.* Redox modification of ryanodine receptors by mitochondria-

derived reactive oxygen species contributes to aberrant Ca2+ handling in ageing rabbit hearts. *J. Physiol.* **591,** 5895–911 (2013).

106. Carnes, C. A. *et al.* Atrial glutathione content, calcium current, and contractility. *J. Biol. Chem.* **282,** 28063–73 (2007).

107. Chopra, N. *et al.* Modest reductions of cardiac calsequestrin increase sarcoplasmic reticulum Ca2+ leak independent of luminal Ca2+ and trigger ventricular arrhythmias in mice. *Circ. Res.* **101,** 617–26 (2007).

108. Postma, A. V *et al.* Absence of calsequestrin 2 causes severe forms of catecholaminergic polymorphic ventricular tachycardia. *Circ. Res.* **91,** e21-6 (2002).

109. Terentyev, D. *et al.* Calsequestrin determines the functional size and stability of cardiac intracellular calcium stores: Mechanism for hereditary arrhythmia. *Proc. Natl. Acad. Sci. U. S. A.* **100,** 11759–64 (2003).

110. Alcalai, R. *et al.* Prevention of ventricular arrhythmia and calcium dysregulation in a catecholaminergic polymorphic ventricular tachycardia mouse model carrying calsequestrin-2 mutation. *J. Cardiovasc. Electrophysiol.* **22,** 316–24 (2011).

111. Hove-Madsen, L. *et al.* The proarrhythmic antihistaminic drug terfenadine increases spontaneous calcium release in human atrial myocytes. *Eur. J. Pharmacol.* **553,** 215–21 (2006).

112. Llach, A. *et al.* Sarcoplasmic reticulum and L-type Ca^{2+} channel activity regulate the beat-to-beat stability of calcium handling in human atrial myocytes. *J. Physiol.* **589,** 3247–62 (2011).

113. Hove-Madsen, L. *et al.* Adenosine A 2A receptors are expressed in human atrial myocytes and modulate spontaneous sarcoplasmic reticulum calcium release. (2006). doi:10.1016/j.cardiores.2006.07.020

114. Molina, C. E. *et al.* Cyclic adenosine monophosphate phosphodiesterase type 4 protects against atrial arrhythmias. *J. Am. Coll. Cardiol.* **59,** 2182–90 (2012).

115. Spencer, K. T. *et al.* Effects of aging on left atrial reservoir, conduit, and booster pump function: a multi-institution acoustic quantification study. *Heart* **85,** 272–7 (2001).

116. Jeevanantham, V. *et al.* Aging reduces left atrial performance during adrenergic

stress in middle aged and older patients. *Cardiol. J.* **19,** 45–52 (2012).

117. Dinanian, S. *et al.* Downregulation of the calcium current in human right atrial myocytes from patients in sinus rhythm but with a high risk of atrial fibrillation. *Eur. Heart J.* **29,** 1190–7 (2008).

118. Goudis, C. A., Kallergis, E. M. & Vardas, P. E. Extracellular matrix alterations in the atria: insights into the mechanisms and perpetuation of atrial fibrillation. *Europace* **14,** 623–30 (2012).

119. Spach, M. S., Heidlage, J. F., Dolber, P. C. & Barr, R. C. Mechanism of origin of conduction disturbances in aging human atrial bundles: experimental and model study. *Heart Rhythm* **4,** 175–85 (2007).

120. Andrés, V. & González, J. M. Role of A-type lamins in signaling, transcription, and chromatin organization. *J. Cell Biol.* **187,** 945–57 (2009).

121. www.progeriaresearch.org.

122. Gordon, L. B. *et al.* Impact of farnesylation inhibitors on survival in Hutchinson-Gilford progeria syndrome. *Circulation* **130,** 27–34 (2014).

123. Merideth, M. A. *et al.* Phenotype and course of Hutchinson-Gilford progeria syndrome. *N. Engl. J. Med.* **358,** 592–604 (2008).

124. Barrowman, J., Wiley, P. A., Hudon-Miller, S. E., Hrycyna, C. A. & Michaelis, S. Human ZMPSTE24 disease mutations: residual proteolytic activity correlates with disease severity. *Hum. Mol. Genet.* **21,** 4084–93 (2012).

125. Osorio, F. G. *et al.* Cell autonomous and systemic factors in progeria development. *Biochem. Soc. Trans.* **39,** 1710–4 (2011).

126. Zhang, H., Kieckhaefer, J. E. & Cao, K. Mouse models of laminopathies. *Aging Cell* **12,** 2–10 (2013).

127. Varela, I. *et al.* Accelerated ageing in mice deficient in Zmpste24 protease is linked to p53 signalling activation. *Nature* **437,** 564–8 (2005).

128. Villa-Bellosta, R. *et al.* Defective extracellular pyrophosphate metabolism promotes vascular calcification in a mouse model of Hutchinson-Gilford progeria syndrome that is ameliorated on pyrophosphate treatment. *Circulation* **127,** 2442–51 (2013).

129. Pendás, A. M. *et al.* Defective prelamin A processing and muscular and adipocyte alterations in Zmpste24 metalloproteinase-deficient mice. *Nat. Genet.* **31,** 94–9 (2002).

130. Jensen, P. N. *et al.* Incidence of and risk factors for sick sinus syndrome in the general population. *J. Am. Coll. Cardiol.* **64,** 531–8 (2014).

131. Strait, J. B. & Lakatta, E. G. Aging-associated cardiovascular changes and their relationship to heart failure. *Heart Fail. Clin.* **8,** 143–64 (2012).

132. Signore, S. *et al.* Late Na(+) current and protracted electrical recovery are critical determinants of the aging myopathy. *Nat. Commun.* **6,** 8803 (2015).

133. Howlett, S. E., Grandy, S. A. & Ferrier, G. R. Calcium spark properties in ventricular myocytes are altered in aged mice. *Am. J. Physiol. Heart Circ. Physiol.* **290,** H1566-74 (2006).

134. London, B. Cardiac arrhythmias: from (transgenic) mice to men. *J. Cardiovasc. Electrophysiol.* **12,** 1089–91 (2001).

135. Wijffels, M. C., Kirchhof, C. J., Dorland, R. & Allessie, M. A. Atrial fibrillation begets atrial fibrillation. A study in awake chronically instrumented goats. *Circulation* **92,** 1954–68 (1995).

136. Voigt, N. *et al.* Cellular and Molecular Mechanisms of Atrial Arrhythmogenesis in Patients with Paroxysmal Atrial Fibrillation. *Circulation* **129,** 145 (2014).

137. Neef, S. *et al.* CaMKII-dependent diastolic SR Ca2+ leak and elevated diastolic Ca2+ levels in right atrial myocardium of patients with atrial fibrillation. *Circ. Res.* **106,** 1134–44 (2010).

138. Vest, J. A. *et al.* Defective cardiac ryanodine receptor regulation during atrial fibrillation. *Circulation* **111,** 2025–32 (2005).

139. Molina, C. E. *et al.* Prevention of adenosine A2A receptor activation diminishes beat-to-beat alternation in human atrial myocytes. *Basic Res. Cardiol.* **111,** 1–15 (2016).

140. Bai, Y. *et al.* Phospholamban knockout breaks arrhythmogenic Ca^{2+} waves and suppresses catecholaminergic polymorphic ventricular tachycardia in mice. *Circ.*

Res. **113,** 517–26 (2013).

141. Hwang, H. S. *et al.* Inhibition of cardiac Ca2+ release channels (RyR2) determines efficacy of class I antiarrhythmic drugs in catecholaminergic polymorphic ventricular tachycardia. *Circ. Arrhythm. Electrophysiol.* **4,** 128–35 (2011).

142. Li, N. *et al.* Ryanodine receptor-mediated calcium leak drives progressive development of an atrial fibrillation substrate in a transgenic mouse model. *Circulation* **129,** 1276–85 (2014).

143. Mahida, S., Lubitz, S. A., Rienstra, M., Milan, D. J. & Ellinor, P. T. Monogenic atrial fibrillation as pathophysiological paradigms. *Cardiovasc. Res.* **89,** 692–700 (2011).

144. Lubitz, S. A. *et al.* Association between familial atrial fibrillation and risk of new-onset atrial fibrillation. *JAMA* **304,** 2263–9 (2010).

145. Sabeh, M. K. & MacRae, C. A. The genetics of atrial fibrillation. *Curr. Opin. Cardiol.* **25,** 186–91 (2010).

146. Sinner, M. F., Ellinor, P. T., Meitinger, T., Benjamin, E. J. & Kääb, S. Genome-wide association studies of atrial fibrillation: past, present, and future. *Cardiovasc. Res.* **89,** 701–9 (2011).

147. Ellinor, P. T. *et al.* Meta-analysis identifies six new susceptibility loci for atrial fibrillation. *Nat. Genet.* **44,** 670–5 (2012).

148. Mommersteeg, M. T. M. *et al.* Pitx2c and Nkx2-5 are required for the formation and identity of the pulmonary myocardium. *Circ. Res.* **101,** 902–9 (2007).

149. Gore-Panter, S. R. *et al.* Atrial Fibrillation Associated Chromosome 4q25 Variants Are Not Associated with PITX2c Expression in Human Adult Left Atrial Appendages. *PLoS One* **9,** (2014).

150. Martin, R. I. R. *et al.* Genetic variants associated with risk of atrial fibrillation regulate expression of PITX2, CAV1, MYOZ1, C9orf3 and FANCC. *J. Mol. Cell. Cardiol.* **85,** 207–214 (2015).

151. Lee, Y. S. Pathophysiological mechanisms of altered transmembrane potentials in diseased human atria. *J. Electrocardiol.* **19,** 41–9 (1986).

152. Lubitz, S. A. *et al.* Novel genetic markers associate with atrial fibrillation risk in

Europeans and Japanese. *J. Am. Coll. Cardiol.* **63,** 1200–10 (2014).

153. Li, N. *et al.* Ryanodine receptor-mediated calcium leak drives progressive development of an atrial fibrillation substrate in a transgenic mouse model. *Circulation* **129,** 1276–85 (2014).

154. Jiang, D. *et al.* RyR2 mutations linked to ventricular tachycardia and sudden death reduce the threshold for store-overload-induced Ca2+ release (SOICR). *Proc. Natl. Acad. Sci. U. S. A.* **101,** 13062–7 (2004).

155. Jiang, D., Xiao, B., Zhang, L. & Chen, S. R. W. Enhanced basal activity of a cardiac Ca2+ release channel (ryanodine receptor) mutant associated with ventricular tachycardia and sudden death. *Circ. Res.* **91,** 218–25 (2002).

156. Watanabe, H. *et al.* Flecainide prevents catecholaminergic polymorphic ventricular tachycardia in mice and humans. *Nat. Med.* **15,** 380–3 (2009).

157. Zhou, Q. *et al.* Carvedilol and its new analogs suppress arrhythmogenic store overload-induced Ca2+ release. *Nat. Med.* **17,** 1003–9 (2011).

158. Lukyanenko, V., Viatchenko-Karpinski, S., Smirnov, A., Wiesner, T. F. & Györke, S. Dynamic regulation of sarcoplasmic reticulum Ca(2+) content and release by luminal Ca(2+)-sensitive leak in rat ventricular myocytes. *Biophys. J.* **81,** 785–98 (2001).

159. Jiang, D., Chen, W., Wang, R., Zhang, L. & Chen, S. R. W. Loss of luminal Ca2+ activation in the cardiac ryanodine receptor is associated with ventricular fibrillation and sudden death. *Proc. Natl. Acad. Sci. U. S. A.* **104,** 18309–14 (2007).

160. Díaz, M. E., O'Neill, S. C. & Eisner, D. A. Sarcoplasmic reticulum calcium content fluctuation is the key to cardiac alternans. *Circ. Res.* **94,** 650–6 (2004).

161. Viatchenko-Karpinski, S. *et al.* Abnormal calcium signaling and sudden cardiac death associated with mutation of calsequestrin. *Circ. Res.* **94,** 471–7 (2004).

162. Dobrev, D. *et al.* Molecular basis of downregulation of G-protein-coupled inward rectifying K(+) current (I(K,ACh) in chronic human atrial fibrillation: decrease in GIRK4 mRNA correlates with reduced I(K,ACh) and muscarinic receptor-mediated shortening of action potentials. *Circulation* **104,** 2551–7 (2001).

163. Van Wagoner, D. R., Pond, A. L., McCarthy, P. M., Trimmer, J. S. & Nerbonne, J. M.

Outward K+ current densities and Kv1.5 expression are reduced in chronic human atrial fibrillation. *Circ. Res.* **80,** 772–81 (1997).

164. Camm, J., Luscher, T. & Serruys, P. *The ESC Textbook of Cardiovascular Medicine*. (Oxford University Press, 2009).

165. Wit, A. L. & Boyden, P. A. Triggered activity and atrial fibrillation. *Heart Rhythm* **4,** S17-23 (2007).

166. Velagapudi, P., Turagam, M. K., Leal, M. A. & Kocheril, A. G. Atrial fibrosis: a risk stratifier for atrial fibrillation. *Expert Rev. Cardiovasc. Ther.* **11,** 155–60 (2013).

167. Corradi, D. Atrial fibrillation from the pathologist's perspective. *Cardiovasc. Pathol.* **23,** 71–84

168. Greiser, M. & Schotten, U. Dynamic remodeling of intracellular Ca^{2+} signaling during atrial fibrillation. *J. Mol. Cell. Cardiol.* **58,** 134–42 (2013).

169. Pang, H., Ronderos, R., Pérez-Riera, A. R., Femenía, F. & Baranchuk, A. Reverse atrial electrical remodeling: a systematic review. *Cardiol. J.* **18,** 625–31 (2011).

170. Gudbjartsson, D. F. *et al.* A sequence variant in ZFHX3 on 16q22 associates with atrial fibrillation and ischemic stroke. *Nat. Genet.* **41,** 876–8 (2009).

171. Benjamin, E. J. *et al.* Variants in ZFHX3 are associated with atrial fibrillation in individuals of European ancestry. *Nat. Genet.* **41,** 879–81 (2009).

172. Ellinor, P. T. *et al.* Common variants in KCNN3 are associated with lone atrial fibrillation. *Nat. Genet.* **42,** 240–4 (2010).

173. Schnabel, R. B. *et al.* Large-scale candidate gene analysis in whites and African Americans identifies IL6R polymorphism in relation to atrial fibrillation: the National Heart, Lung, and Blood Institute's Candidate Gene Association Resource (CARe) project. *Circ. Cardiovasc. Genet.* **4,** 557–64 (2011).

174. Kääb, S. *et al.* Large scale replication and meta-analysis of variants on chromosome 4q25 associated with atrial fibrillation. *Eur. Heart J.* **30,** 813–9 (2009).

175. Zhang, Y. *et al.* Overexpression of microRNA-1 causes atrioventricular block in rodents. *Int. J. Biol. Sci.* **9,** 455–62 (2013).

176. Mahida, S. *et al.* Overexpression of KCNN3 results in sudden cardiac death.

Cardiovasc. Res. **101,** 326–34 (2014).

177. Gage, P. J. *et al.* Dosage requirement of Pitx2 for development of multiple organs. *Development* **126,** 4643–51 (1999).

178. de Lange, F. J., Moorman, A. F. M. & Christoffels, V. M. Atrial cardiomyocyte-specific expression of Cre recombinase driven by anNppa gene fragment. *genesis* **37,** 1–4 (2003).

179. Livak, K. J. & Schmittgen, T. D. Analysis of Relative Gene Expression Data Using Real-Time Quantitative PCR and the 2−ΔΔCT Method. *Methods* **25,** 402–408 (2001).

180. Domínguez, J. N., Navarro, F., Franco, D., Thompson, R. P. & Aránega, A. E. Temporal and spatial expression pattern of beta1 sodium channel subunit during heart development. *Cardiovasc. Res.* **65,** 842–50 (2005).

181. Campione, M. *et al.* Pitx2 expression defines a left cardiac lineage of cells: evidence for atrial and ventricular molecular isomerism in the iv/iv mice. *Dev. Biol.* **231,** 252–64 (2001).

182. Kirchhof, P. *et al.* PITX2c Is Expressed in the Adult Left Atrium, and Reducing Pitx2c Expression Promotes Atrial Fibrillation Inducibility and Complex Changes in Gene Expression. *Circ. Cardiovasc. Genet.* **4,** 123–133 (2011).

183. Yiin, G. S. C. *et al.* Age-specific incidence, outcome, cost, and projected future burden of atrial fibrillation-related embolic vascular events: a population-based study. *Circulation* **130,** 1236–44 (2014).

184. Wagoner, D. R. Van & Nerbonne, J. M. Molecular Basis of Electrical Remodeling in Atrial Fibrillation. *J Mol Cell Cardiol* **32,** 1101–1117 (2000).

185. Burashnikov, A. & Antzelevitch, C. Reinduction of atrial fibrillation immediately after termination of the arrhythmia is mediated by late phase 3 early afterdepolarization-induced triggered activity. *Circulation* **107,** 2355–60 (2003).

186. Bosch, R. F. *et al.* Ionic mechanisms of electrical remodeling in human atrial fibrillation. *Cardiovasc. Res.* **44,** 121–31 (1999).

187. Workman, A. J., Kane, K. A. & Rankin, A. C. The contribution of ionic currents to changes in refractoriness of human atrial myocytes associated with chronic atrial fibrillation. *Cardiovasc. Res.* **52,** 226–35 (2001).

188. Greiser, M., Lederer, W. J. & Schotten, U. Alterations of atrial Ca(2+) handling as cause and consequence of atrial fibrillation. *Cardiovasc. Res.* **89,** 722–33 (2011).

189. Olesen, M. S. *et al.* Genetic Loci on Chromosomes 4q25, 7p31, and 12p12 Are Associated With Onset of Lone Atrial Fibrillation Before the Age of 40 Years. *Can. J. Cardiol.* **28,** 191–195 (2012).

190. Franco, S., Canela, A., Klatt, P. & Blasco, M. A. Effectors of mammalian telomere dysfunction: a comparative transcriptome analysis using mouse models. *Carcinogenesis* **26,** 1613–26 (2005).

191. Marques, F. Z. *et al.* Telomere dynamics during aging in polygenic left ventricular hypertrophy. *Physiol. Genomics* **48,** 42–9 (2016).

192. Lubitz, S. A. *et al.* Independent susceptibility markers for atrial fibrillation on chromosome 4q25. *Circulation* **122,** 976–84 (2010).

193. Gore-Panter, S. R. *et al.* Atrial Fibrillation associated chromosome 4q25 variants are not associated with PITX2c expression in human adult left atrial appendages. *PLoS One* **9,** e86245 (2014).

194. Syeda, F. *et al.* PITX2 Modulates Atrial Membrane Potential and the Antiarrhythmic Effects of Sodium-Channel Blockers. *J. Am. Coll. Cardiol.* **68,** 1881–1894 (2016).

195. Sartori, M. P., Quinones, M. A. & Kuo, L. C. Relation of Doppler-derived left ventricular filling parameters to age and radius/thickness ratio in normal and pathologic states. *Am. J. Cardiol.* **59,** 1179–82 (1987).

196. Borlaug, B. A. *et al.* Impact of arterial load and loading sequence on left ventricular tissue velocities in humans. *J. Am. Coll. Cardiol.* **50,** 1570–7 (2007).